Behavior and Design of Cast-in-Place Anchors under Simulated Seismic Loading

Final Report (Volume I)

Cyclic Behavior of Single Headed Anchors

By

Derek Petersen
Graduate Research Assistant, University of Wisconsin, Milwaukee

Zhibin Lin
Assistant Professor, North Dakota State University, Fargo, ND
(Formerly a graduate student at the University of Wisconsin, Milwaukee)

Jian Zhao
Associate Professor and Principle Investigator, University of Wisconsin, Milwaukee

Submitted to National Science Foundation for the NEESR Project Funded under Grant No. CMMI-990712342

Department of Civil Engineering and Mechanics
University of Wisconsin, Milwaukee, WI 53201

July 2013

Executive Summary

All experimental tests of the NEES-Anchor project were conducted in five phases. The volume of the project report focuses on the cyclic behavior of single anchors subjected to shear, tension, and combined shear-tension. All the described test data can be found in NEES project warehouse at https://nees.org/warehouse/project/725.

Phase I tests focused on the evaluation of code-specified seismic reduction factors for anchor capacities under shear and tension using laboratory tests. The tests provided fundamental understanding of capacity reduction for anchors under cyclic loading. Concrete breakout failure and steel fracture under shear and tension were studied using the reported tests. The rest anchor failure modes, such as the pullout and side face blowout for anchors in tension and the pryout for anchors in shear, were not examined because they are unlikely control the failure of cast-in anchors.

A total of 52 tests were conducted using thirteen test blocks (with four anchors in each block) in Phase I study. The anchor specimens were subjected to displacement-controlled cyclic loading. The observed capacity of anchors under cyclic loads in most tests was lower than that of anchors subjected to monotonic loads. The capacity reduction for anchors with concrete breakout failure ,in both tension and shear, was likely due to accumulative/progressive damage in concrete. The cyclic loading introduced additional uncertainties to the propagation of cracks that led to breakout cones. The capacity reduction for anchors failed in shear fracture was due to crush of concrete around the anchor bolt. The damaged concrete left the top portion of anchor shaft unsupported, and introduced a bending moment, which caused anchor shaft fracture at a lower load than that achieved in monotonic tests. The cyclic loading did not cause any capacity reduction to anchors controlled by fracture in tension.

The seismic reduction factors currently specified in ACI 318-11 were modified according to the results of the described tests and other tests collected from the literature. A database was assembled for cast-in-place anchors and headed studs subjected to stepwise increasing cyclic loading (the tests of post-installed anchors were not included). The database contains about 120 tests for anchors in shear and 20 data for anchors in tension. The ratios of anchor capacities in

cyclic test were calculated with respect to the average capacities of the corresponding monotonic tests. An analysis of the ratios indicated an average capacity reduction of 0.83 for concrete breakout in shear and 0.87 for concrete breakout in tension. A seismic reduction factor of 0.85 is recommended for concrete breakout failure, which is higher than that specified in ACI 318-11. This recommended reduction factor shall not be extended to other failure modes, especially pullout failure. The reduction factor of 0.85 is also recommended for steel fracture in shear based on the data analysis. This is very different from that specified in ACI 318-11, but necessary to consider the impact of local concrete crush. No capacity reduction is needed for anchors controlled by fracture in tension.

Monotonic and cyclic tests of anchor rods were then used to further investigate the seismic capacity reductions for anchors in shear. This additional study was conducted to identify the key parameters that affects the seismic behavior of anchors in shear, focusing on steel fracture. Three types of threaded rods, made of ASTM A193 Grade B7, ASTM A307, and ASTM A304 steel, were tested under monotonic shear and cyclic shear. A gap was introduced in between the loading plates, in terms of 1, 2, and 4 times the anchor diameter. The specific setup represented practical cases, in which the anchor shaft may not be completely embedded in concrete in addition to local concrete crushing.

The cyclic shear tests indicates that low-cycle fatigue had negligible impact on the behavior of anchor rods made of ASTM A193 Grade B7 and ASTM A307 steel, which are most commonly used for anchor bolts. The impact was significant for the anchors made of ASTM A304 steel, a highly ductile steel. These tests indicated that the seismic capacity reduction observed in the reported shear tests of anchors and the tests in the literature may have been largely caused by progressive concrete damage rather than low-cycle fatigue of steel. Further study is needed to better understand the seismic shear behavior of anchor bolts.

The observed large capacity reduction of anchors subjected to cyclic loading indicated that the anchor connections may not be suitable for connections between structural elements. Steel reinforcement is allowed by building codes and design guidelines. Anchor reinforcement was investigated in this study, and the study is documented in the other volumes of the project report.

Acknowledgements

The NEES-Anchor project was supported by the National Science Foundation (NSF) under Grant No. 0724097. The authors gratefully acknowledge the support of Dr. Joy Pauschke, who served as the program director for this grant. The authors also thank the colleagues in ACI committee 355 for their valuable inputs. Any opinions, findings, and recommendations or conclusions expressed in this material are those of the authors and do not necessarily reflect the views of NSF. In addition, the cyclic double shear tests were funded by the department civil engineering and mechanics at UWM through teaching assistantship.

The tests were conducted at the Structures Laboratory at the University of Wisconsin, Milwaukee (UWM), where Dr. Al Ghorbanpoor serves as the director. The authors are grateful for the support Dr. Ghorbanpoor provided throughout the experimental program. The authors would also like to thank Rahim Rashadi for technical support on the hydraulic system.

Many UWM undergraduate students participated in the project, especially Aquilino Dael made a MathCAD program for cast-in-place anchors following three major building codes around the world; Jushua Ollson and Mathew Bushee helped with the specimen preparation and test setup. Chadd Lane (an UWM WiscAMP scholar) also participated the laboratory tests. Some of these undergraduate students were partially funded by Summer Undergraduate Research Fellowship (SURF) at UWM College of Engineering and Applied Science. The project would not be finished without these UWM undergraduate students.

Table of Contents

List of Figures

List of Tables

Nomenclature

α_{eq}	=	Strength reduction factor for earthquake loading
α_{re}	=	Factor accounting for the influence of bend, hook, or loop of reinforcement
λ	=	Factor for considering lightweight concrete
ϕ	=	Strength reduction factor
ψ_e	=	Factor for considering epoxy coated reinforcing bars
ψ_c, ψ_{cp}	=	Factors for considering cracked concrete
ψ_{ed}	=	Factor for considering edge distance effects
A_{nc}	=	Available concrete breakout cone area in tension
A_{nco}	=	Full concrete breakout cone area in tension
A_s	=	Area of steel
A_{se}	=	Effective area of steel
A_{vc}	=	Available concrete breakout cone area in shear
A_{vco}	=	Full concrete breakout cone area in shear
c_{a1}	=	Edge distance measured from center of anchor to edge of concrete
c_{a2}, c_{a3}	=	Side edge distances measured from center of anchor to edge of concrete
d	=	Member depth
d_a	=	Anchor shaft diameter
d_b	=	Diameter of reinforcing bar
e_1	=	Distance from the applied shear force to the concrete surface
e_s	=	Distance between anchor reinforcement and shear force acting on the connection
f_{bd}^0	=	Design bond strength of deformed bars
f'_c	=	Concrete compressive strength
f_{uta}	=	Ultimate tensile strength of a single anchor
F_y	=	Yield strength of material
h_{ef}	=	Embedment depth measured from anchor head to concrete surface
IQR	=	Inter-quartile range
K_{05}	=	Coefficient relating to prediction interval statistics

k_6	=	Factor that considers the position of reinforcement during concreting
k_7	=	Factor to take into account the effect of concrete confinement on the bond strength of reinforcement
k_8	=	Efficiency factor for hairpin anchor reinforcement wrapped around anchor shaft
k_c	=	Constant for calculating the basic tensile breakout capacity
l_d	=	Development length for straight deformed bars
l_{dh}	=	Development length for hooked deformed bars
l_e	=	Load bearing length of the anchor for shear
M_{us}	=	Ultimate bending moment capacity in a bolt
n	=	Number of samples
N_b	=	Basic tension concrete breakout strength of a single anchor unimpeded by edge distances or concrete cracking
N_n	=	Nominal tensile capacity
N_u	=	Applied tension force
Q_1	=	First quartile range being the median of the data that lies below the median of the entire data set
Q_3	=	Third quartile range being the median of the data that lies above the median of the entire data set
S	=	Sample standard deviation
$t_{\alpha,n-1}$	=	100α-percentile values for student t-distribution
u	=	Circumference of reinforcing bar
V_b	=	Basic shear concrete breakout strength of a single anchor unimpeded by edge distances or concrete cracking
V_n	=	Nominal shear capacity
$V_{rk,re}$	=	Steel capacity of anchor reinforcement
V_{sd}	=	Design strength for anchor steel
$V_{sd,re}$	=	Design steel strength for anchor reinforcement
V_u	=	Applied shear force
$\bar{x}$	=	Sample mean
z	=	Internal moment arm of the concrete member

CHAPTER 1 Introduction

1.1 General

Cast-in-place concrete anchors and headed studs are needed to connect structural steel members and concrete. Typical connections utilizing anchors include brace-column connections, column-foundation connections, and girder-wall connections as shown in Figure 1.1. Concrete anchor connections are a critical component of load transfer between steel and concrete members affecting structural performance during earthquake events. Observations of damages in recent major earthquakes have raised concerns about the seismic performance of anchor connections. For example, the 1995 earthquake in Kobe, Japan caused the Osaka Gas Company to lose seventeen transformers that slipped out of place because of anchor failure, causing significant damage to power transmission lines [Asia-Pacific Economic Cooperation, 2002]. The 1994 earthquake in Northridge, California, caused three buildings of a veteran's hospital in Los Angeles to lose power for a week due to a damaged transformer caused by anchor connection failure [Lifeline Earthquake Engineering, 1997]. Also, several column-base connections performed unsatisfactorily in the 1994 Northridge earthquake from excessive anchor elongation and unexpected anchor failure [Grauvilardell et al., 2005].

For cast-in-place anchors, the most common modes of anchor failure encountered in practice are anchor steel failure and concrete breakout failure. Steel or concrete failure of anchored connections can occur under tension, shear, or combined tension-shear loading. Anchor steel failure is shown in Figure 1.2a and Figure 1.2b, where the anchor shaft is fractured near the surface of the concrete in tension or shear respectively. Concrete breakout failure in tension occurs as in Figure 1.3 when the tensile capacity of concrete is insufficient to resist applied tensile forces to the anchor. Upon failure, a concrete cone is broken away from the base concrete in which the connection is located. This breakout cone originates from the head of the anchor and generally follows a 35 degree angle to the concrete surface [Fuchs et al., 1995]. Concrete breakout failure of anchors subject to shear loading occurs when anchors are located close to an edge and loaded in shear toward that edge. In such conditions, a breakout cone is formed at the

concrete surface in front of the anchor shown in Figure 1.4. The breakout cone crack propagates in a 35 degree path toward the free edge in the horizontal and vertical directions. Pullout, side-face blowout, and pryout failures are also considered in anchor design, however, these failure modes are less likely to occur in cast-in-place anchor connections for structural elements and thus are not discussed in this document.

Design standards around the world such as the Precast Concrete Institute (PCI), American Concrete Institute (ACI), Comite Euro-International du Beton (CEB), Canadian Standards Association (CSA), New Zealand Standards (NZS) currently use the concrete capacity design approach developed at the University of Stuttgart in Germany for designing concrete anchor connections. The concrete capacity design method (CCD Method) provides a user-friendly rectangular geometric simplification of the concrete breakout cones discussed previously to calculate concrete breakout capacity. In general, the concrete breakout capacity in tension or shear is dependent on the tensile strength of concrete provided in the breakout cone area. Also, when combined tension-shear loading is present in anchored connections, combined loading interaction equations are used to encompass the conglomerate effects of tension and shear loading in calculating connection capacity.

The test data upon which the CCD method and design code equations are based is largely comprised of anchors subject to static loading. However, when concrete anchors are to be used in seismic risk zones, the effects of cyclic loading must be considered in capacity design as well as connection ductility. Using Appendix D of American Concrete Institute Committee 318 document (ACI 318-08) as a representation of the latest efforts in anchor design for seismic regions, indicates that anchor capacity corresponding to concrete failure is reduced by 25 percent in seismic/cyclic loading conditions. It is not clearly noted whether the motivation of such capacity reduction is intended to account for real behavioral differences of anchors under static loading and cyclic loading, or because it is generally believed that the connected steel element (i.e. beam or column) may develop higher stresses (into strain hardening region of steel behavior) while the anchor connection under the current design and construction does not have such room for developing additional load capacity.

If the motivation of anchor capacity reduction for seismic design is to account for the behavioral difference of the connection, very little data related to cast-in-place anchor behavior under cyclic loading regarding concrete breakout failure exists. For steel failure, the literature shows very contradictory observations: capacity reduction up to 40 percent has been observed in some load controlled cyclic tests [Klingner et al., 1982] yet ACI 318-08 does not require the anchor steel capacity to be reduced for seismic design. Such a large reduction in steel anchor/headed stud capacity has been attributed to low-cycle fatigue occurring under cyclic loading. However, a closer look at those earlier tests indicates that the specimens were tested using force-controlled loading which, according to Pallares and Hajjar (2009), does not accurately represent seismic loading for low-cycle fatigue behavior.

Furthermore, past experimental studies have shown that under reversed cyclic shear loading, headed studs may fail by brittle fracture rather than yielding of steel due to the effect of low-cycle fatigue [Tong, 2001; Civjan and Singh, 2003]. Lotze et al. (2001) concluded that brittle anchor steel fracture can occur under shear loading when small, low strength anchors are used in high strength concrete. Presumably, this situation would lead to pure shear of the anchor shaft without substantially crushing the concrete in front of the anchor that would have allowed larger displacements to manifest.

Anchor connections may fail either by steel failure of the anchor itself which is assumed to be ductile, or by concrete failure which is typically brittle without reinforcement. Anchor design capacity in seismic regions is required to be controlled by ductile failure modes in order for force re-distributions to occur. ACI 318-08 D3.3.4 requires that anchor connection capacity in seismic regions be controlled by a ductile steel element. Thus, two options are available to satisfy this requirement: anchor steel capacity and reinforcing steel capacity. The connection can be designed via ACI 318 Appendix D such that the anchor steel capacity is less than that for all concrete failure modes including the seismic reduction factor mentioned previously to ensure that steel failure of the anchor shaft occurs before brittle concrete failure. However, relying on concrete in tension in seismic design is not accepted for the design of any other reinforced concrete members such as beams, columns, or walls. The concept behind concrete design is for reinforcing steel to carry tensile loads occurring in concrete members.

The behavior of cast-in anchors and headed studs subjected to static loading has been extensively studied [CEB, 1997; Cannon, 1995; Cook et al., 1989; Klingner et al., 1982; Eligehausen et al., 2006], and the results have been implemented in design codes (ACI 318 2008; *fib*, 2008). In most existing studies, the steel base plate were placed in contact with the concrete surface; however, a space is frequently needed during construction of such anchor connections to adjust the orientation of the connected steel member, as illustrated in Figure 1.5a, and the space is usually filled afterwards with grouts. The grout pad, due to the lack of confinement, cracks early when the anchors are subjected to shear, leading to an exposed portion in the anchors. Also, exposed portion of anchors can be found in the steel base plate without grout or with a shim isolating anchor bolts with grout for the purpose of ductility requirement, as shown in Figure 1.5b.

The exposed portion of an anchor causes a moment and sometimes tension in the anchor shaft when subjected to shear. The shear capacity of exposed anchor bolts in concrete is thus affected by the exposed length, anchor bolt diameter, and other factors such as restraints of anchor end rotation from the concrete. The combined loadings on anchors subjected to shear forces with an exposed length (or lever arm) have been recognized by design codes. For example, ACI 318-08 stipulates that the design shear strength of anchor bolts with a grout leveling pad shall be reduced by a factor of 0.8. The *fib* guidelines (2008) for anchor design assume that the failure of an exposed anchor in shear is controlled by flexural yielding of the anchor. However, a review of such existing design guidelines [Lin et al., 2011] reveals that shear behavior of anchor bolts with different exposed lengths are not well understood, and methods to characterize strength capacities in shear are not adequately supported by experimental data.

Most studies which investigate anchor rods in concrete anchors focus on concrete failure modes, rather than the failure of anchor rods from shear and bending, even tension. Similarly, no documented studies examine the effects of ductile anchor steel used for ductility requirement in design codes for the strength capacity of anchors. Thus, there is a lack of experimental research which investigates anchor steel ductility and modes of failure that may characterize the shear capacity of anchors. In addition, it is well known that the behavior of anchors under seismic loading can be affected by loading history, concrete and steel materials, and etc. Current seismic design regulations (e.g., ACI 318-08) for anchors specify the ductile steel failure modes as

anchor capacity. For anchors controlled by steel failure in shear, no reduction is required for the anchor capacities corresponding to steel failure. However, there exist strength reductions to some degree in the literature research. For example, Pallarés and Hajjar (2010a, 2010b) suggested the steel capacity of anchor in shear have a reduction by a factor of 0.76. Therefore the behavior of anchors with various exposed lengths under static loading and quasi-static cyclic loading were carried out in this study.

1.2 Overview of NEES-Anchor Project

There are knowledge gaps in the seismic design of headed anchors, both within a single anchor and a group of anchors as a connection: 1) there are no behavioral data on anchors embedded in concrete with substantial damage; thus, an anchor design may have uncontrollable performance; 2) the desired ductile anchor failure may become brittle fracture of anchors under cyclic shear or combined cyclic tension-shear, leading to an unsafe design; and 3) the potential benefits of adding supplementary reinforcement around anchors is overlooked, which may turn a brittle concrete failure into a more ductile behavior. To rectify these gaps in the existing knowledge base, the NEES-Anchor project is to:

- Obtain detailed experimental data for cast-in-place anchors/studs under simulated seismic loadings with a focus on combined tension-shear loading;
- Evaluate the limitations of current seismic design provisions (e.g., Appendix D of ACI 318-05), and develop improved design methodologies and equations; and
- Evaluate proposed design methods and details by testing connections between steel girders and concrete walls.

The experimental tests were conducted in five phases. The experimental tests include

- 61 tests of unreinforced single anchors subjected to cyclic loading (Phase I);
- 20 tests of reinforced single anchors subjected to shear (Phase II);
- 28 tests of reinforced single anchors subjected to tension (Phase III);
- 2 tests of anchor groups in plastic hinge zones of a concrete wall (Phase IV); and
- 6 tests of reinforced single anchors in plastic hinge zones of columns (Phase V).

Additional tests were conducted for anchor rods in shear with various exposed lengths (Phase O). Phase I tests focused on the evaluation of code-specified seismic reduction factors for anchor capacities under shear and tension using laboratory tests. The volume of the project report focuses on the cyclic behavior of single anchors.

1.3 Research Objectives

There is currently limited test data that provides detailed behavioral observations for cast-in-place anchors exhibiting concrete failure under cyclic loading in tension, shear, or combined tension-shear loading. Specifically, there is very limited test data relating to the cyclic capacity behavior of concrete failure modes in the literature, and the data that is available presents a large degree of scatter. Phase I of this research studies concrete breakout behavior of cast-in-place anchors subject to monotonic and cyclic tension, shear, and combined tension-shear loading. Tests designed to represent geometries commonly encountered in practice were used to provide support to the currently used seismic reduction factor for concrete failure as well as the interaction equation used to determine anchor capacity subject to cyclic combined tension-shear loading.

1.4 Report Layout

A review of existing analytical methods, experimental tests, and code provisions for anchors in plain concrete is provided in Chapter 2 focusing on cyclic-loading behavior. Test setup and design of unreinforced cast-in-place anchors is discussed in Chapter 3. Chapter 4 includes a discussion of unreinforced tests including monotonic shear, cyclic shear, monotonic tension, cyclic tension, as well as combined cyclic tension-shear. Cyclic tests of anchor rods are presented in Chapter 5. Chapter 6 includes the summary and recommendations.

Figure 1.1: Typical anchor connections between structural steel and concrete

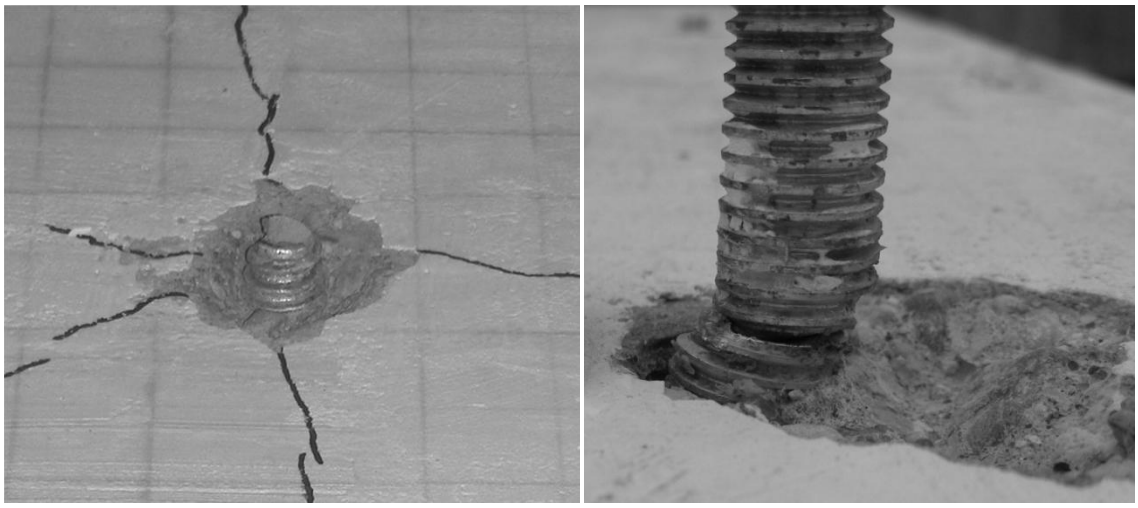

a) Steel failure in tension; b) steel failure in shear

Figure 1.2: Anchor steel failure

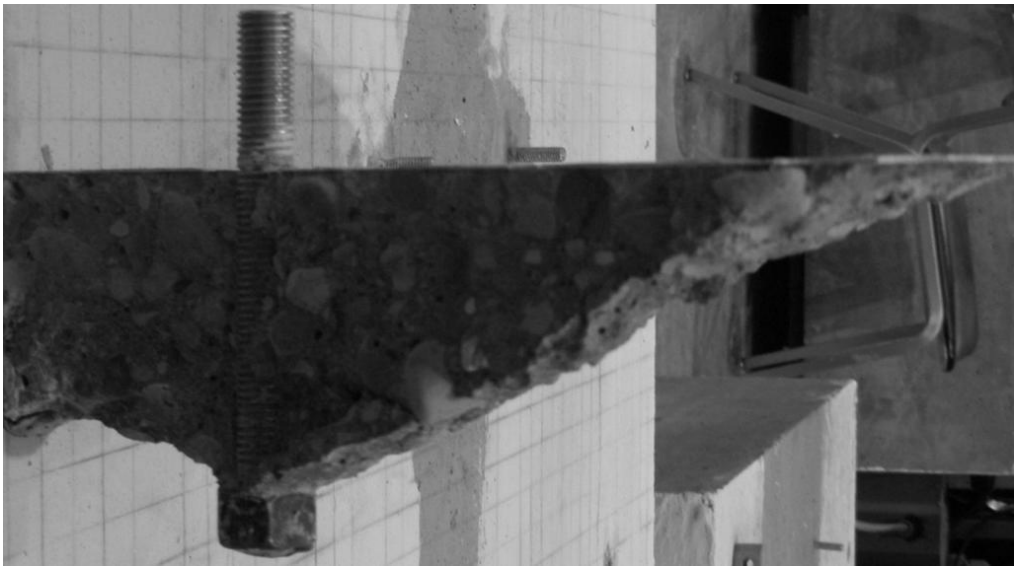

Figure 1.3: Concrete breakout failure in tension

Figure 1.4: Concrete breakout failure in shear

(a) anchors with leveling grout **(b) anchors without grout**

Figure 1.5: Exposed anchor bolts in practice

CHAPTER 2 Literature Review

2.1 General

The behavior of anchors in concrete has been studied and discussed at length in: CEB (1994), Cannon (1995a, 1995b), Cook et al. (1989), Klingner et al. (1998), and Eligehausen et al. (2006). Among the available anchor types, cast-in-place (CIP) anchors/headed studs are most commonly used in the connections shown in Figure1.1.

Most studies have focused on ultimate capacities of anchors under monotonically increasing loads. Design equations as documented in ACI 318-08, ACI 349, CEB 1994, and the PCI design handbook in similar formats are established based on tests of various anchors embedded in both uncracked and cracked concrete and experiencing the following failure modes: steel fracture, concrete breakout, concrete side-face blowout, and anchor pullout for anchors in tension; and steel fracture, concrete breakout, and concrete pryout for anchors in shear (ACI 318-11).

Limited experimental studies exist regarding cyclic shear behavior of anchored connections. Headed anchors located in uncracked and cracked concrete with controlled crack width (up to 0.03in.) under pulsating tension have been studied in Germany with a thorough literature review by Hoehler (2006). It was found that anchor capacity was not significantly affected if the cyclic load level were below the peak anchor capacity. However, a limited number of earlier studies focused on the load-displacement behavior of anchors under cyclic shear. In the tests on single headed studs by Civjan and Singh (2003) and groups of studs by Usami et al. (1980), steel fracture due to low-cycle fatigue was found to be the typical failure mode and considerable pinching and degradation of the force response was observed. Klingner et al. (1982) tested single anchor bolts with varying edge distances under reversed force-controlled cyclic shear. It was observed that the anchor bolts typically failed at much lower loads than those tested monotonically due to the effects of low-cycle fatigue. Similar conclusions were reached in a cyclic loading test of a steel frame with in-filled reinforced concrete walls. Headed studs were used at the steel-concrete interface to ensure composite actions [Tong et al., 2005]. In addition, load-controlled cyclic shear tests have been conducted for headed studs and cast-in anchor bolts, and the tests showed that the anchor shear capacity (corresponding to steel failure) could be

significantly reduced under cyclic loads, and the large capacity reduction (up to 50%) was attributed to low-cycle fatigue. However, ACI 318-11 requires no reduction for the anchor steel capacities. In addition, a reduction factor of 0.75 was proposed for headed studs in composite constructions for both steel and concrete failure.

Anchor behavior under combined cyclic tension-shear has been obtained by testing of groups of anchors [Usami et al., 1980; Okada and Seki, 1984; Hawkins et al., 1980; and Roeder and Hawkins, 1981]. The advantage of such tests is that the ratio of tension and shear loads on individual anchors can be varied with a single hydraulic ram. The disadvantage is that the actual shear and tension in individual anchors cannot be measured directly for evaluating/establishing the interaction equation for design. Combined cyclic testing on single anchor bolts/studs, that provides accurate data for evaluating the shear-tension interaction equation currently used in design codes is limited. The existing studies pertaining to the cyclic behavior of cast-in-place anchors embedded in concrete are reviewed in this section.

2.2 Anchor Behavior under Cyclic Loads

The current design codes use a strength reduction factor for seismic applications. This reduction, coupled with the requirement of ductile anchor steel being the controlling failure mode for connections in moderate to high seismic risk zones are the only considerations that are currently being regulated in worldwide design codes. ACI 318-11 D3.3.3 stipulates a seismic reduction factor of 0.75 applied to all concrete failure modes. Previous research suggests that this may be overly conservative for anchors under cyclic tension loading [Hoehler, 2006; Eligehausen and Balogh, 1995] and un-conservative for anchors under cyclic shear loading [Civjan and Singh, 2003; Klingner et al., 1982]. Also, in seismic events, it is possible for connected steel members to exhibit higher capacities due to plastic behavior. However, it is unclear whether the current seismic reduction for anchor design also includes the strain hardening effects of connected steel members. The reduction factor is likely a combination of both capacity reduction in the anchor connection as well as overcapacity ability of the connected steel members. For the purpose of this study, only cyclic capacity reduction in anchored connections will be explored.

2.2.1 Seismic Loading Protocols

Cyclic tests are used to evaluate the load resistance and energy dissipation capability of structural systems or structural components such that conclusions may be drawn on their seismic performances. This indicates that in addition to the strength and stiffness of the test structure, capturing the dynamic characteristics and history-dependent behavior, such as strain hardening and deterioration, is critical to a simulated seismic test. Limited experimental research has indicated that the quasi-static loading likely cause a small decrease in strength [Krawinkler, 1988]. This may be attributed to the fact that under sloe cyclic loading, the damage in the test specimen would have sufficient time to propagate, leading to increased deterioration. Therefore it is generally accepted that results from quasi-static cyclic tests are conservative. Note that this common view has ignored loading rate-related behavior other than strength. For example, under dynamic loading, breakout cracks may not fully develop such that other failure modes may control the behavior. The impact of dynamic loading rates was not included in this study. While the impact of dynamic loading rates is usually ignored, history-dependent behavior has been the focus of seismic tests. A cyclic loading protocol thus needs to include 1) the number of cycles; 2) the amplitude of each loading cycle; and 3) the sequence of the loading cycles.

Seismic loads on concrete anchors have been represented by various types of loadings in laboratory tests. With a goal to best represent the loading conditions of structures and structural components may experience during an earthquake, most loading protocols are established based on the following assumptions: 1) the deformation demands of a structural component may be well represented by the dynamic responses of a structure; 2) the response of a multi-degrees-of-freedom (MDOF) structure may be well represented by a single-degree-of-freedom (SDOF) structure through its story drift. While detailed studies have been conducted in the literature regarding these two assumptions [Hadidi-Tamjed,1987 and Nassar and Krawinkler,1991] as documented in ACT-24, 1992) for steel structures, Figure 2.2 presents sample responses for illustration purposes. Two idealized SDOF systems were used: one with a natural vibration period of 2 sec, representing a 20-sotry building, and the other with a period of 0.5 sec, representing a stiff structure. The ground acceleration records chosen for the analysis was the Imperial Valley earthquake of May 18, 1940, recorded at El Centro at 270 degrees, with a peak

ground acceleration of 0.34 g. The stiffness of the two structural models was the same and their mass was varied to create the natural periods. The damping ratio was 5% for both models.

All parameters of the structural models were rather arbitrarily assumed for demonstration purposes. The structural model with a natural period of 2 sec was assumed to have bilinear load-displacement behavior without strain hardening. The yield displacement was assumed as 0.75 in. such that the structural response had a ductility coefficient close to 8. The post-yielding stiffness was assumed as 5% of the critical damping. Because of a relative long period, there are roughly three cycles with a peak displacement smaller than the assumed yielding displacement (Δ_y), two cycles at Δ_y, three cycles at $2\Delta_y$, two cycles at $4\Delta_y$, one cycle at $6\Delta_y$, and one cycle at $8\Delta_y$ within the first 32 seconds of the response history. The structural model with a short period had a smaller mass, thus the applied force is much smaller compared with the long-period structure. Therefore the peak displacement of the short-period structure is much smaller than that of the long-period structure. Note that the simulated displacements do not tell that of any real structure. Within the first 32 seconds, the structural model experienced one cycles of peak displacement (Δ), seven cycles at 0.5Δ, six cycles at 0.4Δ, nine cycles at 0.3Δ, fourteen cycles at 0.2Δ, and many cycles below 0.2Δ.

Seismic loading protocols have been designed to reproduce the effects the loading histories similar to Figure 2.3. This has resulted in vastly different observations on the seismic behavior of anchors. The current specifications on seismic capacity reductions for anchors do not all agree with these laboratory observations. For example, seismic loading was represented by ramp-type loading with high loading rates in an extensive study of both cast-in and post-installed anchors (focusing on concrete breakout failure under tension or shear) [Cook et al., 1991]. It was found that the higher anchor capacity than t hat obtained in static tests could be achieved under such impact-type of loading. Expansion and undercut anchors were subjected to low-cycle fatigue loading with constant amplitudes [Hoehler, 2006; Vintzeleou and Eligehausen, 1991; Eligehausen and Balogh, 1995]. Although these tests indicated that the anchor capacities were not reduced by cyclic loading, repeated loading with fixed loading amplitudes may not represent the worst impact of an earthquake on anchor connections.

Various types of loading protocols have been used in quantifying the seismic behavior of anchor bolts as illustrated in Figure 2.1. Only reversed cyclic (alternating) load patterns are shown while pulsating load patterns have also been used in laboratory tests. Many earlier tests were conducted with load-controlled loading protocols (Figures 2.1a through 2.1c) while displacement-controlled tests later become available with sophisticated equipment (Figures 2.1d through 2.1f). Cyclic loading with fixed load or displacement levels have been used to study the effect of low-cycle fatigue on anchor behavior [[Hoehler, 2006; Vintzeleou and Eligehausen, 1991; Klingner et al., 1982]. The loading rate has been selected based on typical seismic responses of structures [Matthew et al., 2011]. More detailed analyses of such seismic responses have led to cyclic loading with variable load/displacement levels (Figures 2.1b, 2.1c and 2.1e): the responses usually start with small-amplitude vibrations before the strong motion that may cause significant damage, and the strong motion phase is usually followed by vibrations with decreasing amplitudes. Such cyclic tests with load-controlled loading (Figure 2.1b) have been specified by the Structural Engineers Association of California (SEAOSC, 1997) and German Institute for Building Technology (DIBt) for seismic qualifications of post-installed anchors. Displacement-controlled cyclic loads (similar to Figure 2.1e) have been widely used for seismic tests of structural components such as columns and beam-column connections). Anchor bolts have also been subjected to pre-calculated seismic displacements (Figure 2.1f). The literature review below focuses on tests with stepwise increasing loads (i.e., Figures 2.1b and 2.1d).

2.2.2 Cyclic Tension

The behavior of headed anchors under cyclic tension has been evaluated extensively for post-installed anchors, however, cyclic testing of cast-in-place anchors is limited. Cyclic tension has been shown to have a negligible effect on anchor strength compared to monotonic loading [Eligehausen and Balogh, 1995; Rodriguez et al., 2001; and Hoehler, 2006]. A series of tests by Hoehler (2006) were used to investigate the effect of cyclic tension loading on the behavior of headed anchors/studs with a focus on ultimate capacity and deformability upon failure. The tests showed minimal capacity change between monotonic and cyclic load cases if the cyclic load level was below the non-cyclic anchor capacity.

The work by Rodriguez et al. (2001) tested cast-in-place as well as various types of post-installed anchors to study the effect of cracking and load type on anchor behavior. The load pattern used

in these tests was a ramp load at rate of 0.1 seconds, whose magnitude exceeded the anchor capacity. It was reasoned in the research by Rodriguez et al. (2001) that this load pattern accurately imitates the typical load behavior produced by earthquakes on non-structural elements. The results however showed that the normalized dynamic ramp loading anchor capacities were approximately 30 percent higher than the monotonic capacities for all types of anchors tested. Hoehler (2006) tested cast-in-place as well as post-installed anchors in a variety of cyclic tension loading situations. Cycling at or below the peak monotonic anchor capacity as well as stepwise increasing tension load level loading was reported to have little or no effect on anchor capacity. Similar observations were made by Silva (2003) testing cast-in-place and post-installed anchors in cyclic tension.

The number of cyclic tension tests is small compared with shear tests. Hasselwander et al. (1974) included two exploratory tests of anchor bolt embedded in concrete piers. Steel failure was observed in tests and the cyclic loads did not cause any reduction in anchor capacities. The negligible steel capacity reduction in tension was also observed in the tests by Nakashima (1999, 2000). The tests by Hoehler (2006) included nine specimens that were subjected to stepwise increasing loads (Figure 2.1b). The cyclic loads did not affect the concrete breakout capacity in tension.

2.2.3 Cyclic Shear

Many of the past studies related to cyclic shear loading of concrete anchors have focused on anchor steel failure. In tests on single headed studs by Civjan and Singh (2003) and groups of studs by Usami et al. (1980), steel fracture due to low-cycle fatigue was found to be the typical failure mode as considerable pinching and degradation of the force response was observed. Civjan and Singh (2003) reported an average loss of anchor steel stud capacity of 10 to 20% under reversed cyclic shear with bare steel specimens with the point of applied shear force 1.85 inches above the surface. This capacity reduction increased to 25% when the height of the shear load was increased to 2.35 inches. They also made generalized conclusions alluding to the effect of bending stresses on anchor steel failure. It was reported that as the distance between the restrained embedded portion of the anchor and the point of applied shear force increases, typically due to the crushing of concrete in front of the anchor; the bending stresses increase as well, producing lower failure capacities.

Similar observations were made by Klingner et al. (1982) testing single anchor bolts under reversed cyclic shear studying anchor steel capacity reduction where anchor bolts typically failed at much lower loads under cyclic loading than those tested monotonically due to the effects of low-cycle fatigue. Research by Saari et al. (2004) for shear studs showed a maximum cyclic shear capacity reduction of 17 percent for all shear failure modes. Similar conclusions were reached in a cyclic loading test of a steel frame connected to infilled reinforced concrete walls with headed studs (Tong, 2001; Tong et al., 2005). The shear studs typically failed at deformations that were less than previously sustained deformation values under monotonic shear loading, indicating that the studs failed due to low cycle fatigue.

Bischof (1978) conducted a series of single-side pushout tests simulating the connections between precast concrete panels. The shear load had an offset such that the concrete pryout controlled the failure. The cyclic load tests showed less than 10% capacity reduction compared with the corresponding monotonic tests. Hawkins and Mitchel (1984) compared the behavior of 10 pushout specimens loaded cyclically with that of 13 monotonically loaded specimens. Specimens failed by stud shearing achieved on average 83% of monotonic capacities with small variations. Hawkins and Mitchel also pointed out that load-controlled loading is more severe type of cyclic loading because specimens subjected to cyclic loads achieved 81% of monotonic capacities compared with 86% for specimens subjected to cyclic displacements. Load-controlled cyclic pushout tests have also been conducted by Nakajima et al.(2003), Taplin and Grundy (1997), Bursi and Gramola (1999), and Civjan and Singh (2003).

Stud fracture due to low-cycle fatigue was found to be the typical failure mode and considerable degradations of the force response (or increases in stud slips) were observed. The typical loss of stud shear capacity is about 20% when the specimens were subjected to cyclic loads. Smaller stud capacity reduction was observed by Gattesco and Giuriani (1996) and Saari et al. (2004) using pushout specimens subjected to displacement-controlled cyclic loading.

The stud shear capacity may include frictions between steel and concrete in the pushout tests while the friction could be minimized in single-anchor shear tests. Swirsky et al. (1978) conducted ninety two shear tests of 1- and 2-in. cast-in-place anchor bolts with and without hairpins, and most cyclic tests were controlled by concrete breakout failure followed by bond

failure of hairpins. The largest load levels varied from 50% to 90% the monotonic anchor capacity. The tests showed that cyclic loading did not affect the anchor capacities. Meanwhile, Klingner et al.(1982) tested single anchor bolts under reversed cyclic shear studying anchor steel capacity reduction where anchor bolts typically failed at much lower loads under cyclic loading than those tested monotonically. The relatively large reduction (e.g., 50%) in anchor steel capacity in shear was also observed in a series of cyclic tests conducted by Nakashima (1999, 2000). The lower observed capacities may have been partly attributed to the grout pads used in the tests, which cracked and crushed, causing combined bending and shear actions in the anchor shaft.

2.2.4 Combined Cyclic Tension-Shear

Anchor behavior under combined cyclic tension-shear has been studied by testing groups of anchors (Roeder and Hawkins, 1981; Usami et al., 1980; Anderson and Meinheit, 2006; Eligehausen et al., 2006). The advantage of the test setups used in these experiments is that the ratio of tension and shear loads on individual anchors can easily be varied by changing the loading angle of a single hydraulic ram. The disadvantage is that the actual shear and tension forces on individual anchors cannot be measured directly for evaluating/establishing an interaction equation for design. Combined cyclic tension-shear testing using two hydraulic actuators on a single anchor bolt/stud can provide more accurate data for evaluating tension-shear interaction because the tension and shear forces on the anchor during the test can be individually measured. McMackin et al. (1973) proposed the following equation for tension-shear loading interaction of concrete anchors:

$$\left(\frac{N_u}{\phi Nn}\right)^{5/3} + \left(\frac{V_u}{\phi Vn}\right)^{5/3} \leq 1 \qquad (2.1)$$

where N_u and V_u correspond to the applied force to the connection while N_n and V_n are the respective nominal tension and shear capacities of the connection to predict the combined load capacity of an anchor connection. This equation is one of the currently accepted combined loading interaction models given in the ACI 318-08 Appendix D. A total of 27 tests were performed by McMackin et al. (1973) on anchors having edge distance of twelve inches embedment lengths ranging from four to eight inches with loading angles of 30 and 60 degrees measured from the pure tension position (zero degrees). The main focus of the research was to

investigate varying embedment depths of anchors as shown by the uniform edge distance for all tests. Since the edge distance selected for the combined loading tests was sufficiently large to resist steel failure in shear, even for the few 7/8 inch diameter anchors that were tested, it can be implied that all reported concrete failures under combined loading were of tension breakout for embedment depths of seven and eight inches and shear pryout for embedment depth of four inches. However, shear or tension breakout failure was not differentiated in the article.

Lotze et al. (2001) suggested that the use of the elliptical interaction equation given by McMackin et al. (1973) may be unconservative and that the tri-linear interaction equation:

$$\frac{N_u}{\phi Nn} + \frac{V_u}{\phi Vn} = 1.2 \tag{2.2}$$

proposed by Bode and Roik (1987) is a better representation of tension/shear interaction where concrete failure controls the capacity of the connection. A modification to the elliptical interaction equation in PCI (1985) used an exponent equal to 4/5 to fit concrete failure interaction under combined loading. The three equations are shown in Figure 2.4 with the elliptical interaction from PCI (1985) being the most conservative. ACI 318-08 accepts the use of either the tri-linear equation or the elliptical interaction using any exponent from 1.0 to 2.0 that is verified by test data. Lotze et al. (2001) concluded that if the elliptical equation was used to predict the interaction behavior for tests experiencing concrete failure under combined loading, using an exponent of 1.6 produced the best results.

2.3 Comparison of Seismic Design Practices

The ACI 318-08, New Zealand Standard 3101 (2006), CEB Design of Fastenings in Concrete (1997), and Prestressed/Precast Concrete Institute design handbook (6th Edition) were reviewed for comparison of design procedures related to anchored connections in seismic risk regions. While all design codes reviewed agree with using the concrete capacity design (CCD) approach for anchor design, they do not agree on all levels of design equations. Seismic effects are treated differently across many of these design codes. For example: The PCI handbook (6th Edition) incorporates an overload factor ranging from 1.0 to 1.33 chosen by the engineer in consideration of mode of failure, consequence of failure, and sensitivity to connection tolerances. ACI 318-08

uses an additional 0.75 capacity reduction to be applied to concrete failure mode capacities for anchors located in seismic risk regions but does not consider overloading. The CEB 1997 design code does not give seismic design requirements but states that the effects of seismic loading should be considered by the engineer while the FIB design guide set to supersede the CEB 1997 report uses an additional multiplication factor of $\alpha_{eq} = 0.75$ to be applied to concrete failure mode capacities similar to the ACI 318-08 code. Neither the ACI 318-08 nor FIB design guide require steel strength to be reduced for consideration of seismic effects.

These seismic factors are applied after all other strength reduction factors for individual failure modes have been considered. Strength reduction (ϕ) factors for anchor capacity calculations are used to address uncertainties in material and design parameters. These reduction factors are chosen based on importance and consequence of the particular failure behavior considered. Reduction factors tend to be larger for failure modes that exhibit less consistent behaviors or that may be sudden/brittle in nature. Strength reduction factors are also used to compensate for inconsistencies between theoretical strength and actual strength. Such inconsistencies can be the result of improper construction or inaccurate models for theoretical strength calculations. While some design codes have very detailed selection for strength reduction factors (ACI318-08), other codes have more general strength reduction assignments [NZS 3101, 2006].

Strength reduction factors and design equations are continuously being optimized as increasing quantity and/or quality of test data becomes available. For example, as more test data has become available for anchor connections, engineers have been able to adapt design equations to more accurately predict the strength of such connections. The anchor design method has evolved from the 45 degree stress cone model, to the kappa factor approach, to the currently used CCD method [Fuchs et al., 1995]. The changes of design methods have made anchor design more accurate and user friendly [Cannon, 1995; Fuchs et al., 1995]. As more accurate design models are introduced, confidence and reliability in design allow for less restrictive strength reduction factors to be used.

A list of anchor design codes considered in this research are as follows: ACI 318-08 (Chile, USA), PCI 6th Edition (USA), CEB 1997 (Germany, Bulgaria, Portugal), CSA A23.3-94 (Canada), NZS 3101-17-2006 (New Zealand), NBR 6118:2003 (Brazil), EHE-2008 (Spain), the

unpublished version of the new FIB anchor design guide, and correspondence regarding the Chinese and Japanese design codes as well. The adoption of the CCD method to design codes worldwide shows international cooperation in anchor design. However, the increasing amount of information relating to anchored connections makes it difficult to stay up to date on the most recent information that can be used for code revisions. Anchor design committees are forced to rely on limited test results when revising code provisions because of this lack of centralized information. For example, the ACI 318-08 methods for anchor design are based largely on post-installed anchor test data, whereas the PCI 6th Edition design handbook relies on test data relating to cast-in-place anchor groups [Anderson and Meinheit, 2007].

Phase I of this research aims to obtain available literature data with single anchor test results from this study in order to explore anchor capacities under monotonic and cyclic loading and use the information to justify the seismic reduction factor of 0.75 used in ACI 318-08. To provide supporting data to existing literature, single anchor tests using anchor diameters and locations carefully chosen to represent commonly encountered cast-in-place anchor conditions seen in engineering practice. In addition, displacement controlled cyclic combined loading was used to inspect the currently used interaction equations of ACI 318-08 for cyclically loaded anchors.

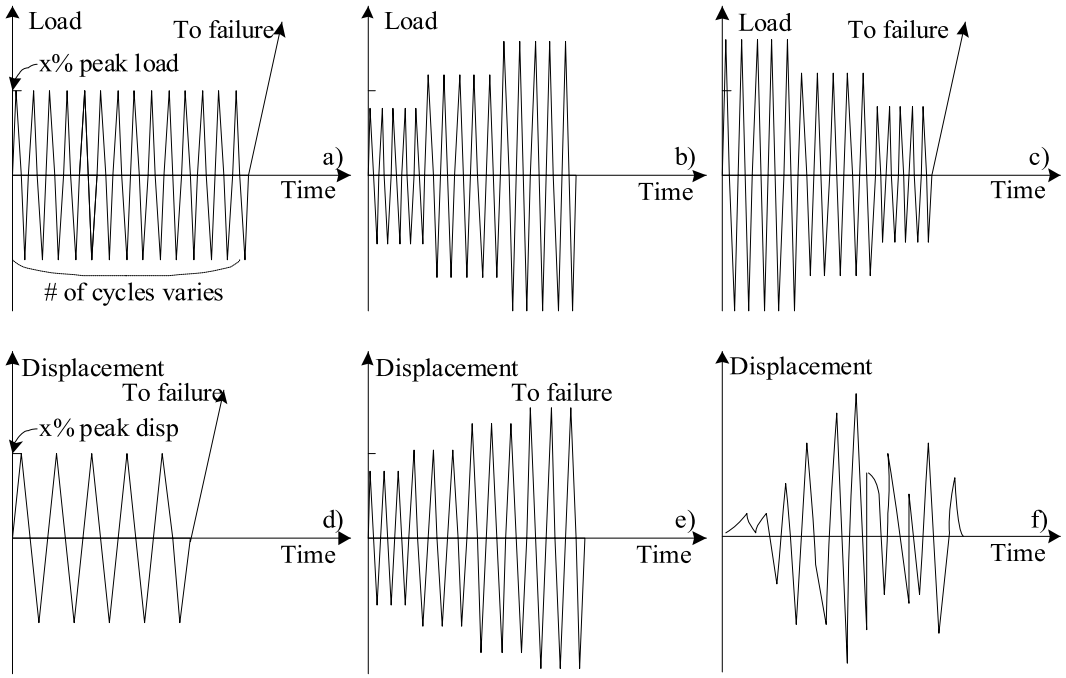

Figure 2.1: Cyclic loading patterns to simulate earthquake actions.

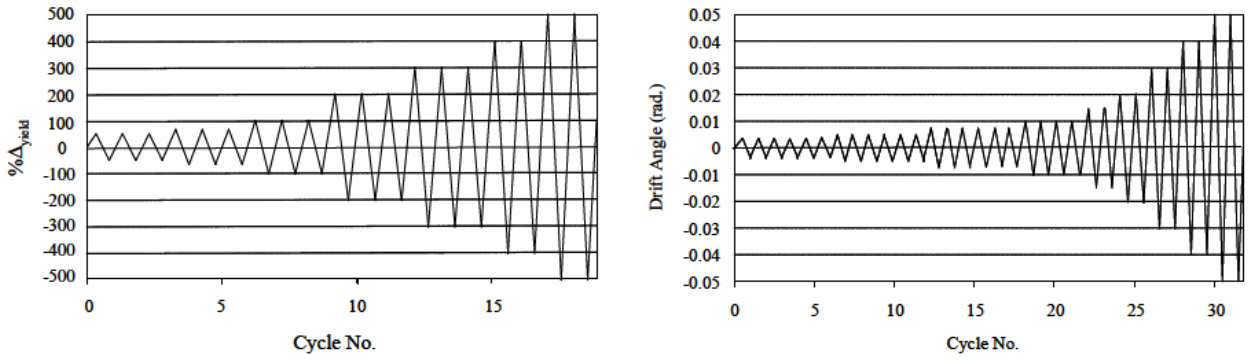

(a) Steel - ATC-24 (ATC-24, 1992)

(b) Steel – SAC (Clark et al., 1997)

Figure 2.2: Typical cyclic loading patterns for testing steel components.

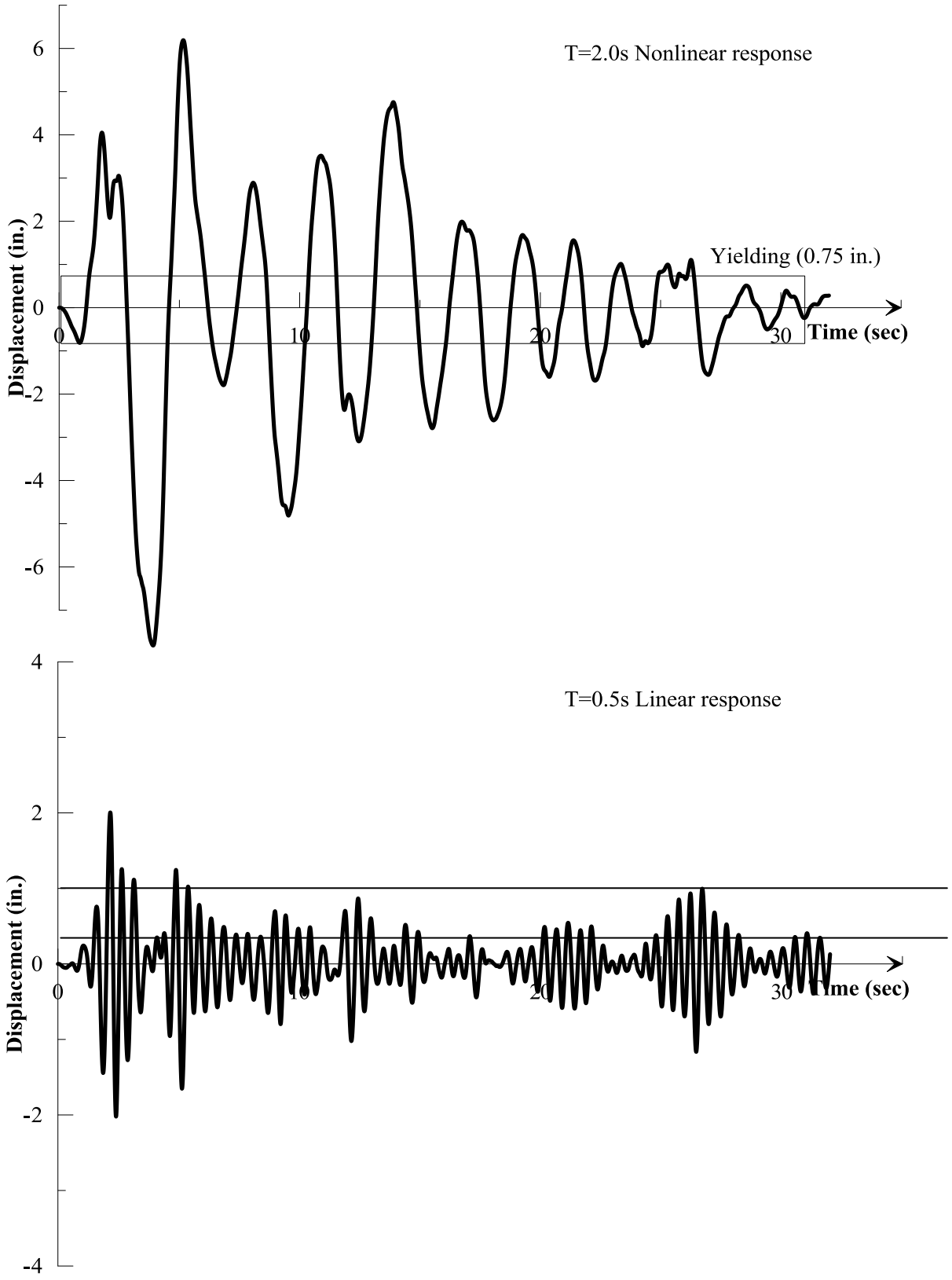

Figure 2.3: Dynamic responses of SDOF systems under El Centro (1940) earthquake.

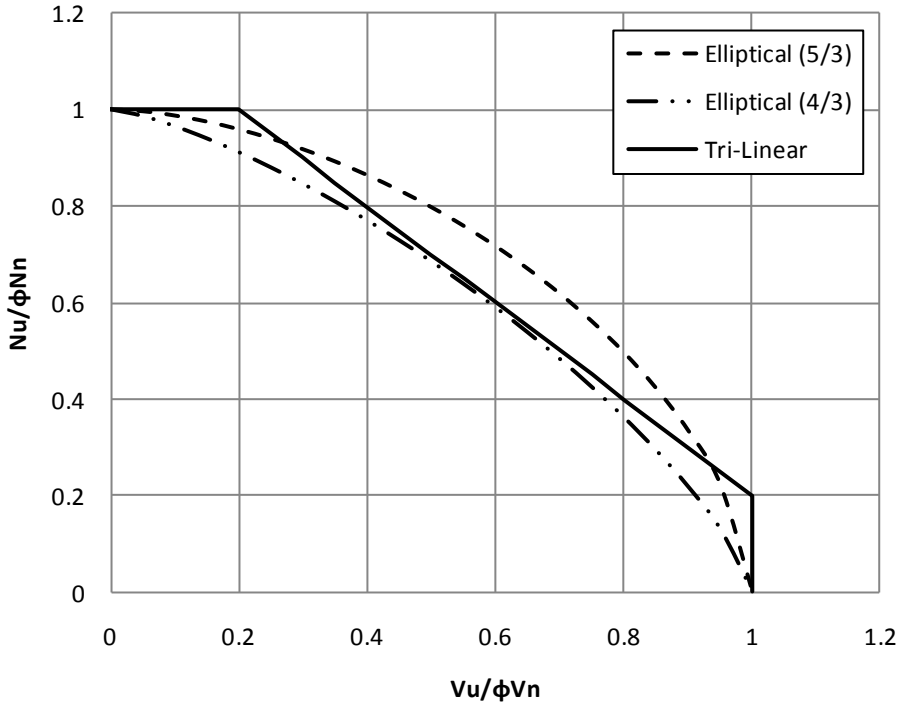

Figure 2.4: Interaction equations used in anchor design

CHAPTER 3 Test Program for Single Anchors in Plain Concrete

3.1 Test Program

The test program for this research was constructed with anchors falling into three geometric categories according to embedment depth, edge distance, and anchor diameter shown in Table 3.1. Embedment depth and edge distance was chosen to observe concrete breakout failure because the cyclic behavior of steel has been addressed in previous literature. Anchors in each of these categories were tested in monotonic shear, cyclic shear, monotonic tension, cyclic tension, and cyclic combined tension-shear loading. By limiting geometric variations, the number of tests was able to be controlled while creating a high degree of comparison across many loading scenarios. In this fashion, the effects of cyclic and combined cyclic loading were able to be directly compared with similar tests conducted within the same testing environment. This chapter will discuss specimen design, setup of the loading frame used for testing, materials used in the specimens, specimen construction, testing equipment and loading protocol, and instrumentation used for measurements

3.2 Specimen Design

The single anchor tests in this study were conducted as full-scale tests. A survey conducted with a number of practicing engineers indicated that the most commonly used cast-in-place anchor bolts range from 0.75 to 1.5 inches in diameter with many applications using 0.75 or 1.0 inch diameter anchors. Hence, 0.75 inch diameter anchors were selected for tests of anchors embedded in plain concrete. Thirteen test blocks (with four anchors on each block) were cast for anchors in plain concrete. The dimensions of the test blocks are shown in Figure 3.1 portrayed in terms of embedment depth (h_{ef}) and edge distance (c_{a1}). Test blocks included four anchors to be tested, six lifting bolts used to transport the test blocks, and a hole between each pair of anchors to be used to restrain the test block using a high strength steel tie-down rod.

The cyclic tests of anchors in plain concrete focused on concrete breakout failure modes with an intention to verify the ACI D.3.3.3 provisions regarding capacity reduction under seismic

loading. The edge distances and embedment depths of anchors were selected to create concrete breakout failure in tension and/or shear. Edge distances of four and six inches in combination with embedment depths of four and six inches were studied for monotonic and cyclic tension, monotonic and cyclic shear, and cyclic combined loading. By retaining the same geometrical properties for monotonic, cyclic, and combined loading tests, maximum cross-comparability between tests was achieved.

Hoehler and Eligehausen (2008), and Klingner (1995) reported that concrete breakout failure cone radii average $2h_{ef}$ and $2c_{a1}$ in tension and shear respectively where h_{ef} denotes the embedment depth of the anchor and c_{a1} is the front edge distance between the anchor and the edge of concrete. Block lengths and anchor spacing were accordingly determined using a concrete failure cone radius $2h_{ef}$ from each anchor plus an additional four inches on the edges of the blocks. For anchors with six inch embedment, 24 inches between anchors and 16 inches of side edge distance were provided. Block widths in the direction of the applied shear load were the resultant of front edge distances and a predetermined distance of 15 inches from the anchors to the center of the test blocks based on geometric restrictions of the loading frame used which is discussed later in this chapter.

The block height was checked for moment capacity based on a 40 kip tension force applied to the anchor. Using the moment arm of 15 inches between the anchor and the tie down rod, the blocks were designed to resist the full applied moment without cracking. Estimating the cracking moment with an assumed concrete strength of 4000 psi and an effective width of 30 inches, the required height of the blocks was calculated as 15.9 inches. After these calculations were performed, a block height of 17 inches was selected providing a cracking moment of 685 k-in, or an approximate applied tensile capacity of 45.7 kips on the anchors.

Many previous tension tests on anchors in the literature were conducted using a self-contained load frame as shown in Figure 3.2. The vertical reaction points, according to Hoehler and Eligehausen (2008) should be placed at a minimum radial distance of $2.5h_{ef}$ from the anchor. However, such surrounding reactions do not exist in field applications of anchor connections shown in Figure 1.l. Laboratory testing environments however are limited by size and cost of specimens making the use of reaction points located close to the tested anchor conducive to both

speed and cost of testing. The locations of the reactions must then be chosen to effectively restrain the test specimen while minimizing effects on the testing area; being the potential concrete breakout cone area for anchor tests. Therefore, in this study, the concrete was held down against the tension forces applied to the anchors during testing using a 1.75-in. diameter tie down rod as shown in Figure 3.3. The tie-down location was 15 inches (equal to $2.5h_{ef}$ for six inch embedment depths) behind the anchor. This setup proved to effectively limit vertical movement of the blocks to less than 0.08 inches under tension loads exceeding 40 kips while minimizing reaction points on the surface of the test block.

For shear, Klingner (1995) suggested that reactions on the test block should be spaced at least $2c_{a1}$ from the anchor shown in Figure 3.4. Clearance limitations through the side of the vertical load frame prevented the use of a self-contained loading system in which the load frame would react against the specimen. The tie-down rod at the center of the block directly behind the test anchor was able to provide some shear resistance, however, due to the restraints that the tie-down rods were not able to be grouted inside the hole in the strong floor through which they passed, the slip of the test block during the reversed cyclic shear loading was inevitable. To minimize the slip of the test block, the specimens were wedged between horizontal beams at their base. Figure 3.5 shows a 4x7x.325 in. HSS section placed on the floor on each side of the specimen bearing against the columns of the vertical load frame. Horizontal braces anchored to the floor on the opposite side of the vertical columns were provided to eliminate any horizontal forces being applied to the vertical loading system. The specimen was then wedged between the HSS sections using shim plates to eliminate horizontal movement of the specimen during shear loading. This method of restraint limited block movement to approximately 0.1 inches under shear loads exceeding 40 kips. The benefit of using this shear reaction system, much the same as for tension, was that the minimized boundary restraints introduced onto the specimen also minimized their affect on the shape of the concrete breakout failure cone.

Block heights were checked for shear loading based in Figure 3.6 using 45 degree stress propagation angle from the HSS shear reaction beam through the test blocks ensuring that the reaction stresses did not intersect the anchors. The most extreme location of anchors proposed for this research of four inch edge distance and six inch embedment was used to determine the required block height of all test specimens.

3.3 Materials for Specimens

The 0.75-inch diameter anchors consisted of F1554 Grade 55 threaded rod and a heavy hex nut tack welded to the base. The F1554 Grade 55 threaded rods had a yield strength of 63 ksi and an ultimate strength of 76 ksi as shown in Figure 3.7.

All concrete specimens used for unreinforced anchor testing were poured at the same time with ready-mixed concrete. Concrete was non-air entrained with a measured air content of 2.3% on the day of pouring and a slump of 3.25 inches. Eighteen 4x8 inch cylinders were cast for testing concrete strengths at various ages throughout testing. All cylinders were kept in their sealed containers for the full 28 days of curing, after which the cylinders were removed and stored at ambient conditions similar to the test specimens. The first strength tests were conducted 56 days after the pour when the first specimen was tested. Subsequent testing resulted in an average concrete strength of 5650 psi for the majority of the specimens.

3.4 Construction of Anchor Specimens

Test blocks were cast with anchors protruding from the bottom of the formwork. This inverted orientation produced a perfect surface finish on the top of the test blocks where the loading plate was placed. The smooth surface around the anchor bolts helped the loading plate rest evenly on the test block. The inverted casting also eliminated any surface obstructions from the open side of the forms while pouring. This improved screeting and troweling efforts and resulted in the best overall surface conditions on all sides of the test blocks. Vertical orientation of the anchors were fixed in the bottom of the formwork through appropriately sized holes drilled into 4x4 blocks that were screwed to the outside of the formwork. This provided two inches of fixity to the anchors protruding out of the concrete test blocks. All anchors were checked for alignment prior to pouring concrete with a T-square. Embedment depth was also checked prior to pouring concrete using a standard template for four and six-inch embedment. The heavy hex nuts used were then tack welded to the anchor rods to prevent any movement while concrete was being poured and compacted. PVC pipes used for the vertical tie down rod were secured in position by a plywood puck cut to the inside diameter of the pipe and bolted to the bottom of the formwork. The free ends of the PVC pipes were tied to temperature and shrinkage reinforcement provided

in the bottom of the test blocks and checked for alignment using a T-square prior to pouring concrete.

Lift bolts measuring 0.375 inches in diameter were secured to the formwork in the same fashion as the anchor bolts. The lift bolts located on the top of the test bocks as shown in Figure 3.1 served a dual purpose: being used to move the block via overhead crane as well as attaching instrumentation for testing as described later in this section. The lift bolts were placed outside a radius of $2.3h_{ef}$ from the anchors so as not to affect the behavior of the breakout cone formed in tension.

After formwork was removed from the test blocks, a thin layer of plaster of paris was applied to assist in identifying concrete cracks during and after testing. The plaster was mixed to a paint-like consistency and applied using a paint brush for even coverage. The thickness of the plaster layer and its contributions to the anchor connection capacity was assumed to be negligible. Chalk lines were also added in a one inch by one inch grid on all surfaces of the test blocks. The chalk lines created a simple measurement system that could easily be seen in pictures for current and future researchers.

3.5 Test Setup

The load frame used to load the test specimens is shown in Figure 3.8. The structure lab at the University of Wisconsin – Milwaukee has a strong floor system with 2.25 inch diameter anchoring holes spaced in a three foot by three foot grid across the testing area. These holes are used to fix test specimens and loading frames securely to the floor. Vertical loading was achieved using an existing test frame at the University of Wisconsin – Milwaukee's structure lab. The frame consisted of four diagonally braced columns spaced 6 feet square tied at the base using W-sections in the direction perpendicular to the applied shear load in this study. This allowed for an unrestricted opening 5 feet 1 inch wide through the load frame perpendicular to the applied shear load. An MTS Model 244.41, 110 kip actuator with a total stroke of 10 inches was suspended from a loading girder at the center of the frame. Height was adjustable by moving the loading girder up and down the columns. The mounting system of the MTS 110-kip vertical actuator to the loading girder was modified to allow adjustability in the direction of the

applied shear by mounting it to a secondary transfer beam which was tied to the loading girder as shown in Figure 3.9 using four one inch diameter dywidag bars.

A braced-column horizontal loading frame was designed specifically for the tests being performed in this research. Holes were drilled in the column at 4.5 inch increments along the height of the column and a transfer block was constructed to provide adjustability in one inch increments for a horizontally mounted MTS Model 244.31, 55-kip actuator with a full stroke of 10 inches. The actuator was braced against the floor at its bearing pad closest to the piston arm. This ensured that the actuator could not be moved downward during shear testing. This prevented the leading edge of the load plate from contacting the front edge of the concrete, hence eliminating any compression induced on the shear breakout cone by the load plate. For monotonic shear loading, the actuator was free to rotate horizontally while during cyclic loading the actuator was restrained using turnbuckles to eliminate the chances of buckling during compression cycles in shear caused by any potential misalignment.

The loading plate fabricated for this research, shown in Figure 3.10, used a modular design to allow the same fixture to be used for both tension and shear loading. The shear plate was one inch thick modeled after a similar load plate used in tests conducted by Klingner et al. (1982). The horizontal actuator was connected to the loading plate with two channels bolted to the top and bottom of the plate using four 0.75 inch diameter ASTM A490 bolts. The shear plate was 12 inches wide to accommodate two 12 inch tall channels that attached to a one inch thick fixture plate for connecting the vertical actuator. For tension tests, the channel module connecting the horizontal actuator was removed for ease of installation during test setup. The 0.75 inch diameter test anchors were inserted through a standard 1/8 inch oversized hole in the load plate and fixed to the loading plate using a heavy hex nut. For each test, a steel sleeve shim was inserted between the anchor and the hole in the load plate. The shim was implemented to reduce the clearance between the anchor and the load plate hole as discussed in Section 4.2. The shims were also useful in preventing damage to the sides of the hole in the load plate when contacted by the higher strength threaded anchor rods during testing.

3.6 Loading Protocol

Tension and shear loading was applied by controlling the displacement of actuator pistons in all tests. Displacement controlled loading has the benefit of allowing the post peak behavior of tests to be captured more accurately than in force controlled loading scenarios. However, cyclic testing provisions for concrete anchors predominantly refer to force-controlled loading. The Structural Engineers Association of Southern California (SEAOSC 1997) standards for cyclic anchor testing employ stepwise increasing load cycles until failure. Loading cycles starting at 25 percent of the anchor's monotonic capacity with increasing step increments of 25 percent until failure occurred was chosen for this study. These provisions were converted in this study to corresponding displacements based on monotonic test results. Programs for individual load types were constructed using the Multi-Purpose Test (MPT) function in the MTS Station manager Version 3.5c. The ability to control the actuators from external inputs was unavailable so programmability was limited to the force and displacement channels of the actuators themselves. For this reason, the actual anchor displacements displayed in the test results later in this report do not match the stated displacement levels used for programming as stated in this section due to test block and frame movements during testing.

Quasi-static loading rates were targeted to avoid the dynamic loading phenomena wherein capacity inflation takes place [Collins, 1988; Hallowell, 1996]. While seismic loading of structures is dynamic in behavior, using quasi-static loading produces conservative capacities which are preferable for the development of design equations. Klingner (2010) suggested that load rates less than 10 mm/min are sufficient in avoiding capacity increase produced by dynamic loading rates.

Monotonic tension and shear tests were conducted first to develop typical load/displacement behaviors of each anchor setup and load direction. Monotonic tension tests used the vertical actuator only, loading as a linear ramp function using a load rate of 1 mm/min. The slow load rate was chosen because relatively small displacements before concrete failure were expected and because it allowed for a greater amount of data to be collected near the peak capacity.

Monotonic shear tests used the vertical actuator to apply a constant small tension force (200 pounds net) to the anchor. This was used to eliminate any friction between the load plate and the

test block during shear tests. The nut fixing the load plate to the anchor was first hand tightened onto the load plate using no tools then loosened 1/8 of a turn to allow slight vertical movement (lifting) of the loading plate when the tension force was applied at the beginning of the test. The horizontal actuator also ran a ramp function with constant displacement rate to apply shear force to the anchors. Initial tests used the same 1 mm/min load rate as the tension tests, however, it was observed that failure displacements were larger in shear and the duration of each test became excessive at a load rate of 1mm/min. The shear load rate was later increased to 2 mm/min with no measured effect on anchor capacity or behavior.

The monotonic test results were then used to develop the displacement intervals of the actuators to be used in cyclic tests as was discussed earlier. Quasi-static cyclic tests at a displacement rate of 2 mm/min cycled the anchors three times at each increasing displacement step as shown in Figure 3.11. Displacement levels were chosen to cycle the anchor at pre-peak, peak, and at least one post peak step. Because of slight variability in monotonic tests however, fixed displacement steps were chosen for tension and for shear and used for all anchors loaded in the respective direction. Shear displacements starting at 2 millimeters increasing at 1 millimeter increments for subsequent cycles were chosen with equal displacements used in cyclic tension. After the post peak cycles were concluded, a monotonic ramp load was used to explore the residual capacity in the connection. For most tests, this monotonic load occurred after the failure of the connection with less than fifty percent of the peak capacity remaining. Ramp or saw tooth loading patterns near the ultimate anchor capacity were determined to be an acceptable model of cyclic loading to create low-cycle fatigue in anchors [Collins et al., 1989]. The simplicity inherent in ramp/saw tooth loading patterns was favorable for the development of the loading profiles developed in the MTS software for this research, especially for combined loading tests.

Displacement-controlled combined loading tests were developed to exhibit pseudo force-controlled loading to match previous combined loading tests in the literature that used force-controlled loading discussed in Chapter 2. Because the current interaction equations such as those in ACI 318-08 D.7 are based on a ratio of applied load to design capacity, the programs for combined loading were designed to follow a similar action. The averages of all cyclic tension and shear tests were used to develop equations for applied force to the anchor as a function of actuator displacement. Cyclic tests results were also used to determine average cyclic tension

and shear capacities for each anchor position to be used in the interaction equations of ACI 318 D.7. Programs for combined loading were then set up to target specific ratios of applied load versus anchor capacity for tension and shear along the interaction curve to generate a moderate spread of data that could be used to verify or disprove the currently used interaction equations.

Peaks of each load cycle in tension and shear were programmed to occur simultaneously. To achieve this, displacement loading rates were calculated and varied for each specific cycle to account for differences in peak displacements of the tension and shear cycles. Generally, tensile actuator displacements were smaller than shear actuator displacements. The displacement loading rates of tension and shear loading were targeted around 2 mm/min with a range between 1 and 3 mm/min. Each cycle was split into four individual ramp components. The first cycle consisted of tension loading and shear loading toward the free edge. The tension load was programmed to reach its target displacement slightly before the shear load reached its peak. The tension load would then hold its displacement until the shear load peaked. This would interrupt the tension hold and both actuators would begin unloading to initial condition. Tension would unload in force control to an end load of 200 pounds tension while shear unloaded in displacement control to zero displacement set at the beginning of the test. Tension would then hold force while the shear load went into compression and back to zero under displacement controlled loading to achieve reversed cyclic shear loading. The process would then repeat itself for each of three successive cycles at each displacement interval.

As tests were performed, a trend developed wherein the anchor would show plastic elongation as cycle displacements grew. Because the vertical actuator was programmed to unload to a 200 pound tension target, the displacement corresponding to this load would stray further and further from initial zero displacement. This caused peak synchronism problems between the two actuators during the test because the vertical actuator was set to load in displacement control to an absolute end level determined as discussed earlier in this section. Because the total piston travel required by the vertical actuator grew smaller as the anchor elongated, the original calculated loading rates became increasingly excessive. The hold function set for the tension peak action alleviated detrimental effects of the unsynchronized loadings by holding the force in tension until the shear toward the free edge could peak, however, in initial tests, the hold time sometimes exceeded 10 seconds when the anchors displayed increasing plastic elongation.

Ultimately, the displacement loading rates of the vertical actuator at each displacement limit cycle were adjusted so that the tension hold time could be limited to a maximum of 5 seconds and in most cases was less than 3 seconds.

3.7 Instrumentation Plan

String pots and linear variable differential transformers (LVDT's) were used to measure the anchor displacements relative to the test block in shear and tension directions respectively. For tension, the high strength tie rod located at the center of the block was used to mount the LVDT's to measure the vertical movement of the load plate relative to the test block. The Trans-tek model 245 DC-DC LVDT's used had a stroke of ± 2 inches with a voltage output of ±10 Volts.

The apparatus shown in Figure 3.12 was attached to the threaded rod and cantilevered into the load plate where the LVDTs were mounted at equal distances of two inches from the anchor in the plane of applied shear load. Using this technique, any vertical movement of the test block was negated leaving only relative vertical movement between the LVDTs and the anchor. Initial tests used a thin (1/8 inch thick) plate that was attached between two nuts on the anchor, on which to rest the vertical LVDTs. This allowed for the tilt of the anchor to be calculated during shear tests. However, during tension tests, it proved to be detrimental because anchor displacements were small for concrete failure modes. The measured tilt of the anchors under tension masked actual vertical movement of the anchors themselves so the small plate was removed and the vertical LVDTs rested on the load plate itself. Because the load plate was assumed to be in contact with the nut located on the anchor at all times, any vertical movement of the load plate was in turn equal to the vertical movement of the anchor. Resting the vertical LVDTs on the load plate eliminated the measurement of anchor tilt, and effectively corrected the accuracy of the vertical anchor displacements.

Horizontal displacements of anchors were measured using three Celesco PT510 DC string pots shown in Figure 3.13. Each string pot has a total stroke of two inches with a voltage output of 0-10 Volts. All three string pots were mounted on a custom made mounting bracket that was in turn suspended on top of the lift bolts provided on the top surface of the test blocks. The

mounting bracket was suspended on the lift bolts using a nut on the top and bottom of the plate and was situated to provide 1/16 inch clearance between the surface of the concrete and the bracket itself to deter interference of horizontal measurements caused by possible contact with concrete tensile breakout cones. Connection of the string pot mounting bracket to the lift bolts provided a secure fastening to the concrete block which allowed for measurements of horizontal anchor movements with respect to the test block to be taken directly through the sting pots.

The middle string pot was attached to the anchor itself to provide a direct measurement of the horizontal displacement of the anchor. However, because it was impossible to locate the point of attachment to the anchor at the surface of the concrete test block, the string pot was ultimately mounted a distance of 1.5 inches above concrete surface for 0.75 inch diameter anchors and two inches above the concrete surface for 1.0 inch diameter anchors. For this reason, the measurements taken from the string pot attached to the anchor contain a combination of the actual horizontal movement of the anchor at the concrete surface as well as some amount of bending displacement at the point of connection. The degree of error for these measurements depends on the hole clearances allowing the anchor to rotate as well as other unforeseen behaviors procured from cyclic shear testing of reinforced anchors discussed later.

Two additional string pots were attached to the load plate itself on the North and South sides of the anchor. Because the load plate acts as a rigid body whose contact with the anchor is responsible for any displacements and imparted loads on the anchor, measurements taken from the load plate can be assumed to be a direct measurement of displacements of the anchor with some exceptions. During testing, a hole clearance was present between the anchor and the load plate. Such clearances produced a lag in displacement measurement between the instances where both the load plate and anchor were moving in unison during cyclic tests. Shim rings were used to surround the anchor which minimized the lag effects with no measurable effect on shear capacity of the anchor. The data from these two string pots was averaged and used to produce all shear load versus displacement graphs displayed in this document.

Two Sensotec spring loaded LVDTs were used to monitor the horizontal and/or vertical displacement of the specimens during testing. The horizontal spring loaded LVDT was positioned on the back side of the test block directly in line with the applied shear load to isolate

any potential rotation of the block. The movement of the horizontal load frame was measured using a dial gauge. Vertical block movements were monitored using a second spring loaded LVDT located at the side edge of the block and oriented equidistant from the loaded edge as the anchor.

3.8 Data Acquisition and Filtering

An IO Tech DaqBook 2000 was used to collect data from all instrumentation as well as force and displacement output channels from the actuators. The DaqBook system was consists of four DBK43A strain gauge modules and a single 16 channel DBK85 module for voltage inputs. The readouts of the DBK43A strain gauge modules were filtered by an internal hardware filter while the DBK85 module does not provide signal filtration. Later a Matlab program was used to filter the obtained data.

The data acquisition system used for this research does not possess a sample and hold function necessary of collecting perfectly time-synchronized data. However, with an inherent physical internal sampling rate of 2 kHz, the lag difference between individual channel recordings was deemed insignificant.

Table 3.1: Phase I testing program (Unreinforced anchors)

h_{ef} - c_{a1}	Loading Type				
	Monotonic Tension	Cyclic Tension	Monotonic Shear	Cyclic Shear	Cyclic Combined
4" – 4"	2	2	2	2 uni-directional	6
				2 FRCS	
6" – 4"	2	2	2	2 uni-directional	5
				2 FRCS	
6" – 6"	1	-	2 w/ shims	2 uni-directional	2
			2 w/o shims	1 FRCS	

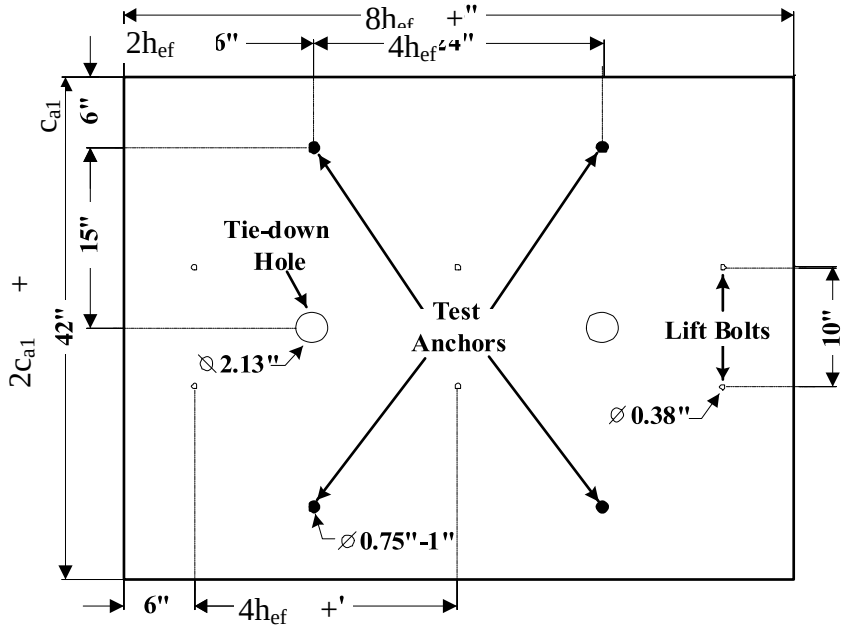

Figure 3.1: Plane view of test specimen containing 4 anchors

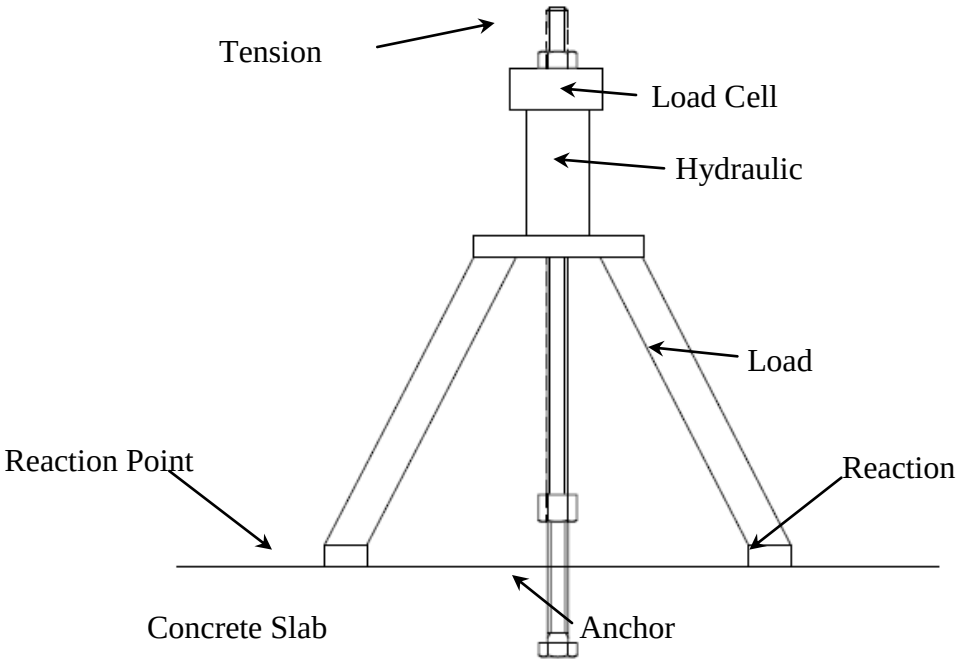

Figure 3.2: Self-contained tension load frame (Hoehler & Eligehausen)

Figure 3.3: Tension restraint mechanism (University of Wisconsin – Milwaukee)

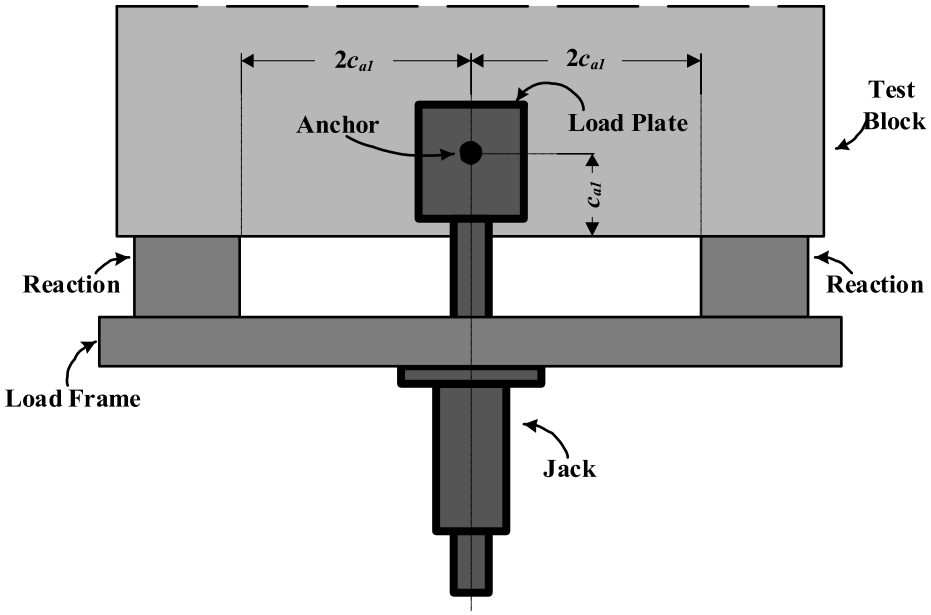

Figure 3.4: Self-contained shear load frame (Klingner)

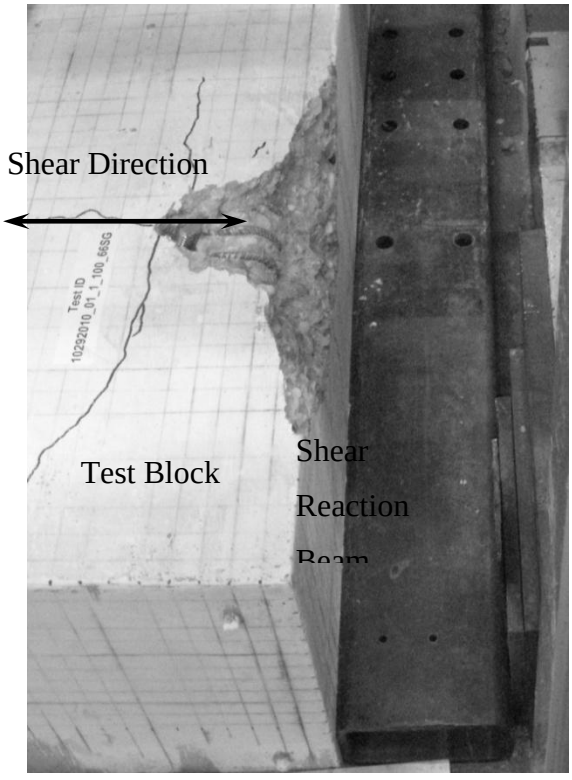

Figure 3.5: Shear restraint mechanism (UWM)

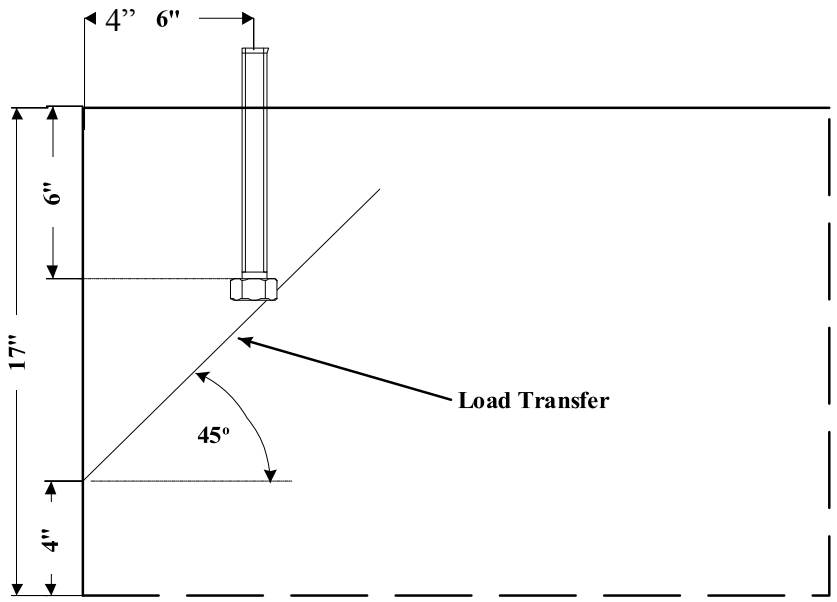

Figure 3.6: Shear reaction stress transfer path

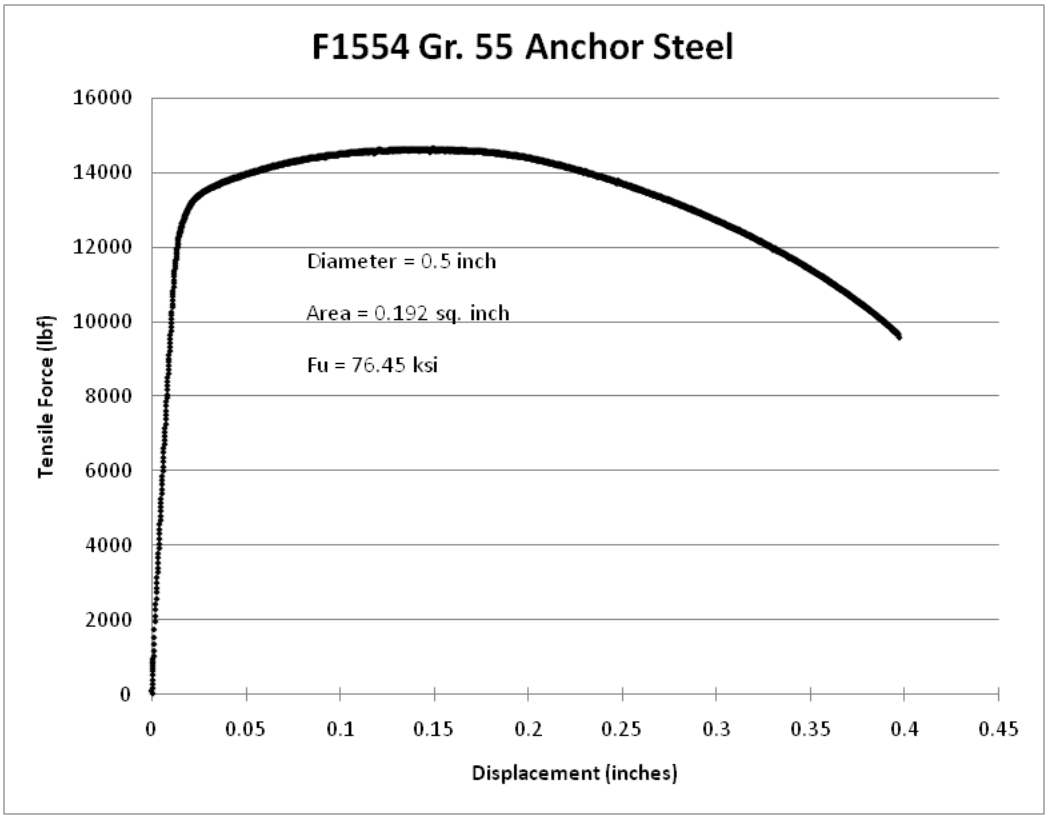

Figure 3.7: Stress-strain behavior of F1554 Grade 50 anchor steel

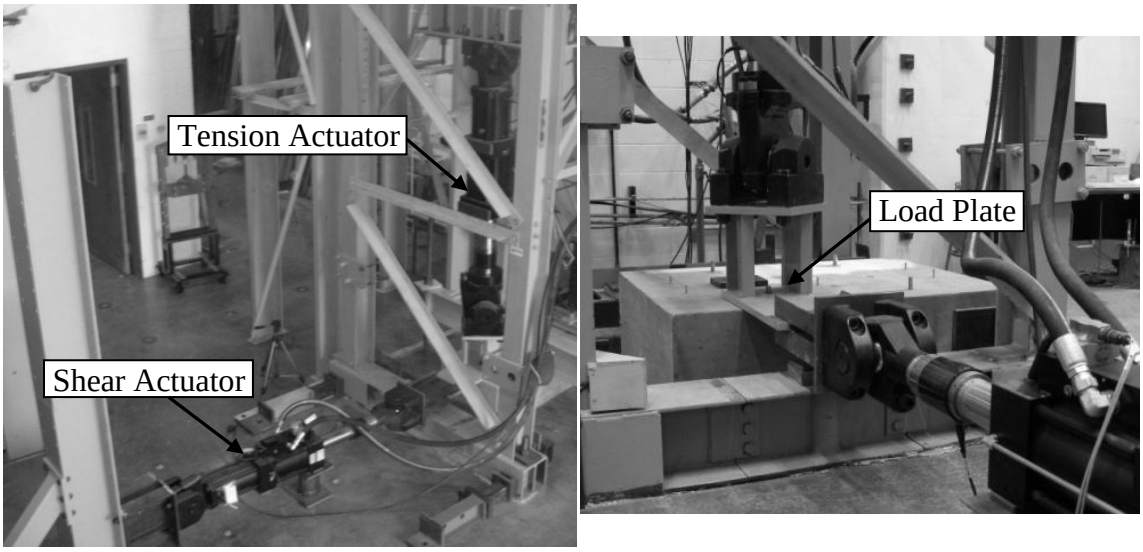

Figure 3.8: Load frame for Phase I tests at UWM

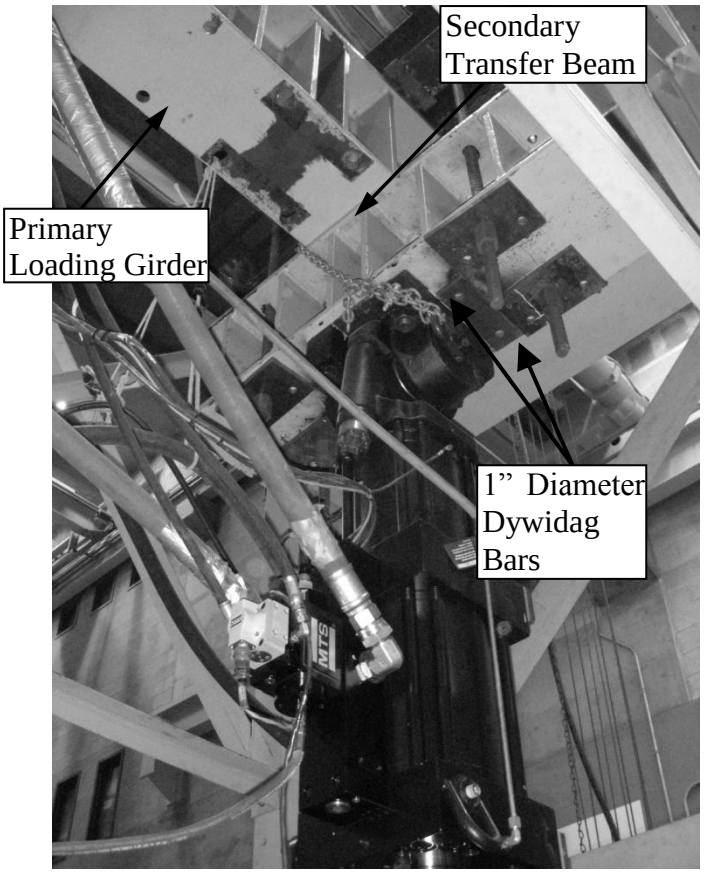

Figure 3.9: Mounting mechanism for tension actuator

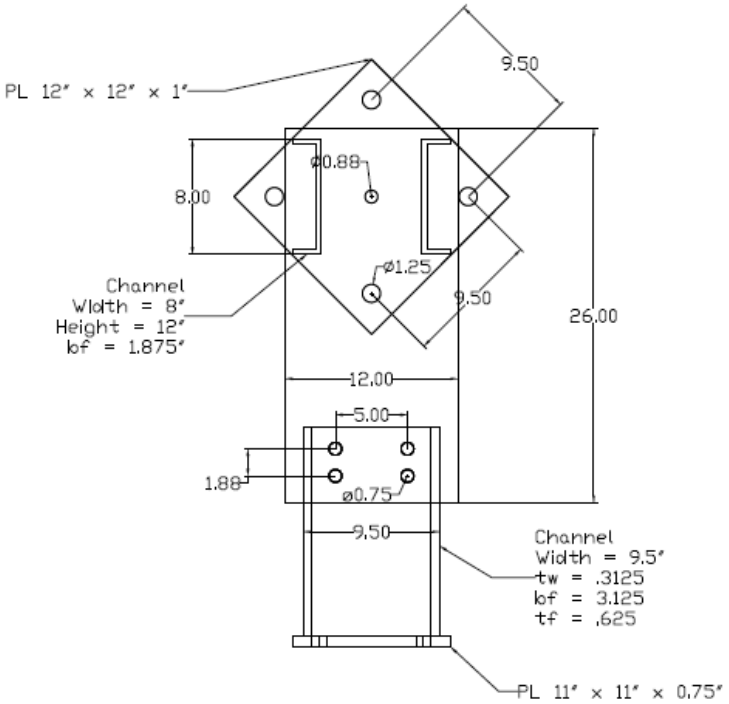

Figure 3.10: Load transfer block between anchor and actuators

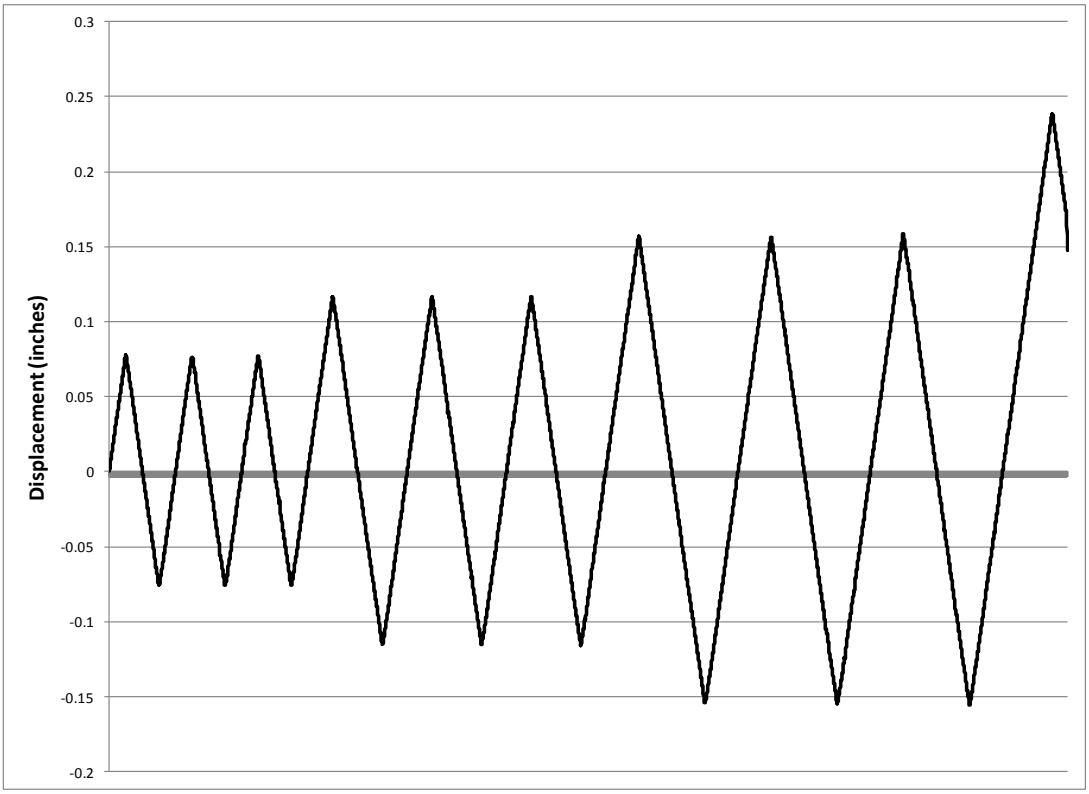

Figure 3.11: Cyclic shear loading profile (Actuator displacement)

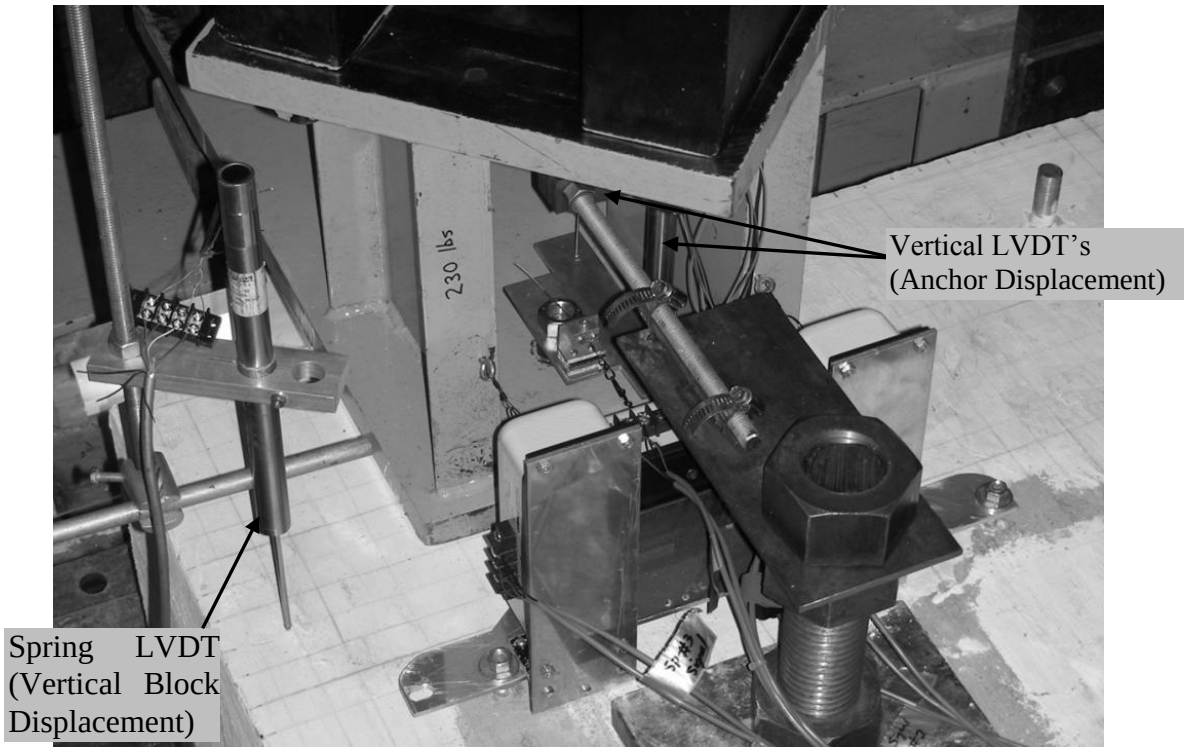

Figure 3.12: Two LVDT's for measuring vertical anchor displacement

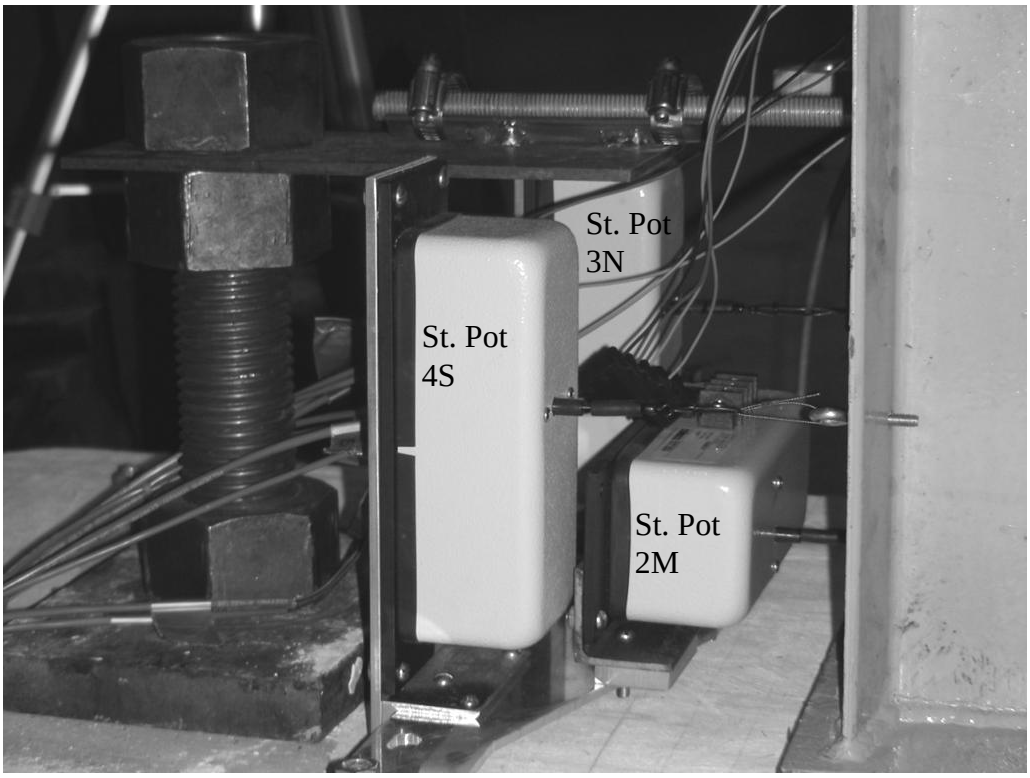

Figure 3.13: Three string pots for measuring horizontal anchor displacement

CHAPTER 4 Test Results of Single Anchors in Plain Concrete

4.1 Introduction

The main goal of Phase I tests was to study the effects of cyclic loading on the behavior of anchor connections focusing on single anchor behavior. Anchor capacity reduction due to cyclic loading in tension and shear, as well as cyclic combined tension-shear loading is addressed in this section. In total, 28 anchors in Table 3.1 were subjected to monotonic or cyclic loading in tension or shear. Table 4.1 shows results from each test including dimensions, concrete strength, loading type and direction, failure load, and mode of failure. The observations from these tests are discussed herein, followed by statistical analysis alongside data collected from the literature. The tension and shear tests from this research were also used in comparing the results of combined tension-shear loading tests. The resulting interaction plot constructed from these test results is also compared to previous literature to verify the currently used interaction equation used in ACI 318-08 Appendix D.

Capacity reduction has been observed in these tests, especially for anchors subjected to shear. Typical failure modes under both monotonic shear and cyclic shear are presented in Figure 1. A detailed analysis of the test data and the collected data from the literature is shown below.

4.2 Anchors in Plain Concrete: Monotonic Shear

Load versus displacement behavior observed in monotonic shear tests are shown in Figures 4.2 through 4.4 for 0.75 inch F1554 Grade 55 anchors having: four inch embedment and four inch edge distance, six inch embedment and four inch edge distance, and six inch embedment and six inch edge distance respectively. Tests having four inch edge distance were controlled by concrete breakout failure, the average capacity recorded from all four tests was 14.5 kips occurring at approximately 0.13 inches displacement with the range between highest and lowest measured capacities being 1.64 kips. Concrete breakout failure was brittle in nature as shown each figure by the sharp loss in capacity after the peak load was reached. Three of the four anchors were not removed from the concrete blocks upon failure as the failure cone typically

propagated 3.5 inches down the face of the anchor shaft before angling toward the front face of the test block as shown in Figure 4.5. The remaining concrete allowed the anchors to retain some level of shear capacity, typically in the range of two to three kips after concrete breakout failure occurred as shown at the end of the load-displacement curves of Figures 4.2 and 4.3. The reserve capacity measured was the bending capacity of the anchors and is larger for anchors where a longer portion of the anchor remained unexposed after the concrete breakout cone formed.

Anchors having six inch edge distance exhibited anchor steel failure exclusively. Two tests were conducted using shims and two were tested without shims. In Figure 4.4, the tests with shims are displayed as solid lines while the tests without shims are displayed as dotted lines. The average capacity with and without shims were similar being 16.7 kips. Anchors having shims generally underwent larger displacement at peak load (0.27 inches) than anchors without shims (0.22 inches) Average capacity of tests using shims was 420 pounds higher than tests without shims showing that: using shims to decrease the size of the hole in the loading plate had a small effect on anchor steel capacity.

4.2.1 Effect of Hole Clearance

Four single anchors with six inch embedment and six in edge distance were tested in monotonic shear to study varying hole clearances on shear load capacity by including or omitting the steel shim sleeve used for testing. During these tests vertical LVDT's were placed on the instrumentation plate above the loaded hex nut spaced 2.5 inches from the anchor in the plane of the shear load as shown in Figure 3.12. The measurements of the LVDT's were used to determine the maximum angle of the anchor during each test. For two tests with no shims (0.125 inch hole clearance), the angle of the anchor was measured as 3.2 degrees and 2 degrees. Two tests with shims (0.05 inch hole clearance) produced anchor tilt angles of 2 degrees and 2.77 degrees. Test data showed that the hole clearance had negligible effect on the angle of anchor tilt or the shear capacity. Because of this observation, all anchors having test ID dates after August 2010 used thicker shims reducing the hole clearance to 0.01 inches to improve system responsiveness for cyclic shear tests in particular. As discussed in Section 3.7, displacement measurements taken from the loading plate are assumed to best represent the displacement of the anchor at the surface of the test block. By reducing the hole clearance between the anchor and

the loading plate, displacement in the load plate at reversals in shear load direction before re-engaging the anchor could also be reduced. The displacement of the load plate is reported for all load versus displacement graphs given in the remainder of this document.

4.2.2 Concrete Breakout Cone Size

The loading frame and restraint system in Section 3.5 used for shear tests created very minimal effects on the size and shape of the concrete breakout cone. Because of this, cone sizes in shear were observed to be much larger than predicted using the 35 degree cone method. As discussed in Section 3.2 the test blocks were designed using an assumed failure cone measuring 2ca1 on each side of the anchor. Measured cone sizes for anchors having four inch edge distance ranged from 3 - 3.75c_{a1} under monotonic shear and 2 - 3.25c_{a1} under cyclic shear loading. Also, reversed cyclic shear produced smaller breakout cones than uni-directional cyclic shear, and the size of the shear cone toward the outside of the test block was oftentimes limited by the side edge of 3c_{a1} for anchors with four inch front edge distance . Because spacing between anchors on each side of the test blocks was only 4c_{a1}, some of the larger breakout cones of the first tested anchors interfered with the size of the failure cone for the second tested anchor on the same side of the test block; however, there was no significant effect on the shear capacity of the second anchor. This phenomena was accompanied by an observation that there were commonly two apparent angles in each shear breakout cone as shown in Figure 4.5. The first angle measured very near the 35 degrees used in the code, propagated approximately 2/3 c_{a1} from the anchor toward the loaded edge of the concrete specimen, after which a noticeably flatter angle protruded the remaining distance to the edge significantly enlarging the total dimensions of the failure cone. The inner 35 degree failure cone of anchors that were "affected" by previous tests was never observed to be reduced in any way by the previous cone formation. From this observation, it can be concluded that although the actual measured size of the failure cone formed in shear may be much larger than the 1.5c_{a1} radius used in the ACI 318 code, it is this smaller cone that is responsible for the majority of the concrete breakout capacity.

4.2.3 Statistical Analysis: Monotonic Shear

An extensive collection of literature data was obtained from 15 sources as listed in Table 4.2 along with the number of tests from each source. In total, 278 sets of test data were collected when examining the monotonic shear behavior of headed steel anchors. The data was collected

for cast-in-place anchor bolts and headed studs despite the large data body existing for post-installed anchors since this research was aimed at the behavior of cast-in-place anchors only. The collected data focuses on two failure modes of anchors under shear loading: concrete breakout failure when the anchor is embedded close to an edge; and anchor steel failure when the anchor is embedded away from an edge. Tests related to group anchors, pryout failures (in which the anchor/stud has small embedment depth), anchor bolts in lightweight concrete, anchors experiencing steel failure of the anchor shaft, and reinforced shear tests were removed leaving 155 tests controlled by concrete breakout failure. Existing data was used to statistically analyze the fit of the concrete breakout capacity equation used to design cast-in-place concrete anchors.

The general form of the design formulas used to compute the nominal strength of an individual anchor controlled by concrete breakout failure as provided by ACI 318-08 is:

$$V_b = 7 * \left(\frac{l_e}{d_a}\right)^{0.2} * \sqrt{d_a} * \sqrt{f'_c} * (c_{a1})^{1.5} \quad (4.1)$$

where: d_a represents the anchor shaft diameter, l_e is load bearing length of the anchor for shear, which is equal to h_{ef} for anchors having constant stiffness over the full length of the embedded section, f_c' is the concrete compressive strength (psi), and c_{a1} is the front edge distance measured from the axis of the anchor to the edge of concrete.

The equations for anchor capacity are based on the 5% fractile; that is, the formulas are developed such that there is a 90% confidence level that over 95% of failures will occur above the calculated limit state value for an individual anchor. The ACI 318-08 D.1 calculates the five percent fractile values using the equation: $\bar{x} - K_{05}S$,, where $\bar{x}$ is the sample mean, S is the sample standard deviation, and K_{05} is a coefficient relating to prediction interval statistics that is dependent on the number of samples (n). The ACI 318 code gives values for K_{05} as: 1.645 for n = ∞, 2.010 for n = 40, and 2.568 for n = 10.

The determination of K-factor in the ACI 318 code is related to student t-distribution,

$$K = t_{\alpha,n-1}\sqrt{1 + \frac{1}{n}} \quad (4.2)$$

where n is the sample size (the number of tests), and $t_{\alpha,n-1}$ is the 100α-percentile values for student t-distribution with n-1 degrees of freedom as shown in the following table.

n	1	5	10	20	40	50	100	200	400	500	1000	2000	∞
K_{05}-value	8.929	2.335	1.922	1.772	1.718	1.701	1.672	1.664	1.652	1.651	1.649	1.646	1.645

As the number of samples increase, the 100α-percentile values for student t-distribution with n-1 degrees of freedom approaches the 100α-percentile values for a normal distribution. Comparing the few values for K_{05} in the ACI 318 code being larger than the values determining K_{05} for a normal distribution in the following table, it is possible that the ACI 318 code may be assuming log-normal distribution; however, it is unclear if this assumption is true. For this study, the data will be assumed to follow normal distribution characteristics.

The obtained shear load capacities from this research were plotted alongside existing data shown in Figure 4.7 to display good correlation in which measured shear capacities divided by the ACI 318-08 D.6.2 predicted capacities of all collected cast-in-place anchors undergoing concrete breakout failure in shear are plotted with front edge distance increasing along the horizontal axis. The plot shows that the ACI 318 code equation is conservative for much of test data collected from the literature with 28 of the 155 data points falling below 1.0 being the code predicted capacity. However, the 28 tests falling below the ACI 318 predicted values make up 18 percent of the total data set.

The coefficient used to calculate the concrete breakout capacity V_b in the code was plotted versus the provided shear cone area A_{vc} in Figure 4.8 to explore the validity of the coefficient in relation to cast-in-place anchors. The hysteretic distribution of the collected data from the literature plotted in Figure 4.9 with an overlaid normal distribution curve shows that the literature data exhibits a large amount of variability. It is apparent that the standard deviation of historical shear tests is large, making the statistical calculation of the coefficient for shear breakout capacity using all data points inaccurate. Therefore, it is necessary to attempt to eliminate outlier data from the sample to achieve a more accurate analysis. Of the 155 collected data points collected, 5 were removed as statistical outliers defined by the interquartile range defined as follows:

$$\text{Lower Limit} = Q_1 - 1.5 * IQR \tag{4.3}$$

$$\text{Upper Limit} = Q_3 - 1.5 * IQR \quad (4.4)$$

where: Q_1 represents the first quartile range being the median of the data that lies below the median of the entire data set, Q_3 being the third quartile as the median of the data that lies above the median of the entire data set, and IQR is the inter-quartile range = $Q_3 - Q_1$.

The ACI 318 code specifies a coefficient of 7.0 for cast in place anchors bolted to a base plate and 8.0 for anchors welded to the plate. The average value of the coefficient for V_b is calculated as 9.49 with a standard deviation of 2.76 excluding outliers. Using the equation $\bar{x} - K_{05}S$ with K_{05} interpolated as 1.668 for a sample number of 150, the coefficient used in the calculation of the basic breakout strength in shear (V_b) can statistically be taken as 4.89. Therefore, it is apparent that additional data treatment is needed to eliminate outliers based on testing methods as well in order to procure a data sample with less variability.

4.3 Anchors in Plain Concrete: Cyclic Shear

Under cyclic shear, the ultimate capacity of the anchors was not significantly reduced compared to the monotonically loaded anchors as shown in Figures 4.10 through 4.12 which compare the load-displacement behavior of anchors loaded in cyclic shear. Cyclic tests are shown in solid lines and monotonic tests are shown in dashed lines. Each anchor placement scenario contained two cyclic tests where anchors were loaded with cyclic displacements toward the shear edge only and two tests where anchors were subject to fully reversed cyclic displacements. In general, fully reversed loading caused only slightly lower capacities compared to uni-directional cyclic loading in tests controlled by concrete breakout failure. For all concrete breakout failure tests, the capacity decrease due to cyclic shear loading is minimal if not nonexistent as shown in Table 4.1. For anchors having six inch edge distance and anchor steel failure, the uni-directional cyclic capacity reduction averaged only 2 percent whereas a single fully reversed cyclic test showed nearly 8 percent reduction from the monotonic average capacity.

As discussed in Section 2.1, it is commonly recognized that cyclic loading and low cycle fatigue has a negative effect on anchor connection capacity. The fatigue of materials stems from the process of load reversal occurring in cyclic loading which causes increased damage at the material level with each subsequent load cycle. Under low cycle fatigue loading, materials are

subject plastic deformation reversals and in turn endure a lower number of loading cycles before failure compared to high cycle fatigue when load reversals are within the elastic range. The load reversal effect (i.e. tension/compression) exists in all materials, including concrete. Cyclic shear results from this study showed that for tests that were controlled by concrete failure; the cyclic capacity reduction was much smaller than for those where steel failure occurred. On average, cyclic shear loading caused less than 3 percent capacity reduction for concrete failures but 8 percent reduction for steel failure. When cyclic shear is applied to anchors, the concrete failure cone area undergoes cycling in tension (loading toward the free edge) only. It is currently believed that the anchor head loads the failure cone in compression cycles (loading away from the edge) by developing a pivot point located near the surface of the concrete. While this theory is sensible, the actual load that the head of the anchor applies to the concrete cone during compression cycles has never been measured. The slenderness of the anchor also needs to be taken into consideration here. For two anchors of equal diameters, by the general definition of a lever, the anchor with smaller embedment would impart a larger force on the concrete cone during compression cycles and in turn the capacity reduction would be inversely related to the ratio of embedment depth to anchor diameter. For cases where the embedment depth to anchor diameter is smaller, the capacity reduction under fully reversed cyclic shear would be greater.

4.4 Anchors in Plain Concrete: Monotonic Tension

Load versus displacement behaviors of monotonic tension tests are given in Figure 4.13 for 0.75 inch F1554 Gr. 55 anchors having four inch embedment and four inch edge distance, six inch embedment and four inch edge distance, and six inch embedment and six inch edge distance. Tests having four inch edge distance were controlled by concrete breakout failure. Of those tests, anchors having four inch embedment underwent concrete breakout failure in tension before significant yielding of the anchor took place. Average tensile capacities for anchors with four inch embedment and four inch edge distance was 20.44 kips. Anchors with four inch edge distance but six inch embedment showed some measures of anchor steel yielding before concrete breakout failure occurred in Figure 4.13. Average capacity for anchors with six inch embedment and four inch edge distance was 26.75 kips.

Only one anchor was tested with six inch edge distance exhibiting anchor steel failure exclusively at 28.37 kips of load. Although the ACI 318 code predicts concrete breakout capacity of these anchors to be 24.86 kips, concrete breakout failure was also observed in preliminary tests with anchors embedded six inches with six inch edge distance using higher strength steel. The test showed only minimal concrete cracking in Figure 4.14a, most likely the product of localized concrete spalling near the surface of the concrete due to anchor elongation displayed in Figure 4.14b with fully formed concrete spalling. Because the scope of this research was to study the concrete breakout capacity of anchored connections, no additional monotonic or cyclic tension tests were conducted for unreinforced anchors having six inches embedment and six inches edge distance.

4.4.1 Concrete Breakout Cone Size

Load frame reaction effects on the concrete breakout cone size and shape were also small for tension loading. In tension, the block was restrained with a 6 x 8 x 1 inch rectangular plate washer and tie rod located in the center of the block 15 inches behind the tested anchors as detailed in Section 3.2. For tension, similar observations regarding larger than predicted breakout failure cones were made as well. Cone radii for anchors having four inches of embedment measured 4hef and for anchors having six inches of embedment measured an average of $4.33h_{ef}$. Again, with $4h_{ef}$ spacing provided between anchors on the test blocks, in some cases the large failure cone from the first tested anchor intersected a large portion of the assumed failure cone of the second anchor as shown in Figure 4.15. The depth of the failure cone overlapping the 35 degree failure cone of the second anchor was less than two inches for all locations. However, even with the effective embedment depth of the second anchor reduced in approximately a quarter of the area of the 35 degree failure cone shown in Figure 4.15, the difference in capacity was typically less than 1 kip with only the most extremely effected test showing a capacity decrease of 3 kips or 11 percent .

Flattening of the failure cone angle for tension tests was similar to the observations made in shear loading as in Figure 4.16. The flattening of the failure cone angle typically occurred approximately $1/3h_{ef}$ from the surface of the concrete. Also, the failure cone angle toward the front edge distance of four inches was observed to be nearly flat, rising less than one inch from the anchor head to the front edge. The failure cone angle toward the tie rod restraint retained a

constant angle all the way to the concrete surface of approximately 26 degrees or $2h_{ef}$. Lee et al. (2007) discovered that anchors having shallower embedment depth subject to tension loading produce a flatter angled concrete breakout failure cone than anchors having larger embedment depths. This observation could also be used to predict that with decreasing edge distances, the angle of the tensile breakout cone would also decrease; and for edge distances less than a certain limit the breakout failure cone angle may become zero.

4.4.2 Statistical Analysis: Monotonic Tension

A collection of literature data was obtained from 20 sources listed in Table 4.3 along with the number of tests from each source. In total, 599 tests were considered when examining the monotonic tension behavior of headed steel anchors. Anchors having embedment depth less than 1.5 inches and edge distance less than three inches were removed from the data set along with reinforced tests and anchor tests in lightweight concrete to leave a data set representing concrete breakout failure of cast-in-place anchors in typical installations consisting of 415 samples. This data was used to statistically analyze the fit of the concrete breakout capacity equation used to design cast-in-place concrete anchors loaded in tension.

Basic tensile breakout capacity of concrete anchors unaffected by edge distance limitations and cracking in concrete is calculated in the ACI 318 code as follows:

$$N_b = k_c * \sqrt{f'_c} * \left(h_{ef}\right)^{1.5} \tag{4.5}$$

where: k_c = 24 for cast-in-place anchors in cracked concrete, f'_c is the concrete compressive strength (psi), and h_{ef} is the effective embedment depth of the anchor typically being measured from the concrete surface to the point at which bearing stresses are developed at the head of the anchor. The basic tensile breakout capacity (N_b) can be multiplied by 1.25 for cast-in-place anchors used where no concrete cracking is ensured before loading. If the k_c variable is multiplied by the uncracked concrete factor, a value of 30 is produced.

Figure 4.17 plots the measured tensile capacities from the literature divided by the ACI 318 predicted capacities of cast-in-place anchors undergoing concrete breakout failure in tension. The database was organized so that embedment depths increase along the horizontal axis of the plot. The figure was plotted without eliminating any outliers and shows that the ACI 318 code

equation is conservative for nearly all test data collected from the literature with only 11 of the 415 data points falling below 1.0 being the code predicted capacity.

Figure 4.18 plots the "k_c" factor solved for every sample versus the available concrete shear cone area (A_{nc}). Because not all collected data provided sufficient concrete dimensions to allow a full 35 degree breakout cone to form (A_{nco}) in shear, plotting k_c versus A_{nc} effectively normalizes all data regardless of whether a full concrete breakout cone was formed or not. Plotting the existing data in this fashion shows that the value k_c is independent of A_{nc} and as a result, independent of embedment depth. Again, without eliminating any outliers, the values of kc were calculated from the collected literature with an average 39.68 with a standard deviation of 7.97. The five percent fractile K_{05} = 1.652 given in Section 4.2.3 for 400 sample size to calculate the constant kc in the basic concrete breakout capacity by taking: $k_c = \bar{x} - K_{05}S,$, gives k_c = 26.5. Considering statistical outliers as in Section 4.2.3, 40 of the 415 collected data points are removed from the data set, keeping all data for $24.61 \leq k_c \leq 53.76$, the five percent fractile k_c value increases to 29.58 in good agreement with the ACI 318-08 code using $1.25(k_c) = 30$ for cast-in-place anchors in uncracked concrete. Figure 4.19 shows the hysteretic distribution of test data collected from the literature fitting closer to lognormal distribution but with acceptable normal distribution correlation as well.

4.5 Anchors in Plain Concrete: Cyclic Tension

It is observed in the literature that the tension capacity of anchors is less affected by cyclic loading than shear [Hoehler, 2006; Hasselwander et al., 1974; Klingner et al., 1982; Civjan and Singh, 2003]. In this study, the average reduction in tensile breakout capacity of anchors subjected to cyclic loading was 11 percent for anchors having four inch embedment and a maximum of 4 percent for anchors having six inch embedment. Anchors with six inch embedment and four inch edge distance in Figure 4.20 exhibited steel failure under cyclic tension loading whereas concrete breakout failure was observed for monotonic tension tests. Because those anchors nearly reached the calculated anchor steel capacity under monotonic tension loading, it can be concluded that the cyclic capacity reduction for steel failure in tension is approximately 4 percent.

The cause of the relatively small capacity reductions is due in part that under cyclic tension loading of cast-in-place anchors, the anchor could not undergo load reversal. Because anchors were bolted on top of the loading plate, any applied axial compression forces would thus be transferred directly to the concrete block and a zero net force would exist in the anchors themselves. When the anchors are only loaded in one direction, material fatigue caused by load reversal is avoided and the material destruction and subsequent cyclic capacity reduction is greatly reduced.

4.6 Anchors in Plain Concrete: Cyclic Combined Loading

As discussed in Section 3.6, displacement controlled loading was used to test anchors in cyclic combined tension-shear loading. Because displacement loading was used however, the exact load values of each cycle between various tests were not able to be controlled with a great degree of accuracy. This produced an anticipated scatter of applied tension and shear loads in each test that was beneficial in spreading collected data throughout the tension shear interaction range. Because the ACI 318 code predictions for seismic shear and tension consistently underestimated the average measured capacities in studies, the interaction plot in Figure 4.21 was developed using the individual cyclic tension and cyclic shear capacities measured from this research as the ultimate capacities of tension and shear capacities of the connection. Using the tested cyclic capacities allowed researchers to evaluate an interaction situation where the code would predict the exact cyclic capacity of the connection in cyclic shear and tension. This capacity would correspond to the five percentile capacity of all currently available test data upon which the code equations are based. In this case, the tri-linear interaction equation of ACI 318-08 D.7.3 showed good fit to the test data. Plotted interaction values for anchors with four inch embedment and edge distance following the tri-linear interaction model ranged from 1.11 to 1.43 with an average of 1.23, and interaction values for anchors with six inch embedment and four inch edge distance ranged from 1.13 to 1.31 with an average of 1.2. Using the code equation for the nominal capacity of the anchor produces an interaction equation as shown in Figure 4.22 where an average safety factor of 1.7 is provided. Combined loading interaction curves are also given from Eligehausen et al. (2006), Anderson and Meinheit (2006), as well as Lotze and Klingner

(1997) in Figures 4.23, 4.24, and 4.25 respectively. Those plots are in close agreement with the interaction plot procured from this research shown in Figure 4.26 with all combined loading test data from the literature and this study shown. Considering these observations, it can be concluded that the current design equations for concrete breakout capacity in tension and shear paired with the tri-linear interaction equation given in ACI 318-08 can safely predict the interaction behavior of anchor connections subject to cyclic combined tension and shear loading.

4.6.1 Failure Behavior

For combined loading, regardless of the ratio of the applied shear versus tension, concrete failure in shear occurred first for every test. This trend was especially pronounced for test data in the upper left corner of the interaction plot in Figure 4.21 where applied shear load was a relatively small percentage of the ultimate shear capacity, hinting that concrete breakout failure in shear is much more sensitive to combined loading than tension. For one test in Figure 4.27, the program was allowed to continue running even after peak shear capacity had been achieved. With the shear breakout cone formed, the anchor was still able to achieve 87 percent of the predicted cyclic tensile capacity, however, the total tension-shear interaction value given by: $\frac{N_u}{N_n} + \frac{V_u}{V_n}$ was similar for both points.

This behavior can be reasonably explained by the method in which the concrete cone is formed in tension and shear. Tension breakout cone cracking forms at the head of the anchor whereas the load is applied at the surface of the concrete. A transfer of tensile forces from the nut on the base plate down to the head of the anchor inside the concrete is needed to produce such behavior. As tension is applied, the anchor begins to elongate through the base plate and slightly into the concrete itself. The concrete acts to restrain the force transfer through the anchor and reduces anchor elongation with increasing depth until the force ultimately reaches the head of the anchor. As more force is applied, the anchor elongation increases above and below the concrete surface.

This process can be verified simply by reviewing anchor steel failures under tension loading as in Figure 4.14 for anchors with six inch embedment and four inch edge distance in which concrete breakout and ultimate anchor steel capacity were nearly equal. The small amount of concrete failure, perhaps better termed spalling, is produced by the anchor elongating inside the concrete causing the brittle concrete to crack. As the tensile force in the anchor exceeds the yield

strength, plastic deformation allows increasingly large elongation of the anchor with little increase in capacity. However, even for anchors loaded in tension below their yield strength, elongation is present.

In shear, it is well established that the concrete failure cone develops at the concrete surface in front of the anchor where greatest force concentration is located. For reversed cyclic tests, the surface of the concrete behind the anchor is also damaged in compression cycles. By combining the failure patterns of both tension and shear, the critical effect of tension loading can be seen. With both tension and shear loading being applied to the anchor, shear forces are producing a crack in the horizontal direction at the surface of the concrete while elongation of the anchor in tension is producing additional damage at the concrete surface in the formation of concrete spalling around the anchor. As a result, both tension and shear forces are producing damage at the concrete surface. With relatively high tension loads and low shear loads under combined loading, it could be assumed that tension cracks concrete with anchor elongation, and shear forces act to increase the propagation of such cracks. As the shear failure plane travels further down into the concrete, the depth at which the tension forces cause anchor steel elongation also increases, hence a continually destructive system of combined loading forces is created. The graph in Figure 4.28 compares vertical displacements of anchors loaded in tension only with vertical displacements of anchors under combined shear. The increase in displacement "ductility" can be accredited largely to the aforementioned cracking behavior.

4.7 Seismic Reduction Factors

Cyclic loading introduces additional uncertainties to the behavior of anchors controlled by concrete breakout. The uncertainties are likely related to the propagation of breakout cracks in concrete. In addition, concrete crushing under cyclic loading also changes the stress states in the anchor shaft subjected to shear. These additional uncertainties often time lead to a reduction in the ultimate capacities of anchors subjected to cyclic loading. Because the design of anchor connections is based on their ultimate capacity, the cyclic load induced capacity reduction must be considered in seismic design.

The cyclic tests of anchors in the literature (18 sources in total) can be categorized into load-controlled tests and displacement-controlled tests as shown in Table 4.4. Note that there are a large amount of tests that utilized fatigue-type of loading (i.e., loading cycles of constant loads/displacements as illustrated in Figures 3.1a and 3.1d). However theses tests are not included in the data analysis because such cyclic loading was deemed different from earthquake-induced loading. Only tests with stepwise increasing loading (Figures 3.1b and 3.1e) are included in the data analysis. In addition, direct comparison of the collected cyclic tests with monotonic tests in Figures 4.17 and 4.18 (also listed in Appendix A and Appendix B) is not practical because the cyclic data is much less than the monotonic data, and the tests are from many different laboratories with various original intended research goals. Instead corresponding monotonic test(s) were identified for all the collected cyclic tests, and the ratios of the reported ultimate cyclic loads to the average of the corresponding monotonic loads are analyzed in Figures 4.29 and 4.30.

4.7.1 Anchors Subjected to Cyclic Shear

The collected tests were divided into two groups depending upon their reported failure modes as shown in Figure 4.29. Most of these tests with stepwise increasing loading had load levels close to the ultimate load except those from Swirsky et al.,(1978) the cyclic load levels of which varied from 50% to 90% of the ultimate loads. The collected data includes those with reported concrete failure in pushout tests characterized as concrete crushing in front of the studs and/or concrete pryout. In addition, anchors in the tests reported by DeRenzis et al. (2010) were subjected to shear parallel to the free edge. The anchors were placed with very small edge distances (e.g., 1.75 in.), and most tests stopped because concrete broke out towards the free edge, which is perpendicular to the shear direction. These shear tests (No. 23 through No. 54 in Figure 4.29a) are included because they provided information on the impact of cyclic loads on concrete failure: smaller cyclic loads are needed to cause concrete breakout. Load controlled tests by Nakashima (1999, 200) showed an opposite trend. A closer look at the tests indicates that the anchors were placed in specimens simulating columns, in which stirrups were provided. Concrete breakout may have been affected by the stirrups. Despite the limited number of tests available, capacity reduction for anchors under cyclic shear loading controlled by concrete breakout failure is obvious as shown in Figure 4.29. The average ratio of cyclic capacities vs. monotonic capacities

is 0.87 and the ratio drops to 0.83 if load controlled tests are excluded. The lower ratio is partly due to a reported abnormal test (with a ratio of 0.59) by Hawkins and Mitchell (1984).

For anchors controlled by steel failure in shear, almost all tests showed outstanding capacity reductions. The steel capacity reduction is largely related to the complex stress states in the anchor shaft: concrete crushes around the anchor in shear, and the damage to concrete can be more severe under cyclic loads. Deeper concrete crush leads to a larger exposed anchor shaft (a larger bending moment) and a smaller anchor shear capacity. In addition, load-controlled tests in general showed larger capacity reduction than the displacement-controlled tests. This is in line with the observation by Hawkins and Mitchell (1984) that load-controlled loading is more severe type seismic loading. The larger capacity drops in load-controlled tests may be explained as follows: concrete crush further and the anchor bolt deforms further in each consecutive load cycle to the same load in load-controlled tests; and the anchor fracture at certain deformation. This is shown in the observed load vs. displacement behavior by Klingner et al. (1982). Note that further increases in the exposed length will alter the stress state again such that the anchor shaft would be subjected to combined tension, bending and shear. The tension in the anchor shaft would contribute to the anchor shear capacity as illustrated by the two tests reported by Swirsky et al. (1978) in Figure 4.29b (data No. 1 and 2). The ultimate shear capacity increased because the shear load was applied 2.25 in. above the concrete surface.

Further studies are needed to quantify the depth of crushed concrete around an anchor subjected to shear. A group of tests were conducted for anchor rods subjected in cyclic shear to clarify the contributing factors for the observed cyclic capacity reduction. In addition, the friction between the base plate and concrete surface needs to be included if the shear resistance of anchor bolt itself is to be calculated separately. The Data analysis shown in Figure 4.29 indicates that the average seismic reduction factor for the anchor steel capacity in shear is 0.76, which is close to that proposed by Pallarés and Hajjar (2010). Consider that the load-controlled loading protocols are different from typical earthquake-induced actions; the seismic reduction factor for the anchor steel capacity in shear may be increased to 0.86 from the average ratio observed in all displacement-controlled tests.

4.7.2 Anchors Subjected to Cyclic Tension

The available data for anchors subjected to cyclic tension (see Figure 4.30) is very limited partly because the collected data did not include the tests with fatigue-type loading. Among the tests controlled by concrete breakout failure, load-controlled tests showed no capacity reduction while the displacement-controlled conducted in this study clearly showed noticeable reductions. The average capacity reduction is 0.97, however, it is recommended to use the lowest ratio (0.87) due to limited tests available. This ratio is comparable to that of shear tests described above for the concrete breakout failure mode. For the tests controlled by steel fracture, none of the collected tests indicated any cyclic capacity reduction. This is in line with the fact that the cyclic behavior of steel in construction is enveloped by the monotonic behavior.

Table 4.1: Summary of Unreinforced Anchor Tests

Reported Test No.	Anchor Dia. da (in)	Embed. Depth hef (in)	Steel Strength F_{ut} (ksi)	Head Area A_{brg} (in^2)	Conc. Strength f'_c (psi)	Front Edge c_{a1} (in)	Side Edge 1 c_{a2} (in)	Side Edge 2 c_{a3} (in)	Back Edge c_{a4} (in)	Block Height h (in)	Crack in Concrete	Load Type (Mono/ Cyclic)	Load Direction (Shear/ Tension)	Failure Load (kips)	Reported Failure Mode
2222010	0.75	4.00	76.00	0.91	5650	4.058	12.00	NA	15.00	17.00	None	Mono	Shear	14.18	Cone
2232010	0.75	4.00	76.00	0.91	5650	3.995	12.00	NA	15.00	17.00	None	Mono	Shear	14.46	Cone
3162010	0.75	4.00	76.00	0.91	5650	3.995	12.00	NA	15.00	17.00	None	Uni-Cyclic	Shear	13.44	Cone
3172010	0.75	4.00	76.00	0.91	5650	4.058	12.00	NA	15.00	17.00	None	Uni-Cyclic	Shear	14.28	Cone
9032010	0.75	4.00	76.00	0.91	5650	3.995	12.00	NA	15.00	17.00	None	Rev. Cyclic	Shear	14.125	Cone
9032010_2	0.75	4.00	76.00	0.91	5650	3.995	12.00	NA	15.00	17.00	None	Rev. Cyclic	Shear	14.76	Cone
1132010	0.75	6.00	76.00	0.91	5650	4.058	16.00	NA	15.00	17.00	None	Mono	Shear	13.41	Cone
3012010	0.75	6.00	76.00	0.91	5650	4.058	16.00	NA	15.00	17.00	None	Mono	Shear	15.82	Cone
3022010	0.75	6.00	76.00	0.91	5650	4.058	16.00	NA	15.00	17.00	None	Uni-Cyclic	Shear	14.84	Cone
3052010	0.75	6.00	76.00	0.91	5650	4.183	16.00	NA	15.00	17.00	None	Uni-Cyclic	Shear	15.18	Cone
4092010	0.75	6.00	76.00	0.91	5650	3.995	16.00	NA	15.00	17.00	None	Rev. Cyclic	Shear	14.33	Cone
6162010	0.75	6.00	76.00	0.91	5650	4.058	16.00	NA	15.00	17.00	None	Rev. Cyclic	Shear	14.57	Cone
3092010	0.75	6.00	76.00	0.91	5650	6.058	16.00	NA	15.00	17.00	None	Mono	Shear	16.11	Steel
3102010	0.75	6.00	76.00	0.91	5650	5.933	16.00	NA	15.00	17.00	None	Mono	Shear	17.74	Steel
3222010	0.75	6.00	76.00	0.91	5650	6.188	16.00	NA	15.00	17.00	None	Mono	Shear	16.84	Steel
3232010	0.75	6.00	76.00	0.91	5650	6.245	16.00	NA	15.00	17.00	None	Mono	Shear	16.17	Steel
3122010	0.75	6.00	76.00	0.91	5650	5.995	16.00	NA	15.00	17.00	None	Uni-Cyclic	Shear	16.14	Steel
3222010	0.75	6.00	76.00	0.91	5650	5.995	16.00	NA	15.00	17.00	None	Uni-Cyclic	Shear	16.57	Steel
3242010	0.75	6.00	76.00	0.91	5650	6.058	16.00	NA	15.00	17.00	None	Rev. Cyclic	Shear	15.4	Steel
2052010	0.75	4.00	76.00	0.91	5650	4.058	12.00	NA	15.00	17.00	None	Mono	Tension	19.66	Cone
2122010	0.75	4.00	76.00	0.91	5650	4.120	12.00	NA	15.00	17.00	None	Mono	Tension	21.22	Cone
3252010	0.75	4.00	76.00	0.91	5650	4.058	12.00	NA	15.00	17.00	None	Cyclic	Tension	18.44	Cone
3252010_2	0.75	4.00	76.00	0.91	5650	4.120	12.00	NA	15.00	17.00	None	Cyclic	Tension	17.96	Cone
3252010	0.75	6.00	76.00	0.91	5650	4.058	16.00	NA	15.00	17.00	None	Mono	Tension	28.30	Cone
3302010	0.75	6.00	76.00	0.91	5650	4.120	16.00	NA	15.00	17.00	None	Mono	Tension	25.20	Cone
3312010	0.75	6.00	76.00	0.91	5650	3.870	16.00	NA	15.00	17.00	None	Cyclic	Tension	28.14	Steel
4062010	0.75	6.00	76.00	0.91	5650	3.995	16.00	NA	15.00	17.00	None	Cyclic	Tension	27.80	Steel
1292010	0.75	6.00	76.00	0.91	5650	6.058	16.00	NA	15.00	17.00	None	Mono	Tension	28.37	Steel

Table 4.2: Literature data for anchors in shear

Reference	# Tests	Reinforcement	Failure Mode
Viest (1956)	4	Surface	Steel
Ollgaard et al. (1971)	21	Surface	Steel
McMackin et al. (1973)	12	None	2 Steel
			10 Cone
Bailey and Burdette (1977)			
Swirsky et al. (1978)	37	17 None	31 Cone
		20 Hairpin	6 Other
Klingner et al. (1982)	33	22 None	8 Steel
		11 Hairpin	25 Cone
Klingner and Mendonca (1982)	14	None	2 Steel
			12 Cone
Ueda et al. (1990)	20	None	Cone
Hallowell (1996)	20	None	Cone
Gattesco and Giuriani (1996)	2	None	Steel
Wong et al. (1988)	5	None	1 Steel
			4 Cone
Anderson and Meinheit (2000)	44	None	6 Steel
			38 Cone
Gross et al. (2001)	6	2 None	Cone
		4 Hairpin	
Kawano et al. (2003)	16	None	4 Steel
			12 Cone
Muratli et al. (2004)	4	None	Cone
Lee et al. (2010)	27	None	Cone

Table 4.3: Literature data for anchors in tension

Reference	# Tests	Reinforcement	Failure Mode
Nordlin et al. (1968)	52	None	22 Steel
			30 Cone
McMackin et al. (1973)	22	None	11 Steel
			11 Cone
Hasselwander et al. (1974)	55	Longitudinal Bars	12 Steel
			12 Steel-Incomplete
Cannon et al. (1975)	43	None	19 Steel
			24 Cone
Bode and Hanenkamp (1985)	165	None	Cone
Cook et al. (1992)	8	None	Steel
Carraio et al. (1996)	8	None	3 Steel
			5 Cone
Hallowell (1996)	20	None	Cone
Primavera et al. (1997)	62	None	Cone
Shirvani (1998)	100	None	Cone
Rodriguez et al. (2001)	2	None	Cone
Kawano et. al. (2003)	8	None	Steel
Hoehler (2006)	5	None	Cone
Solomos and Berra (2006)	5	None	Cone
Jang and Suh (2006)	21	None	Cone
Lee et al. (2007)	20	12 None	12 Cone
		8 Stirrups	12 Incomplete
Ando et al. (2007)	3	Stirrups	Cone

Table 4.4: Cyclic tests of anchors in the literature

References	Specimen[#]	Tension tests[*]	Shear tests[*]	Loading type
Hasselwander et al. (1974)	Single anchor	2 (s:2)		Cyclic load
Swirsky et al. (1978)	Single anchor		10 (s:2 c:8)	Reversed load
Bischof (1978)	Pushout-2		2 (c:2)	Cyclic load
Klingner et al. (1982)	Single anchor		3 (s:3)	Reversed load
Hawkins and Mitchell (1984)	Pushout-4		9 (s:6 c:3)	Reversed load
Nakajima et al. (1996)	Pushout-4		2 (s:2)	Reversed load
Gattesco and Giuriani (1996)	Single anchor		2 (s:2)	Cyclic load
Taplin and Grundy (1997)	Pushout-8		2 (s:2)	Cyclic load
Bursi and Gramola (1999)	Pushout-8		5 (s:5)	Reversed Disp.
Nakashima (1999)	Single anchor		12 (s:6 c:6)	Reversed load
Nakashima (2000)	Single anchor	2 (s:2)	4 (s:4)	Reversed load
Civjan and Singh (2003)	Pushout-8		7 (s:7)	Reversed load
Saari et al. (2004)	Pushout-4		1 (s:1)	Reversed load
Yoshimori and Nakashima (2004)	Single anchor	2 (s:2)		Cyclic Disp.
Hoehler (2006)	Single anchor	5 (c:5)		Cyclic load
Fennel et al. (2009)	Single anchor		4 (c:4)	Reversed Disp.
DeRenzis et al. (2010)	Single anchor		32 (c:32)	Reversed Disp.
Petersen (2011)	Single anchor	8 (s:4 c:4)	19 (s:11 c:8)	Reversed Disp.

#: Single anchor specimens include structural bolts and threaded rods headed studs; the number of studs in pushout specimens is shown. *: s = tests with steel failure; c = tests with concrete failure, mainly breakout failure

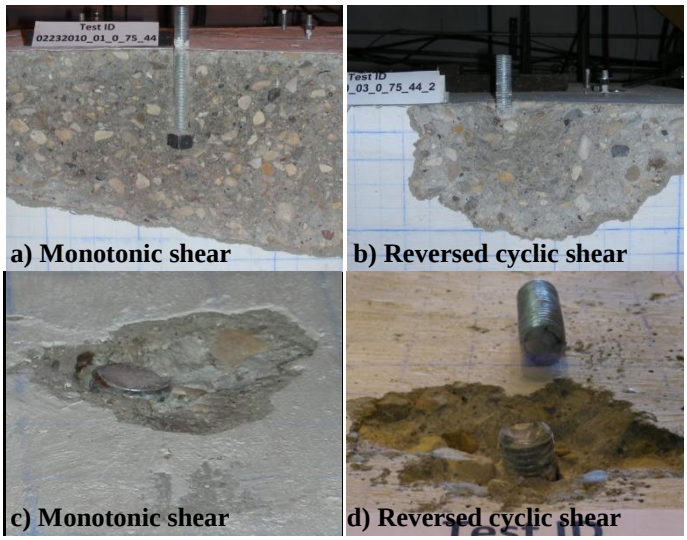

Figure 4.1: Typical failure modes of anchor bolts in shear

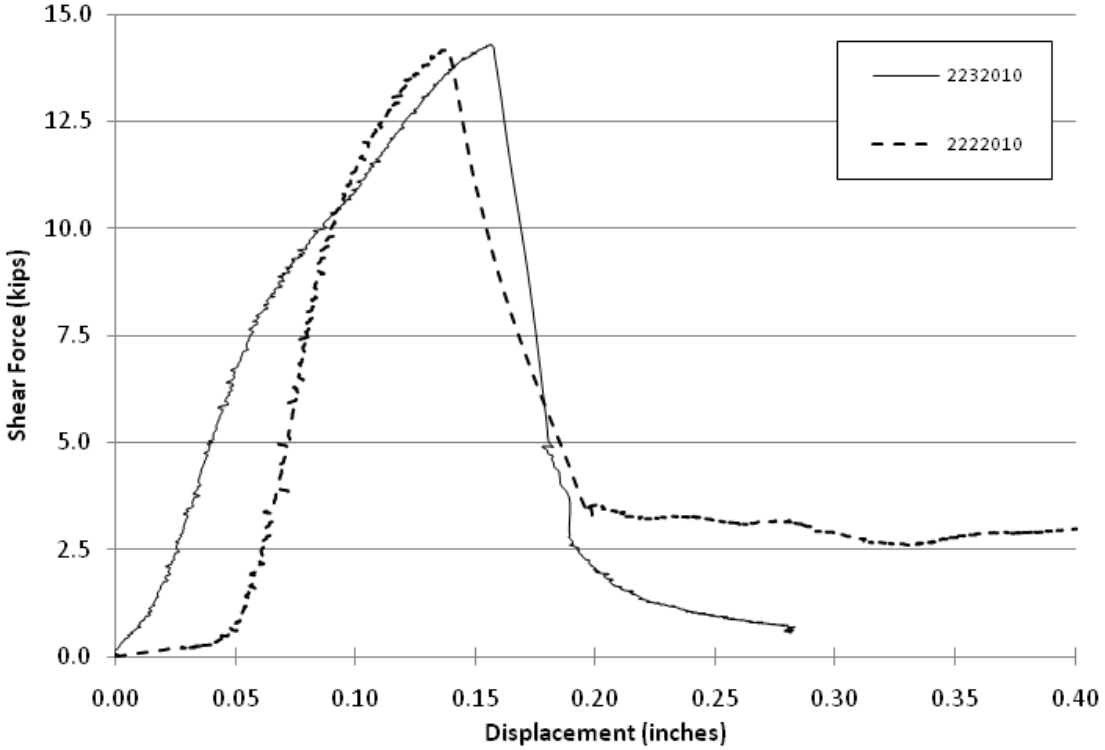

Figure 4.2: Monotonic shear concrete breakout failure (d_a = 0.75", h_{ef} = 4", c_{a1} = 4")

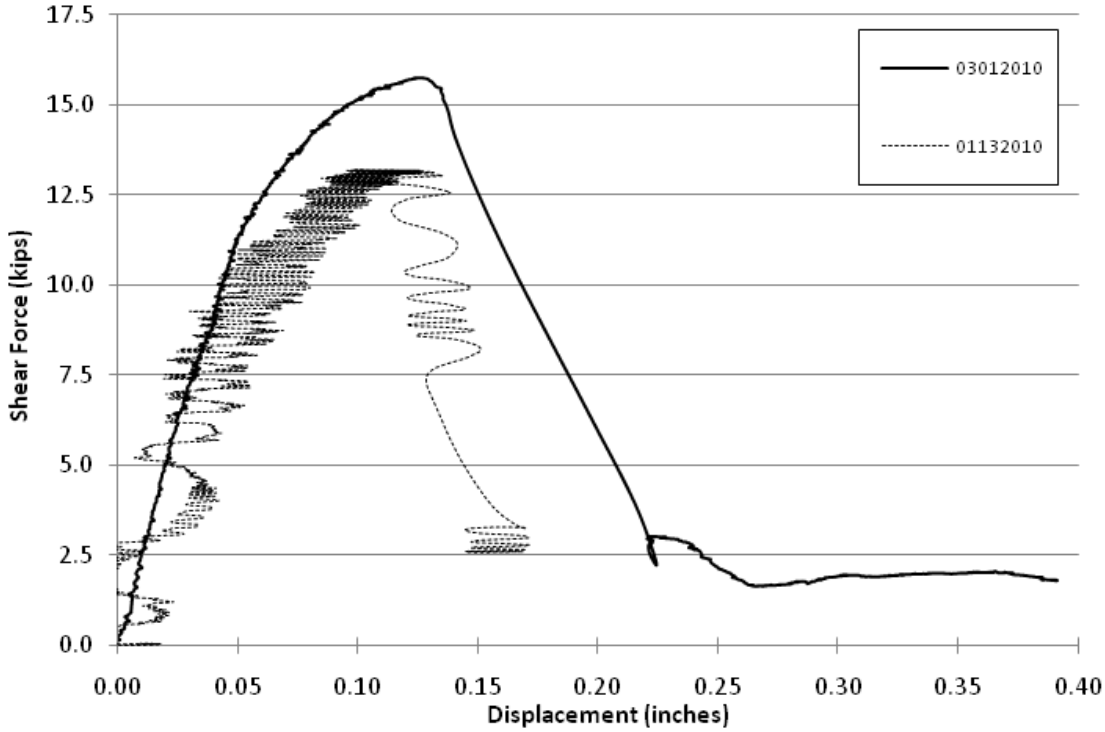

Figure 4.3: Monotonic shear concrete breakout failure (d_a = 0.75", h_{ef} = 6", c_{a1} = 4")

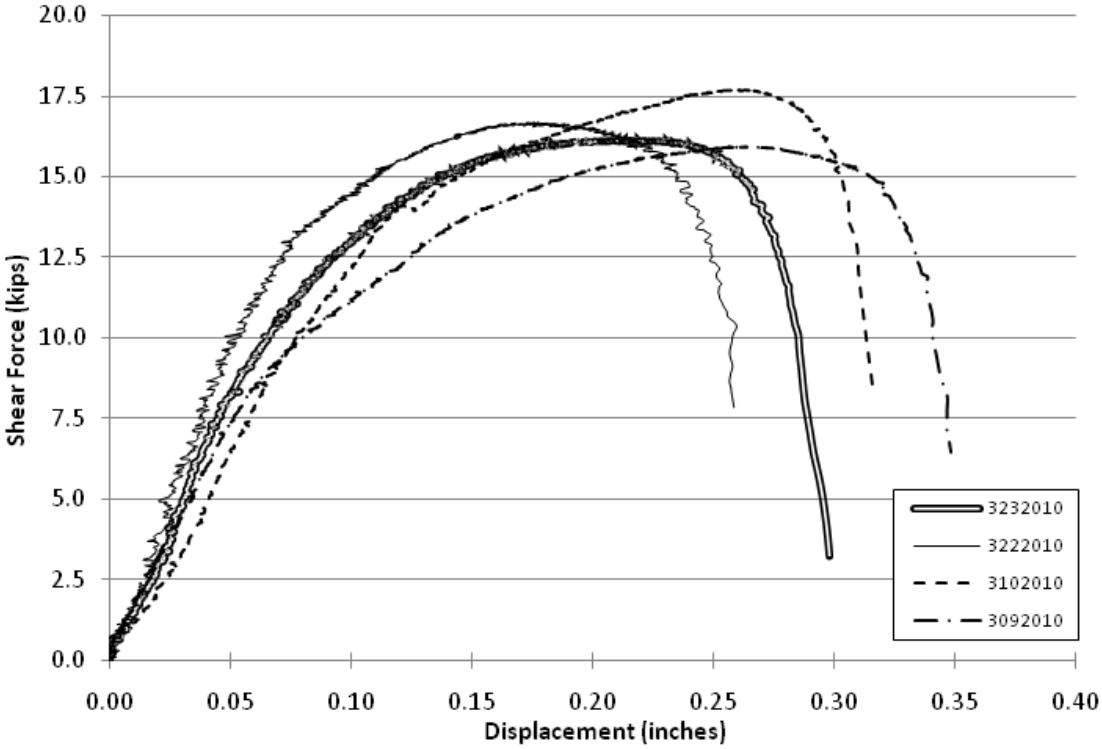

Figure 4.4: Monotonic shear steel failure (d_a = 0.75", h_{ef} = 6", c_{a1} = 6")

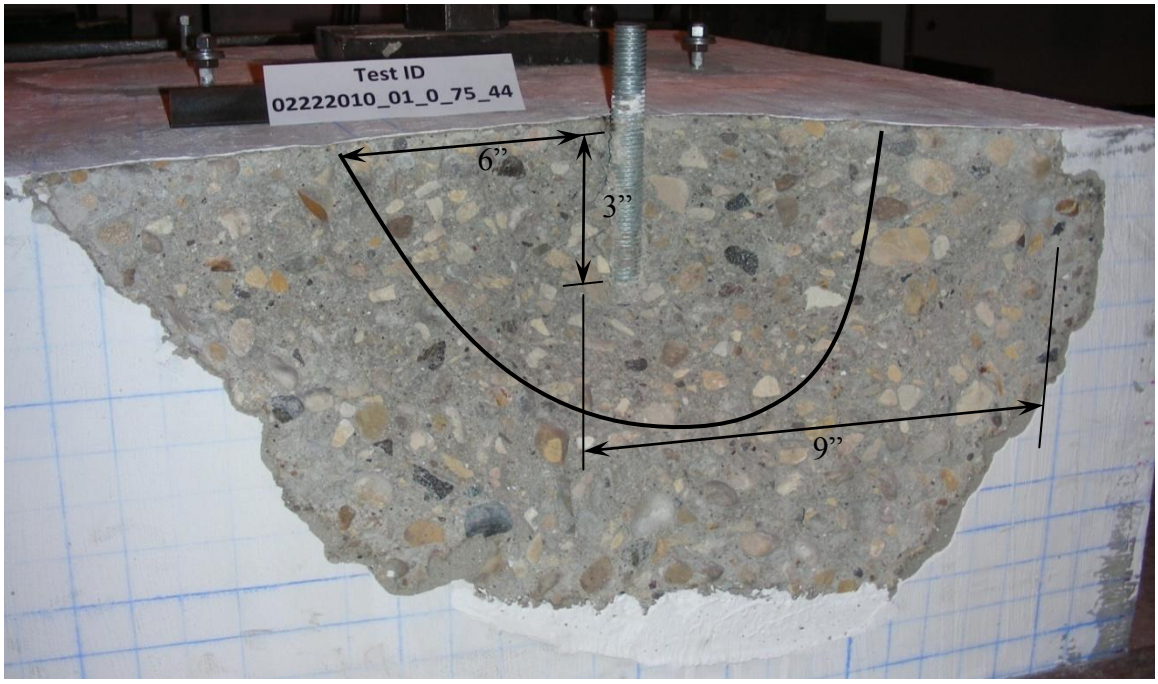

Figure 4.5: Typical monotonic shear breakout failure (c_{a1} = 4")

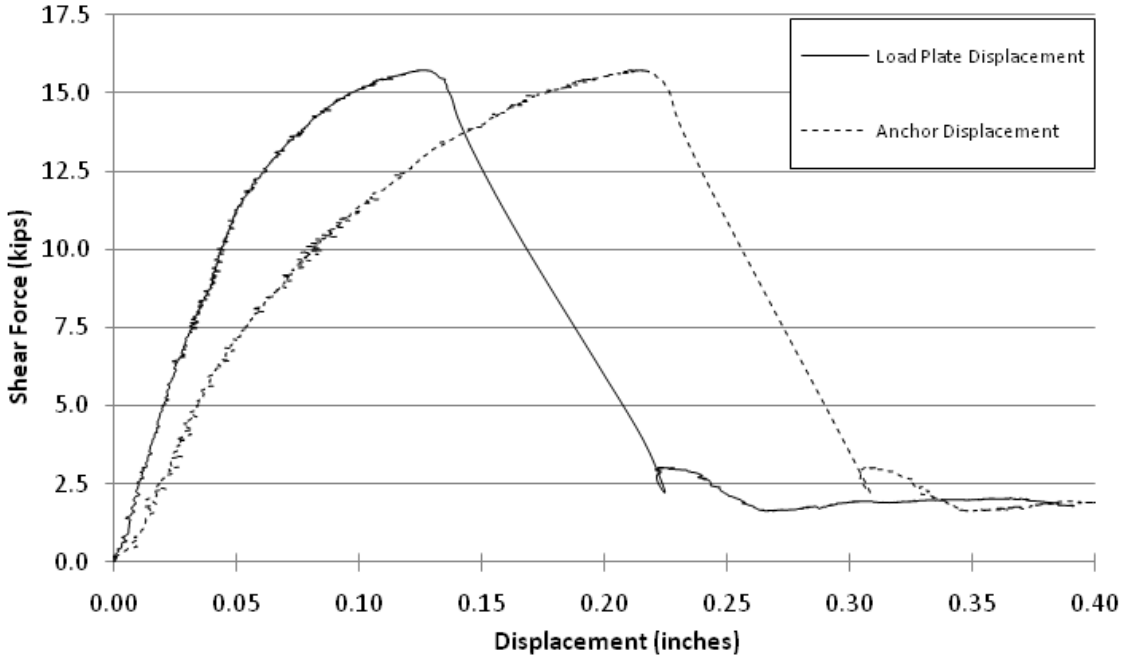

Figure 4.6: Disp. comparison from anchor and load plate (d_a = 0.75", h_{ef} = 6", c_{a1} = 4")

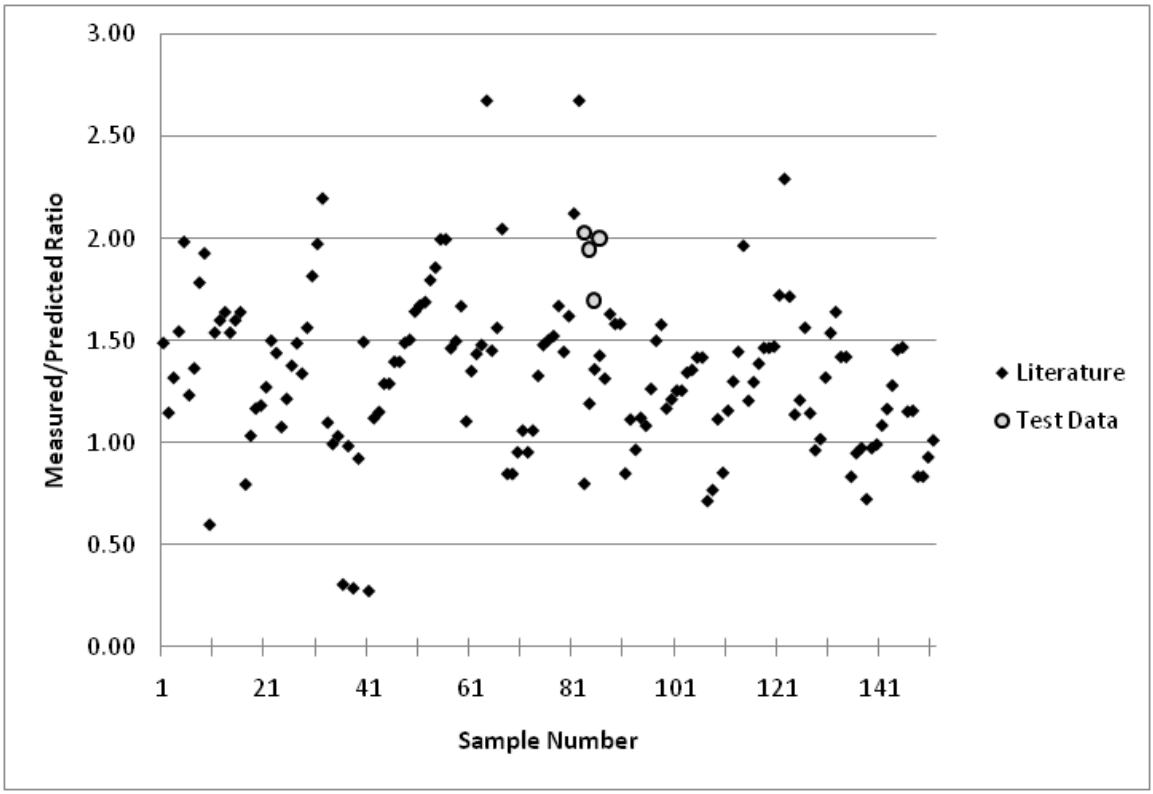

Figure 4.7: Measured/Predicted monotonic shear breakout capacity

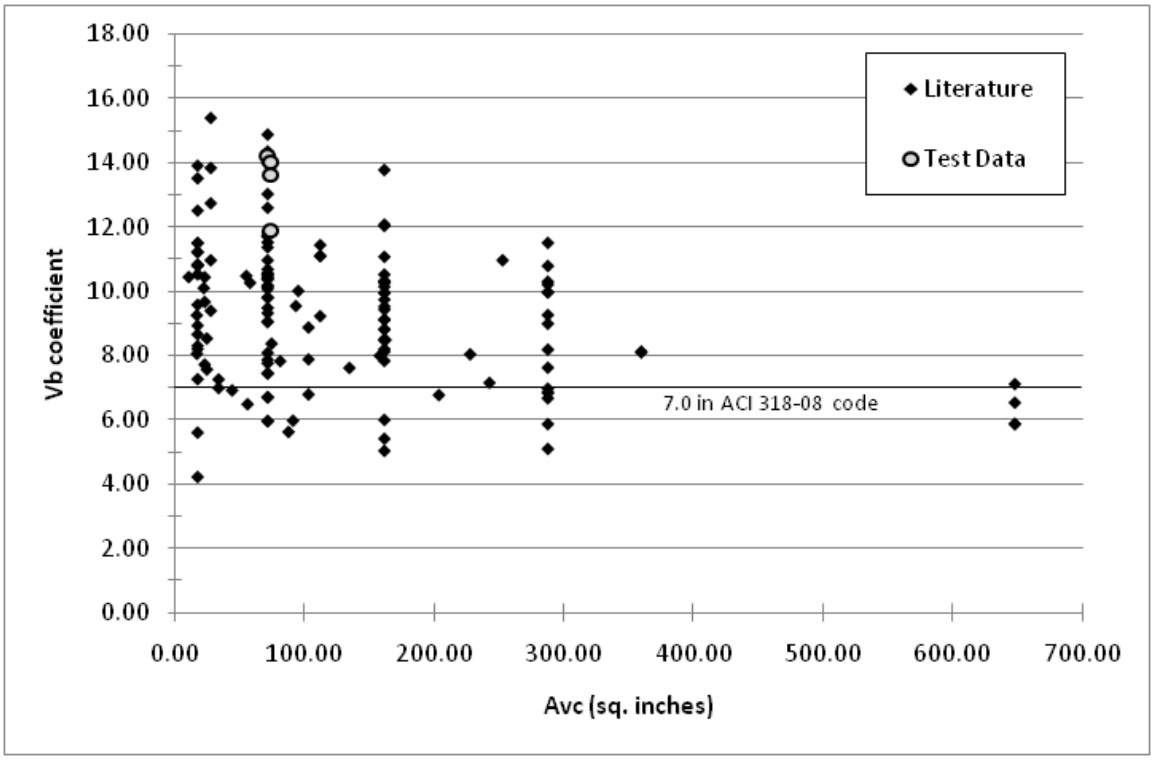

Figure 4.8: Shear breakout coefficient for V_b versus A_{nc} (Outliers excluded)

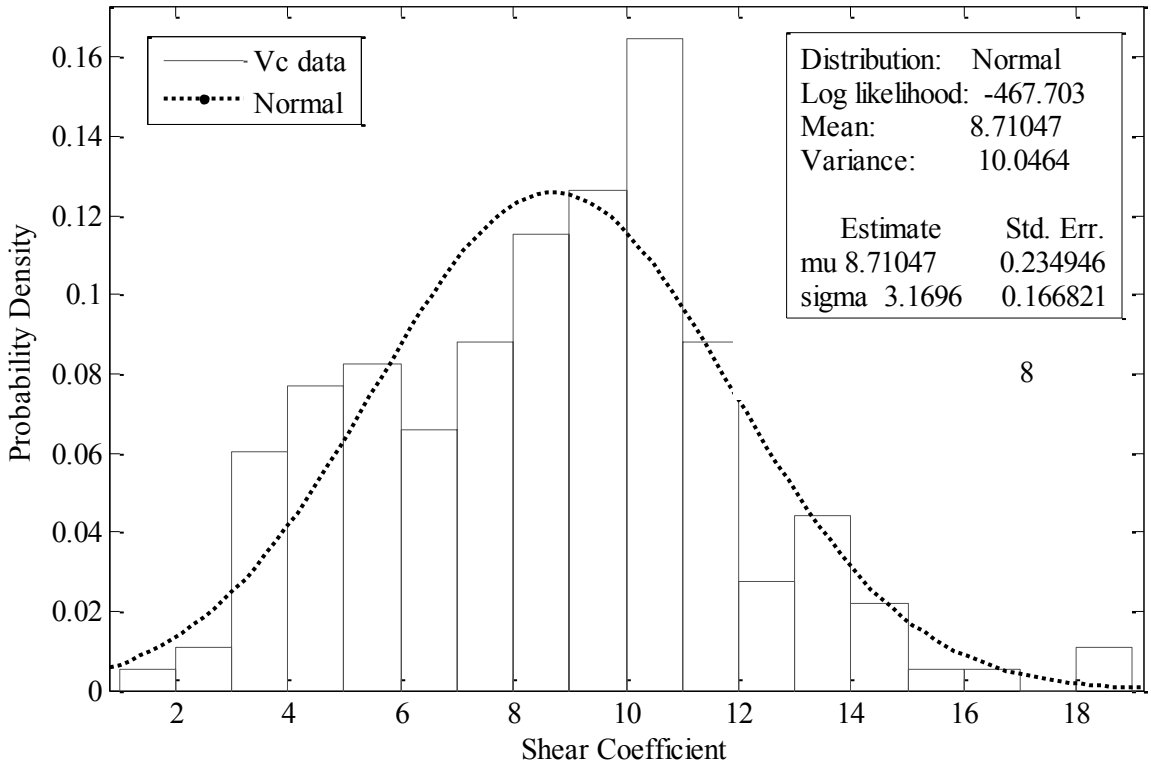

Figure 4.9: Hysteretic Monotonic Shear Data Distribution

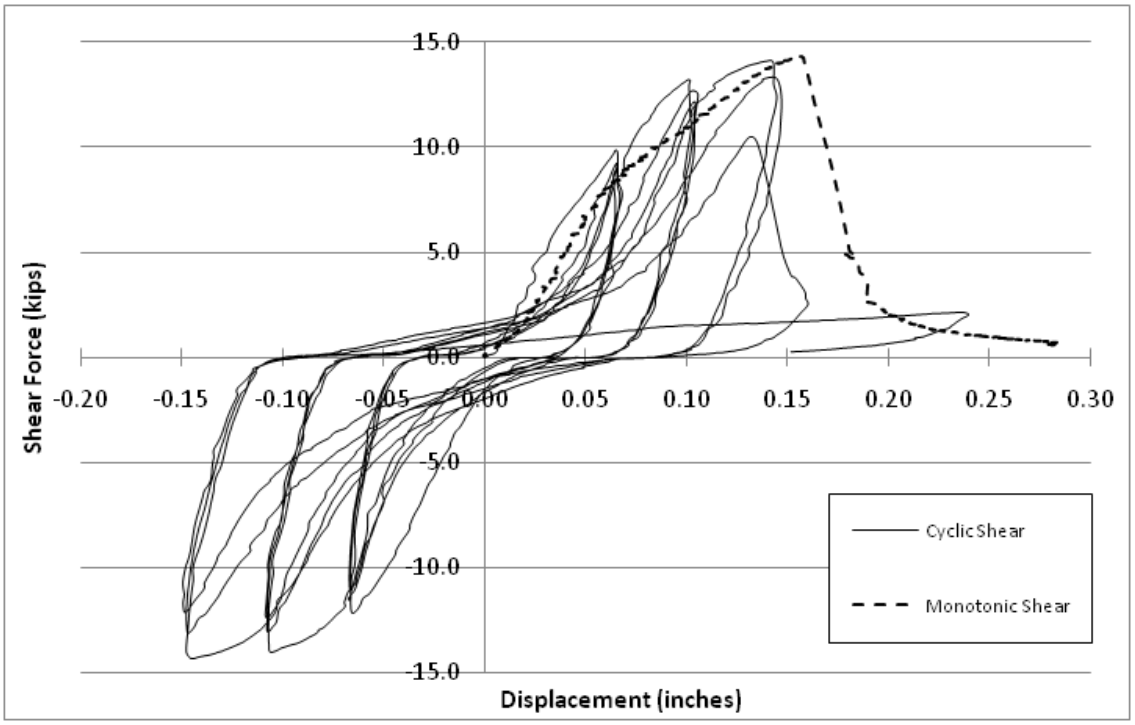

Figure 4.10: Cyclic shear concrete failure (d_a = 0.75", h_{ef} = 4", c_{a1} = 4")

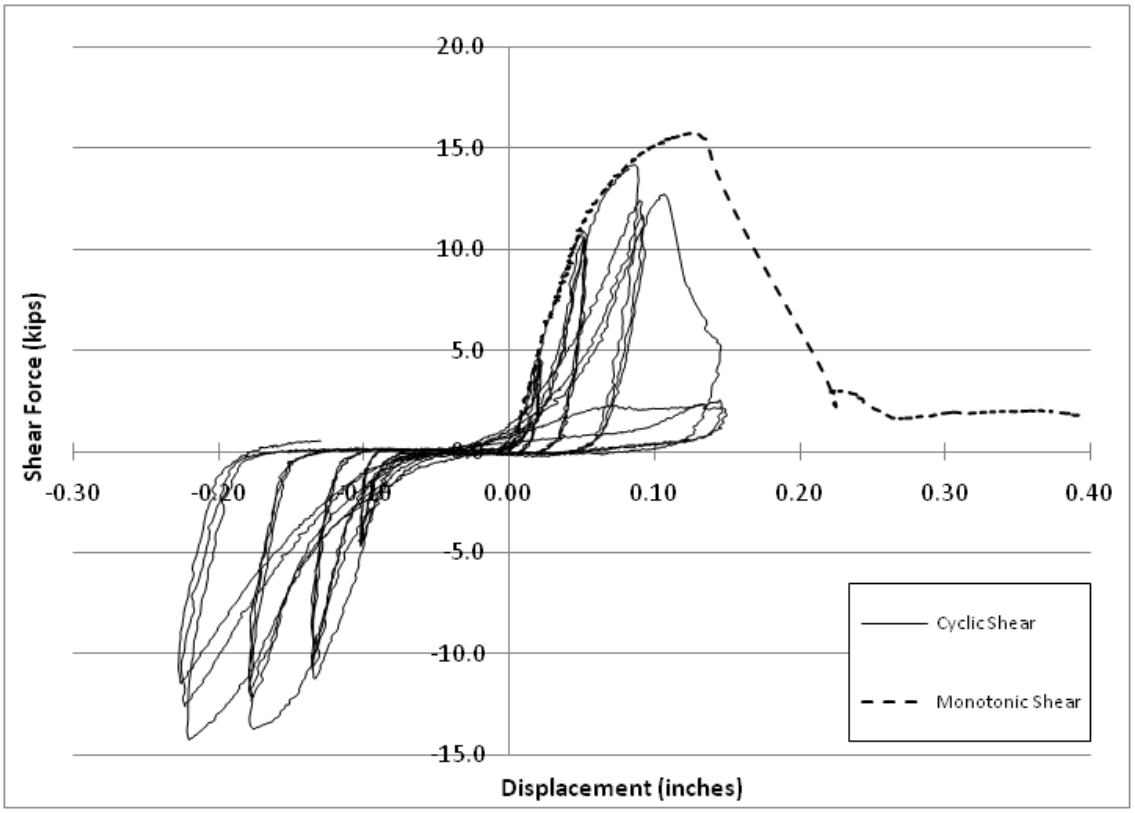

Figure 4.11: Cyclic shear concrete failure (d_a = 0.75", h_{ef} = 6", c_{a1} = 4")

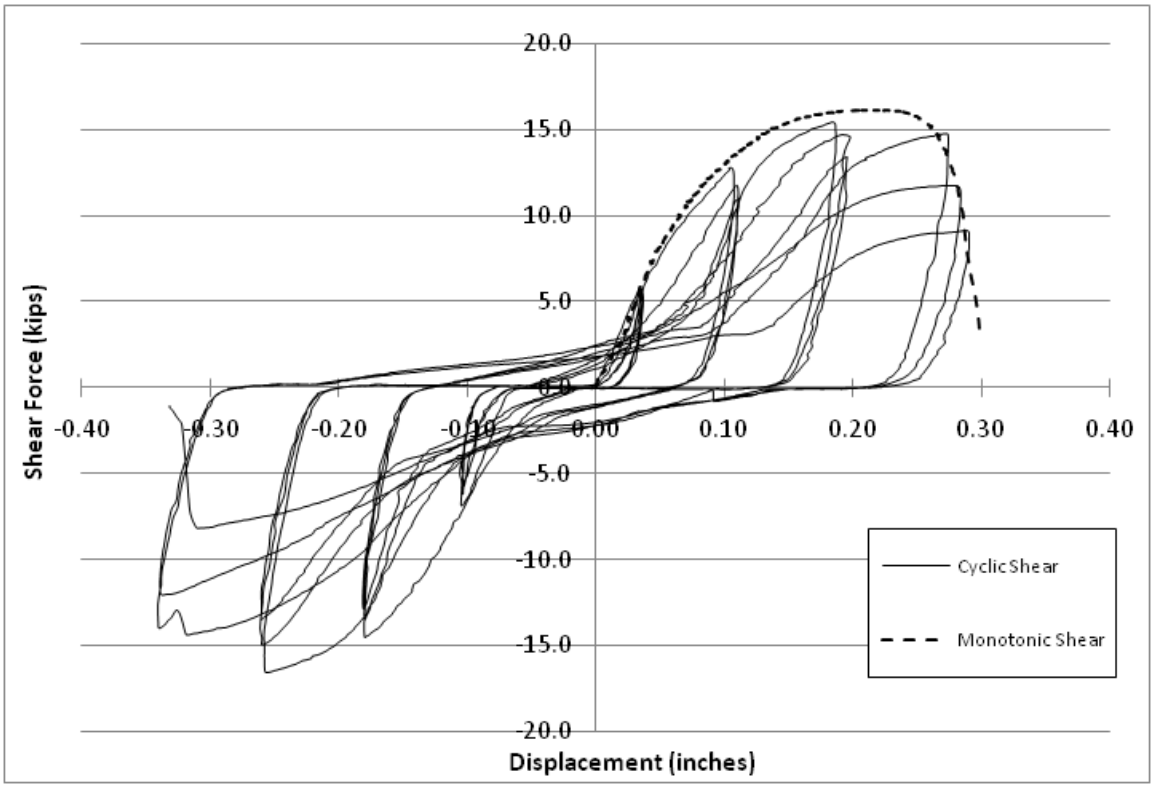

Figure 4.12: Cyclic shear steel failure (d_a = 0.75", h_{ef} = 6", c_{a1} = 6")

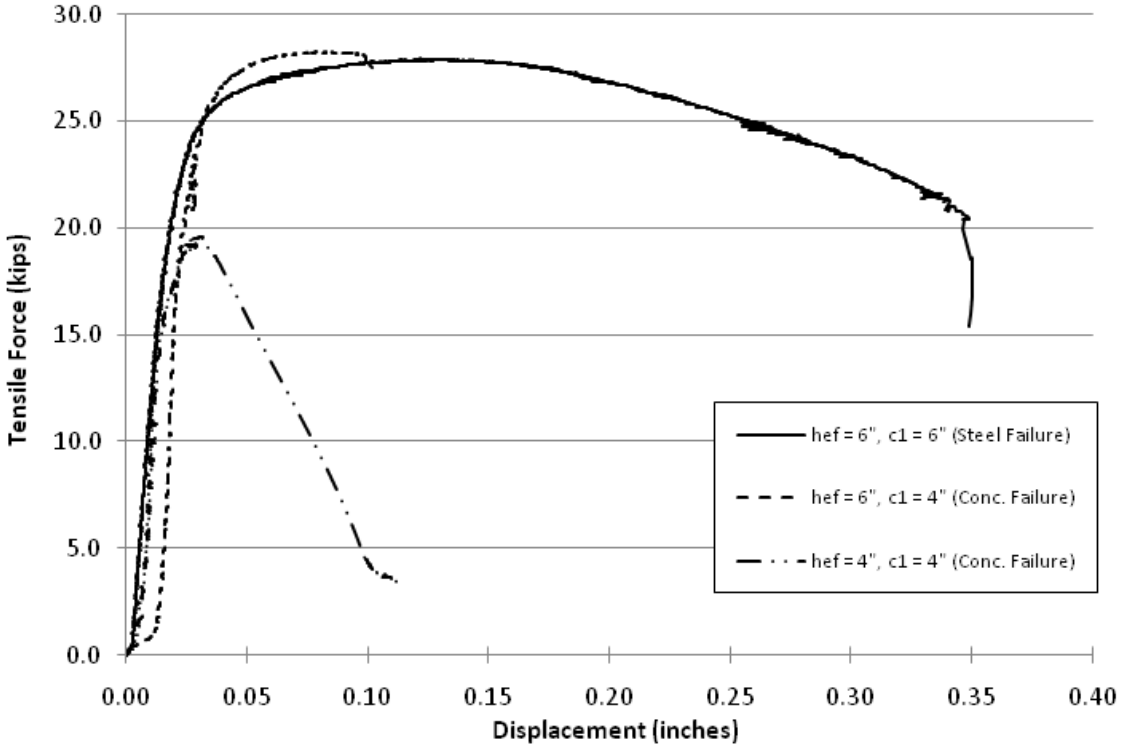

Figure 4.13: Summary of unreinforced monotonic tension tests

Figure 4.14: Concrete spalling during tensile steel failure

Figure 4.15: Tension breakout cone interference (d_a = 0.75", h_{ef} = 6", c_{a1} = 4")

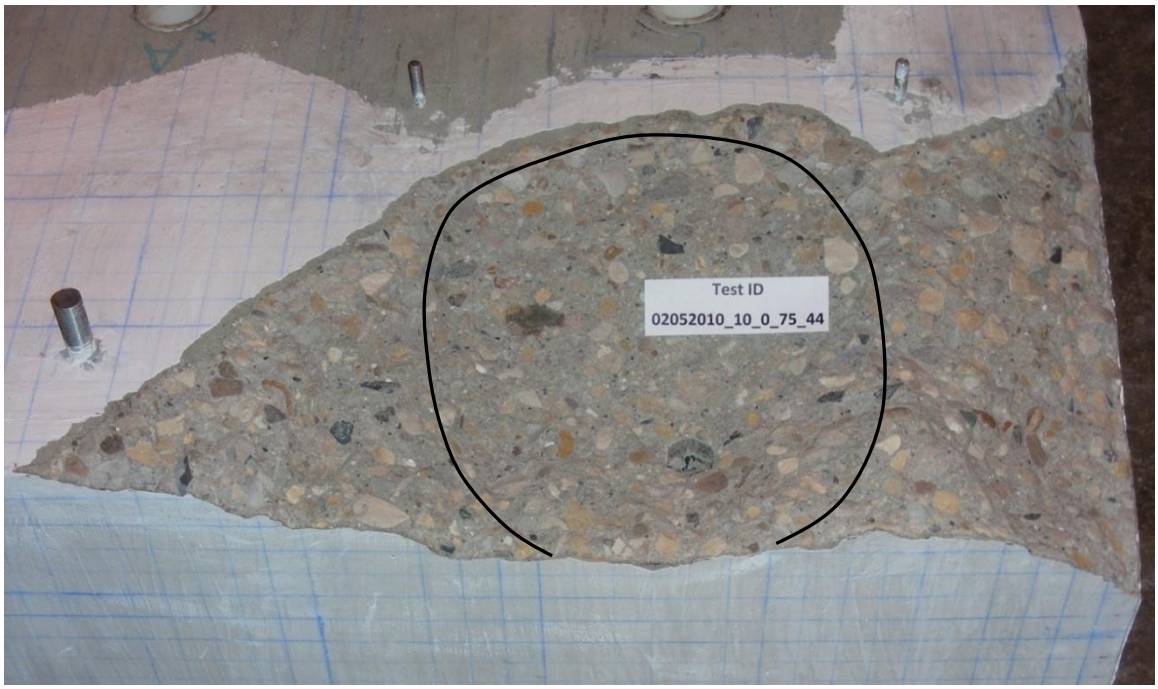

Figure 4.16: Tension breakout cone angle change (d_a = 0.75", h_{ef} = 4", c_{a1} = 4")

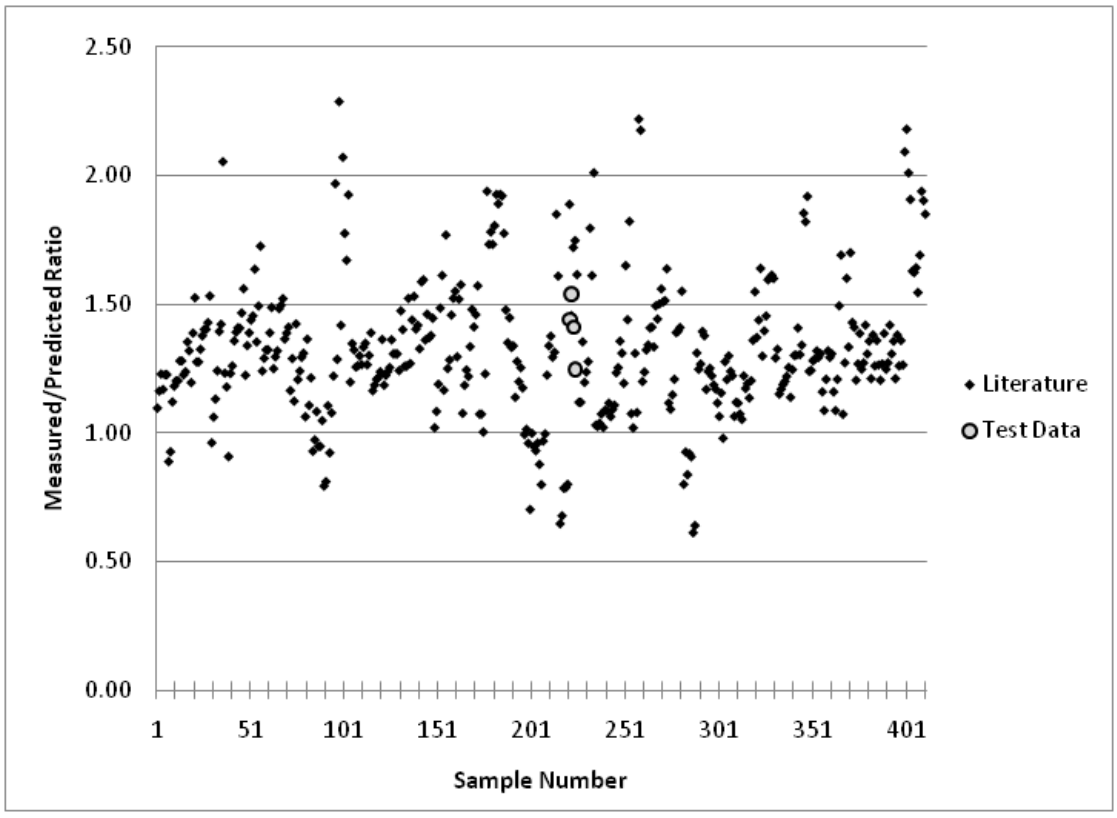

Figure 4.17: Measured/Predicted monotonic tension capacity

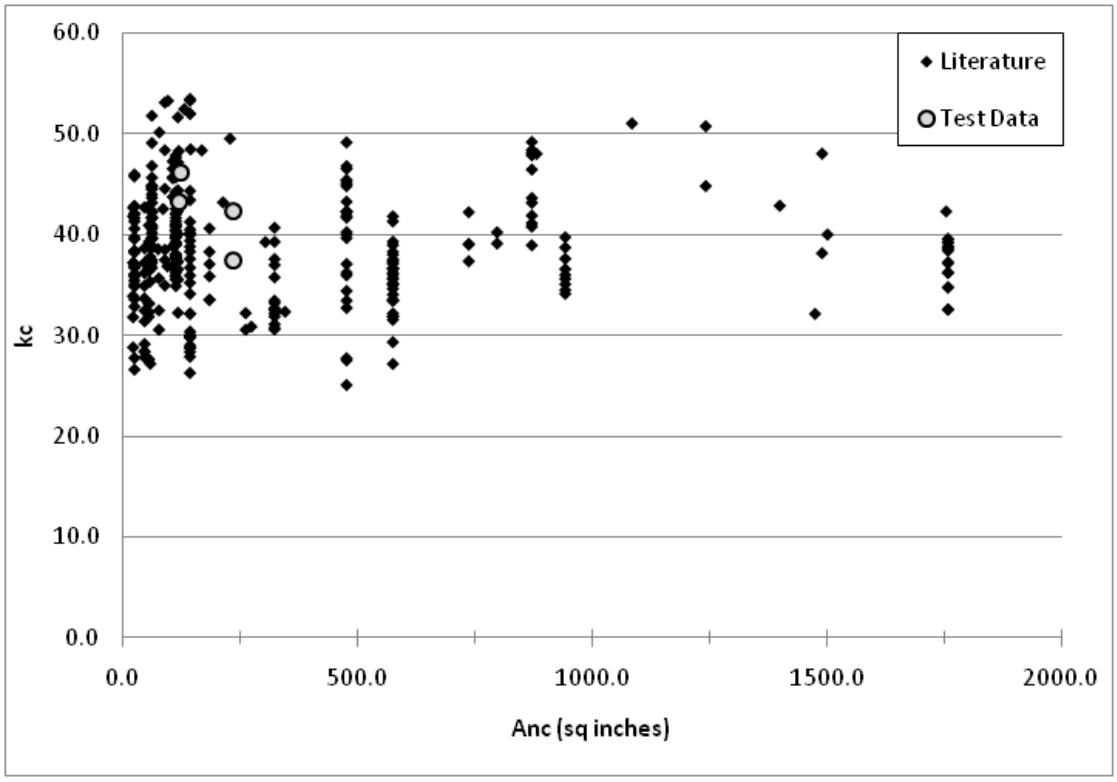

Figure 4.18: Tension breakout constant k_c versus A_{nc} (Outliers excluded)

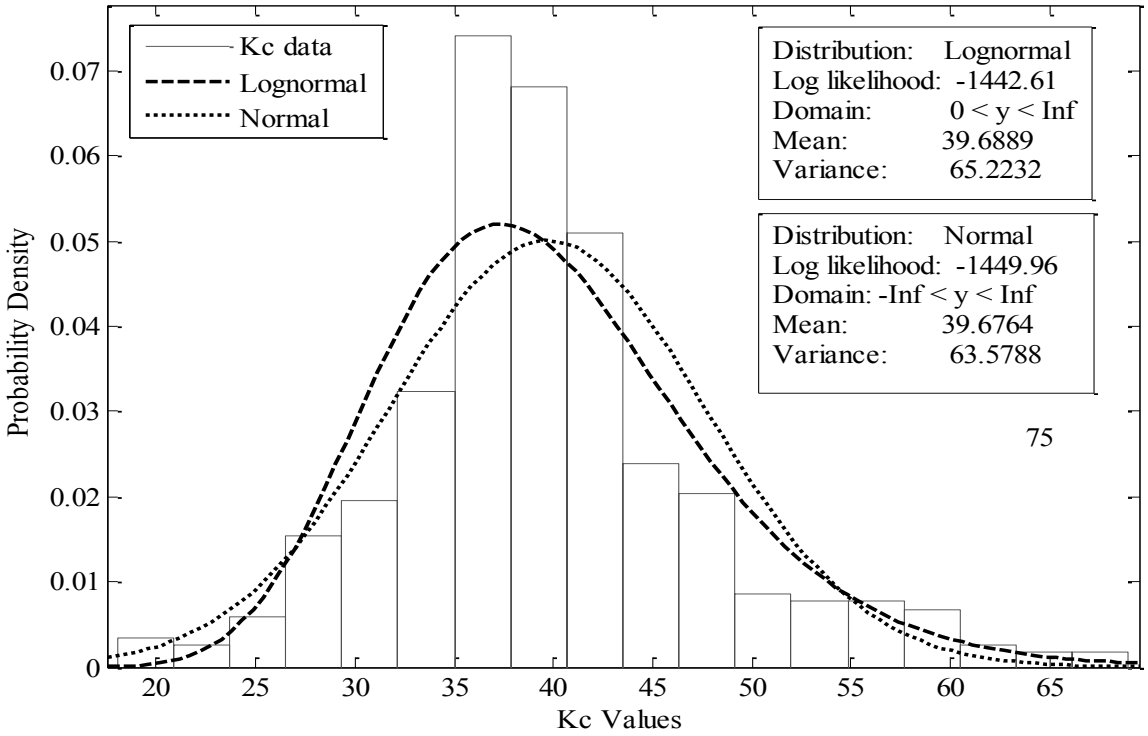

Figure 4.19: Hysteretic distribution of monotonic tension data from literature

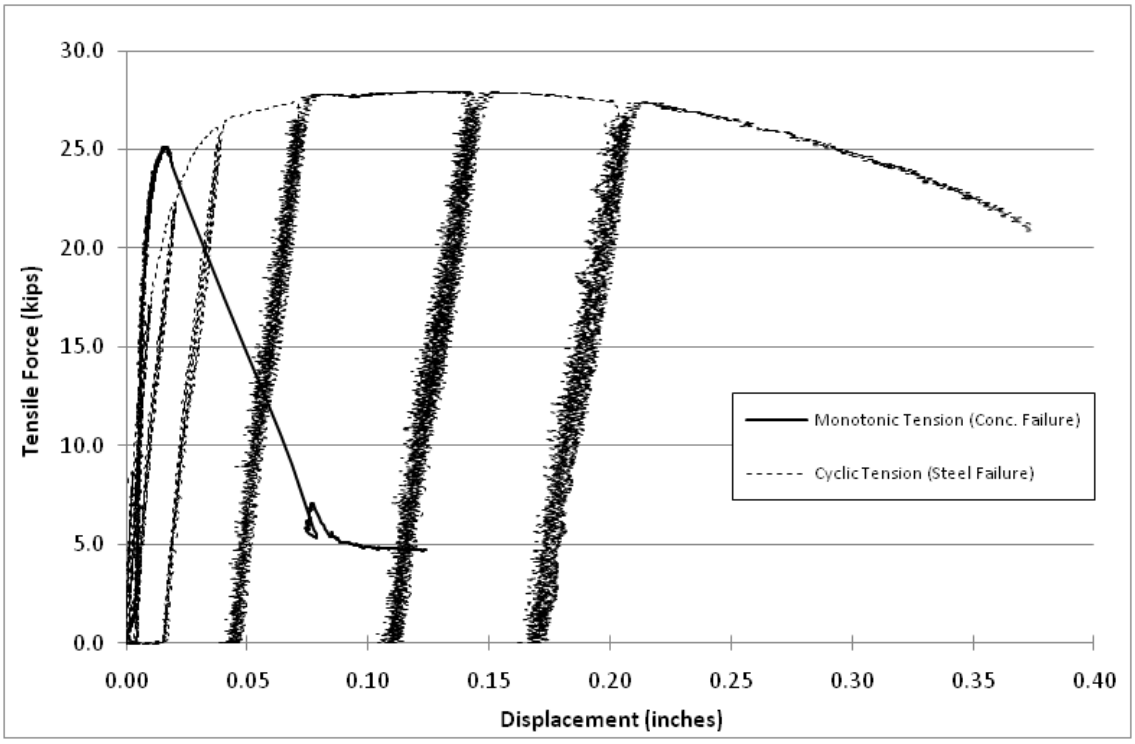

Figure 4.20: Cyclic tension failure mode change (d_a = 0.75", h_{ef} = 6", c_{a1} = 4")

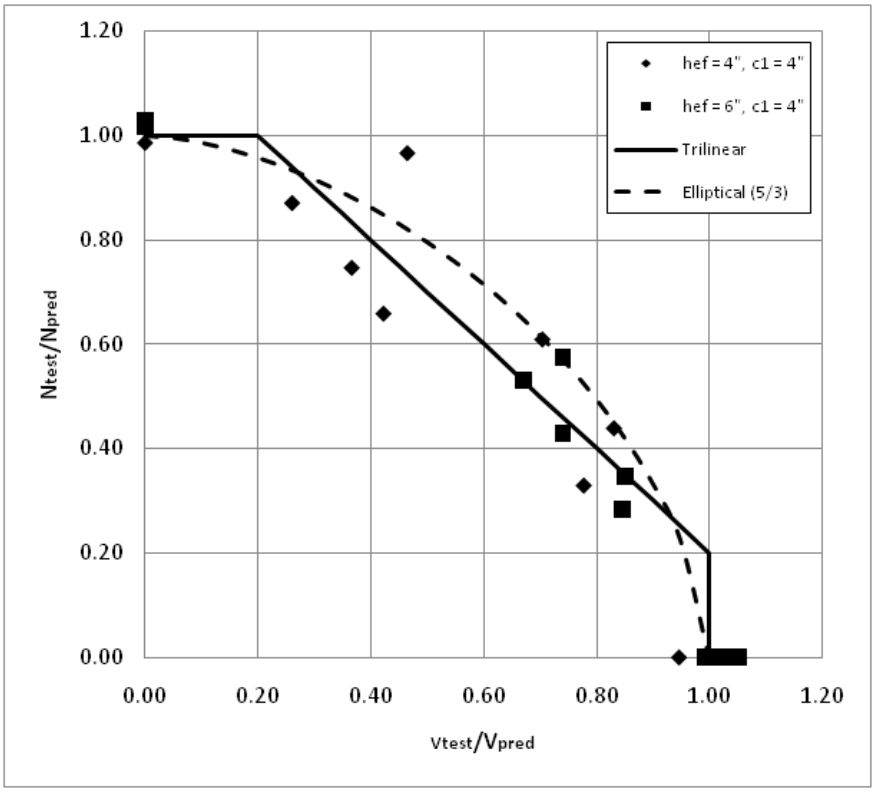

Figure 4.21: Cyclic combined loading interaction plot (using test avg. for N_n and V_n)

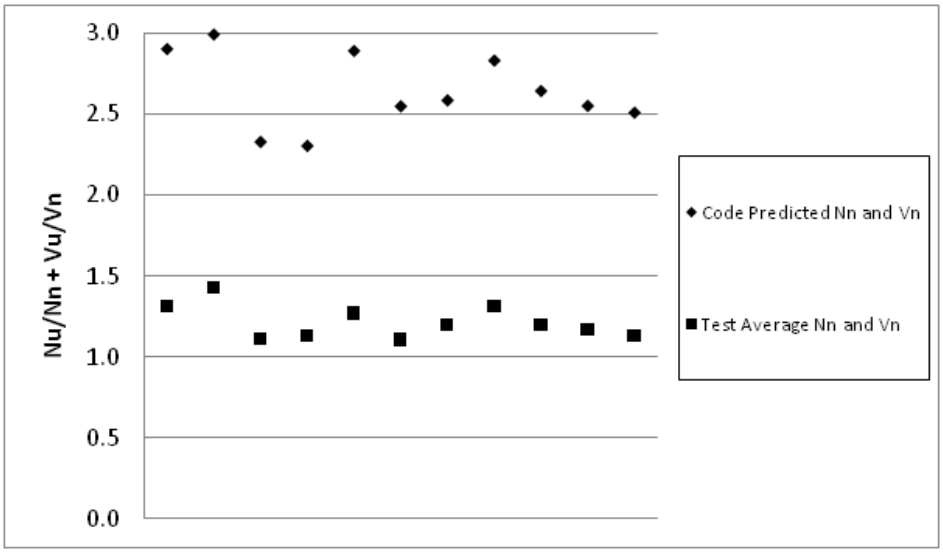

Figure 4.22: Cyclic tension-shear interaction values

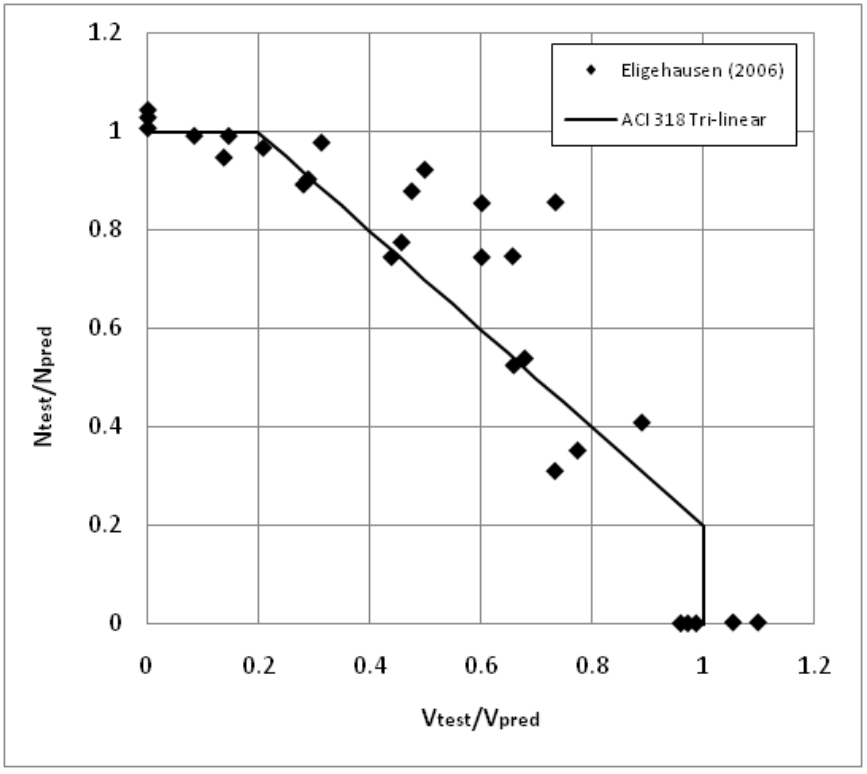

Figure 4.23: Combined interaction test data (Eligehausen et al. 2006)

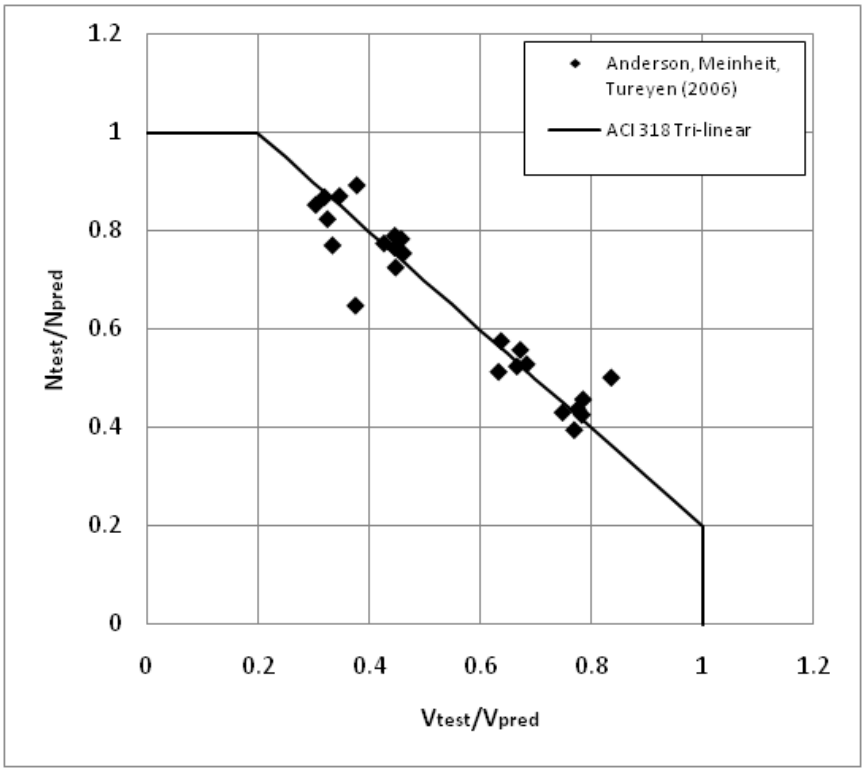

Figure 4.24: Combined interaction test data (Anderson et al. 2006)

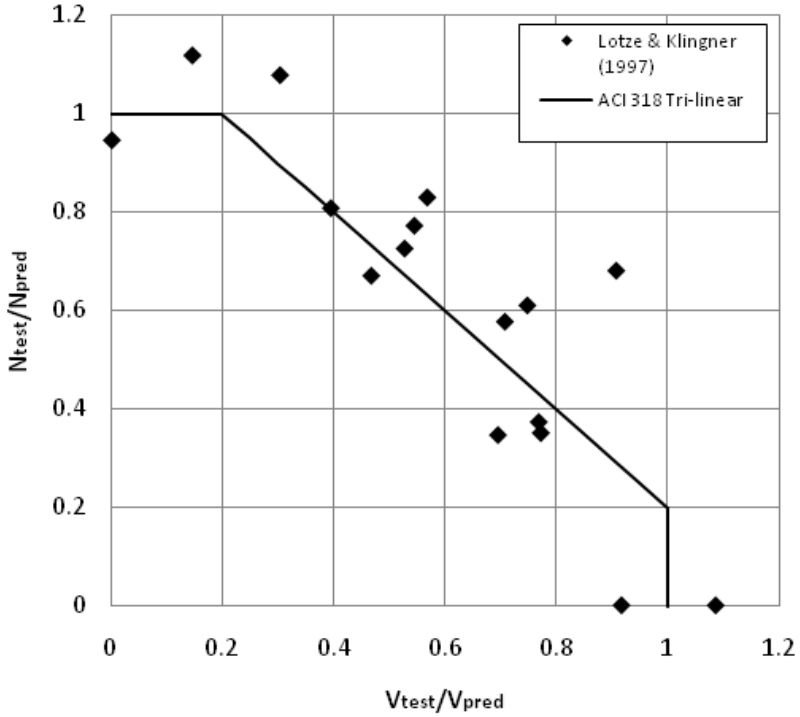

Figure 4.25: Combined interaction test data (Lotze & Klingner 1997)

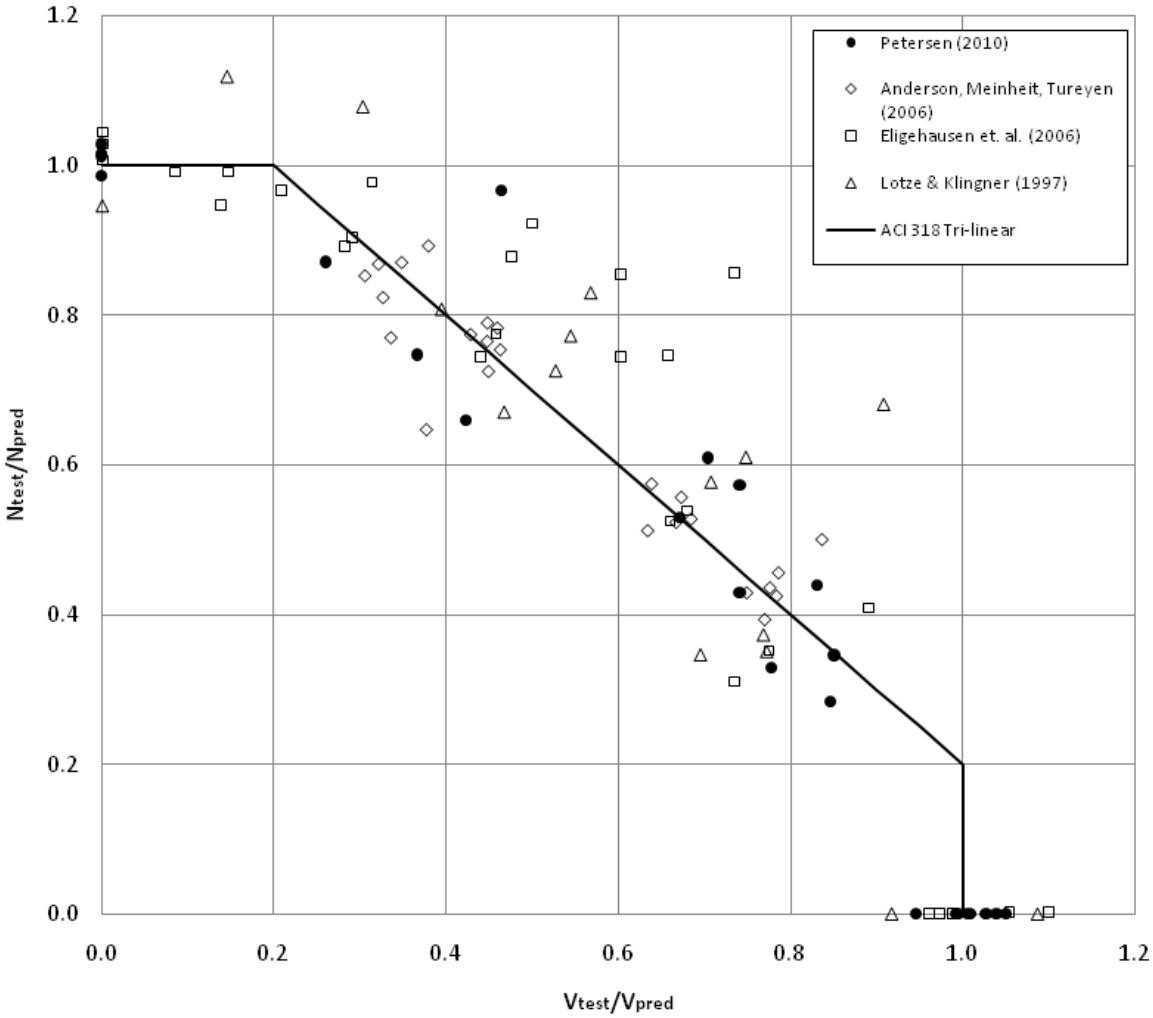

Figure 4.26: Summary of combined interaction test data

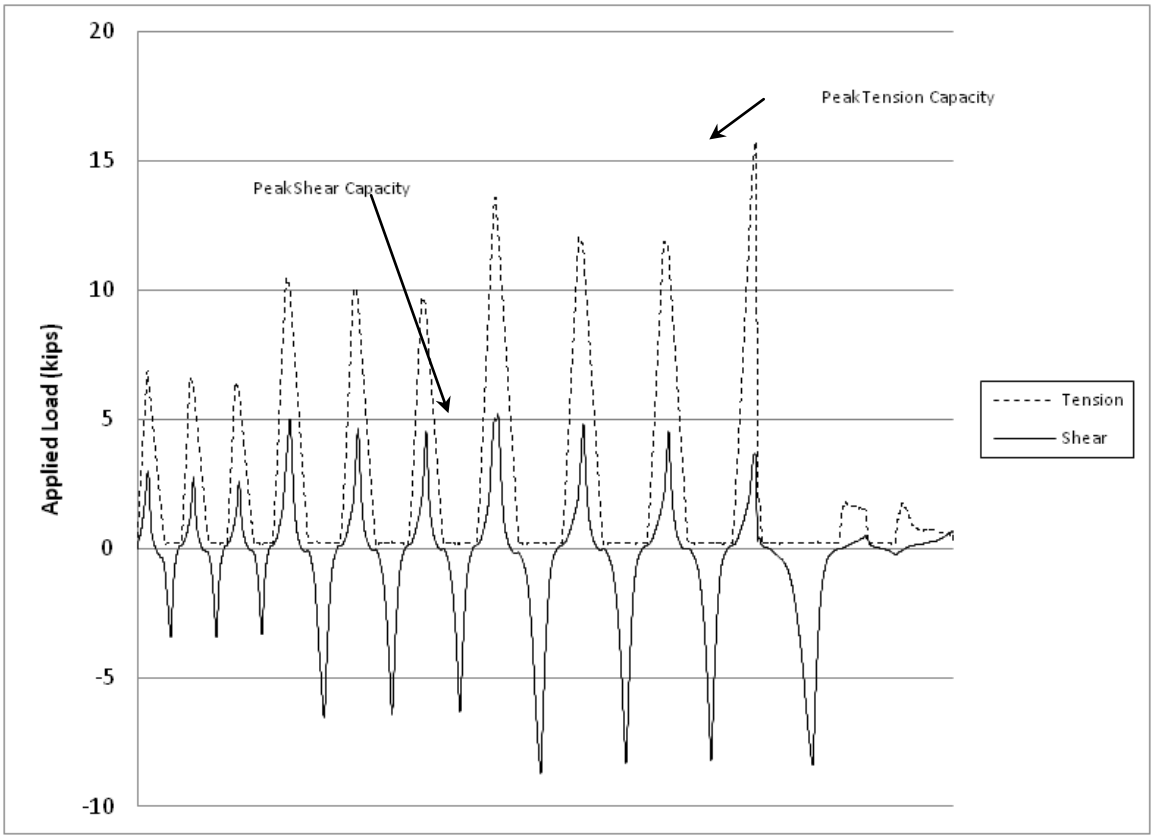

Figure 4.27: Cyclic combined loading continued after shear capacity peak

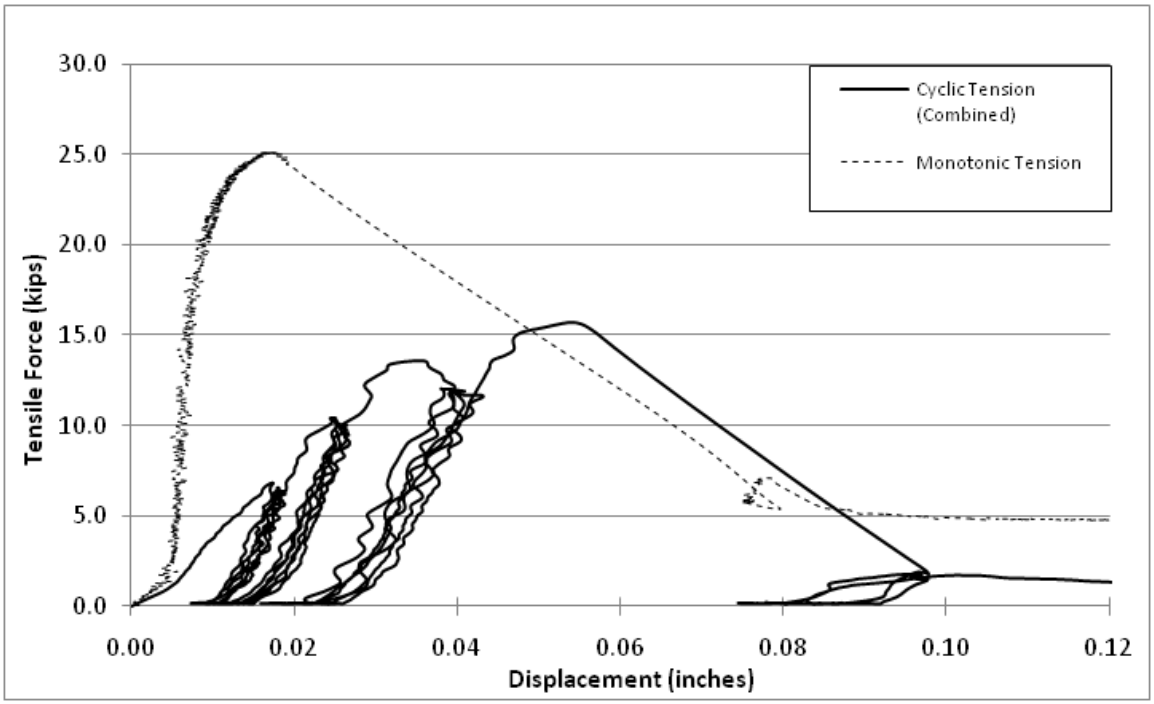

Figure 4.28: Tensile displacement comparison for cyclic combined loading

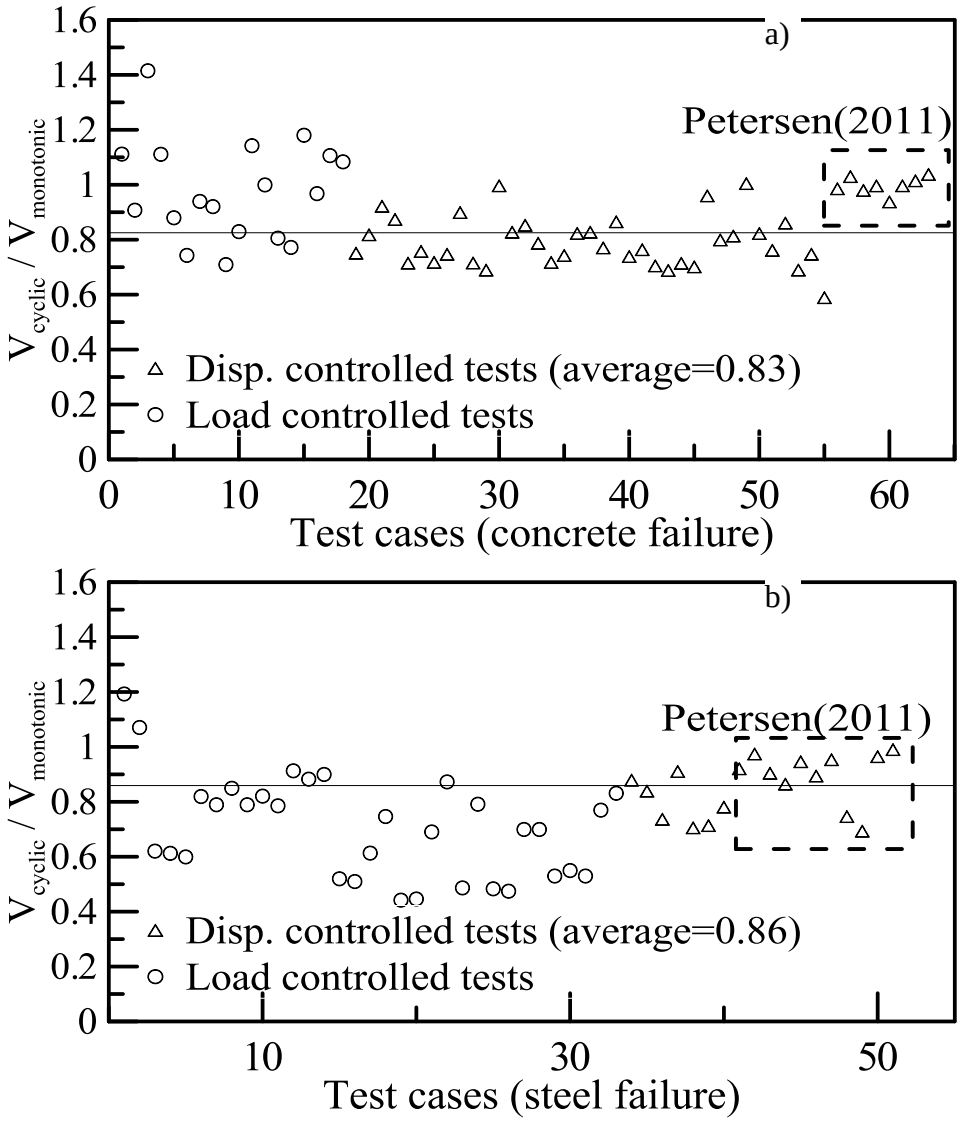

Figure 4.29: Capacity reduction factors for anchors in shear. a) tests with concrete breakout failure; b) tests with steel fracture

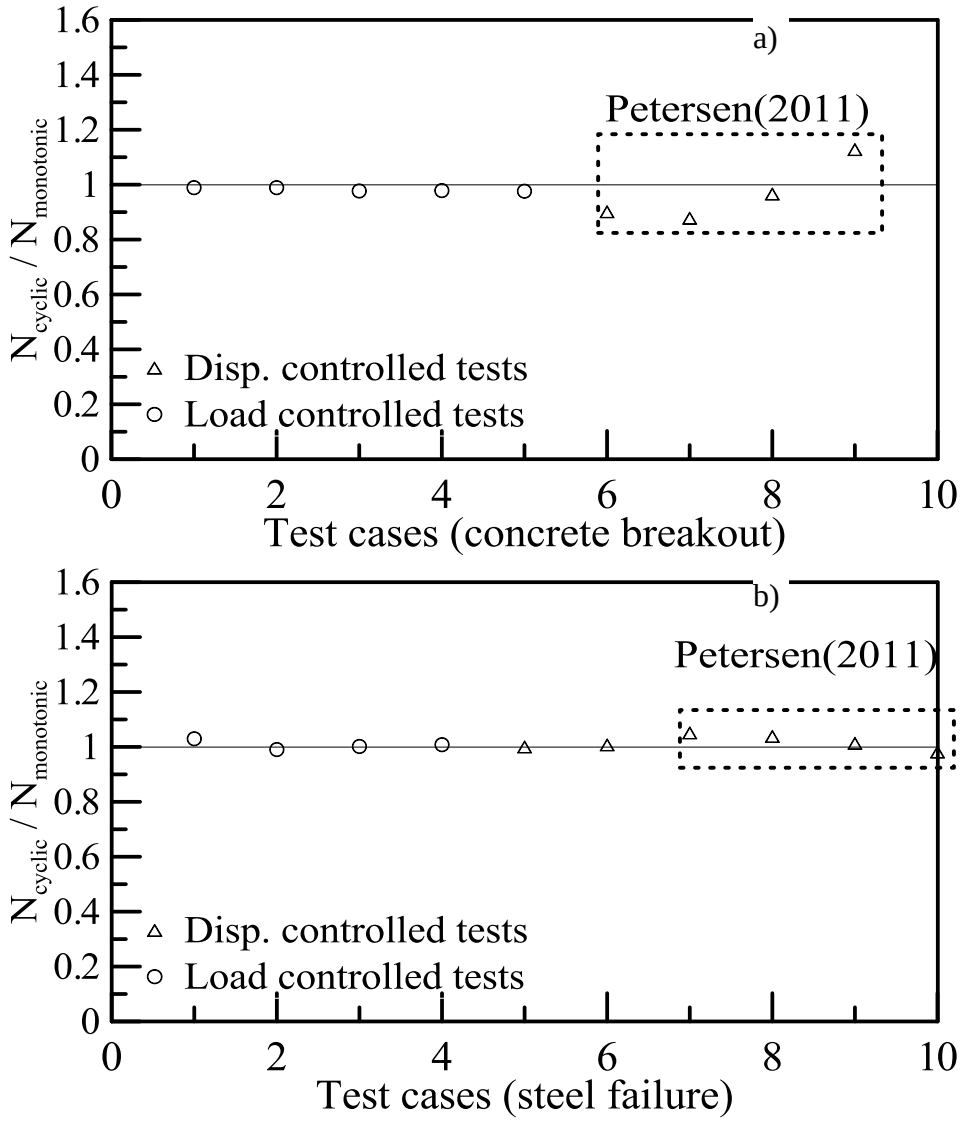

Figure 4.30: Capacity reduction factors for anchors in tension. a) tests with concrete breakout failure; b) tests with steel fracture

CHAPTER 5 Cyclic Tests of Anchor Rods in Shear

5.1 Introduction

This chapter presents an experimental study investigating the impact of low-cycle fatigue on the cyclic shear behavior of anchor bolts. The investigation considered the effects of ductility of anchor steel material on the shear capacity. Double-shear tests, along with the uniaxial tension tests, were carried out using three types of anchor steel: ASTM A193 Grade B7, referred as A193, ASTM A307 Grade 55, referred as A307, and ASTM A304 Grade 105, referred as A304 hereafter.

This report describes the experimental program in detail by providing an overview of the small scale test setup, testing procedures and test results associated with the discussion of experimental observations, detailed data for all experiments. An analysis of observations and a brief assessment of current design guidelines are provided for each shear investigated. Complete experimental programs and results of the anchor rod tests were provided in the following sections.

5.1.1 Test Setup

A total of 6 double shear tests for each type of anchor steel were conducted using 0.75-in. diameter ASTM A193 Grade B7 threaded rods. As shown in Figure 5.1, two threaded rods were subjected to shear simultaneously between a fabricated (1-in. thick) load plate and two (1-in. thick) plates fixed to the load frame mounted on the strong wall, and the shear load was applied using a MTS Model 244.31, 55 kip actuator with a full stroke of 5 inches horizontally mounted on the braced-column horizontal load frame. The test assembly, including such those fabricated load plate and the fixed plates, was designed to remain undamaged during testing and was reused for all eighteen tests.

In this group of tests, the test rods were inserted through a standard 1/8-in. oversized hole in both the load plate and the fixed plates, and the standard washers were removed to allow end rotations. The exposed lengths in this group of tests (i.e., the distance between the load plates and the fixed plates) varied from d_a to $4d_a$. To protect the holes in load plates, standard washers

were welded to each contact surface on the plates, as shown in Figure 5.8a. Additional plates were welded as webs on the fixed plates to prevent damages of the fixed plates due to the large out-plane bending moment along the fixed plates (Figure 5.8b). Nuts were hand tightened.

5.1.2 Instrumentation and Loading Protocol

The applied monotonically/cyclically shear forces (for two specimens) were monitored using a load cell with a sensitivity factor of 2mV/V. Two spring-loaded LVDT's from Sensotec with a measurement range of 6 in. were used to measure the displacements of the load plate, which is assumed to be the shear displacements of the specimens. The sensor data (i.e., force and displacement output channels from the actuators, and displacement from two LVDT's) were collected using an IO Tech DaqBook 2000 data acquisition system (four DBK43A strain gauge modules and a single 16 channel DBK85 voltage module) with a sampling rate of 2 kHz.

Monotonic shear loading (displacement) was applied linearly increasing load until failure by controlling the displacement of actuator in the first group of tests. Displacement controlled loading has the benefit of allowing the post peak behavior of tests to be captured more accurately than in force controlled loading scenarios. However, cyclic shear testing on the second group of tests applied force-controlled loading. The cyclic loading history consists of sets of increasing reversed lateral load cycles (three cycles per set/group), with amplitudes of 4, 8, 12, 16, 20, 28, 32, and 40 kips, as shown in Figure 5.1b.

5.2 ASTM A193 Grade B7 (A193)

5.2.1 Coupon Tension Tests

Equipments for full-size testing of these 0.75-in. diameter anchor rods were not available, thus three tests using 0.50-in. diameter coupons, milled from ASTM A193 Grade B7 rods as shown in Figure 5.2, were conducted in accordance with Test Methods and Definitions A 370. The tests were conducted under monotonic displacement control using a MTS loading frame with 55 kips tension/compression load cell and LVDT for displacement control as shown in the insert photos of Figure 5.3. The data acquisition system dependent of the testing machine is allowed to capture the displacement and the corresponding loads from load cell.

A typical loading history of A193 anchor rods is shown in Figure 5.4, where a tensile test with necking localization was captured. The A193 anchor rods exhibited the local necking, and the cup-cone tensile fracture surfaces (Figure 5.5), which is typical for ductile metals. It also can be confirmed from the load vs. displacement curve, as shown in Figure 5.6. The stresses were calculated from measured load by dividing the initial net area. The average engineering strains were calculated from measured displacement by dividing the 2-in (50.8-mm) gauge length. Figure 5.7 showed the stress-strain response of A193 anchor steel.

The yield strength f_y (as determined by the 0.2% offset method) is 130 ksi and f_{ut} is140 ksi for the A193 anchor steel. The yield strength and ultimate strength were approximately 19% and 11% greater than the minimum specified strength of 105 ksi and 125 ksi according to the ASTM standard. The elongation of test coupon is 17%, larger than the minimum elongation of 16% specified in the ASTM standards. In general, if there are no coupon tests available, it is conservative to use specified yield strength, ultimate strength and the minimum elongation specified in the ASTM standards.

5.2.2 Double Shear Tests

The anchor exposed length is the key point among the influential factors for the shear behavior of an exposed anchor under monotonic and cyclic loadings. Hence, two groups of double-shear tests using threaded rods with various exposed lengths were conducted: under monotonic shear displacement in the first group of tests while under reversed cyclic shear load for the specimens in the second group. Table 5.1 presents the test matrix for the double-shear tests. The table includes key information about each experiment, including information regarding the exposed lengths investigated and the ultimate capacities. A193 anchor rods were shown in the first row of Table 5.1 under monotonic and cyclic loadings cases. Description of the test setup was provided below followed by the discussion of results.

5.2.3 Monotonic shear test results

The load vs. displacement curves of the A193 anchor rods under monotonic loading were shown in Figure 5.9 and ultimate shear capacities were listed in Table 5.1, in which the experimental information and results are summarized for all anchor rod tests, including the peak shear loads. The stiffness and ultimate capacity generally decrease with an increase in the exposed length.

The specimen with an exposed length of d_a showed a shear-dominant behavior (see the first solid lines in Figure 5.9). There was obvious shear deformation with sudden failure based on the load-displacement curve, even though flexural yielding was also inspected in fractured surfaces for these rods discussed in the later section. The behavior changed for specimens with larger exposed lengths. The load vs. displacement curves indicated a flexural-dominant behavior for the specimens with an exposed length of $2d_a$. Flexural yielding of the specimens as shown by the stiffness degradation indicated a larger impact from bending and a larger reduction of cross sectional area, which may explain the lower capacity observed in these specimens. The initial part of the load vs. displacement behavior for specimens with an exposed length of $4d_a$ showed a flexural-dominant behavior as well. However the stiffness and shear capacity increased at larger displacements (Figure 5.9 and Table 5.1). Such post-yield, strain hardening type of behavior was observed due to tension close to failure.

A 193-d_a-MD

Anchor rods having an exposed length of d_a subjected to shear force represents a shear-dominant failure mode. The deformation of A193 anchor rod with an exposed length of d_a and the fracture surface were plotted in Figure 5.10 and Figure 5.11. On the fracture surface in Figure 5.11, it illustrated that the fracture of the anchor rod initiated a flexural crack at the location of yellow solid line in Figure 5.11 and then failed in shear fracture after crack opening till purple dashed line in Figure 5.11. The fracture surface confirmed the shear-dominant fracture with a shining flat zone due to crystal slip.

A 193-2d_a-MD

The deformation of A193 anchor rod with an exposed length of $2d_a$ and the fracture surface were plotted in Figure 5.12 and Figure 5.13. The shear capacity of the specimen with an exposed length of $2d_a$ dropped significantly, as shown in Figure 5.9. This might have been due to a reduced cross sectional area that was subjected to shear fracture. Such reduction was likely caused by flexural cracks as described in Figure 5.13a and Figure 5.13b. Figure 5.13a and Figure 5.13b showed two fracture surfaces from one fractured anchor rods in the double shear tests (Figure 5.12). On the fracture surface of one side of the rod in Figure 5.13a, the flexural crack initiation sites were present, with one main crack that led to failure. The cracks initiated at a diameter transition opposite to the support bearing and the most area of final failure (the area as

shown intersected by yellow solid line and purple dashed line (in Figure 5.13a and Figure 5.13b), was caused by opening of the flexural crack associated with the main crack. There was a small fracture area near the fracture edge along shear direction. This was most likely caused by mechanical damage of the fracture surface that occurred due to tension prior to final failure (However, the area of tension was relative small and thus final capacity had no apparent increase). It was easy to observe this change from the fracture surface of the other side of the same rod in Figure 5.13b. The fracture surface exhibited an obvious transition (illustrated in purple dashed line) from different fracture modes, which initially showed flexural-dominant fracture and then presented a failure mode with a 45 degree shear slip due to the tension.

A 193-4d_a-MD

The A193 anchor rods with an exposed length of 4d_a, plotted in Figure 5.14a, experienced much larger deformation compared with anchor rods with an exposed length of d_a or 2d_a. The local bearing deformation and the crack opening were observed in Figures 5.14b and 5.14c, respectively. Unlike the shear- or flexural-dominant failure modes of anchor rods with an exposed length of d_a or 2d_a, this rod exhibited an apparent tension-dominant mode, as shown in Figure 5.15a and Figure 5.15b.

5.2.4 Cyclic test results

This series of tests were used to investigate the shear capacities under cyclic shear loading. As described previously, the test setup was identical to those under monotonic loading. All ASTM A193 Grade B7 anchor rods were mounted on the rigid load plates. Similar behavior was observed in the cyclic tests. Specifically, flexural crack was initiated after the yielding of the specimen. The damage to the anchor rods progressively increased due to the propagation of the crack, resulting in reduced strength and stiffness, compared to those results obtained under monotonic loading. In fact, such degradation in strength and stiffness were not significant because of the following post-hardening behavior. Since it is well known that for a typical steel coupon under tension, the cyclic behavior is enveloped by the monotonic behavior without marked reduction. Compared to the measured shear capacities of anchor rods under monotonic loading presented previously in Figure 5.9 and Table 5.1, the ultimate load (of all three anchor rods) was approximately 4% lower than those under monotonic loading.

Figure 5.16 plots the displacement during the course of the cyclic shear loading. Similar to those results under monotonic loadings as described previously, the stiffness and ultimate capacity generally decrease with an increase in the exposed length. The behavior for specimens with larger exposed lengths and failure modes (of anchor rods) were likely dominated by shear, flexural and even tension action. Particularly for the rods with an exposed length of $4d_a$, prior to failure, the rod displaced significantly higher stiffness and capacities with larger displacements.

A 193-d_a-RL

As shown in Figure 5.16, there was no apparent flexural yielding during the force cycles. Figure 5.17 plotted the final deformation of A193 anchor rod with an exposed length of d_a and the fractured rods. Figure 5.18 showed the fracture surfaces in details. Inspections made after the test revealed damage in the form of localized flexural crack initiation was clearly displayed at the location of yellow solid line (in Figure 5.18a and Figure 5.18c). Also Figure 5.18 showed the evidence of shear-dominant fracture for this type of rods because flexural crack opened till purple dashed line and most of the cross area were fractured by shear, which also could be confirmed by the slight change in stiffness before the failure in Figure 5.16.

A 193-2d_a-RL

Figure 5.19 plotted the final deformation of A193 anchor rod with an exposed length of $2d_a$. It should be mentioned from the observation of the experimental test that the second fractured anchor rod had further deformation and fractured into three pieces after the first rod was broken, in which local bearing and crack opening were shown in Figure 5.19b and Figure 5.19c. Such failure was an artifact of the loading history since they coincide with further displacements under force-controlled loading after the first rod had already fractured. Thus, it is not appropriate to consider such fracture as one of failure modes from the experiments. However, this failure (Figure 5.19b and Figure 5.19c) provided important information regarding overall response of the anchor rod, which may be used to analyze the considerations of the fracture process for anchor steel.

As observed in Figure 5.16, flexural yielding of the anchor rods started during the 8 kips (35.6 kN) amplitude force cycle. Note that the stiffness had a slight change under the same amplitude

force cycles before yielding and, in general, the cumulative fatigue damge due to cyclic loading was not marked.

Figure 5.20 illustrated the fracture path, identical to those under monotonic loading, which revealed damage was mainly controlled by the flexural crack (shown in the area within yellow solid line and purple dashed line (refer schematic in Figure 5.20)). The extensive damage due to tension action was observed from the fracture surface near the failure.

A 193-4d_a-RL

Figure 5.21 displayed the final deformation, local bearing and crack opening for the A193 anchor rods with an exposed length of 4d_a. As identically observed for the rods under monotonic loadings in previous section, these rods exhibited significant residual deformations up to about one inch and evidence of tension-dominant mode (Figure 5.22). The stiffness and capacities had a significant increase after initially flexural yielding.

5.3 ASTM A307 Grade 55 (A307)

5.3.1 Coupon Tension Tests

Three standard 0.50-in. diameter coupons of A307 Grade 55 (in Figure 5.23) were tested to provide the constitutive relationship for the anchor steel. The tests were carried out using the MTS loading frame (Figure 5.24). A typical loading history of A307 anchor rods was shown in Figure 5.25, where localized necking and the cup-and-cone tensile failure mode (Figure 5.26) were observed. It confirmed that the A307 anchor rods exhibited the evidence of a typical ductile metal. Figure 5.27 plotted the load vs. displacement behavior.

The stresses were calculated from measured load by dividing the initial net area. The average engineering strains were calculated from measured displacement by dividing the 2-in gauge length. Figure 5.27 showed the stress-strain response of A307 anchor steel. It was observed that A 307 had a relatively short plateau and strain hardening with a slight increase in strength before the localized necking occurred, however, the total behavior generally displayed a ductile material with 24.5%.

The yield strength f_y (as determined by the 0.2% offset method) was 70 ksi and f_{ut} was 71.6 ksi for the 3/4" diameter rod. The yield strength and ultimate strength of the 3/4" diameter rod is approximately 27% greater and 4% smaller than the minimum specified strength of 55 ksi and 75 ksi in the ASTM standards. The elongation of test coupon is 24.5%, larger than the minimum elongation of 23% specified in the ASTM standards standard. In general, if there are no coupon tests available, it is conservative to use specified yield strength, ultimate strength and the minimum elongation in the ASTM standards.

5.3.2 Double-Shear Tests

Two groups of double-shear tests with were performed using threaded rods with various exposed lengths from d_a to $4d_a$ under two different loading cases (i.e., monotonic shear displacement and reversed cyclic shear load). As shown in Table 5.1 for the test matrix for the double-shear tests, the test setup and load protocol were identical to those for A193 anchor rods as mentioned in the earlier section. This section described the experimental program and results in detail. Also this section presented key data and representative response plots associated with the discussion of experimental observations, detailed data for all experiments.

5.3.3 Monotonic test results

Figure 5.28 plotted the load vs. displacement curves of the A307 anchor rods under monotonic loading and also ultimate shear capacities were listed in Table 3.1. The stiffness at initial loading generally decreases with an increase in the exposed length. Unlike the measured results for A193 anchor rods with decreasing shear capacities, the capacities of such specimens had no marked drop, even a significant increase in the specimen with an exposed length of $2d_a$. The behavior changed for specimens with larger exposed lengths. Yielding of the specimens as shown by the stiffness reduction indicated a larger impact from bending and a larger reduction of cross sectional area, which may explain the lower capacity observed in these specimens. The load vs. displacement curves (in Figure 5.28) indicated a tension-dominant behavior for the specimens with an exposed length of $2d_a$ and $4d_a$. Note that significant increase in the displacement of the specimen with an exposed length of $2d_a$ may be explained by its fracture mode in the following sub-section.

A 307-d_a-MD

Figure 5.29 plotted the deformation of A307 anchor rod with an exposed length of d_a and the fractured pieces. As observed for this double-shear test in Figure 5.29, only one anchor bolt exhibited severe damages, failing into pieces while the other bolt had a small deformation, indicating that the dominant failure mode for these rods was controlled by shear. The fracture surfaces of A307 anchor rod, illustrated in Figure 5.30, showed that the fracture of the anchor rod initiated a flexural crack at the location of yellow solid line and then failed by shear fracture.

A 307-2d_a-MD

Figure 5.31 showed the final deformation/fractured pieces of the specimen A307-2d_a-MD. Both anchor bolts were fractured to failure and exhibited significant deformation, indicating that the dominant failure mode was controlled by flexure or even tension. Figure 5.32 plotted four fractured surfaces from two rods in double shear test. Unlike those identical exposed-length specimens A193-2d_a-MD or A304-2d_a-MD which experienced an obvious transition from flexural crack opening and tension, it was found that the first two fractured surfaces of specimens A307-2d_a-MD, identical to those for A193-4d_a-MD or A304-4d_a-MD, exhibited obvious tension-dominant failure modes with a 45 degree fracture. It may be the reason why shear capacity of A304-2d_a-MD is higher than those for A307-d_a-MD. Inspection made after the test indicated that the second two fractured surfaces were caused by the further deformation to failure after the first rod was fractured to pieces. Note that the typical cup-and-cone fracture surface was displayed in this rod.

A 307-4d_a-MD

Figure 5.33 showed the final deformation/fractured pieces of the specimens A307-4d_a-MD. Like the identical group in specimens A193-4d_a-MD and A304-4d_a-MD, the tension-controlled fracture can be seen in Figure 5.34.

5.3.4 Cyclic test results

Figure 5.35 plotted the load vs. displacement curves during the course of the cyclic shear loading. Compared to the measured shear capacities of anchor rods under monotonic loading presented previously in Figure 5.28 and Table 5.1, the ultimate capacity was approximately 3% lower than that obtained in the monotonic tests. Similar to those results under monotonic

loadings as described previously, the ultimate capacity of these rods have no obvious decrease with an increase in the exposed length while significant increase in shear capacity for specimens A 307-2d_a-RL were displayed. Also the stiffness of load vs displacement curves exhibited apparent "strain-hardening" behavior due to tension earlier at specimens with an exposed length of 2d_a rather than 4d_a at A 193 or A 304 (observed at later section).

A 307-d_a-RL

Figure 5.36 plotted the deformation of A307 anchor rod with an exposed length of d_a (A 307-2d_a-RL) and the fractured pieces. As observed for this double-shear test (Figure 5.37), both anchor bolts fail by fracture and had a slight deformation before failure, indicating that the dominant failure mode for these rods was controlled by shear. It was also found that the deformation had a slight increase during the following cycles of the same displacement group (Figure 5.35). The fracture surfaces of A307 anchor rod, illustrated in Figure 5.37, showed that the fracture of the anchor rod initiated a flexural crack at the location of yellow solid line and then failed by shear fracture.

A 307-2d_a-RL

Figure 5.38 showed the final deformation/fractured pieces of the specimens A307-2d_a-RL. Both anchor bolts were fractured to failure and exhibited significant deformation. Figure 5.39 plotted four fractured surfaces from two rods in double shear test and both rods were fractured into pieces approximately at the same time based on the inspection made after experimental test. Such fractured surfaces exhibited obvious tension-dominant failure modes with a 45 degree fracture or cup-and-cone fracture.

A 307-4d_a-RL

Figure 5.41 showed the final deformation/fractured pieces of the specimens A307-4d_a-RL. Like the identical group in specimens A193-4d_a-MD and A304-4d_a-MD, the tension-controlled fracture can be seen in Figure 5.42.

5.4 ASTM A304 Grade 36 (A304)

5.4.1 Coupon Tension Tests

ASTM A304 is a stainless steel with great ductility (min. 30% elongation). Three standard 0.50-in. diameter coupons of A304 Grade 55 (in Figure 5.43) were tested to provide the constitutive relationship for anchor steel. The tests were carried out by the MTS loading frame (Figure 5.45). A typical loading history of A304 anchor rods was shown in Figure 5.44, where severe localized necking and the cup-and-cone tensile failure mode (Figure 5.44) were observed. It confirmed that the A304 anchor rods exhibited the evidence of a typical ductile metal. Figure 5.46 plotted the load vs. displacement behavior.

The stresses were calculated from measured load by dividing the initial net area. The average engineering strains were calculated from measured displacement by dividing the 2-in (50.8-mm) gauge length. Figure 5.47 showed the stress-strain response of A304 anchor steel.

The yield strength f_y (as determined by the 0.2% offset method) was 80 ksi and f_{ut} was 100.5 ksi. The yield strength and ultimate strength of the 3/4" diameter rod is approximately 166.7% and 85% greater than the minimum specified strength of 30 ksi and 70 ksi in the ASTM standards standard. The 63% elongation of stainless steel test coupon displayed excellent ductile compared to the minimum elongation of 30% specified in the ASTM standards. Again, if there are no coupon tests available, it is conservative to use specified yield strength, ultimate strength and the minimum elongation in the ASTM standards.

5.42 Double-Shear Tests

In this series of double-shear tests, identical two groups of double-shear tests with were conducted using threaded rods with various exposed lengths from d_a to $4d_a$ under two different loading cases (i.e., monotonic shear displacement and reversed cyclic shear load). As shown in Table 3.1 for the test matrix for the double-shear tests, the test setup and load protocol were identical to those for A193 anchor rods as mentioned in the earlier section. This section described the experimental program and results in detail.

5.4.3 Monotonic test results

Stainless steel A304 exhibited great ductility, as shown in Figure 5.48. Figure 5.49 plotted the load vs. displacement curves of the A304 anchor rods under monotonic loading and also ultimate

shear capacities were listed in Table 3.1. The stiffness and capacities at initial loading generally decrease with an increase in the exposed length. Unlike the observation from those in A193 and A 307 anchor rods which had tension effects in much larger exposed length, the stiffness (of all types of rods) displayed "strain-hardening" behavior after initial flexural yielding. It can also be confirmed from the load vs. displacement curves (in Figure 5.49) that a tension behavior was observed to various extent for all the specimens with an exposed length of d_a, $2d_a$ and $4d_a$.

A 304-d_a-MD

Figure 5.50 plotted the deformation of A304 anchor rod with an exposed length of d_a (A304-4d_a-MD) and the fractured pieces. As observed for this double-shear test in Figure 5.50, anchor bolts exhibited significant deformation and localized area reduction near support bearing. The fracture surfaces of specimen A304-4d_a-MD, illustrated in Figure 5.51, showed that the fracture of the anchor rod initiated a flexural crack at the location of yellow solid line and then failed by shear fracture with shining surfaces after crack opened till purple dashed lines.

A 304-2d_a-MD

Figure 5.52 showed the final deformation/fractured pieces of the specimens A304-2d_a-MD. Both anchor bolts were fractured to failure and exhibited significant deformation, indicating that the dominant failure mode was controlled by flexure or even tension. The shear capacity of the specimens A304-2d_a-MD dropped significantly. This might have been due to a reduced cross sectional area that was subjected to shear fracture. Such reduction was likely caused by flexural cracks as described in Figure 5.53a and Figure 5.53b. Two fracture surfaces from one fractured anchor rods in the double shear tests (Figure 5.53). The cracks initiated at a diameter transition opposite to the support bearing and the most area of final failure (the area as shown intersected by yellow solid line and purple dashed line (accordingly, in Figure 5.53a and 3.51b), was caused by opening of flexural crack associated with the main crack. There was a small fracture area near the fracture edge along shear direction. This was most likely caused by mechanical damage of the fracture surface that occurred due to tension prior to final failure. It will be easy to observe this change from the fracture surface of the other side of the same rod in Figure 5.53b. The fracture surface exhibited an obvious transition (illustrated in purple dashed line) from different fracture modes, which initially showed flexural-dominant fracture and then presented a failure mode with a 45 degree shear lip due to the tension.

A 304-4d_a-MD

Figure 5.54 showed the final deformation/fractured pieces of the specimens A307-4d_a-MD. Like the identical group in specimens A193-4d_a-MD and A304-4d_a-MD, the tension-controlled fracture can be seen in Figure 5.55.

5.4.4 Cyclic test results

Figure 5.56 plotted the load vs. displacement curves during the course of the cyclic shear loading. Compared to the measured shear capacities of anchor rods under monotonic loading presented previously in Figure 5.49 and Table 3.1, Similar to those results under monotonic loadings as described previously, the stiffness and final capacities in accordance with load vs. displacement curves generally decreased with the increase of exposed length. The ultimate capacities for specimens A304-d_a, A304-4d_a and A304-4d_a were approximately 25%, 11% and 12% lower than those obtained under monotonic loading, respectively. Especially anchor rods with larger exposed length exhibited tension behavior.

A 304-d_a-RL

Figure 5.57 plotted the deformation of A304 anchor rod with an exposed length of d_a (A 304-d_a-RL) and the fractured pieces. As observed for this double-shear test (Figure 5.58), the dominant failure mode for these rods was controlled by shear, even though flexural fracture was observed with a fracture area covered between yellow solid lines and purple dashed lines). It was also found, however, that anchor rod had a more severe accumulative damage during cyclic loading than that observed under monotonic loading.

A 304-2d_a-RL

Figure 5.59 showed the final deformation/fractured pieces of the specimens A307-2d_a-RL. Figure 5.60 plotted a fractured surface. Such fractured surfaces exhibited obvious tension-dominant failure modes with a cup-and-cone fracture after a small portion of flexural cracking opening, as shown in Figure 5.60.

A 304-4d_a-RL

Figure 5.61 showed the final deformation/fractured pieces of the specimens A307-4d_a-RL. Like the identical group in specimens A193-4d_a-MD/RL and A304-4d_a-MD/RL, the tension-controlled fracture can be seen in Figure 5.62.

5.5 Summary

All three types of steel widely used in tests (i.e., A193, A307 and A304) had great ductility (ductile material is defined to have at least 14% elongation for anchor steel in ACI 318-08). Figure 5.63 displayed the monotonic behavior of all three types of specimens with various exposed lengths. The failure was likely controlled by shear fracture when the exposed length was short (e.g., $1.0d_a$, which represents the anchors in a typical shear key connection in Figure 5.65). The ultimate strength of the anchor steel dominates the ultimate shear strength in this case. Note that the A304 steel in this study had exceptionally large ductility, therefore the tensile fracture may have likely affected the failure as indicated by the deformed shapes in Figure 5.50. This hypothesis can be verified by the fact that the exposed length did not affect the ultimate capacity of A304 anchor rods as shown in Figure 5.63. As the exposed length increased to $2.0d_a$, which represents the anchors in a column base connection in Figure 5.65, the shear-dominating failure was replaced by shear-tension failure. Both A193 and A307 anchor rods had a higher shear capacity. Meanwhile the stiffness of all three specimens reduced. The shear stiffness was further reduced when the exposed the length was increased to $4.0d_a$, which is close to the anchors in a bridge girder bearing connection in Figure 5.65. In this case, the failure is controlled by tension fracture after a large lateral displacement. The shear stiffness may be recovered as the anchors start to resist the shear loads through tension action.

In summary, the anchor rods with a relatively short exposed length (e.g., less than or equal to d_a in Figure 5.63a) may exhibit shear-dominant failure mode while the failure mode may combine the flexural fracture and shear when anchor rods with a moderate exposed length (e.g., $2d_a$). Such fracture mode can be featured by an obvious transition from flexural crack to shear fracture. Anchor rods with a larger exposed length (e.g., $4d_a$ and larger) may be controlled by the tension failure mode.

The behavior of the anchor rods under cyclic loading was similar to that observed in the monotonic tests, as illustrated in Figure 5.64. In most cases, the monotonic curves enveloped the cyclic curves. The cyclic loading was under load control, which caused negligible accumulative damage to the specimens. Specifically, only slight increases were observed after the first peak loads in each loading group. Such observed increase in the displacement after consecutive peak

loads in each load group may have also attributed to the local deformation of the loading plates near the holes. Therefore, the low-cycle fatigue of the anchor rods may have caused negligible impact on the anchor shear behavior. Furthermore, the shear capacities of anchors rods under cyclic loading had slight reduction, that is within 5%, compared to monotonic loading for A193 or A307 steel. However, the stainless steel A304 had much larger reduction in the shear capacities (a maximum of 25% reduction was observed in the test of anchor with an exposed length of $1.0d_a$). All the A304 specimens were controlled by tensile fracture after large lateral displacements. Therefore the propagation of flexural cracks may have contributed to the large capacity reduction. Further study is needed to better understand the impact of low-cyclic fatigue.

Table 5.1: Test matrix of double-shear tests

Steel Type	No.	l/d_a	Load type (Mono/Cyclic)	Ultimate Capacity P_v, (kips)	percentage
A 193	A 193-d_a-MD	1	Monotonic disp.	16.77	/
	A 193-2d_a-MD	2	Monotonic disp.	12.98	/
	A 193-4d_a-MD	4	Monotonic disp.	17.00	/
	A 193-d_a-RL	1	Reversed cyclic load	16.95	96%
	A 193-2d_a-RL	2	Reversed cyclic load	12.40	96%
	A 193-4d_a-RL	4	Reversed cyclic load	16.15	96%
A 307	A 307-d_a-MD	1	Monotonic disp.	10.82	/
	A 307-2d_a-MD	2	Monotonic disp.	12.50	/
	A 307-4d_a-MD	4	Monotonic disp.	9.84	/
	A 307-d_a-RL	1	Reversed cyclic load	10.40	101%
	A 307-2d_a-RL	2	Reversed cyclic load	11.95	96%
	A 307-4d_a-RL	4	Reversed cyclic load	9.45	95%
A 304	A 304-d_a-MD	1	Monotonic disp.	24.30	/
	A 304-2d_a-MD	2	Monotonic disp.	15.40	/
	A 304-4d_a-MD	4	Monotonic disp.	17.95	/
	A 304-d_a-RL	1	Reversed cyclic load	18.30	75%
	A 304-2d_a-RL	2	Reversed cyclic load	13.70	89%
	A 304-4d_a-RL	4	Reversed cyclic load	15.85	88%

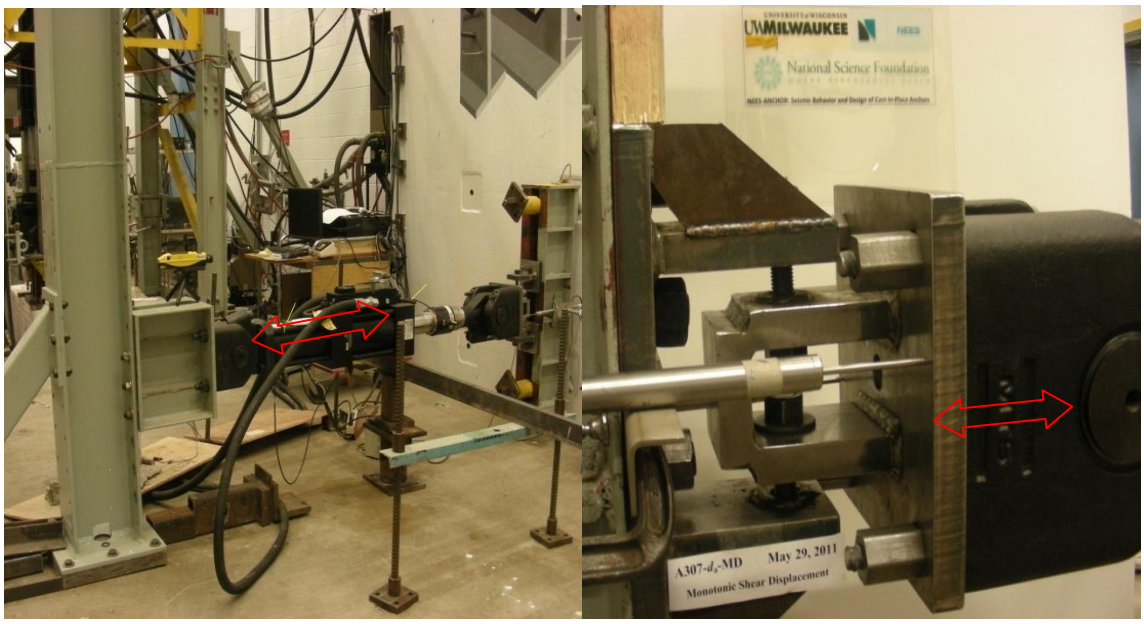

(a) Test setup

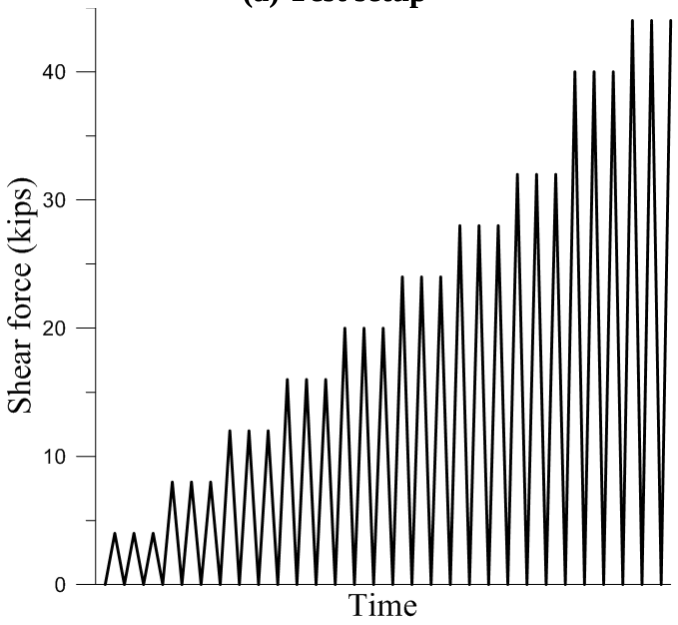

(b) load history for cyclic loading

Figure 5.1: Experimental program for double-shear test

Figure 5.2: Standard 0.5-in (12.7-mm) diameter coupon of A193 anchor rods

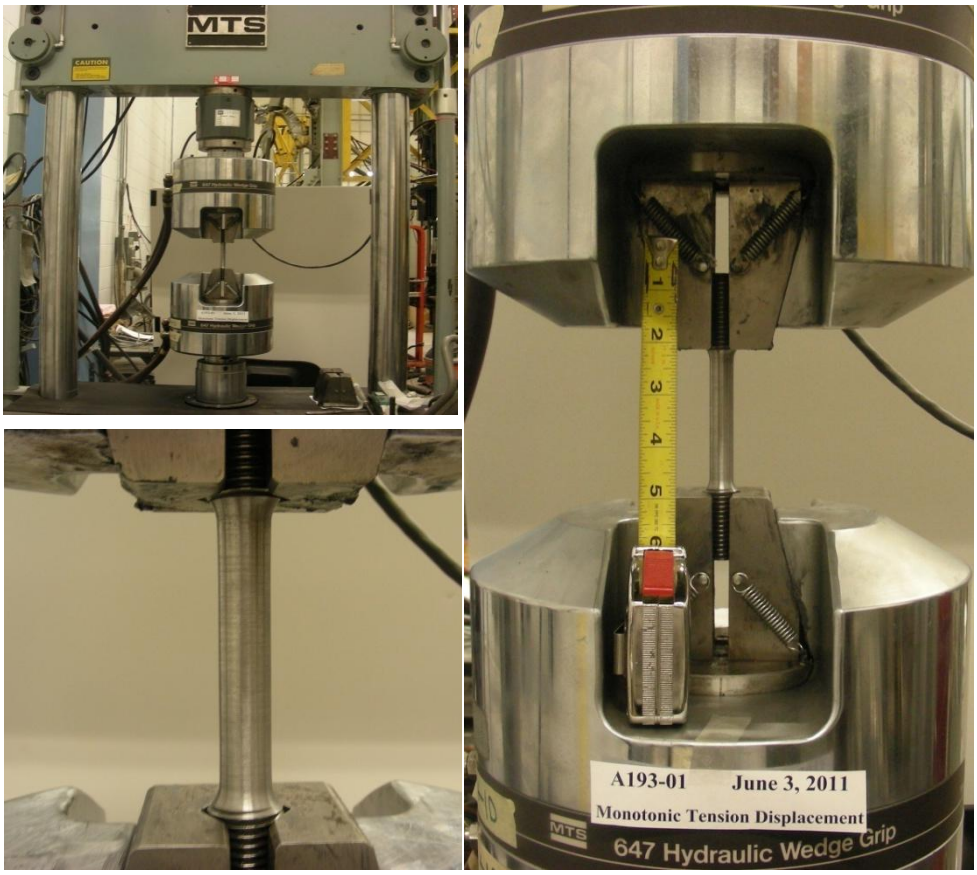

Figure 5.3: Coupon test in MTS testing machine

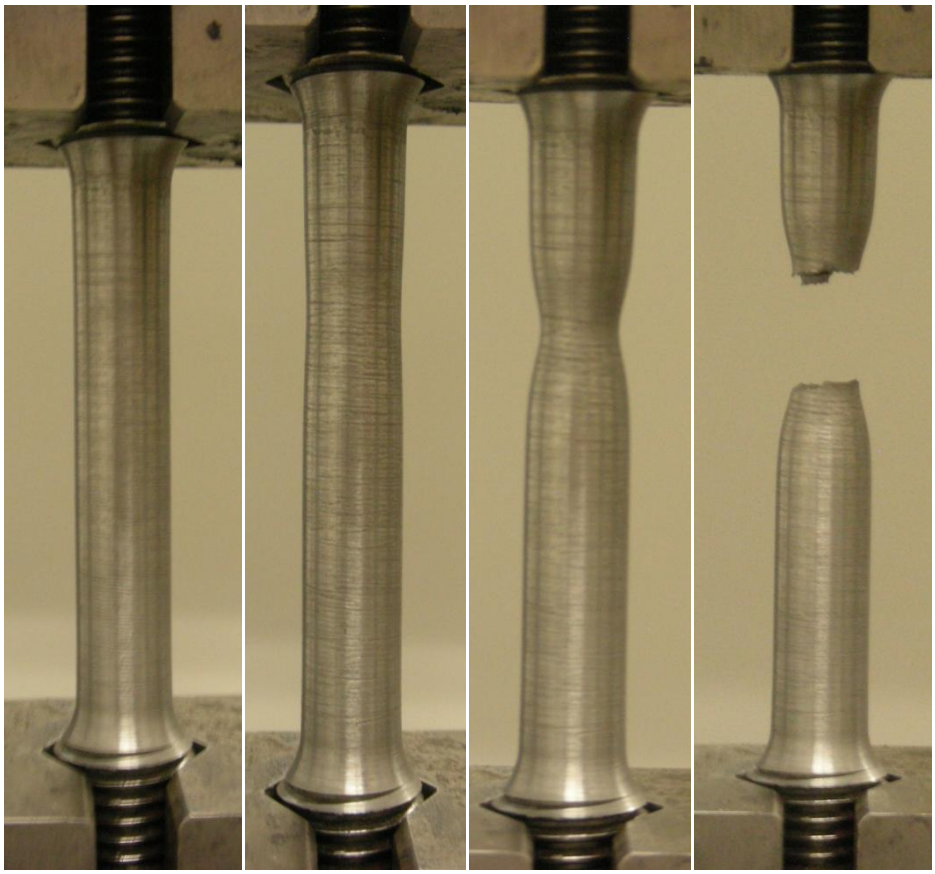

(a) (b) (c) (d)

Figure 5.4: load history: a) after yielding; b) starting necking; c) necking; d) fracture and failure

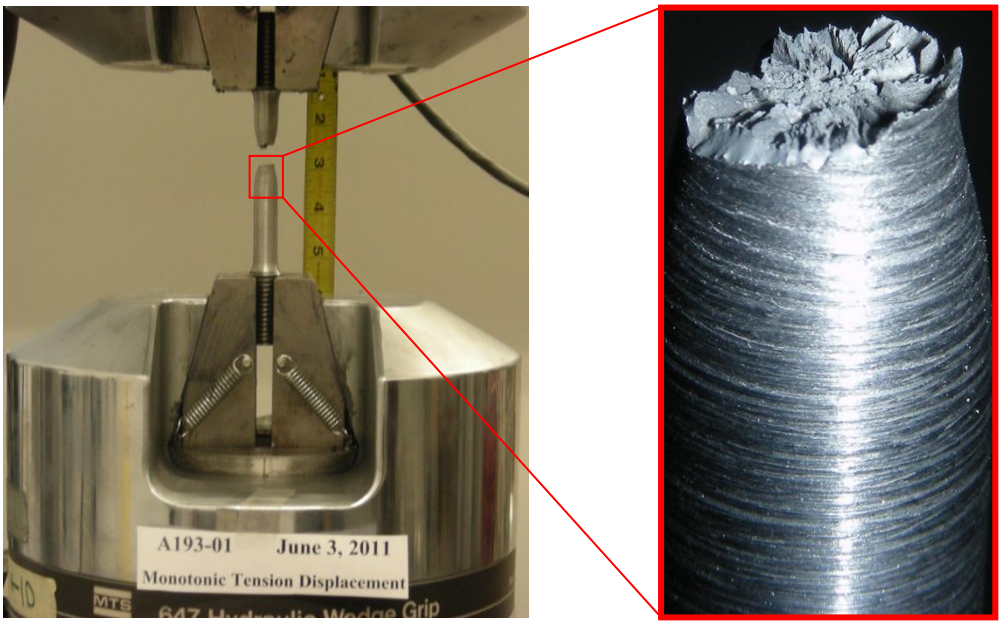

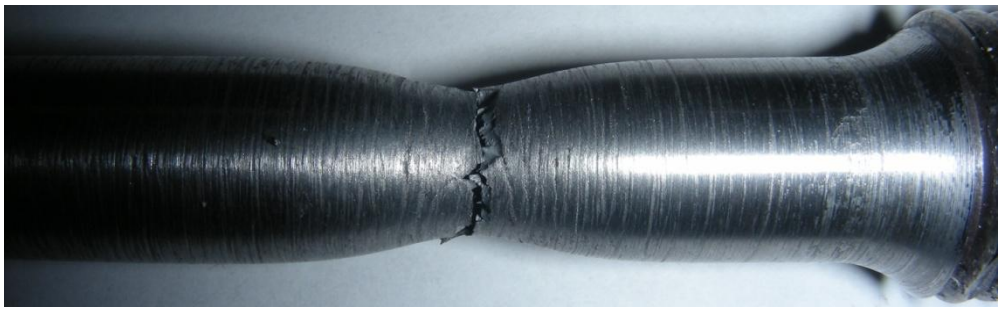

Figure 5.5: Tensile fracture surface of A193 anchor rod

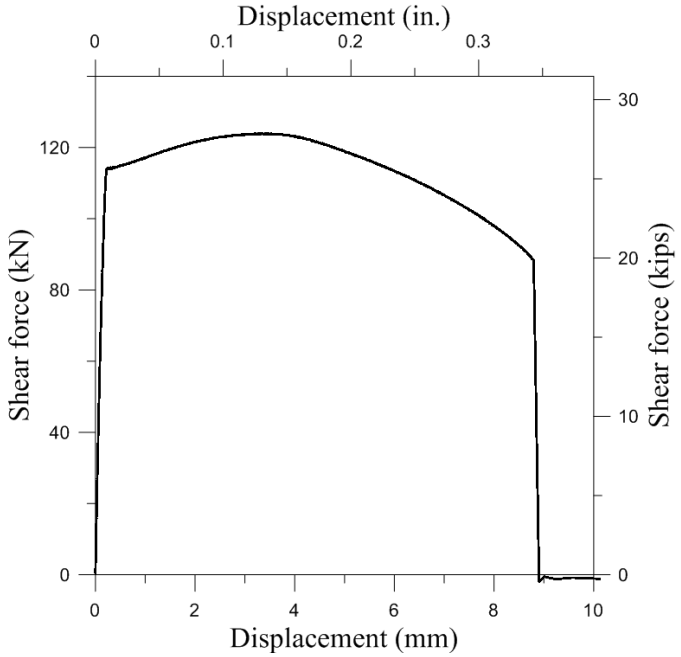

Figure 5.6: Load verse displacement of A193 anchor rod

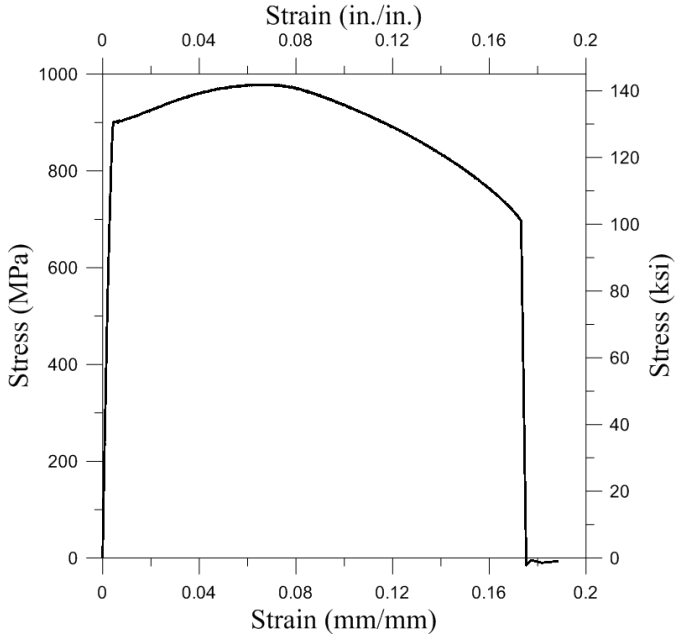

Figure 5.7: Stress verse strain curve of A193 anchor rod

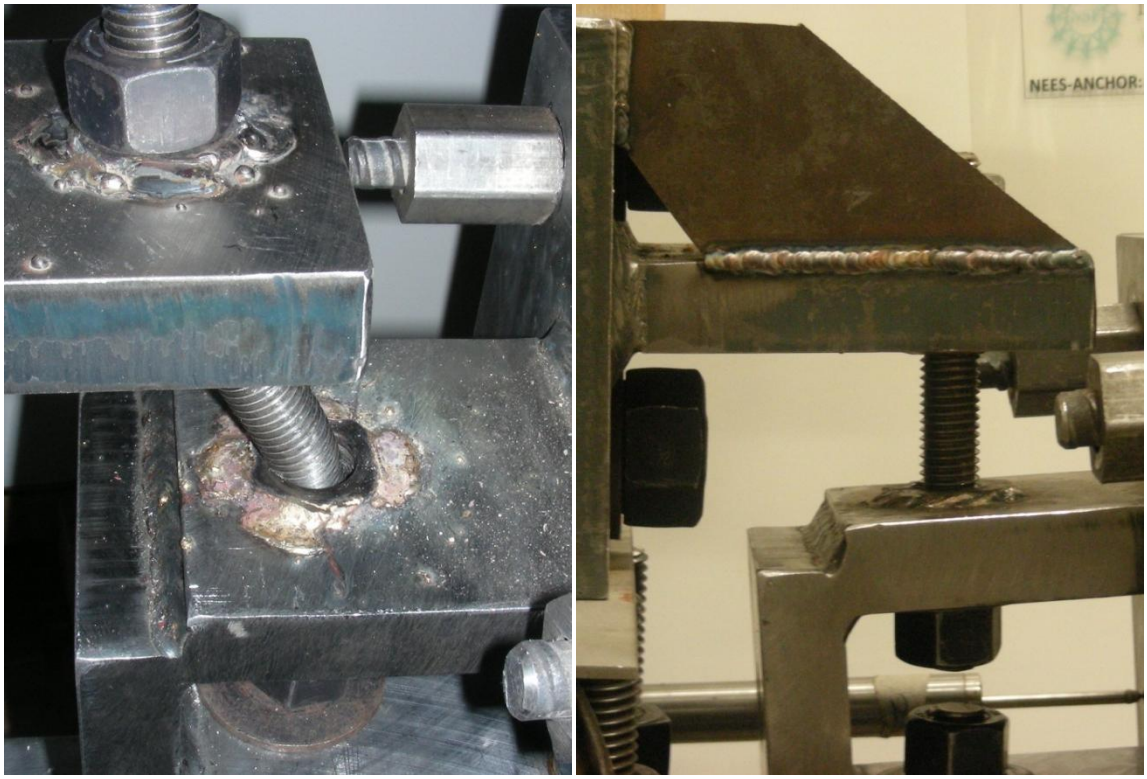

Figure 5.8: welded washers on the contact surfaces and plates welded on the fixed plates

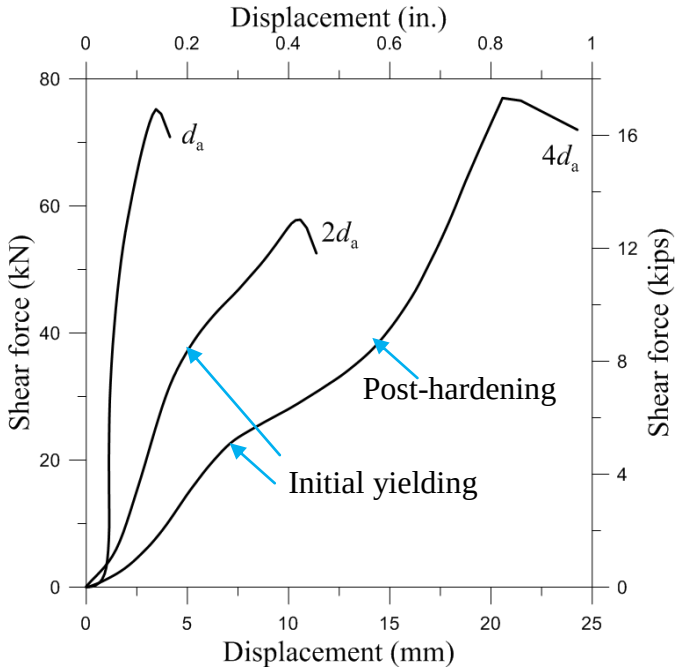

Figure 5.9: Load-displacement behavior of A193 anchor rods under monotonic loading

Figure 5.10: A193-da-MD

(a) one side of the fractured rod **(b) the other side of the rod**

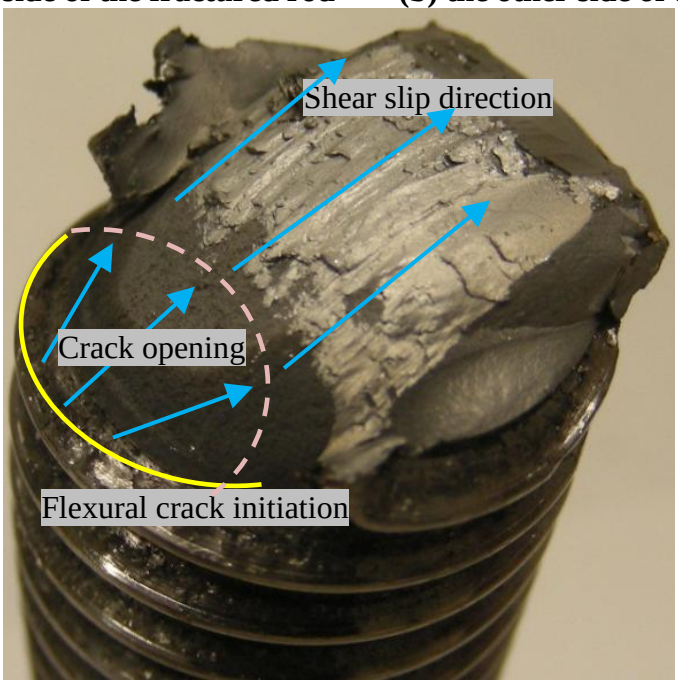

(c) fracture mode

Figure 5.11: fracture surfaces of A193-da-MD

Figure 5.12: A193-2da-MD

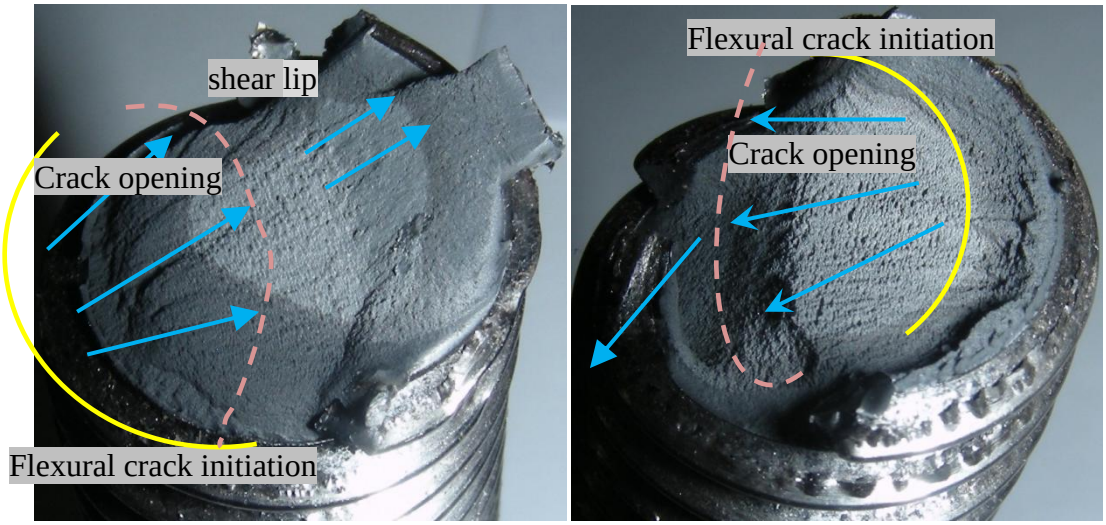

(a) one side of the fractured rod (b) the other side of the fractured rod

Figure 5.13: fracture surfaces of A193-2da-MD

(a) deformation of two anchor rods

(b) local bearing deforamtion

(c) flexural crack opening

Figure 5.14: A193-4da-MD

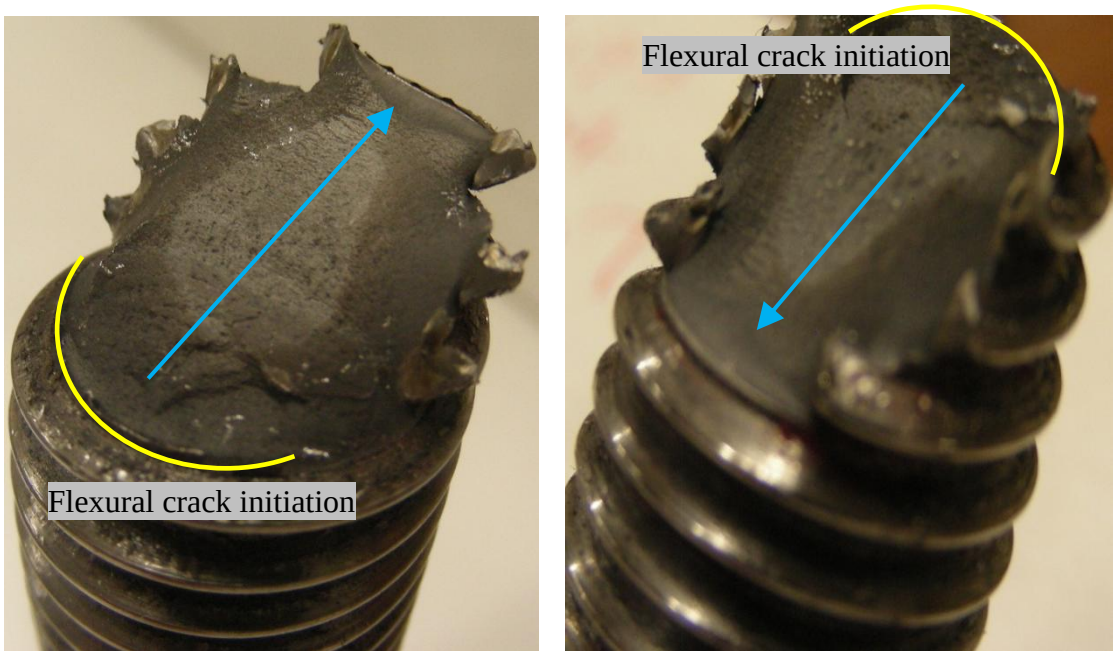

Figure 5.15: fracture surfaces of A193-4da-MD

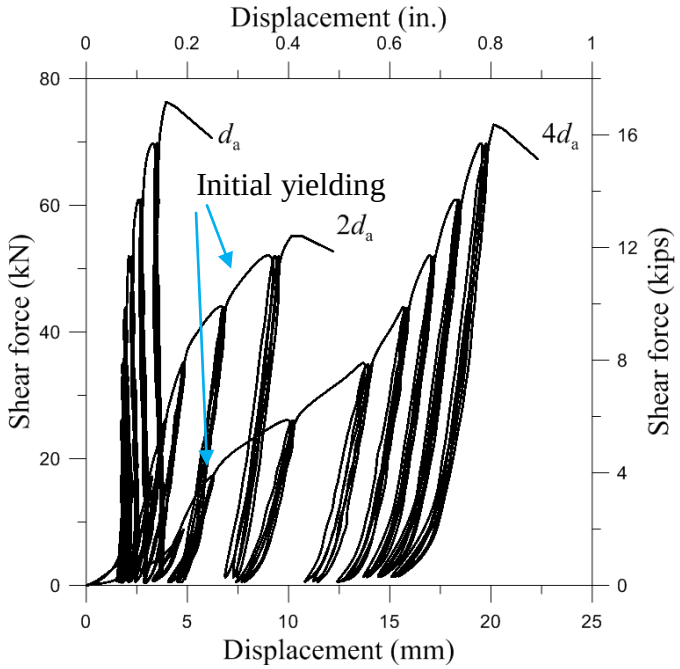

Figure 5.16: Load-displacement behavior of A193 anchor rods under cyclic loading

Figure 5.17: A193-da- RL

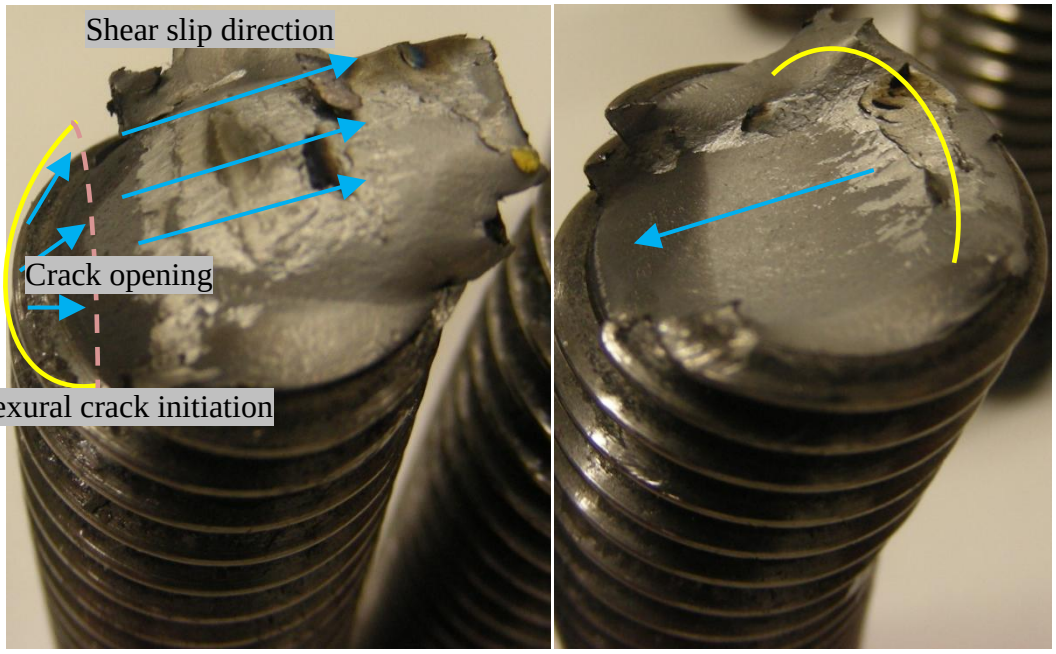

(a) one side of the first fractured rod (b) the other side of the first fractured rod

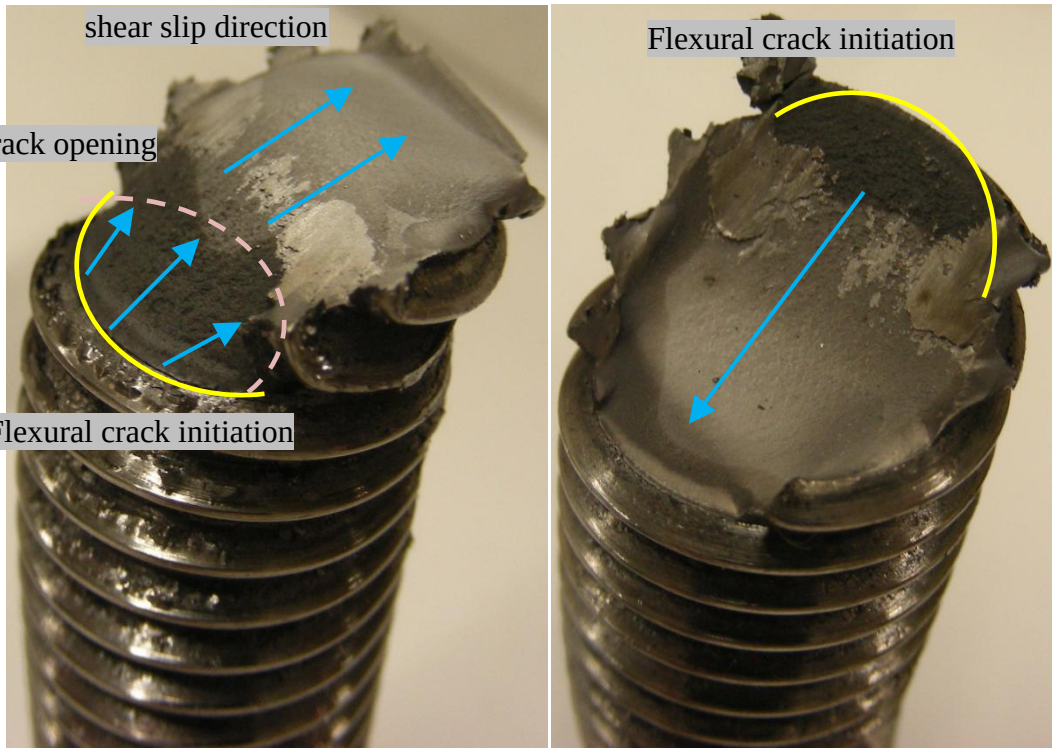

(c) one side of the second fractured rod (d) the other side of the second fractured rod

Figure 5.18: fracture surfaces of A193-da- RL

(a) deformation of two anchor rods

(b) local bearing deformation

(c) crack opening

Figure 5.19: A193-2da- RL

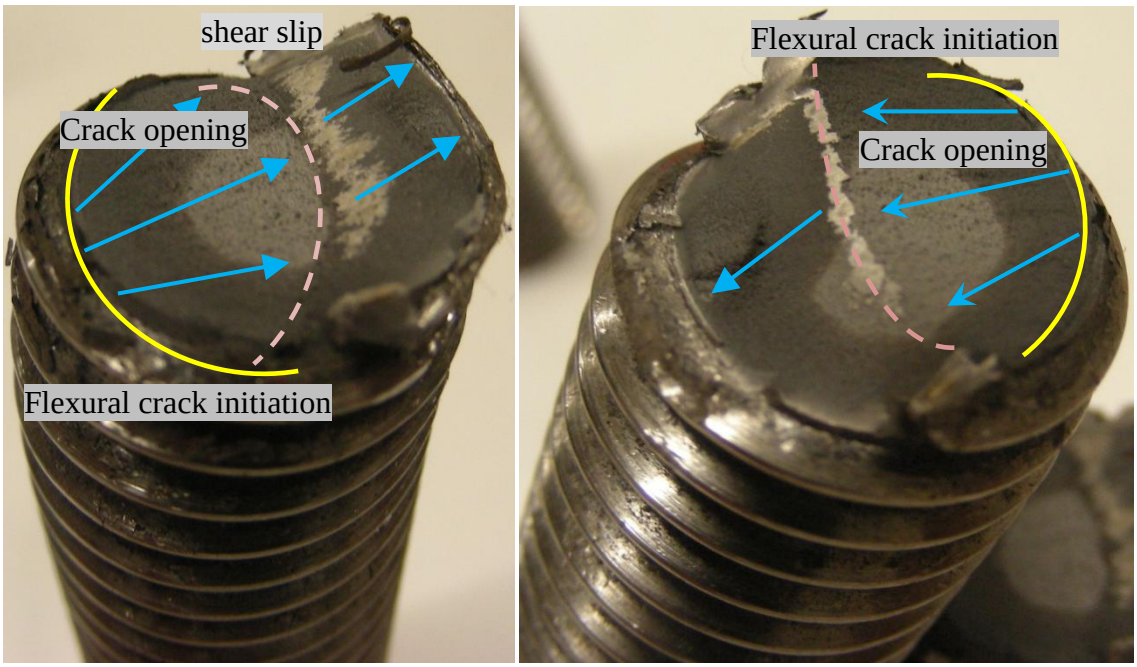

(a) one side of the fractured rod (b) the other side of the fractured rod

Figure 5.20: fracture surfaces of A193-2da-RL

Figure 5.21: A193-4da- RL

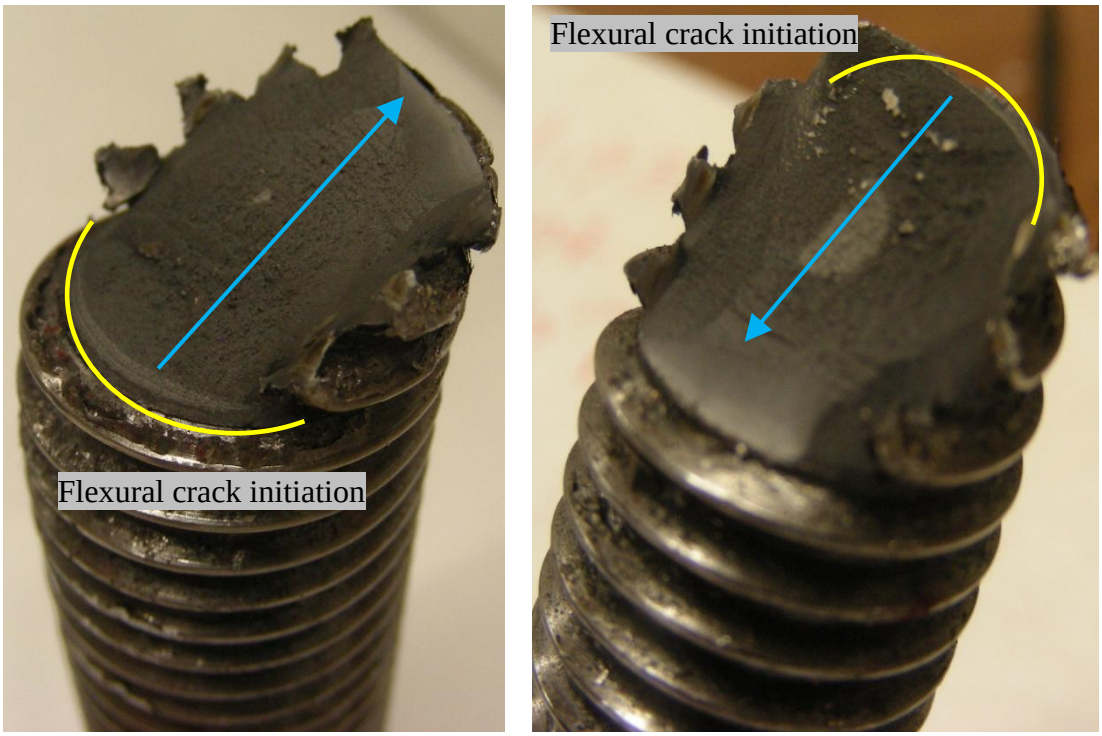

Figure 5.22: fracture surfaces of A193-4da-RL

Figure 5.23: Standard 0.5-in (12.7-mm) diameter coupon of A307 anchor rods

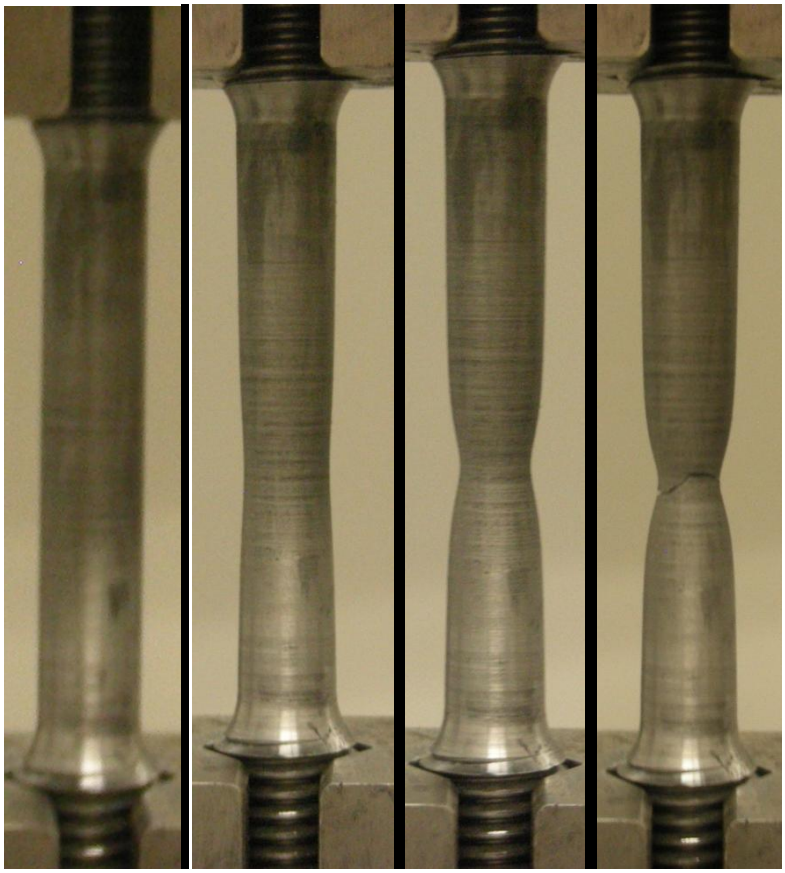

(a) (b) (c) (d)

Figure 5.24: load history: a) after yielding; b) starting necking; c) necking; d) fracture and failure

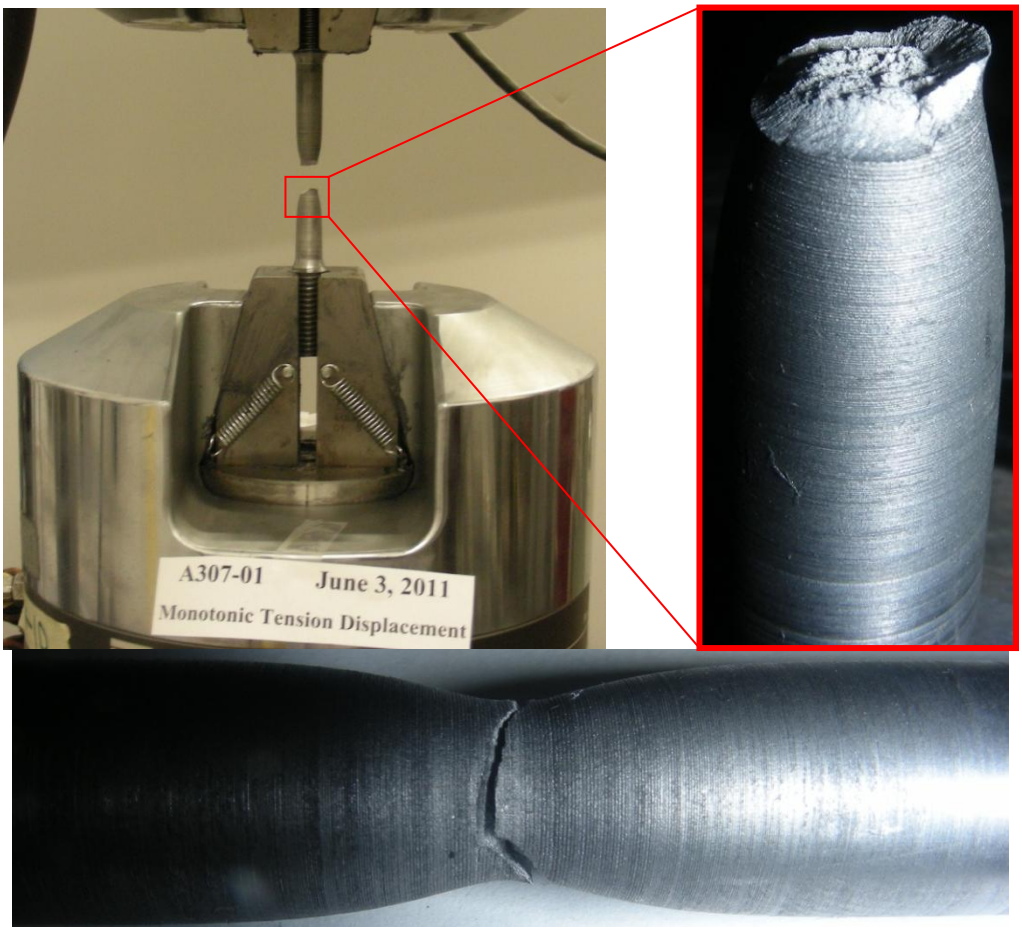

Figure 5.25: Tensile fracture surface of A307 anchor rod

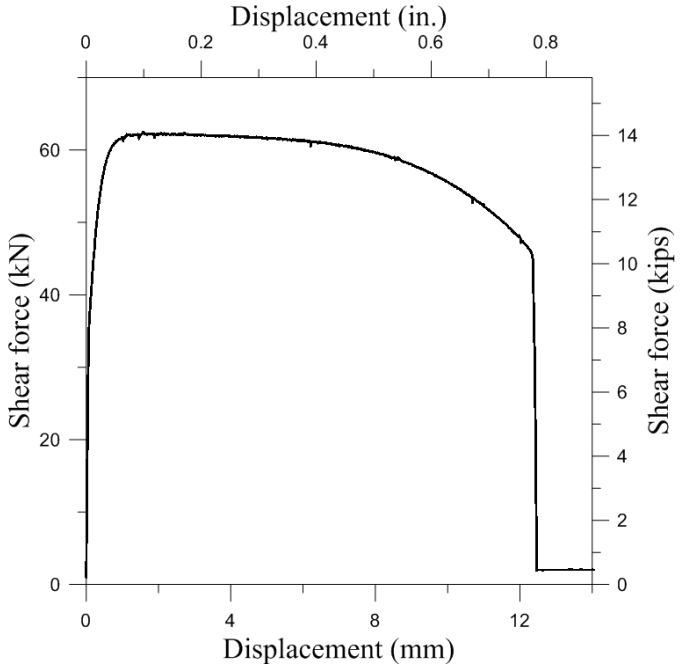

Figure 5.26: Load verse displacement of A307 anchor rod

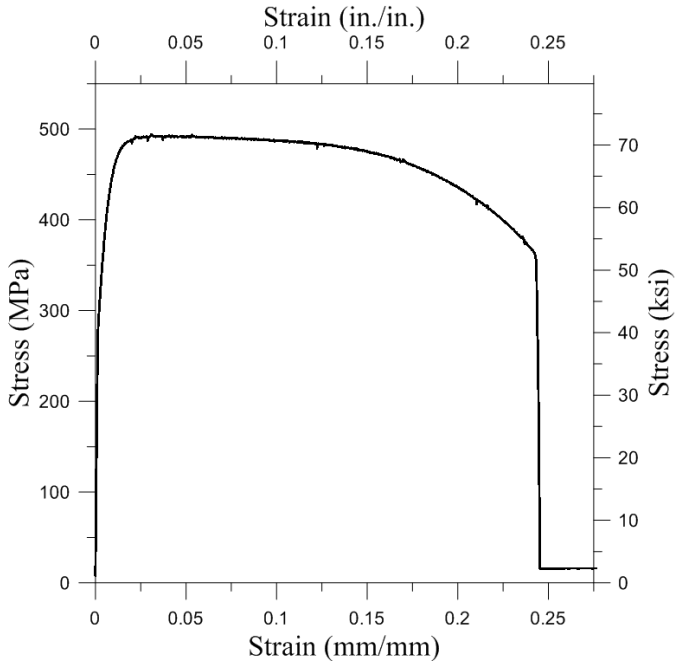

Figure 5.27: Stress verse strain curve of A307 anchor rod

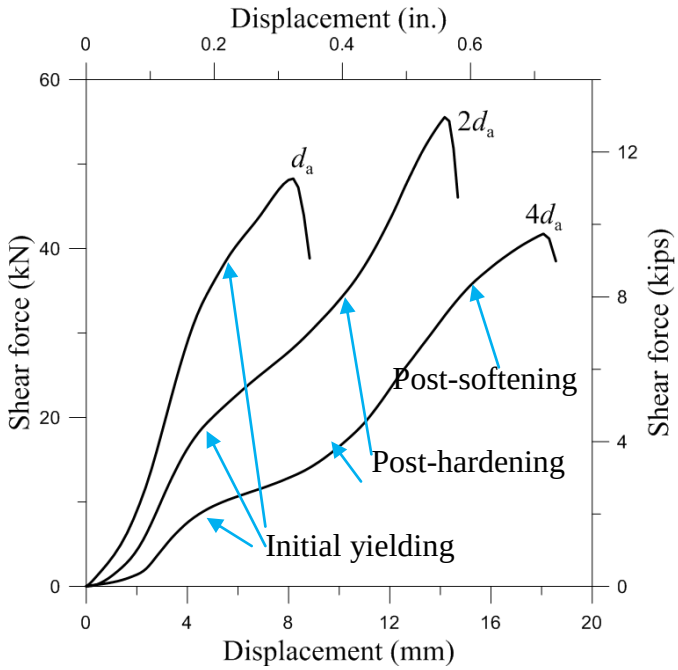

Figure 5.28: Load-displacement behavior of A307 anchor rods under monotonic loading

Figure 5.29: A307-da- MD

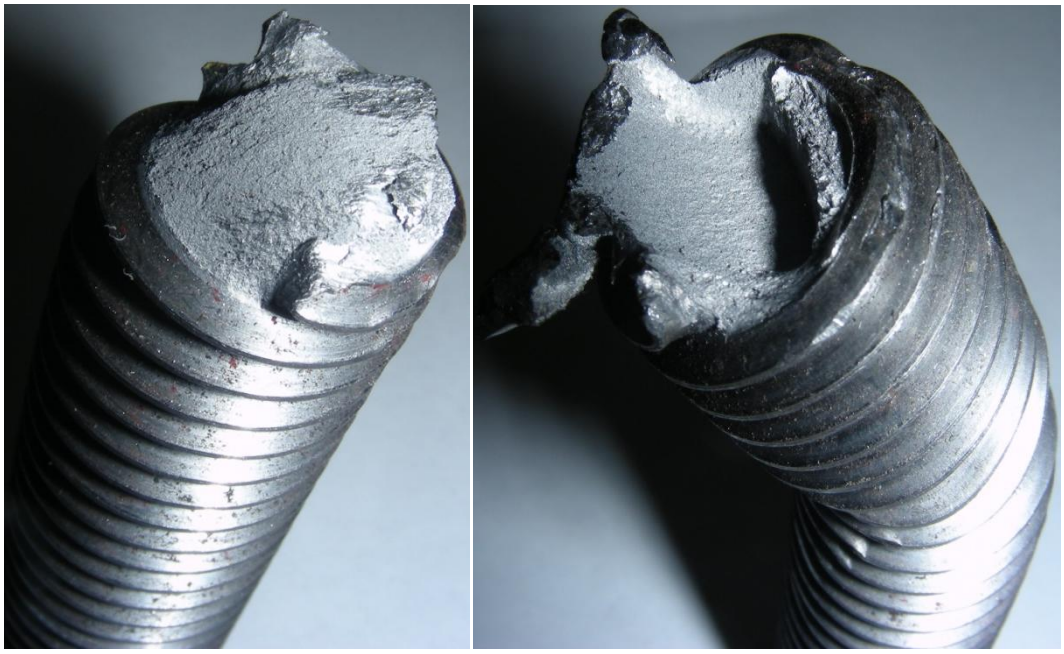

(a) one side of the fractured rod **(b) the other side of the rod**

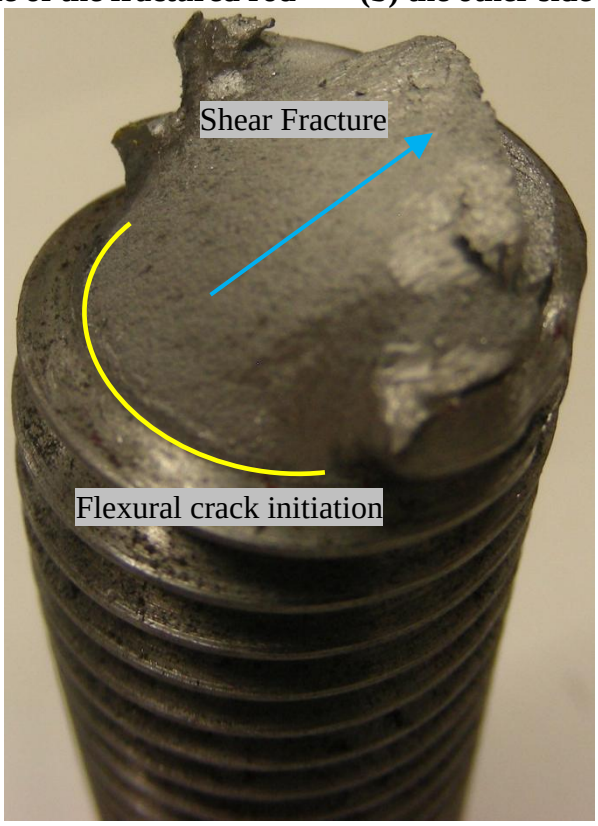

(c) fracture mode

Figure 5.30: fracture surfaces of A307-da-MD

Figure 5.31: A307-2da-MD

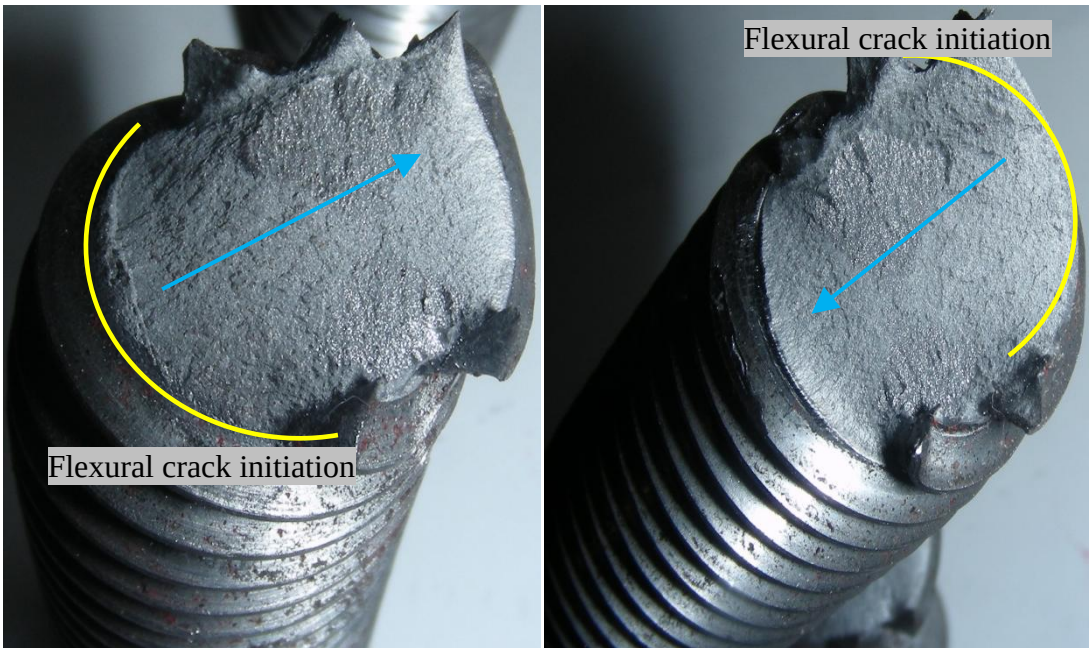

one side of the fractured rod (b) the other side of the fractured rod

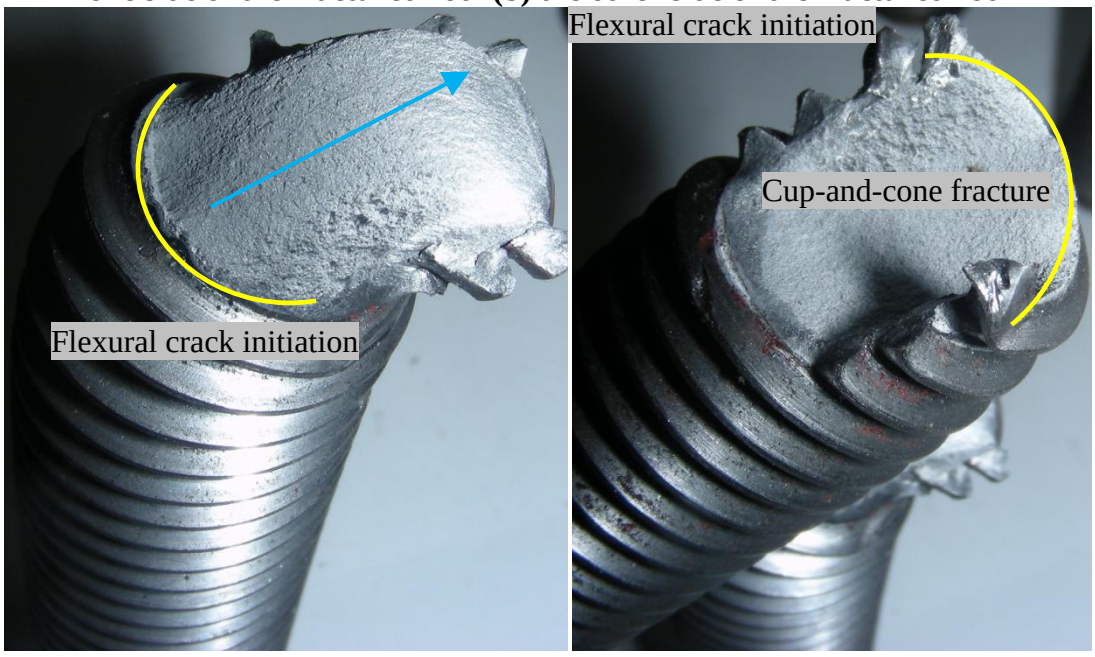

(c) one side of the second fractured rod (d) the other side of the second fractured rod

Figure 5.32: fracture surfaces of A307-2da-MD

Figure 5.33: A307-4da-MD

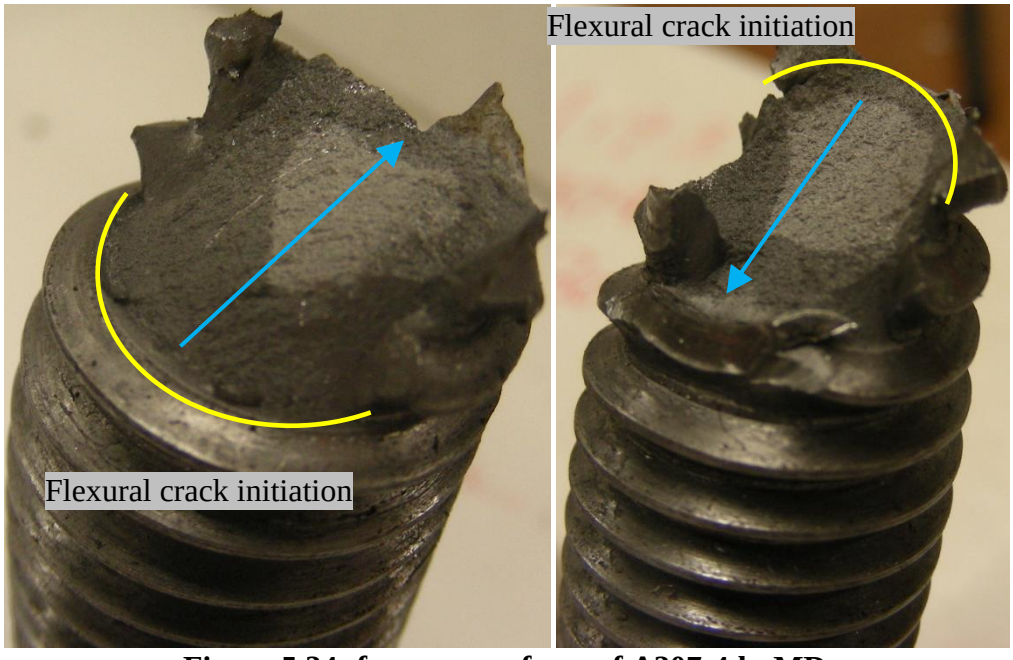

Figure 5.34: fracture surfaces of A307-4da-MD

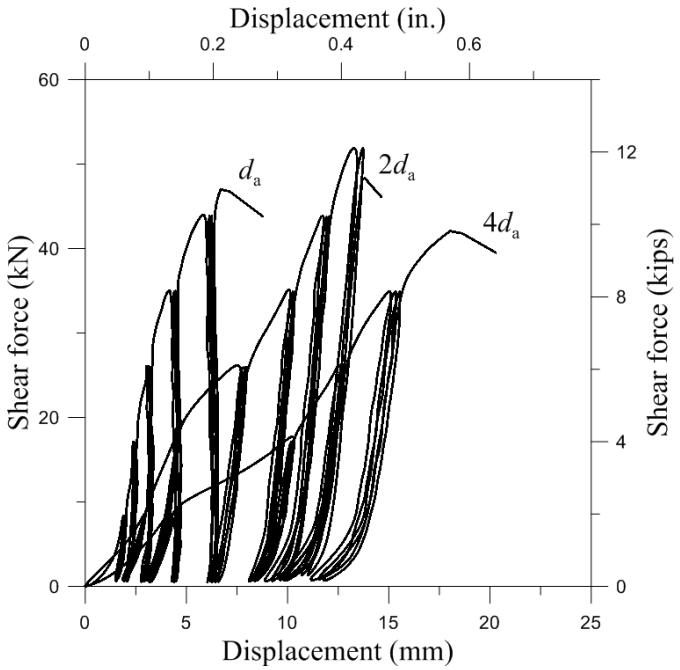

Figure 5.35: Load-displacement behavior of A307 anchor rods under cyclic loading

Figure 5.36: A307-da- RL

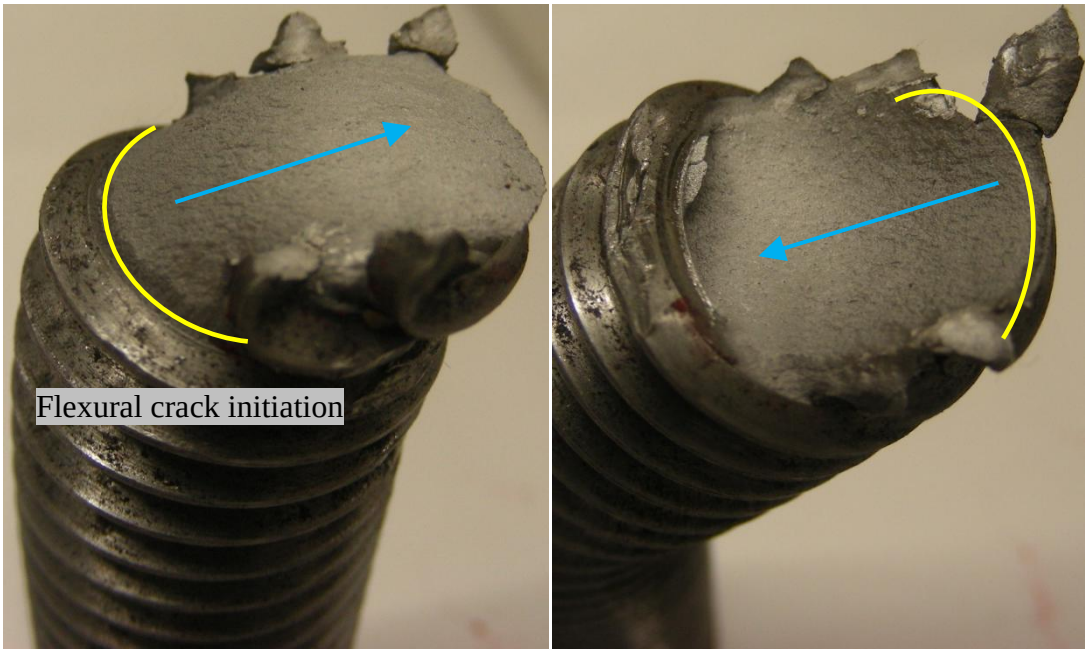

(a) one side of the fractured rod (b) the other side of the fractured rod

Figure 5.37: fracture surfaces of A307-da- RL

Figure 5.38: A307-2da- RL

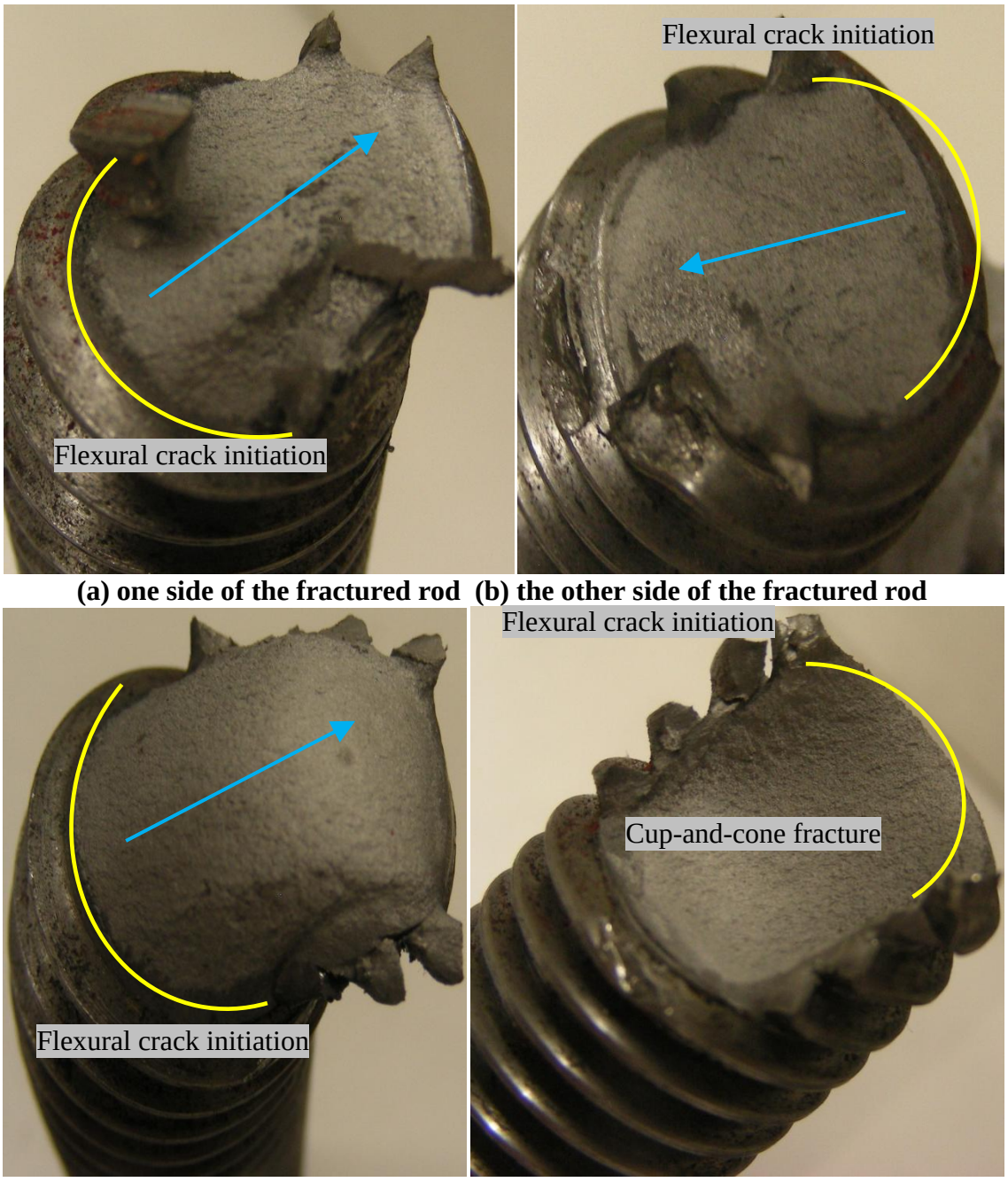

(a) one side of the fractured rod (b) the other side of the fractured rod

(c) one side of the second fractured rod (d) the other side of the second fractured rod

Figure 5.39: fracture surfaces of A307-2da-RL

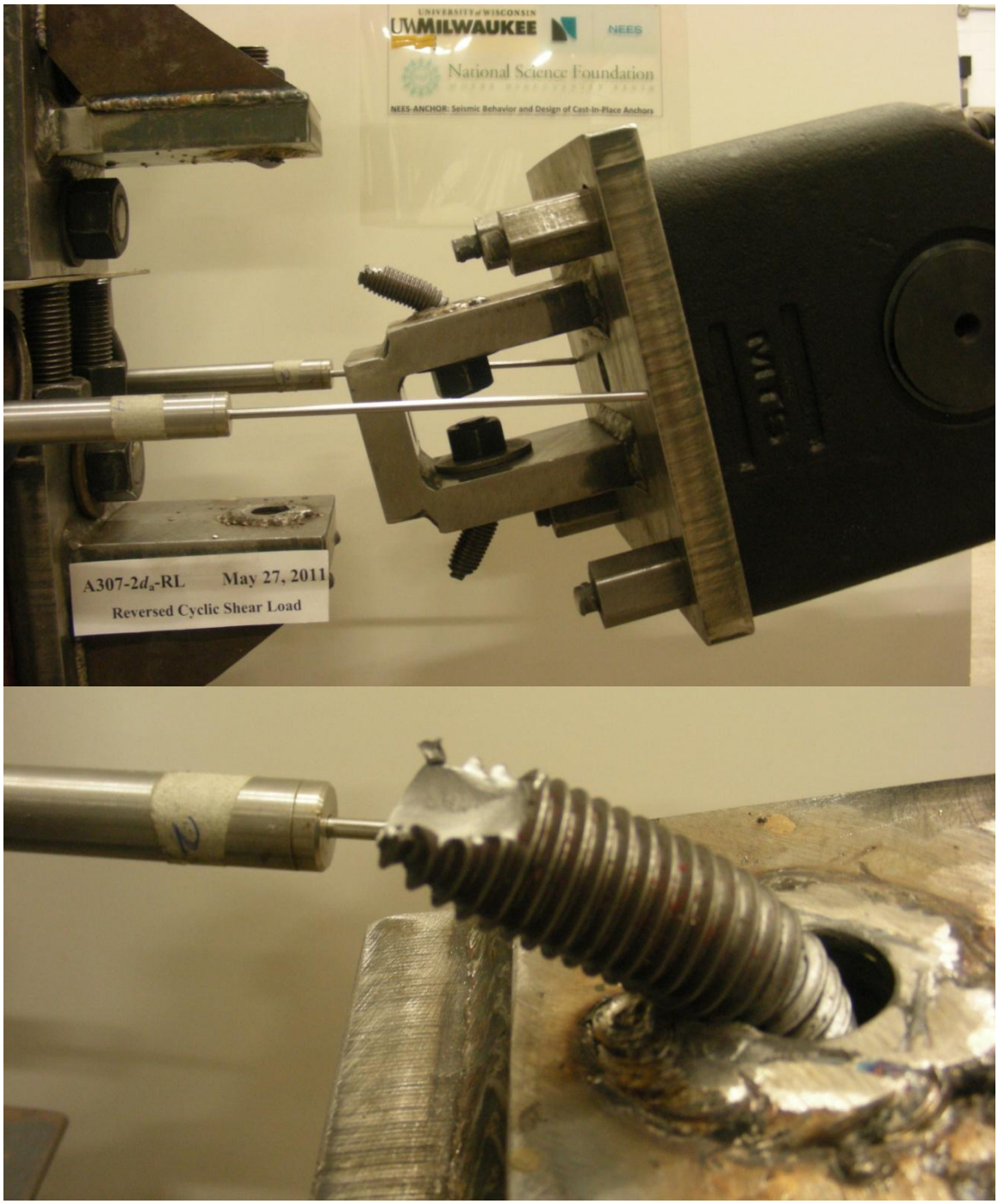

Figure 5.40: fractured rods in double-shear tests

Figure 5.41: A307-4da- RL

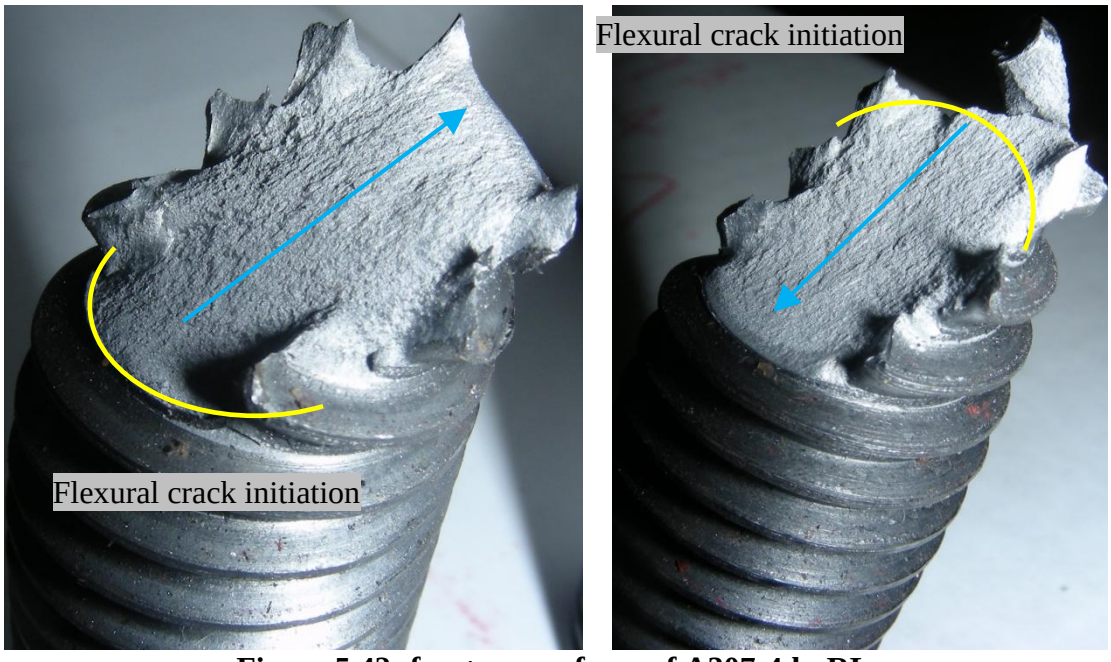

Figure 5.42: fracture surfaces of A307-4da-RL

Figure 5.43: Standard 0.5-in (12.7-mm) diameter coupon of A304 anchor rods

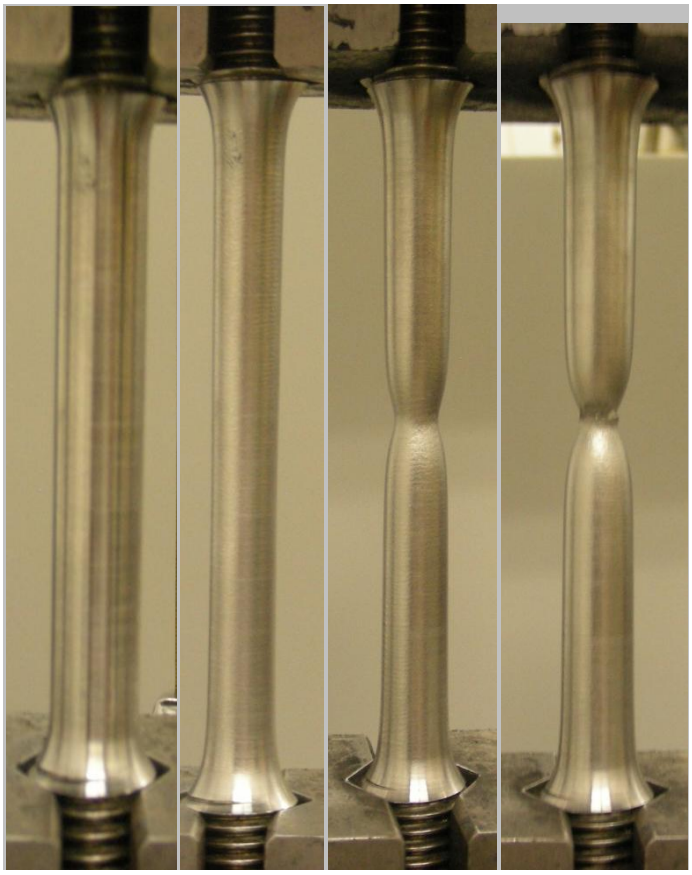

(a) (b) (c) (d)

Figure 5.44: load history: a) before yielding; b) after yielding; c) necking; d) failure

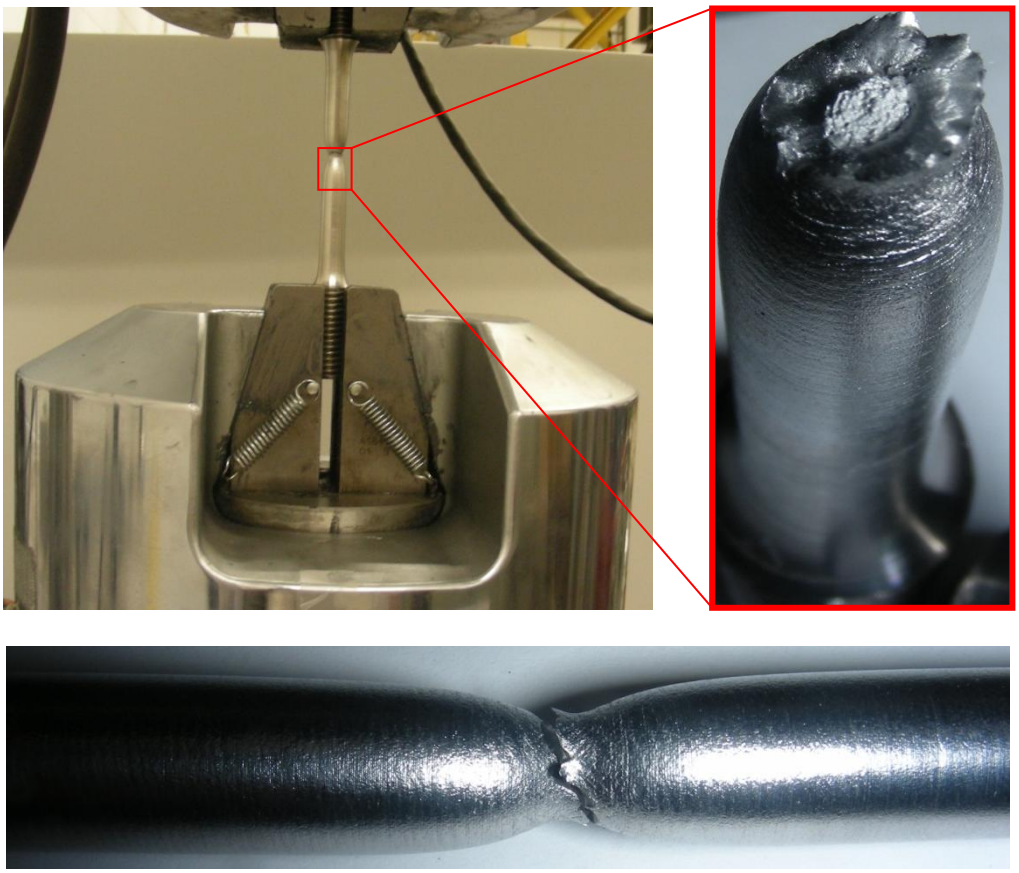

Figure 5.45: Tensile fracture surface of A307 anchor rod

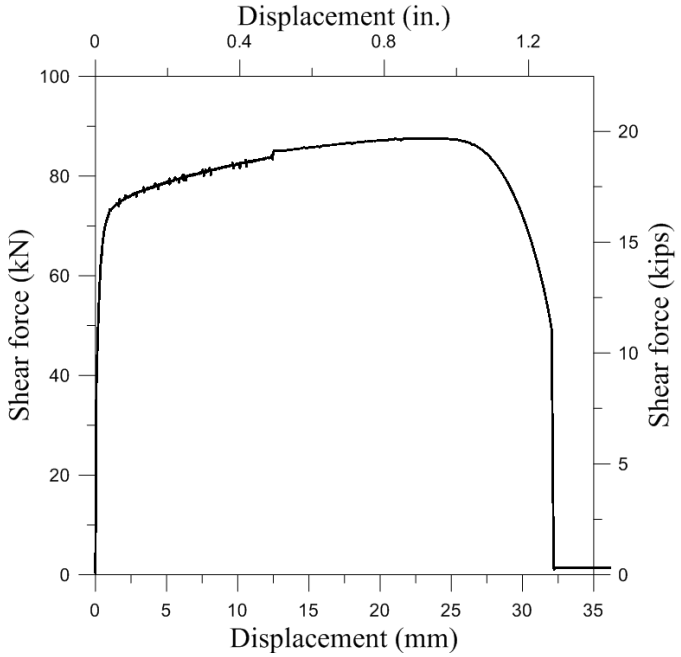

Figure 5.46: Load verse displacement of A304 anchor rod

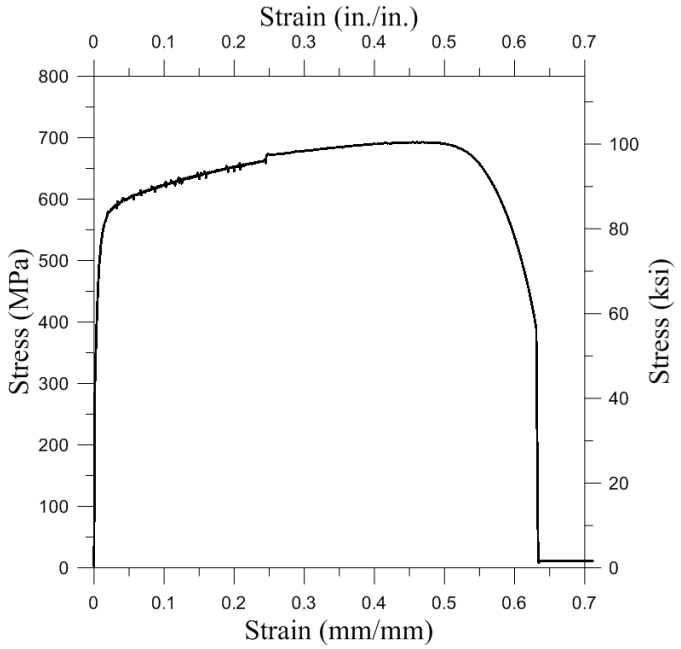

Figure 5.47: Stress verse strain curve of A304 anchor rod

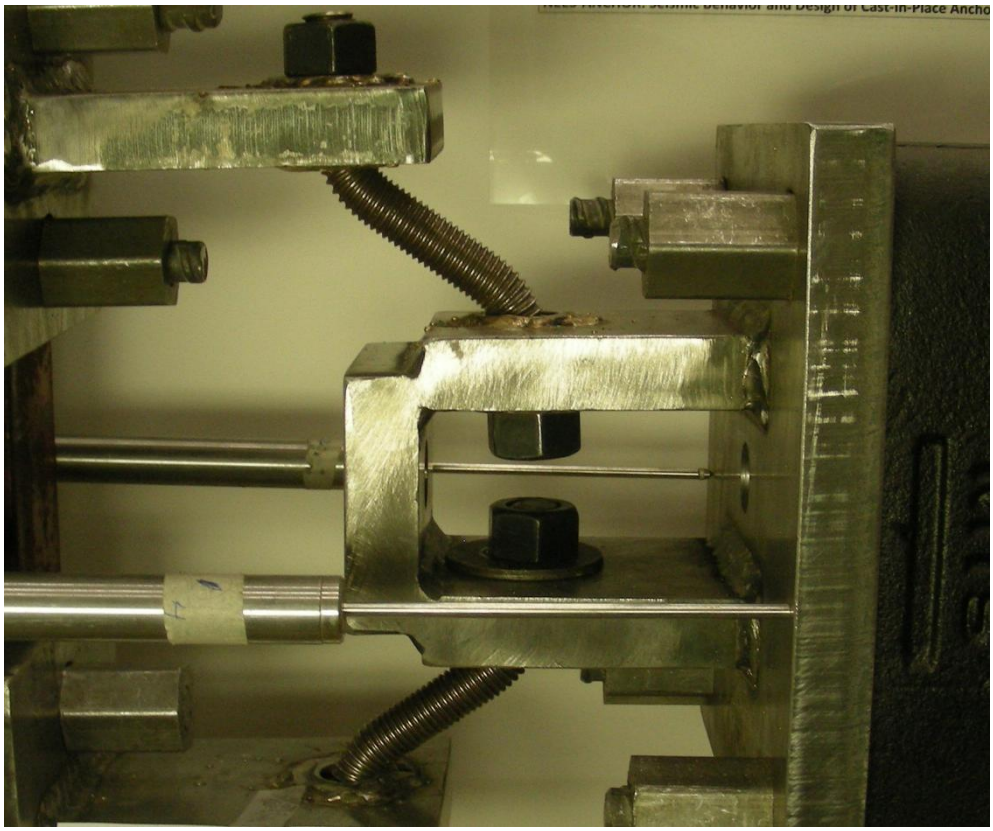

Figure 5.48: deformation of stainless steel A304

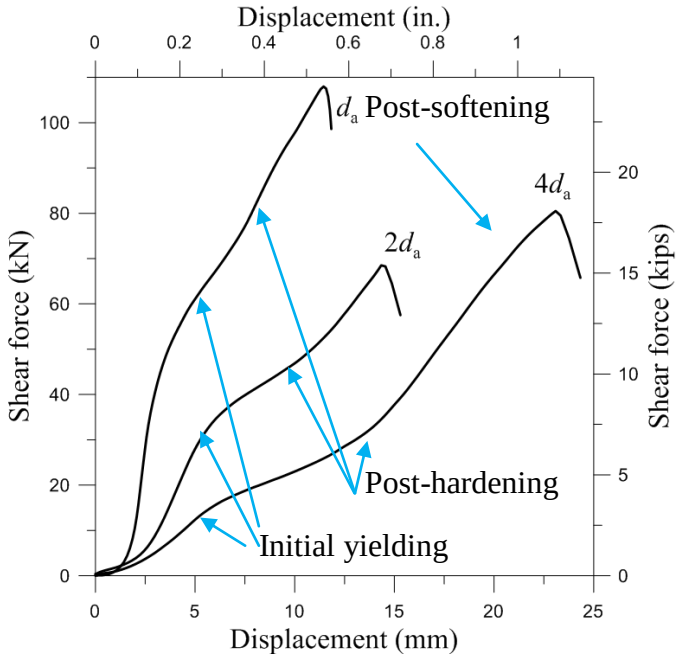

Figure 5.49: Load-displacement behavior of A304 anchor rods under monotonic loading

Figure 5.50: A304-da- MD

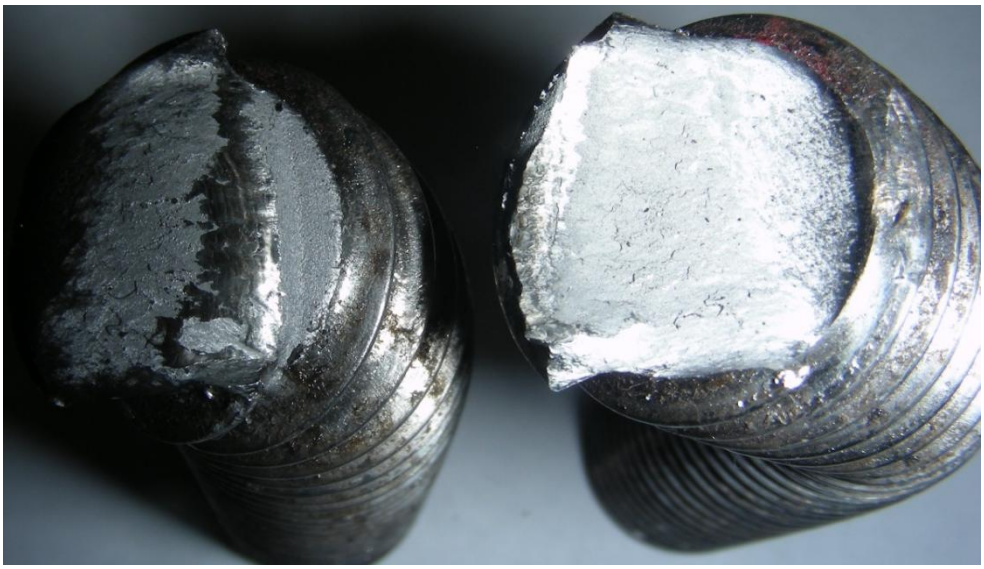

(a) one side of the fractured rod (b) the other side of the rod

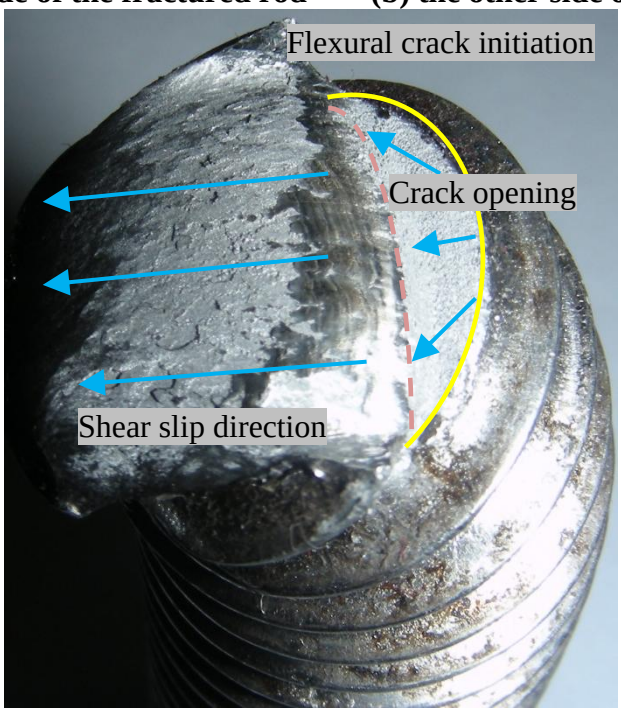

(c) fracture mode

Figure 5.51: fracture surfaces of A304-da-MD

Figure 5.52: A304-2da-MD

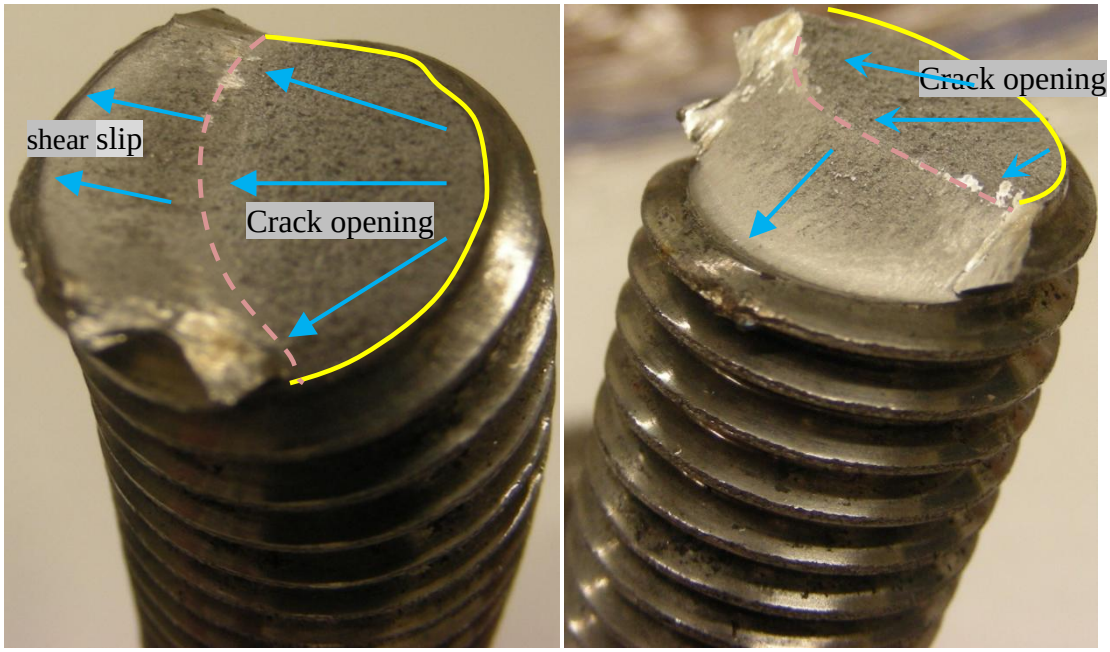

(a) one side of the fractured rod (b) the other side of the fractured rod

Figure 5.53: fracture surfaces of A304-2da-MD

Figure 5.54: A304-4da-MD

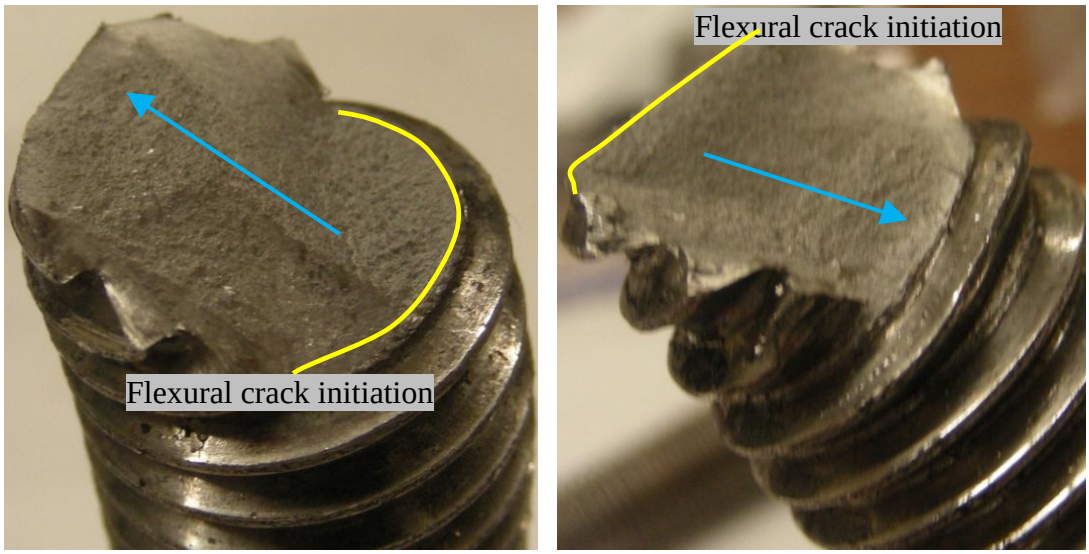

Figure 5.55: fracture surfaces of A304-4da-MD

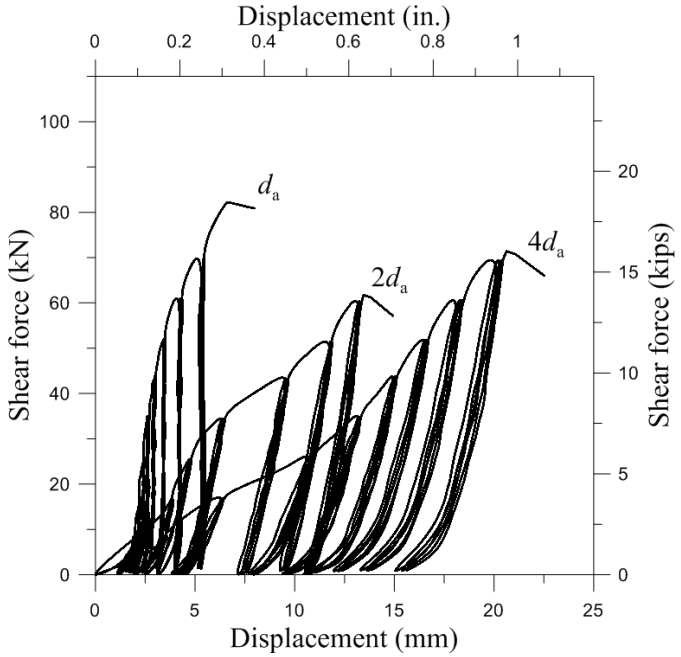

Figure 5.56: Load-displacement behavior of A304 anchor rods under cyclic loading

Figure 5.57: A304-da- RL

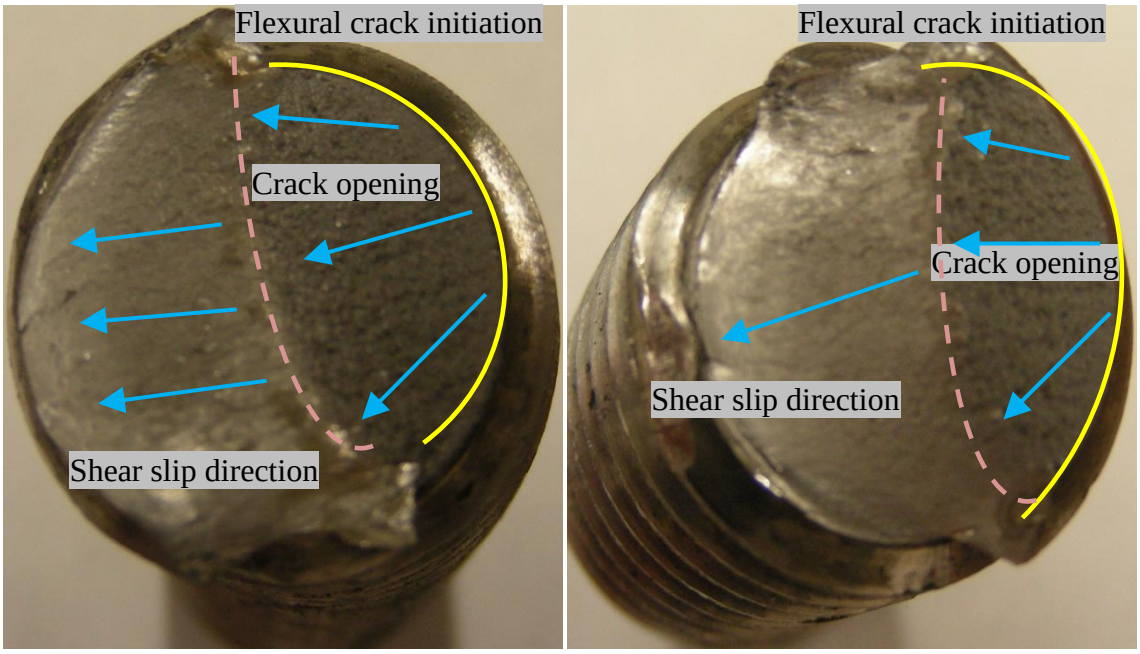

(a) one side of the fractured rod (b) the other side of the fractured rod
Figure 5.58: fracture surfaces of A304-da- RL

(a) deformation of two anchor rods

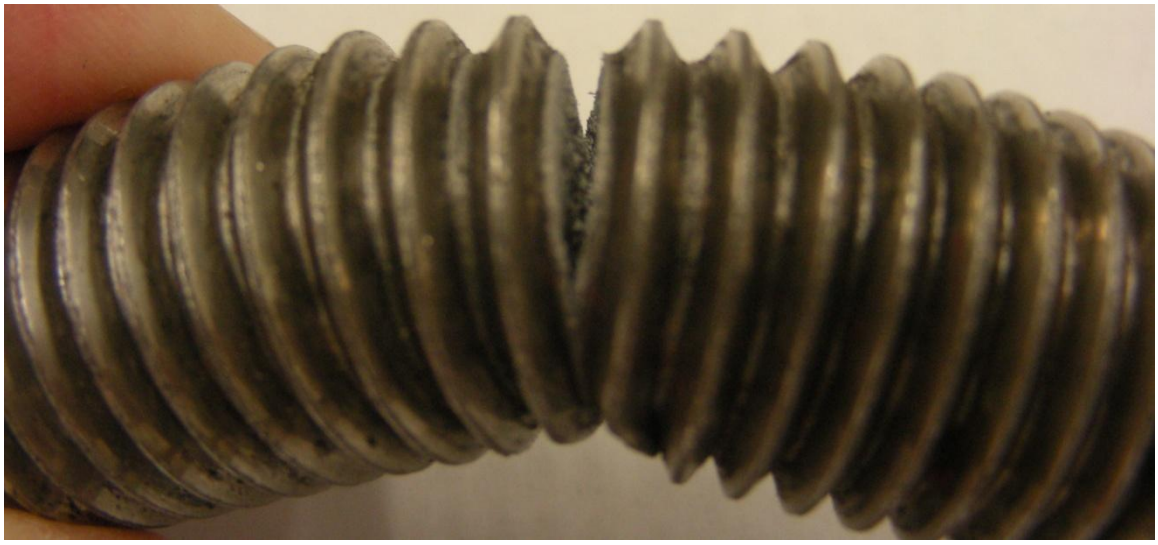

(b) flexural crack opening

Figure 5.59: A304-2da- RL

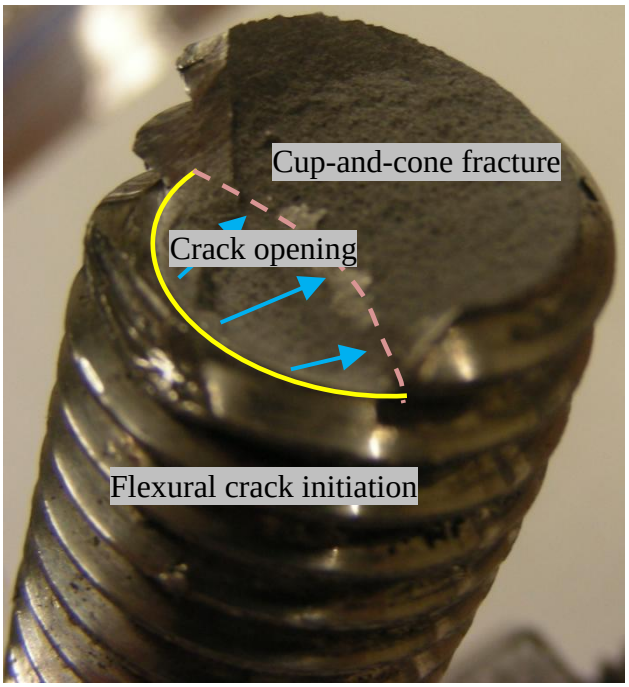

Figure 5.60: fracture surfaces of A304-2da-RL

Figure 5.61: A304-4da- RL

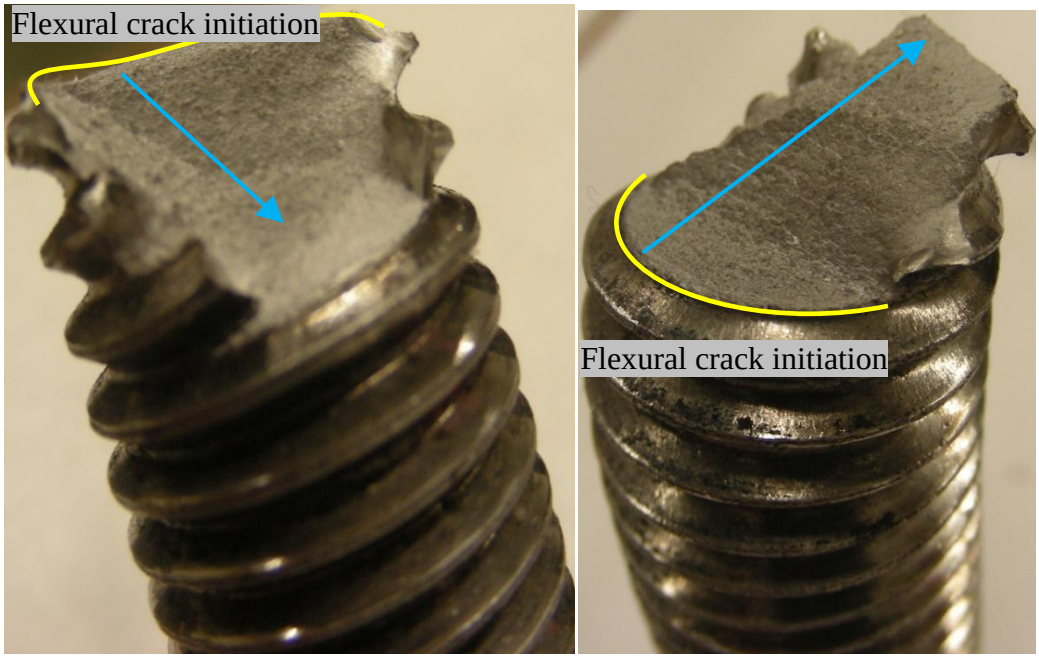

Figure 5.62: fracture surfaces of A304-4da-RL

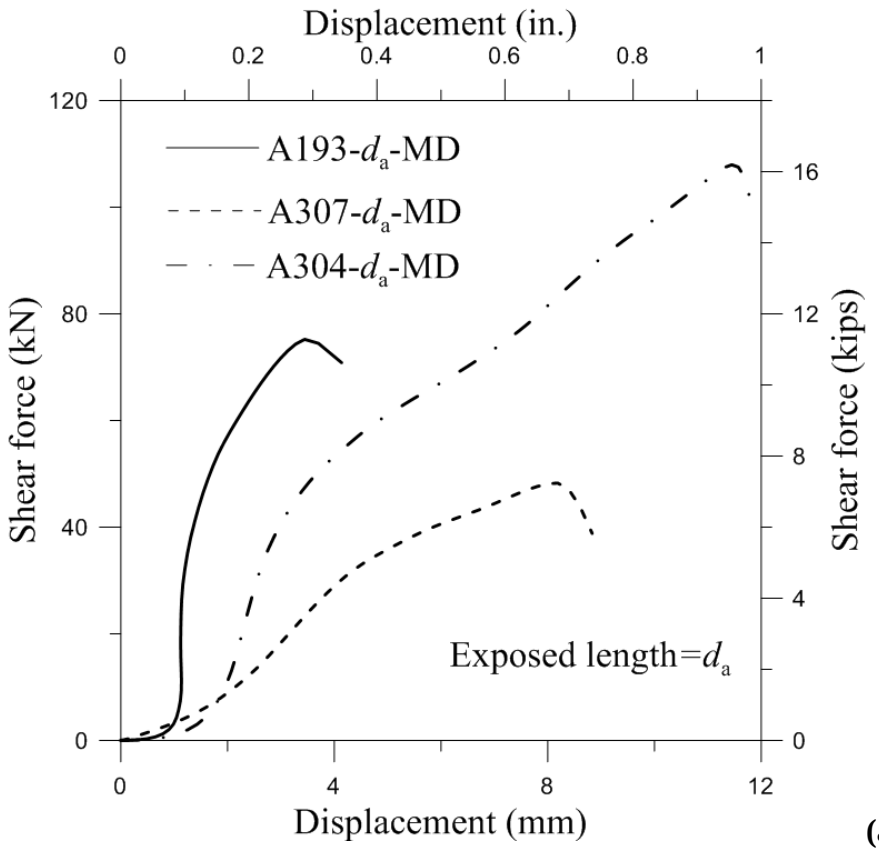
Displacement (in.)
0
0.2
0.4
0.6
0.8
1
120
80
40
0
A193-d_a-MD
A307-d_a-MD
A304-d_a-MD
Exposed length=d_a
Shear force (kN)
16
12
8
4
0
Shear force (kips)
0
4
8
12
Displacement (mm)

(a)

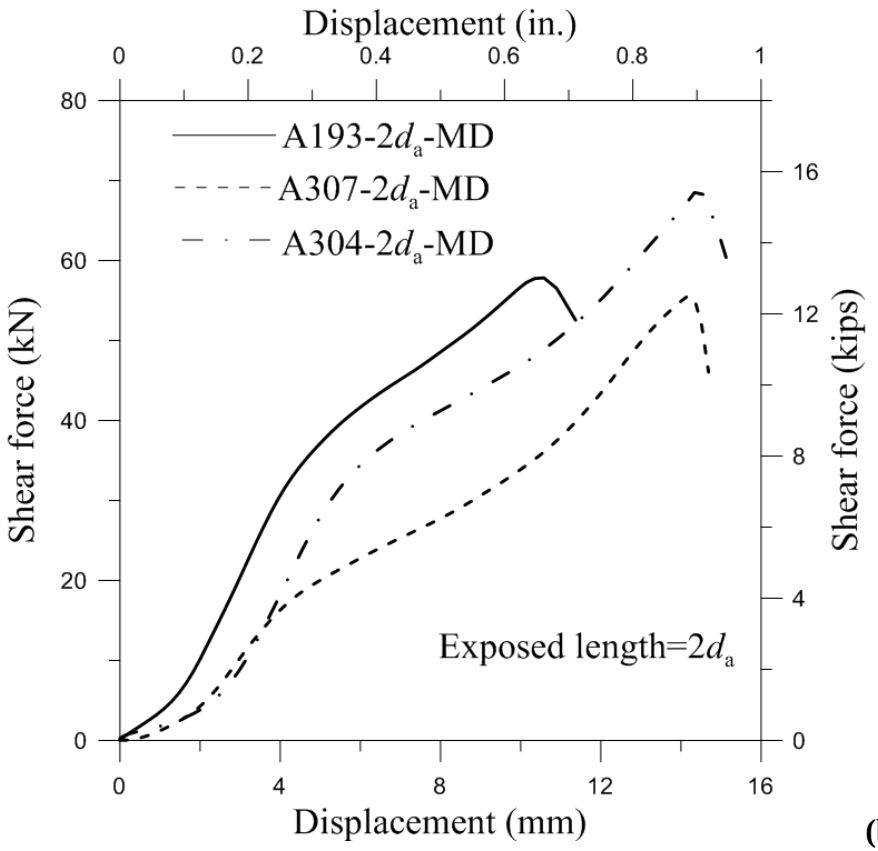
Displacement (in.)
0
0.2
0.4
0.6
0.8
1
80
60
40
20
0
A193-2d_a-MD
A307-2d_a-MD
A304-2d_a-MD
Exposed length=2d_a
Shear force (kN)
Shear force (kips)
16
12
8
4
0
0
4
8
12
16
Displacement (mm)

(b)

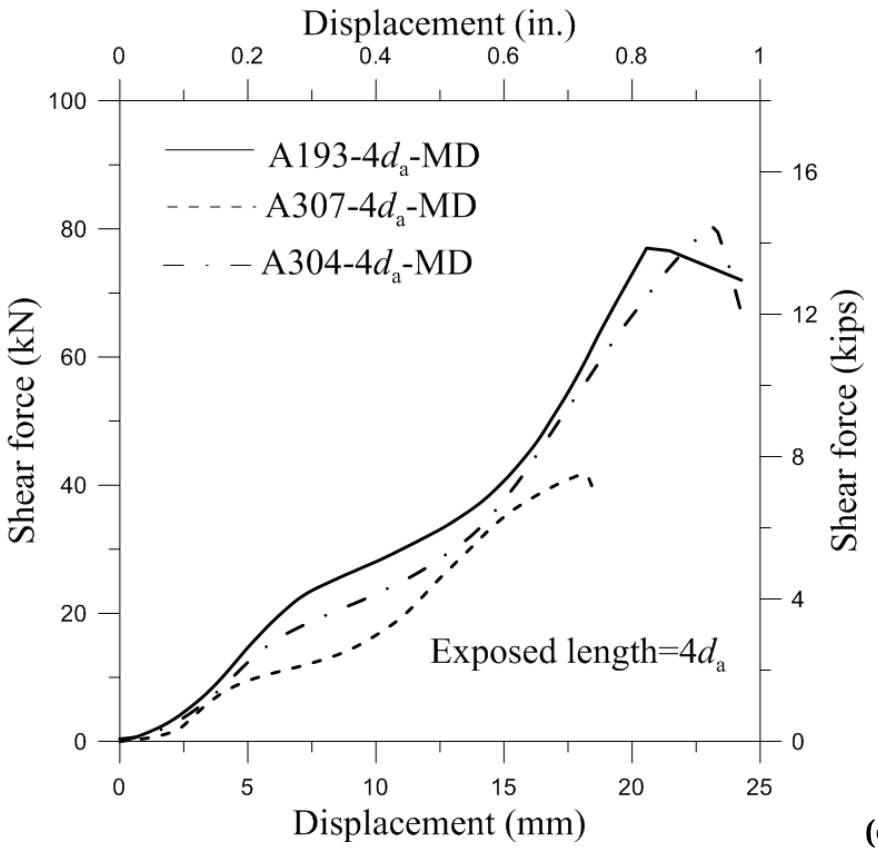

(c)

Figure 5.63: Comparison of different types of steel under monotonic loading

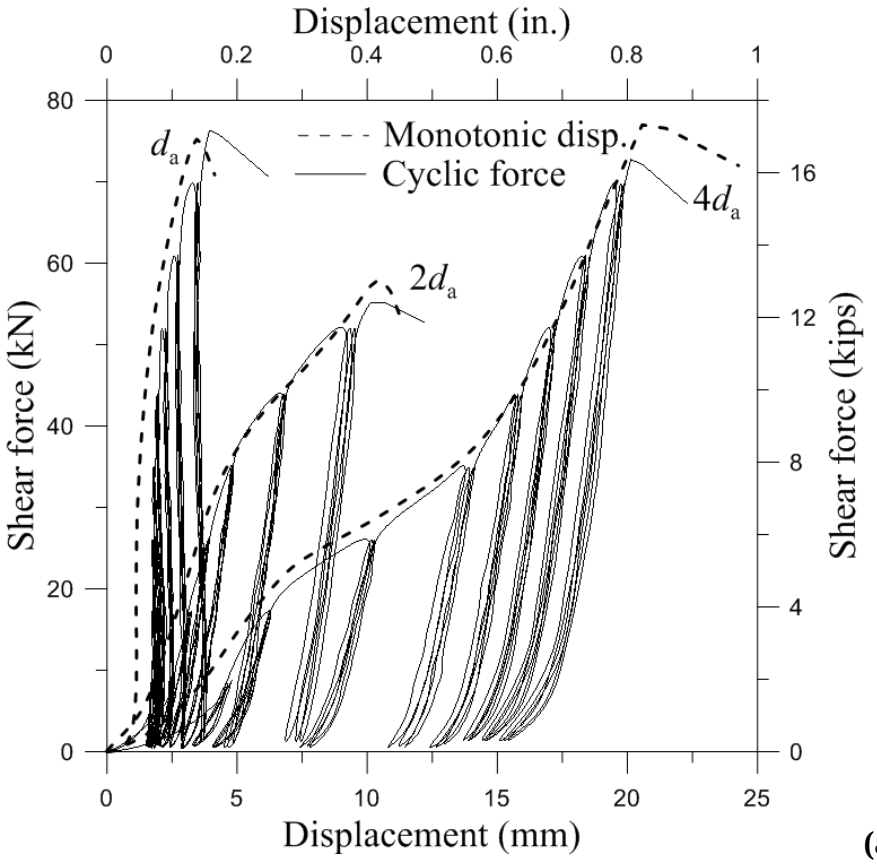
Displacement (in.)
0
0.2
0.4
0.6
0.8
1
80
60
40
20
0
Shear force (kN)
16
12
8
4
0
Shear force (kips)
Monotonic disp.
Cyclic force
d_a
$2d_a$
$4d_a$
0
5
10
15
20
25
Displacement (mm)

(a) A307

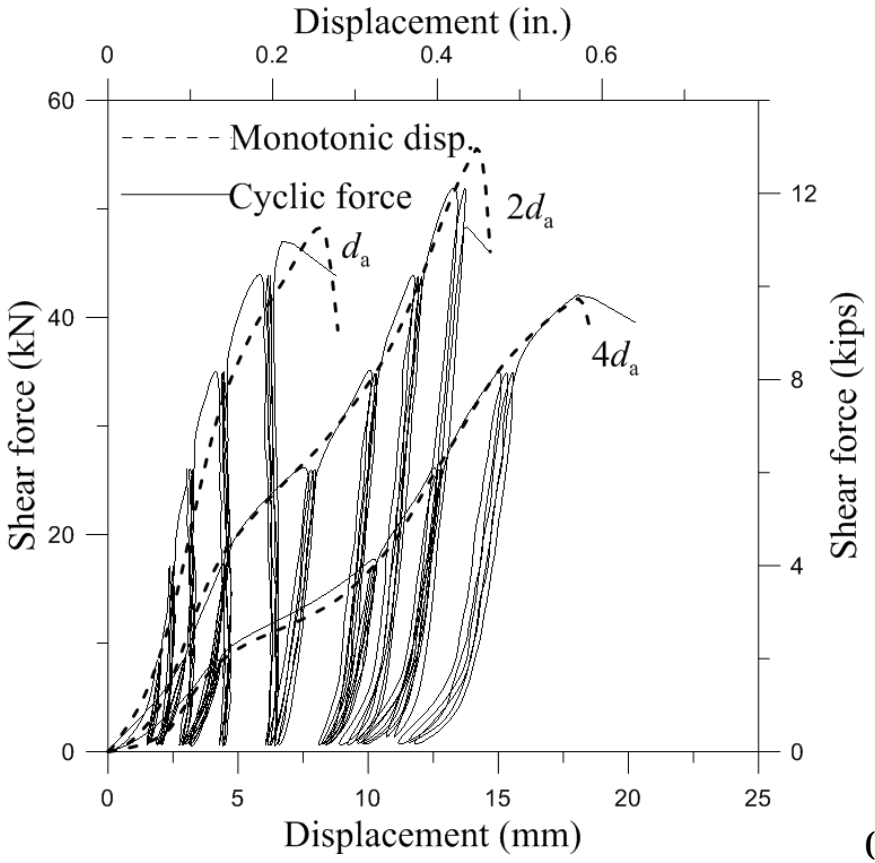
Displacement (in.)
0
0.2
0.4
0.6
60
40
20
0
Monotonic disp.
Cyclic force
d_a
$2d_a$
$4d_a$
12
8
4
0
Shear force (kN)
Shear force (kips)
0
5
10
15
20
25
Displacement (mm)

(b) A193

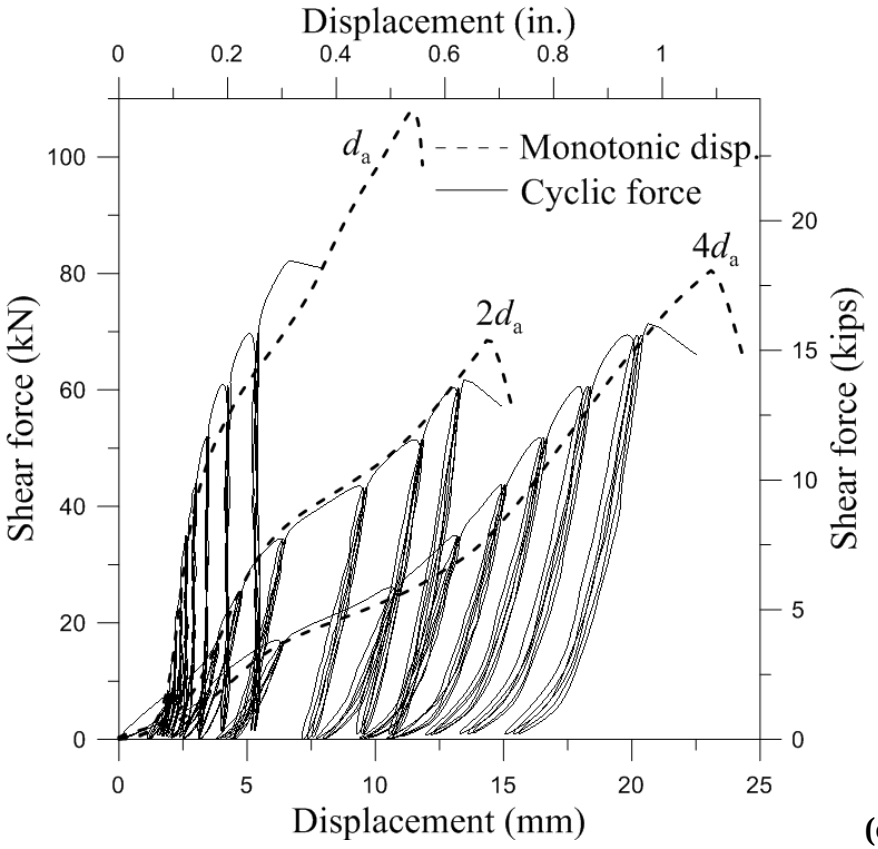

(c) A304

Figure 5.64: Comparison of different types of steel under cyclic loading

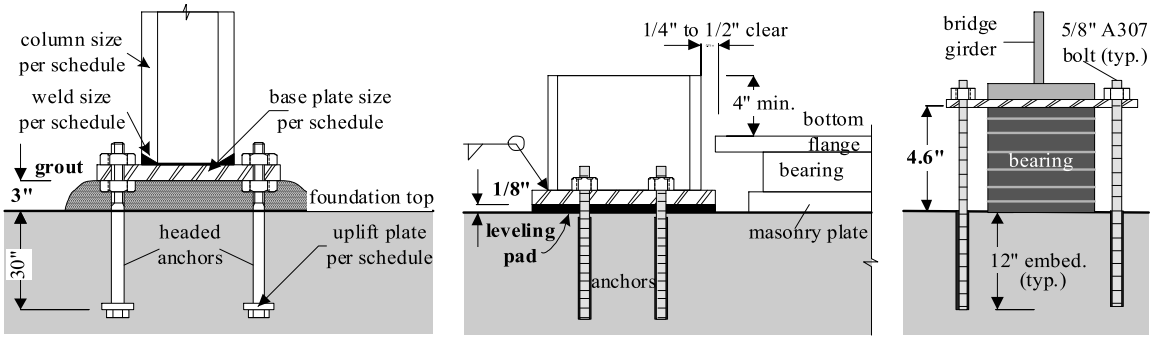

(a) Column base connection; (b) Shear key on bridge cap; (c) Bearing for bridge girder

Figure 5.65: Exposed anchor bolts in various types of connections

CHAPTER 6 Summary and Conclusion

6.1 Summary

This study (Phase I of NEES-Anchor project) provides experimental data for a rational analysis of seismic design of anchor connections targeted at current anchor design equations in the ACI 318-08 Appendix D. The presented investigation focused on cast-in-place single anchors in plain concrete experiencing concrete breakout failure. The anchors were subjected to static as well as simulated seismic loading to study the behavioral differences of cast-in-place anchors under seismic loading conditions.

This study used 0.75 inch diameter anchor bolts that were first subjected to monotonic tension or shear loading and the measured anchor capacities were compared with a database compiled from a literature review focusing on cast-in-pace anchor bolts and headed studs experiencing concrete breakout failure. The monotonically loaded tests were used to provide reference behavior for comparison with anchors subjected to quasi-static cyclic tension or shear loadings. Using these comparisons alongside past literature, the current seismic capacity reduction requirements for anchor connections was analyzed. Anchor bolts were also subjected to combined cyclic tension-shear loading, and the measured capacities were used to evaluate the combined loading interaction equations currently being used for anchor design.

In part 2 of this report, monotonic and cyclic tests and exposed anchor rods were presented. The motivation of this additional study was to identify the key parameters that affects the seismic behavior of anchors in shear, focusing on steel fracture. Three types of threaded rods were tested under monotonic tension, monotonic shear, and cyclic shear. For the shear tests, a gap was introduced in between the loading plates. The gap, in terms of 1, 2 and 4 times the anchor diameter, represent several practical applications, in which the anchor shaft may not be completely embedded in concrete.

6.2 Conclusions

The behavioral observations of experimental tests in which anchors were subjected to monotonic and cyclic tension or shear were used to explore the seismic reduction factor of 0.75 used in the ACI 318-08 code. Results showed average maximum cyclic capacity reductions of less than 11 percent for concrete failure modes in tension and shear while cyclic loading reduced anchor steel capacity by 13 percent for shear but less than 3 percent for tension. Anchor steel capacity reductions up to 40 percent have been reported in the literature for cyclic shear loading, however capacity reduction of anchor steel under cyclic loading is currently excluded from the ACI 318-08 code. If the seismic reduction factor in ACI 318 Appendix D is used to purely consider capacity reduction of anchored connections, test observations show that implying a 25 percent capacity reduction to concrete failure modes of anchors used in seismic zones may be overly conservative. Also, the negated seismic capacity reduction for steel failure modes in ACI 318-08 code was shown in this study and in existing literature to be un-conservative.

Cyclic combined tension-shear loading tests in Phase I, supported by existing literature data, support the use of the tri-linear interaction equation in ACI 318-08 D.7.3 for cyclic combined cyclic loading scenarios. This research shows the accuracy of the interaction equation (disregarding phi factors) to be sufficient even for cases when the cyclic tension and shear capacity of anchors match the five percent fractile values upon which the code equations for anchor capacities are based. As a result, the currently used tri-linear interaction equation is assumed to be satisfactory as long as the individual predicted nominal cyclic tension and shear capacities remain adequately conservative.

The cyclic double shear tests indicates that low-cycle fatigue caused by cyclic shear loading had impact on the capacity of anchor rods. The impact is significant for ASTM A304 steel, a highly ductile steel for use in concrete anchors. The impact is negligible for ASTM A193 Grade B7 and ASTM A307 steel, most commonly used steel for anchor bolt. These tests indicated that the seismic capacity reduction observed in the shear tests of anchors in the literature may have been largely caused by progressive concrete damage rather than low-cycle fatigue of steel. Further study is needed to better understand the behavior.

6.3 Recommendations for Future Studies

The lever arm behavior discussed in Section 7.1.5 for reinforced anchors in shear is more complex than the currently proposed equation by Eligehausen (2006) considers. This research has shown that lever arm development is the largest contribution to capacity (both monotonic and cyclic) as well as ductility for reinforced anchors subject to shear loading. This behavior should be examined in greater detail relating to concrete anchors to produce a more accurate representation of lever arm effects in the presence of, and resulting from, anchor reinforcement. Upon developing a model for this behavior, the benefits of anchor reinforcement can be fully and safely utilized in anchor connection design.

References

1. American Concrete Institute. (2008). “Building Code Requirements for Structural Concrete (ACI 318-08).” Farmington Hills, Michigan.
2. Anderson, N., and Meinheit, D., (2000). “Design criteria for headed stud groups in shear: Part I – steel capacity and back edge effects.” *PCI Journal*, 45(5), 46-75.
3. Anderson, N. and Meinheit, D. (2006). “Design criteria for headed stud groups in shear.” Wiss, Janney, Elstner Associates Inc., Northbrook, IL.
4. Anderson, N., Tureyen, K., and Meinheit, D. (2007). “Design criteria for headed studs, Phase II tension and combined tension and shear.” Second draft report, Wiss, Janney, Elstner Associates Inc., Northbrook, IL.
5. Anderson, N. and Meinheit, D. (2007). “A review of headed-stud design criteria in the sixth edition of the PCI design handbook.” *PCI Journal*, Jan.-Feb. 2007.
6. Ando, Y., Sakai, S., and Nakano, K. (2007). "Study on structural performance of anchor bolt embedded in rc footing beams." *Architectural Institute of Japan*, (50), 117-120.
7. Asia-Pacific Economic Cooperation. (2002). Earthquake Disaster Management of Energy Supply System of APEC Member Economies, Energy Commission, Ministry of Economic Affairs, Chinese Taipei.
8. Bailey, J. W. and Burdette, E. G. (1977). "Edge effects on anchorage to concrete." *Civil Engineering Research Series No. 31*,The University of Tennessee, Knoxville, TN.
9. Bode, H. and Hanenkamp, W. (1985). “Zur tragfähigkeit von kopfbolzen bei zugbeanspruchung (Strengh of headed studs embedded in concrete and loaded in tension).” *Bauingenieur*, 60(9), 361–367.
10. Bode, H. and Roik, K. (1987). “Headed studs embedded in concrete and loaded in tension.” *Anchorage to Concrete*, SP-103, G.B. Hasselwander, ed., American Concrete Institute, Farmington Hills, Mich.,61-88.
11. Cannon, R. (1995). “Straight talk about anchorage to concrete-part I.” *ACI Structural Journal*, 92(56), 1-7.
12. Cannon, R. (1995). “Straight talk about anchorage to concrete-part II.” *ACI Structural Journal*, 92(69), 1-11.

13. Cannon, R., Burdette, E., and Funk, R. (1975). “Anchorage to concrete.” *Report No. CEB 75-32*, Civil Engineering Branch, Tennessee Valley Authority, Knoxville, TN.
14. Carraio, P. J., Krauss, K. W. and Kim, J. B. (1996). “Tension tests of heavy-duty anchors with embedments of 8 to 19 inches.” *ACI Structural Journal*, 93(33),1-9.
15. Civjan, S., and Singh, P. (2003). “Behavior of shear studs subjected to fully reversed cyclic loading.” *Journal of Structural Engineering ASCE*, November 2003, 1466-1474.
16. Collins, D. M. (1988). “Load-deflection behavior of cast-in-place and retrofit concrete anchors subjected to static, fatigue, and impact tensile loads.” M.S. thesis, University of Texas at Austin, Austin, TX.
17. Collins, D., Klingner, R. E., and Polyzois, D. (1989). “Load-deflection behavior of cast-in-place and retrofit concrete anchors subjected to static, fatigue, and impact tensile loads.” *Research Report CTR 1126-1*, Center for Transportation Research, University of Texas at Austin, Austin, TX.
18. Comité Euro-International du Béton (CEB). (1994). “Fastenings to concrete and masonry structures: State of the art report.” Thomas Telford Service Ltd., London.
19. Comité Euro-International du Béton (CEB). (1997). “Fastenings to concrete and masonry structures: State of the art report.” Thomas Telford Service Ltd., London.
20. Cook, R. A., Doerr, G. T., and Klingner, R.E. (1989). "Design guide for steel-to-concrete connections." *Research report No. 1126-4*, Center for Transportation Research, University of Texas at Austin, Austin, TX.
21. Cook, R. A. and Klinger, R. E. (1991). "Behavior of ductile multiple anchor steel-to-concrete connections with surface-mounted baseplates." *Anchors in Concrete–Design and Behavior, SP-130*, G. A. Senkiw and B. Lancelot, III, eds., American Concrete Institute, Farmington Hills, MI.
22. Cook, R. A., Collins, D. M., Klinger, R. E., and Polyzois, D. (1992). "Load- deflection behavior of cast-in-place and retrofit concrete anchors." *ACI Structural Journal*, 89(12), 639-649.
23. Eligehausen, R. and Balogh, T. (1995). "Behavior of fasteners loaded in tension in cracked reinforced concrete." *ACI Structural Journal*, 92(35), 365-379.

24. Eligehausen, R., Mallée, R., and Silva, J. (2006). “Anchorage in concrete construction.” Wilhelm Ernst & Sohn, Berlin, Germany.
25. Federation Internationale du Beton (FIB). (2008). “Fastenings to concrete and masonry structures.” in press.
26. Fuchs, W., Eligehausen, R., and Breen, J. (1995a). “Concrete capacity design approach for fastening to concrete.” *ACI Structural Journal*, 92(1), 73-94.
27. Fuchs, W., Eligehausen, R., and Breen, J. (1995b). “Concrete capacity design approach for fastening to concrete, authors' closure to discussions.” *ACI Structural Journal*, 92(6), 794-802.
28. Gattesco, N. and Giuriani, E. (1996). “Experimental study on stud shear connectors subjected to cyclic loading.” *Journal of Construction Steel Research*, 38(1), 1–21.
29. Grauvilardell, J., Lee, D., Hajjar, J., and Dexter, R. (2005). “Synthesis of design, testing and analysis research on steel column base plate connections in high-seismic zones.” *Structural Engineering Report No. ST-04-02*, University of Minnesota, Minneapolis, MN.
30. Gross, J., Klingner, R., and Graves, H. (2001). “Dynamic behavior of single and double near-edge anchors loaded in shear.” *ACI Structural Journal*, 98(64), 665-676.
31. Hallowell, J. (1996). “Tensile and shear behavior of anchors in uncracked and cracked concrete under static and dynamic loading.” M.S. thesis, University of Texas at Austin. Austin, TX.
32. Hasselwander, G. B., Jirsa, J. O., Breen, J. E., and Lo, K. (1974). "Strength and behavior of anchor bolts embedded near edges of concrete piers." *Research Report 29-2F*, Center for Transportation Research, the University of Texas at Austin, Austin, TX.
33. Hawkins, N., Mitchell, D., and Roeder, C. (1980). "Moment resisting connections for mixed construction." *AISC Engineering Journal*, 17(1), 1-10.
34. Hawkins, N. (1987) "Strength in shear and tension of cast-in-place anchor bolts." *Anchorage to Concrete, SP-103*, G. B. Hasselwander, ed., American Concrete Institute, Farmington Hills, MI., 233-257.
35. Hoehler, M. (2006). “Behavior and testing of fastenings to concrete for use in seismic applications.” Ph.D. thesis, University of Stuttgart, Stuttgart, Germany.

36. Hoehler, M. and Eligehausen, R. (2008). “Behavior and testing of anchors in simulated seismic cracks.” *ACI Structural Journal*, 105(34), 348-357.
37. Jang, J. B. and Suh, Y. P. (2006). “The experimental investigation of a crack’s influence on the concrete breakout strength of a cast-in-place anchor,” *Nuclear Engineering and Design*, (236), 948-953.
38. Kawano, H., Kutani, K., and Masuda, K. (2003)."Experimental studies on the shear resistance of anchor bolts in exporsed type of steel column bases.” *Journal of Structural and Construction Engineering*. Transactions of AIJ (567), 141-148.
39. Klingner, R. E., Mendonca, J. A., and Malik J. B. (1982). “Effect of reinforcing details on the shear resistance of anchor bolts under reversed cyclic loading.” *ACI Journal*, 79(1), 471-479.
40. Klingner, R. E., and Mendonca, J. A. (1982). "Shear capacity of short anchor bolts and welded studs: a literature review." *ACI Journal, Proceedings*,79(5), 339-349.
41. Klinger, R. E., Hallowell, J., Lotze, D., Park, H., Rodriguez, M. and Zhang, Y. (1998). “Anchor bolt behavior and strength during earthquakes.” *U.S. Nuclear Regulatory Commission*, NUREG/CR-5434.
42. Klingner, R. E. (2010). Personal contact regarding quasi-static loading rates and concrete failure behavior using hairpins for shear anchor reinforcement.
43. Lee, N. H., Kim, K. S., Bang, C. J., and Park, K. R. (2007). “Tensile-headed anchors with large diameter and deep embedment in concrete.” *ACI Structural Journal*, 104(46), 479-486
44. Lee, N. H., Park, K. R., Suh, Y. P. (2010). "Shear behavior of headed anchors with large diameters and deep embedments in concrete." *Nuclear Engineering and Design*, in press.
45. Lifeline Earthquake Engineering (ASCE). (1997). “Northridge earthquake: lifeline performance and post-earthquake response. a report to U.S. department of commerce; technology administration.” *National Institute of Standards and Technology*; Building and Fire Research Laboratory. Gaithersburg, MD 20899.
46. Lotze, E., and Klingner, R. (1997). "Behavior of multiple-anchor connections to concrete from the perspective of plastic theory." *PMFSEL Report No. 96-4*, University of Texas at Austin, TX.
47. Lotze, D., Klingner, R., and Graves, H., (2001). "Static behavior of anchors under combinations of tension and shear loading." *ACI Structural Journal*, 98(50), 525-536.

48. Nakashima, M. and Chusilp, P. (2003). “A partial view of Japanese post-Kobe seismic design and construction practices.” *Earthquake Engineering and Engineering Seismology*, 4(1), 3-13.
49. New Zealand Standards 3101 Part I. (2006). “Embedded items, fixings, and secondary structural elements.” New Zealand, Ch. 17.
50. Okada, T. and Seki, M. (1984). "Nonlinear earthquake response of equipment system anchored on rc building floor." *Proceedings of the 8th World Conference on Earthquake Engineering*, San Francisco, 1151-1158.
51. Ollgaard, J., Slutter, R., and Fisher, J. (1971). "Shear strength of stud connectors in lightweight and normal weight concrete." *AISC Engineering Journal*, 8(2), 55-64.
52. McMackin, P., Slutter, R., and Fisher, J. (1973). “Headed steel anchors under combined loading.” *AISC Engineering Journal*, 10(2), 43-52.
53. Muratli, H., Klingner, R., Graves, H. (2004). “Breakout capacity of anchors in concrete – Part II:Shear.” *ACI Structural Journal*, 101(81), 821-829.
54. Nordlin, E. F., Ames, W. H., and Post, E. R. (1968). “Evaluation of concrete anchor bolts.” Caltrans Report 19601-762500-36390.
55. Pallarés, L. and Hajjar, J. (2009). “Headed steel stud anchors in composite structures, Part I: Shear.” *Journal of Constructional Steel Research*. 66, 198-212.
56. Pallarés, L. and Hajjar, J. (2009). “Headed steel stud anchors in composite structures, Part II: Tension,” *Journal of Constructional Steel Research*. 66, 213-228.
57. Prestressed Concrete Institute (PCI). (1985). “PCI Design Handbook – Precast and Prestressed Concrtete, 3rd Edition.” Chicago, IL.
58. Prestressed Concrete Institute (PCI). (2004). “PCI Design Handbook – Precast and Prestressed Concrtete, 6th Edition.” Chicago, IL.
59. Primavera, E., Pinelli, J., and Kalajian, E. (1997). "Tensile behavior of cast-in-place and undercut anchors in high-strength concrete." *ACI Structural Journal*, 94(5), 583-594.
60. Rodriguez, M., Lotze, D., Gross, J. H., Zhang, Y. G., Klingner, R. E., and Graves, H. L. (2001). “Dynamic behavior of tensile anchors to concrete.” *ACI Structural Journal*, 98(4), 511-524.

61. Roeder, C. and Hawkins, N. (1981). “Connections between steel frames and concrete walls.” *Engineering Journal (AISC)* First Quarter, 22-29.
62. Shirvani, M. (1998)."Behavior of tensile anchors in concrete: statistical analysis and design recommendations." M.S. thesis, University of Texas at Austin, Austin, TX.
63. Structural Engineers Association of Southern California (SEAOSC). (1997). “Standard method of cyclic load testing for anchors in concrete or grouted masonry.” *SEAOSC*, Whittier, California.
64. Shahrooz, B., Deason, J., and Tunc, G. (2004a). “Outrigger beam–wall connections. I: component testing and development of design model.” *Journal of Structural Engineering*, 130(2), 253-261.
65. Shahrooz, B., Tunc, G., and Deason, J. (2004b). “Outrigger beam–wall connections. II: subassembly testing and further modeling enhancements.” *Journal of Structural Engineering*, 130(2), 262-270.
66. Silva, J. F. (2003). “U.S. codes and standards governing the design of anchors for seismic applications.” *Conference Proceedings of the fib Symposium on Concrete Structures in Seismic Regions*, Athens, Greece.
67. Solomos, G. and Berra, M. (2006). "Testing of anchorages in concrete under dynamic tensile loading." *Materials And Structures Journal*, 39, 695-706.
68. Stephens, T. (2004). “Skinner building gets a seismic skeleton.” *Architecture and Engineering Perspectives: Seattle Daily Journal of Commerce*, November 2004.
69. Swirsky, R., Dusel, J., Crozier, W., Stoker, J., and Nordlin, E. (1978). "Lateral resistance of anchor bolts installed in concrete," *Report No. FHWA-CA-ST-4167-77-12*, California Department of Transportation, Sacramento, CA.
70. Technical Council on Lifeline Earthquake Engineering. (1995). “Northridge earthquake – lifeline performance and post-earthquake response, monograph No. 8.” *ASCE*, New York, NY.
71. Tong, X. (2001). “Seismic behavior of composite steel frame–reinforced concrete infill wall structural system.” Ph.D. thesis, Department of Civil Engineering, University of Minnesota, Minneapolis, MN.

72. Tong, X., Hajjar, J. F., Schultz, A. E., and Shield, C. K. (2005). “Cyclic behavior of composite steel frame-reinforced concrete infill wall structural system.” *Journal of Constructional Steel Research*, 61(4), 531-552.
73. United States Department of Labor, Directorate of Construction. (2003). Presentation at the construction safety council’s 13th annual construction safety and health conference exposition. *Electronic Library of Construction Occupational Safety and Health*.
74. Ueda, T., Kitipornchai, S., and Ling, K. (1990). “Experimental investigation of anchor bolts under shear.” *Journal of Structural Engineering*, ASCE, 116(4), 910-924.
75. Usami, S., Abe, U. and Matsuzaki, Y. (1980). "Experimental study on the strength of headed anchor bolts under alternate shear load and combined load (shear and axial)." *Proceedings of the Annual Meeting of the Kantou Branch of the Architectural Institute of Japan*.
76. Viest, I. M. (1956). “Investigation of stud shear connectors for composite concrete and steel t-beams,” *Journal of the American Concrete Institute*, 27(8), 875-891.

Appendix A Collected data on cast-in anchors in tension

Number	No.	d_a (in)	h_{ef} (in)	F_{uta} (ksi)	A_{brg} (in^2)	$A_{se,N}$	f'_c (psi)	c_{a1} (in)	c_{a2} (in)	c_{a3} (in)	x (in)	y (in)	h (in)	Crack	Reinf.	A_s (in^2)	f_y (ksi)	T (kips)	Mode
Ref.	of	Anchor	Embed	Steel	Head	Net	Concrete	Front	Side	Side	Block	Block	Block	in	Anchor	Reinf.	Yield	Measured	Reported
Paper	Test	Dia.	Depth	Strength	Area	Area	Strength	Edge	Edge 1	Edge 2	Length	Width	Height	Concrete	Pattern	Area	Strength	Tension	Failure
[1]	No1-1	0.63	3	66	0.45	0.30	4250	3	12	12	NA	NA	NA	None	None	0.00	NA	10.50	Cone
[1]	No1-2	0.63	3	66	0.45	0.30	4250	3	12	12	NA	NA	NA	None	None	0.00	NA	11.50	Cone
[1]	No1-3	0.63	3	66	0.45	0.30	4250	3	12	12	NA	NA	NA	None	None	0.00	NA	11.80	Cone
[1]	No1-4	0.63	3	66	0.45	0.30	4250	5	12	12	NA	NA	NA	None	None	0.00	NA	14.10	Cone
[1]	No1-5	0.63	3	66	0.45	0.30	4250	5	12	12	NA	NA	NA	None	None	0.00	NA	15.00	Cone
[1]	No1-6	0.63	3	66	0.45	0.30	4250	5	12	12	NA	NA	NA	None	None	0.00	NA	13.90	Cone
[1]	No1-7	0.63	3	66	0.45	0.30	4250	7	12	12	NA	NA	NA	None	None	0.00	NA	14.40	Cone
[1]	No1-8	0.63	3	66	0.45	0.30	4250	7	12	12	NA	NA	NA	None	None	0.00	NA	13.70	Cone
[1]	No1-9	0.63	3	66	0.45	0.30	4250	7	12	12	NA	NA	NA	None	None	0.00	NA	12.80	Cone
[1]	No1-10	0.63	4	66	0.45	0.30	4250	3	12	12	NA	NA	NA	None	None	0.00	NA	19.00	Steel
[1]	No1-11	0.63	4	66	0.45	0.30	4250	3	12	12	NA	NA	NA	None	None	0.00	NA	18.90	Steel
[1]	No1-12	0.63	4	66	0.45	0.30	4250	3	12	12	NA	NA	NA	None	None	0.00	NA	18.40	Steel
[1]	No1-13	0.63	4	66	0.45	0.30	4250	5	12	12	NA	NA	NA	None	None	0.00	NA	18.50	Steel
[1]	No1-14	0.63	4	66	0.45	0.30	4250	5	12	12	NA	NA	NA	None	None	0.00	NA	18.90	Steel
[1]	No1-15	0.63	4	66	0.45	0.30	4250	5	12	12	NA	NA	NA	None	None	0.00	NA	18.70	Steel
[1]	No1-16	0.63	4	66	0.45	0.30	4250	7	12	12	NA	NA	NA	None	None	0.00	NA	18.70	Steel
[1]	No1-17	0.63	4	66	0.45	0.30	4250	7	12	12	NA	NA	NA	None	None	0.00	NA	18.10	Steel
[1]	No1-18	0.63	4	66	0.45	0.30	4250	7	12	12	NA	NA	NA	None	None	0.00	NA	19.10	Steel
[1]	No1-19	0.63	6	66	0.45	0.30	4250	3	12	12	NA	NA	NA	None	None	0.00	NA	19.50	Steel
[1]	No1-20	0.63	6	66	0.45	0.30	4250	3	12	12	NA	NA	NA	None	None	0.00	NA	19.70	Steel
[1]	No1-21	0.63	6	66	0.45	0.30	4250	3	12	12	NA	NA	NA	None	None	0.00	NA	16.50	Steel
[1]	No1-22	0.63	6	66	0.45	0.30	4250	5	12	12	NA	NA	NA	None	None	0.00	NA	19.10	Steel
[1]	No1-23	0.63	6	66	0.45	0.30	4250	5	12	12	NA	NA	NA	None	None	0.00	NA	19.00	Steel
[1]	No1-24	0.63	6	66	0.45	0.30	4250	5	12	12	NA	NA	NA	None	None	0.00	NA	20.30	Steel
[1]	No2-1	1.00	3	66	1.16	0.61	4250	5	12	12	NA	NA	NA	None	None	0.00	NA	12.20	Cone
[1]	No2-2	1.00	3	66	1.16	0.61	4250	5	12	12	NA	NA	NA	None	None	0.00	NA	11.90	Cone
[1]	No2-3	1.00	3	66	1.16	0.61	4250	5	12	12	NA	NA	NA	None	None	0.00	NA	14.50	Cone
[1]	No2-4	1.00	3	66	1.16	0.61	4250	7	12	12	NA	NA	NA	None	None	0.00	NA	14.30	Cone
[1]	No2-5	1.00	3	66	1.16	0.61	4250	7	12	12	NA	NA	NA	None	None	0.00	NA	15.20	Cone
[1]	No2-6	1.00	3	66	1.16	0.61	4250	7	12	12	NA	NA	NA	None	None	0.00	NA	14.20	Cone
[1]	No2-7	1.00	4	66	1.16	0.61	4250	5	12	12	NA	NA	NA	None	None	0.00	NA	19.30	Cone
[1]	No2-8	1.00	4	66	1.16	0.61	4250	5	12	12	NA	NA	NA	None	None	0.00	NA	22.70	Cone
[1]	No2-9	1.00	4	66	1.16	0.61	4250	5	12	12	NA	NA	NA	None	None	0.00	NA	22.50	Cone
[1]	No2-10	1.00	4	66	1.16	0.61	4250	7	12	12	NA	NA	NA	None	None	0.00	NA	20.80	Cone
[1]	No2-11	1.00	4	66	1.16	0.61	4250	7	12	12	NA	NA	NA	None	None	0.00	NA	20.90	Cone

[1]	No2-12	1.00	4	66	1.16	0.61	4250	7	12	12	NA	NA	NA	None	None	0.00	NA	22.60	Cone
[1]	No2-13	1.00	4	66	1.16	0.61	4250	12	12	12	NA	NA	NA	None	None	0.00	NA	23.30	Cone
[1]	No2-14	1.00	4	66	1.16	0.61	4250	12	12	12	NA	NA	NA	None	None	0.00	NA	24.40	Cone
[1]	No2-15	1.00	4	66	1.16	0.61	4250	12	12	12	NA	NA	NA	None	None	0.00	NA	24.10	Cone
[1]	No2-16	1.00	6	66	1.16	0.61	4250	3	12	12	NA	NA	NA	None	None	0.00	NA	31.40	Cone
[1]	No2-17	1.00	6	66	1.16	0.61	4250	3	12	12	NA	NA	NA	None	None	0.00	NA	32.40	Cone
[1]	No2-18	1.00	6	66	1.16	0.61	4250	3	12	12	NA	NA	NA	None	None	0.00	NA	28.60	Cone
[1]	No2-19	1.00	6	66	1.16	0.61	4250	5	12	12	NA	NA	NA	None	None	0.00	NA	33.50	Cone
[1]	No2-20	1.00	6	66	1.16	0.61	4250	5	12	12	NA	NA	NA	None	None	0.00	NA	33.70	Cone
[1]	No2-21	1.00	6	66	1.16	0.61	4250	5	12	12	NA	NA	NA	None	None	0.00	NA	39.30	Cone
[1]	No2-22	1.00	6	66	1.16	0.61	4250	7	12	12	NA	NA	NA	None	None	0.00	NA	44.70	Steel
[1]	No2-23	1.00	6	66	1.16	0.61	4250	7	12	12	NA	NA	NA	None	None	0.00	NA	39.20	Steel
[1]	No2-24	1.00	6	66	1.16	0.61	4250	9	12	12	NA	NA	NA	None	None	0.00	NA	42.50	Steel
[1]	No2-25	1.00	6	66	1.16	0.61	4250	9	12	12	NA	NA	NA	None	None	0.00	NA	39.80	Steel
[1]	No2-26	1.00	6	66	1.16	0.61	4250	12	12	12	NA	NA	NA	None	None	0.00	NA	39.20	Steel
[1]	No2-27	1.00	6	66	1.16	0.61	4250	12	12	12	NA	NA	NA	None	None	0.00	NA	37.80	Steel
[1]	No2-28	1.00	6	66	1.16	0.61	4250	12	12	12	NA	NA	NA	None	None	0.00	NA	40.50	Steel
[2]	A1-1	0.75	7	64	0.79	0.44	5270	12	12	12	84	24	24	None	None	0.00	NA	28.30	Steel
[2]	A1-2	0.75	7	64	0.79	0.44	5270	12	12	12	84	24	24	None	None	0.00	NA	28.50	Steel
[2]	A1-3	0.75	7	64	0.79	0.44	5270	12	12	12	84	24	24	None	None	0.00	NA	28.00	Steel
[2]	D3-1	0.75	7	64	0.79	0.44	5300	12	12	12	84	24	24	None	None	0.00	NA	28.70	Steel
[2]	A1-4	0.75	7	64	0.79	0.44	5270	2	12	12	84	24	24	None	None	0.00	NA	19.50	Cone
[2]	A1-5	0.75	7	64	0.79	0.44	5270	2	12	12	84	24	24	None	None	0.00	NA	18.50	Cone
[2]	A2-4	0.75	7	64	0.79	0.44	5270	4	12	12	84	24	24	None	None	0.00	NA	31.50	Steel
[2]	A2-5	0.75	7	64	0.79	0.44	5270	4	12	12	84	24	24	None	None	0.00	NA	29.30	Steel
[2]	B3-5	0.75	7	64	0.79	0.44	4900	4	12	12	84	24	24	None	None	0.00	NA	29.40	Steel
[2]	C2-4	0.75	7	64	0.79	0.44	5180	4	12	12	84	24	24	None	None	0.00	NA	29.40	Cone
[2]	A3-4	0.75	7	64	0.79	0.44	5270	6	12	12	84	24	24	None	None	0.00	NA	29.30	Steel
[2]	A3-5	0.75	7	64	0.79	0.44	5270	6	12	12	84	24	24	None	None	0.00	NA	28.80	Steel
[2]	B3-4	0.75	7	64	0.79	0.44	4900	6	12	12	84	24	24	None	None	0.00	NA	31.50	Steel
[2]	C3-4	0.75	7	64	0.79	0.44	5180	6	12	12	84	24	24	None	None	0.00	NA	29.50	Cone
[2]	C3-5	0.75	7	64	0.79	0.44	5180	6	12	12	84	24	24	None	None	0.00	NA	27.30	Steel
[2]	B1-1	0.88	8	64	0.79	0.60	4900	12	12	12	84	24	24	None	None	0.00	NA	43.00	Cone
[2]	D1-1	0.75	8	64	0.79	0.44	5300	12	12	12	84	24	24	None	None	0.00	NA	30.10	Cone
[2]	D1-2	0.75	8	64	0.79	0.44	5300	12	12	12	84	24	24	None	None	0.00	NA	31.50	Cone
[2]	C1-1	0.75	4	64	0.79	0.44	5180	12	12	12	84	24	24	None	None	0.00	NA	18.50	Cone
[2]	C1-2	0.75	4	64	0.79	0.44	5180	12	12	12	84	24	24	None	None	0.00	NA	18.50	Cone
[2]	C1-3	0.75	4	64	0.79	0.44	5180	12	12	12	84	24	24	None	None	0.00	NA	17.30	Cone
[2]	B1-5	0.75	4	64	0.79	0.44	4900	2	12	12	84	24	24	None	None	0.00	NA	11.00	Cone
[3]	1.00x15Dx1.0x2.5	1.00	15	125	4.12	0.61	5500	2	18	18	36	36	96	None	Long. bars	8.00	60.00	62.00	Steel-
[3]	1.00x15Dx2.5x2.5	1.00	15	125	4.12	0.61	3910	4	18	18	36	36	96	None	Long. bars	8.00	60.00	77.00	Steel-

[3]	1.00x15Dx3.5x2.5	1.00	15	125	4.12	0.61	3520	5	18	18	36	36	96	None	Long. bars	8.00	60.00	76.80	Steel-
[3]	1.00x15Dx3.5x2.5	1.00	15	125	4.12	0.61	4290	5	18	18	36	36	96	None	Long. bars	8.00	60.00	81.60	Steel-
[3]	1.00x15Dx4.5x2.5	1.00	15	125	4.12	0.61	4910	6	18	18	36	36	96	None	Long. bars	8.00	60.00	78.30	Steel-
[3]	1.75x15Dx2.5x4	1.75	26	135	10.16	2.08	3950	5	18	18	36	36	96	None	Long. bars	8.00	60.00	139.80	Steel-
[3]	1.75x15Dx3.5x4	1.75	26	135	10.16	2.08	3630	6	18	18	36	36	96	None	Long. bars	8.00	60.00	149.40	Steel-
[3]	1.75x15Dx4.5x4	1.75	26	135	10.16	2.08	4680	7	18	18	36	36	96	None	Long. bars	8.00	60.00	178.30	Steel-
[3]	1.75x15Dx4.5x4	1.75	26	135	10.16	2.08	4310	7	18	18	36	36	96	None	Long. bars	8.00	60.00	168.00	Steel-
[3]	1.75x15Dx6.0x4	1.75	26	135	10.16	2.08	3980	8	18	18	36	36	96	None	Long. bars	8.00	60.00	212.90	Steel-
[3]	1.00x20Dx2.5x2.5	1.00	20	125	4.12	0.61	3880	4	18	18	36	36	96	None	Long. bars	8.00	60.00	79.30	Steel
[3]	1.00x20Dx3.5x2.5	1.00	20	125	4.12	0.61	3930	5	18	18	36	36	96	None	Long. bars	8.00	60.00	75.50	Steel
[3]	1.75x20Dx3.5x4	1.75	35	135	10.16	2.08	3680	6	18	18	36	36	96	None	Long. bars	8.00	60.00	143.40	Steel-
[3]	1.75x20Dx4.5x4	1.75	35	135	10.16	2.08	4910	7	18	18	36	36	96	None	Long. bars	8.00	60.00	188.30	Steel-
[3]	1.00x10Dx2.5x2.5	1.00	10	125	4.12	0.61	5110	4	18	18	36	36	96	None	Long. bars	6.00	60.00	61.00	Steel-
[3]	1.75x10Dx3.5x4	1.75	18	135	10.16	2.08	5480	6	18	18	36	36	96	None	Long. bars	8.00	60.00	139.60	Steel-
[3]	1.75x10Dx6x4	1.75	18	135	10.16	2.08	5120	8	18	18	36	36	96	None	Long. bars	8.00	60.00	157.00	Steel-
[3]	1.00x15Dx2.5x3.25	1.00	15	125	4.12	0.61	5480	4	18	18	36	36	96	None	Long. bars	8.00	60.00	81.70	Steel
[3]	1.00x15Dx4.5x4.5	1.00	15	125	4.12	0.61	4290	7	18	18	36	36	96	None	Long. bars	8.00	60.00	81.70	Steel
[3]	1.75x15Dx3.5x3	1.75	26	135	10.16	2.08	2640	5	18	18	36	36	96	None	Long. bars	8.00	60.00	68.00	Steel-
[3]	1.75x15Dx3.5x3.25	1.75	26	135	10.16	2.08	4300	5	18	18	36	36	96	None	Long. bars	8.00	60.00	155.40	Steel-
[3]	1.75x15Dx3.5x3.5	1.75	26	135	10.16	2.08	5470	6	18	18	36	36	96	None	Long. bars	8.00	60.00	148.90	Steel-
[3]	1.75x15Dx3.5x5	1.75	26	135	10.16	2.08	2770	6	18	18	36	36	96	None	Long. bars	8.00	60.00	117.80	Steel-
[3]	1.00x15Dx2.5x2.5U	1.00	15	125	4.12	0.61	5260	4	18	18	36	36	96	None	Long. bars	8.00	60.00	79.80	Steel
[3]	1.75x15Dx3.5x4U	1.75	26	135	10.16	2.08	5380	6	18	18	36	36	96	None	Long. bars	8.00	60.00	163.50	Steel-
[3]	1.75x15Dx3.5x5U	1.75	26	135	10.16	2.08	3960	6	18	18	36	36	96	None	Long. bars	8.00	60.00	157.00	Steel-
[3]	0.5x15Dx0.5	0.50	8	125	1.13	0.14	3460	1	5	5	9	9	36	None	Long. bars	0.44	60.00	11.50	Steel-
[3]	0.5x15Dx0.75	0.50	8	125	1.13	0.14	3460	1	5	5	9	9	36	None	Long. bars	0.44	60.00	16.00	Steel-
[3]	0.5x15Dx0.75	0.50	8	125	1.13	0.14	3260	1	5	5	9	9	36	None	Long. bars	0.44	60.00	16.82	Steel-
[3]	0.5x15Dx1.0	0.50	8	125	1.13	0.14	5025	1	5	5	9	9	36	None	Long. bars	0.44	60.00	16.86	Steel-
[3]	0.5x15Dx1.0	0.50	8	125	1.13	0.14	5450	1	5	5	9	9	36	None	Long. bars	0.44	60.00	19.00	Stee
[3]	0.5x15Dx1.0	0.50	8	125	1.13	0.14	3090	1	5	5	9	9	36	None	Long. bars	0.44	60.00	13.00	Steel-
[3]	0.5x15Dx1.0	0.50	8	125	0.69	0.14	3260	2	5	5	9	9	36	None	Long. bars	0.44	60.00	15.33	Steel-
[3]	0.5x15Dx1.0	0.50	8	125	2.21	0.14	3260	2	5	5	9	9	36	None	Long. bars	0.44	60.00	13.00	Steel-
[3]	0.5x15Dx1.25	0.50	8	125	1.13	0.14	5960	1	5	5	9	9	36	None	Long. bars	0.44	60.00	21.41	Steel
[3]	0.5x15Dx1.25	0.50	8	125	1.13	0.14	3660	1	5	5	9	9	36	None	Long. bars	0.44	60.00	15.05	Steel-
[3]	0.5x15Dx1.25	0.50	8	125	0.69	0.14	3450	2	5	5	9	9	36	None	Long. bars	0.44	60.00	14.20	Steel-
[3]	0.5x15Dx1.25	0.50	8	125	2.21	0.14	3260	2	5	5	9	9	36	None	Long. bars	0.44	60.00	17.84	Steel
[3]	0.5x15Dx1.5	0.50	8	125	1.13	0.14	3950	1	5	5	9	9	36	None	Long. bars	0.44	60.00	15.48	Steel-
[3]	0.5x15Dx1.75	0.50	8	125	1.13	0.14	3400	1	5	5	9	9	36	None	Long. bars	0.44	60.00	18.00	Steel
[3]	0.5x15Dx1.75	0.50	8	125	0.69	0.14	3090	2	5	5	9	9	36	None	Long. bars	0.44	60.00	10.48	Steel-
[3]	0.5x15Dx2.0	0.50	8	125	1.13	0.14	3090	1	5	5	9	9	36	None	Long. bars	0.44	60.00	18.75	Steel
[3]	0.5x15Dx2.25	0.50	8	125	0.69	0.14	3500	3	5	5	9	9	36	None	Long. bars	0.44	60.00	21.00	Steel

[3]	0.5x20Dx0.75	0.50	10	125	1.29	0.14	2970	1	5	5	9	9	36	None	Long. bars	0.44	60.00	14.95	Steel-
[3]	0.5x20Dx1.0	0.50	10	125	1.29	0.14	5000	2	5	5	9	9	36	None	Long. bars	0.44	60.00	16.50	Stee
[3]	0.5x20Dx1.0	0.50	10	125	1.29	0.14	3090	2	5	5	9	9	36	None	Long. bars	0.44	60.00	13.96	Steel-
[3]	0.5x20Dx1.0	0.50	10	125	1.29	0.14	5655	2	5	5	9	9	36	None	Long. bars	0.44	60.00	21.50	Steel
[3]	0.5x20Dx1.25	0.50	10	125	1.29	0.14	3460	2	5	5	9	9	36	None	Long. bars	0.44	60.00	17.50	Steel-
[3]	0.5x20Dx1.25	0.50	10	125	0.69	0.14	3500	2	5	5	9	9	36	None	Long. bars	0.44	60.00	16.54	Steel-
[3]	0.5x10Dx1.0	0.50	5	125	1.29	0.14	4530	2	5	5	9	9	36	None	Long. bars	0.44	60.00	9.48	Stee
[3]	0.5x10Dx1.25	0.50	5	125	1.29	0.14	4025	2	5	5	9	9	36	None	Long. bars	0.44	60.00	11.50	Steel-
[3]	0.5x10Dx1.5	0.50	5	125	1.29	0.14	5040	2	5	5	9	9	36	None	Long. bars	0.44	60.00	15.50	Steel
[3]	0.5x10Dx1.5	0.50	5	125	1.29	0.14	3610	2	5	5	9	9	36	None	Long. bars	0.44	60.00	8.41	Steel-
[3]	0.5x10Dx1.75	0.50	5	125	0.69	0.14	3430	2	5	5	9	9	36	None	Long. bars	0.44	60.00	9.61	Steel-
[3]	0.5x10Dx2.0	0.50	5	125	0.69	0.14	3120	3	5	5	9	9	36	None	Long. bars	0.44	60.00	13.40	Steel-
[4]	#1	0.75	3	60	0.65	0.33	4315	15	NA	NA	NA	NA	NA	None	None	0.00	NA	16.00	Cone
[4]	#2	0.75	4	60	0.65	0.33	4315	15	NA	NA	NA	NA	NA	None	None	0.00	NA	25.40	Cone
[4]	#3	0.75	6	60	0.65	0.33	5050	5	NA	NA	NA	NA	NA	None	None	0.00	NA	26.10	Steel
[4]	#4	0.75	6	60	0.65	0.33	5050	6	NA	NA	NA	NA	NA	None	None	0.00	NA	26.20	Steel
[4]	#5	0.75	7	60	0.65	0.33	4000	2	NA	NA	NA	NA	NA	None	None	0.00	NA	23.80	Cone
[4]	#6	0.75	7	60	0.65	0.33	5050	2	NA	NA	NA	NA	NA	None	None	0.00	NA	25.40	Steel
[4]	#7	0.75	7	60	0.65	0.33	5050	4	NA	NA	NA	NA	NA	None	None	0.00	NA	26.30	Steel
[4]	#8	0.75	7	60	0.65	0.33	5050	5	NA	NA	NA	NA	NA	None	None	0.00	NA	29.60	Steel
[4]	#9	0.75	8	60	0.65	0.33	3500	2	NA	NA	NA	NA	NA	None	None	0.00	NA	23.20	Steel
[4]	#10	0.75	8	60	0.65	0.33	3500	4	NA	NA	NA	NA	NA	None	None	0.00	NA	24.40	Steel
[4]	#11	0.75	5	60	0.65	0.33	5500	3	NA	NA	NA	NA	NA	None	None	0.00	NA	23.20	Cone
[4]	#12	0.75	5	60	0.65	0.33	5500	4	NA	NA	NA	NA	NA	None	None	0.00	NA	29.90	Steel
[4]	#13	0.75	6	60	0.65	0.33	5500	3	NA	NA	NA	NA	NA	None	None	0.00	NA	25.40	Steel
[4]	#14	0.75	4	60	0.65	0.33	4870	2	NA	NA	NA	NA	NA	None	None	0.00	NA	9.90	Cone
[4]	#15	0.75	4	60	0.65	0.33	4315	2	NA	NA	NA	NA	NA	None	None	0.00	NA	16.60	Cone
[4]	#16	0.75	4	60	0.65	0.33	4870	3	NA	NA	NA	NA	NA	None	None	0.00	NA	13.30	Cone
[4]	#17	0.75	4	60	0.65	0.33	4315	3	NA	NA	NA	NA	NA	None	None	0.00	NA	18.30	Cone
[4]	#18	0.75	4	60	0.65	0.33	4870	4	NA	NA	NA	NA	NA	None	None	0.00	NA	19.90	Cone
[4]	#19	0.75	5	60	0.65	0.33	4635	2	NA	NA	NA	NA	NA	None	None	0.00	NA	14.50	Cone
[4]	#20	0.75	5	60	0.65	0.33	3500	2	NA	NA	NA	NA	NA	None	None	0.00	NA	14.90	Cone
[4]	#21	0.75	5	60	0.65	0.33	4635	3	NA	NA	NA	NA	NA	None	None	0.00	NA	20.50	Cone
[4]	#22	0.75	5	60	0.65	0.33	4635	4	NA	NA	NA	NA	NA	None	None	0.00	NA	22.00	Cone
[4]	#23	0.75	5	60	0.65	0.33	4635	5	NA	NA	NA	NA	NA	None	None	0.00	NA	21.00	Steel
[4]	#24	0.75	6	60	0.65	0.33	4635	2	NA	NA	NA	NA	NA	None	None	0.00	NA	22.70	Cone
[4]	#25	0.75	6	60	0.65	0.33	3500	2	NA	NA	NA	NA	NA	None	None	0.00	NA	17.70	Cone
[4]	#26	0.75	6	60	0.65	0.33	4315	3	NA	NA	NA	NA	NA	None	None	0.00	NA	28.20	Cone
[4]	#27	0.75	6	60	0.65	0.33	5050	3	NA	NA	NA	NA	NA	None	None	0.00	NA	26.00	Steel
[4]	#28	0.75	6	60	0.65	0.33	5050	4	NA	NA	NA	NA	NA	None	None	0.00	NA	26.10	Steel
[4]	#29	0.75	6	60	0.65	0.33	5500	3	NA	NA	NA	NA	NA	None	None	0.00	NA	26.00	Steel

[4]	#30	0.75	7	60	0.65	0.33	5500	1	NA	NA	NA	NA	NA	None	None	0.00	NA	22.10	Cone
[4]	#31	0.75	7	60	0.65	0.33	5500	3	NA	NA	NA	NA	NA	None	None	0.00	NA	30.40	Steel
[4]	#32	0.75	8	60	0.65	0.33	5500	3	NA	NA	NA	NA	NA	None	None	0.00	NA	29.30	Steel
[4]	#33	0.75	8	60	0.65	0.33	5500	3	NA	NA	NA	NA	NA	None	None	0.00	NA	27.70	Steel
[4]	#34	0.75	4	60	0.65	0.33	5500	2	NA	NA	NA	NA	NA	None	None	0.00	NA	14.40	Cone
[4]	#35	0.75	4	60	0.65	0.33	5500	2	NA	NA	NA	NA	NA	None	None	0.00	NA	16.60	Cone
[4]	#36	1.00	10	150	1.16	0.33	4300	18	NA	NA	NA	NA	NA	None	None	0.00	NA	98.00	Cone
[4]	#37	1.00	13	150	1.16	0.33	4300	18	NA	NA	NA	NA	NA	None	None	0.00	NA	116.00	Steel
[4]	#38	1.00	15	150	1.16	0.33	4245	18	NA	NA	NA	NA	NA	None	None	0.00	NA	118.00	Steel
[4]	#39	1.00	17	150	1.16	0.33	4200	18	NA	NA	NA	NA	NA	None	None	0.00	NA	118.00	Steel
[4]	#40	1.00	12	150	1.16	0.33	4300	5	NA	NA	NA	NA	NA	None	None	0.00	NA	76.00	Cone
[4]	#41	1.00	14	150	1.16	0.33	4300	5	NA	NA	NA	NA	NA	None	None	0.00	NA	82.00	Cone
[4]	#42	1.00	16	150	1.16	0.33	4300	5	NA	NA	NA	NA	NA	None	None	0.00	NA	82.00	Cone
[4]	#43	1.00	18	150	1.16	0.33	4245	5	NA	NA	NA	NA	NA	None	None	0.00	NA	94.00	Cone
[5]	GER4-001	0.37	2	63	0.33	NA	1695	3	39	39	NA	NA	NA	None	None	0.00	NA	2.97	Cone
[5]	GER4-002	0.37	2	63	0.33	NA	1695	3	39	39	NA	NA	NA	None	None	0.00	NA	3.15	Cone
[5]	GER4-003	0.37	2	63	0.33	NA	1695	3	39	39	NA	NA	NA	None	None	0.00	NA	3.33	Cone
[5]	GER4-004	0.37	2	63	0.33	NA	3491	3	39	39	NA	NA	NA	None	None	0.00	NA	4.54	Cone
[5]	GER4-005	0.37	2	63	0.33	NA	3491	3	39	39	NA	NA	NA	None	None	0.00	NA	4.77	Cone
[5]	GER4-006	0.37	2	63	0.33	NA	3491	3	39	39	NA	NA	NA	None	None	0.00	NA	4.77	Cone
[5]	GER4-007	0.37	2	63	0.33	NA	3429	8	39	39	NA	NA	NA	None	None	0.00	NA	3.42	Cone
[5]	GER4-008	0.37	2	63	0.33	NA	3491	8	39	39	NA	NA	NA	None	None	0.00	NA	3.60	Cone
[5]	GER4-009	0.37	2	63	0.33	NA	3085	8	39	39	NA	NA	NA	None	None	0.00	NA	4.09	Cone
[5]	GER4-010	0.37	2	63	0.33	NA	3085	8	39	39	NA	NA	NA	None	None	0.00	NA	4.32	Cone
[5]	GER4-011	0.37	2	63	0.33	NA	3429	8	39	39	NA	NA	NA	None	None	0.00	NA	4.63	Cone
[5]	GER4-012	0.37	2	63	0.33	NA	3429	8	39	39	NA	NA	NA	None	None	0.00	NA	4.63	Cone
[5]	GER4-013	0.37	2	63	0.33	NA	3085	8	39	39	NA	NA	NA	None	None	0.00	NA	4.68	Cone
[5]	GER4-014	0.37	2	63	0.33	NA	3085	8	39	39	NA	NA	NA	None	None	0.00	NA	4.68	Cone
[5]	GER4-015	0.37	2	63	0.33	NA	3429	8	39	39	NA	NA	NA	None	None	0.00	NA	4.72	Cone
[5]	GER4-016	0.37	2	63	0.33	NA	3429	8	39	39	NA	NA	NA	None	None	0.00	NA	4.77	Cone
[5]	GER4-017	0.37	2	63	0.33	NA	3085	8	39	39	NA	NA	NA	None	None	0.00	NA	4.95	Cone
[5]	GER4-018	0.37	2	63	0.33	NA	3429	8	39	39	NA	NA	NA	None	None	0.00	NA	5.08	Cone
[5]	GER4-019	0.37	2	63	0.33	NA	4326	8	39	39	NA	NA	NA	None	None	0.00	NA	5.17	Cone
[5]	GER4-020	0.37	2	63	0.33	NA	3491	8	39	39	NA	NA	NA	None	None	0.00	NA	5.40	Cone
[5]	GER4-021	0.37	2	63	0.33	NA	3085	8	39	39	NA	NA	NA	None	None	0.00	NA	5.58	Cone
[5]	GER4-022	0.37	2	63	0.33	NA	4486	8	39	39	NA	NA	NA	None	None	0.00	NA	5.62	Cone
[5]	GER4-023	0.37	2	63	0.33	NA	4486	8	39	39	NA	NA	NA	None	None	0.00	NA	5.62	Cone
[5]	GER4-024	0.37	2	63	0.33	NA	4326	8	39	39	NA	NA	NA	None	None	0.00	NA	5.73	Cone
[5]	GER4-025	0.37	2	63	0.33	NA	4486	8	39	39	NA	NA	NA	None	None	0.00	NA	6.07	Cone
[5]	GER4-026	0.37	2	63	0.33	NA	4326	8	39	39	NA	NA	NA	None	None	0.00	NA	6.07	Cone
[5]	GER4-027	0.37	2	63	0.33	NA	4326	8	39	39	NA	NA	NA	None	None	0.00	NA	6.07	Cone

[5]	GER4-028	0.37	2	63	0.33	NA	4326	8	39	39	NA	NA	NA	None	None	0.00	NA	6.18	Cone
[5]	GER4-029	0.37	2	63	0.33	NA	4326	8	39	39	NA	NA	NA	None	None	0.00	NA	6.63	Cone
[5]	GER4-030	0.87	3	63	0.88	NA	3749	8	39	39	NA	NA	NA	None	None	0.00	NA	6.86	Cone
[5]	GER4-031	0.87	3	63	0.88	NA	3749	8	39	39	NA	NA	NA	None	None	0.00	NA	9.31	Cone
[5]	GER4-032	0.87	3	63	0.88	NA	3749	8	39	39	NA	NA	NA	None	None	0.00	NA	9.53	Cone
[5]	GER4-033	0.63	3	63	0.92	NA	1695	5	39	39	NA	NA	NA	None	None	0.00	NA	7.19	Cone
[5]	GER4-034	0.63	3	63	0.92	NA	1695	5	39	39	NA	NA	NA	None	None	0.00	NA	7.37	Cone
[5]	GER4-035	0.63	3	63	0.92	NA	1695	5	39	39	NA	NA	NA	None	None	0.00	NA	7.46	Cone
[5]	GER4-036	0.63	3	63	0.92	NA	3491	5	39	39	NA	NA	NA	None	None	0.00	NA	10.70	Cone
[5]	GER4-037	0.63	3	63	0.92	NA	3491	5	39	39	NA	NA	NA	None	None	0.00	NA	11.15	Cone
[5]	GER4-038	0.63	3	63	0.92	NA	3491	5	39	39	NA	NA	NA	None	None	0.00	NA	11.87	Cone
[5]	GER4-039	0.63	3	63	0.92	NA	2791	8	39	39	NA	NA	NA	None	None	0.00	NA	8.32	Cone
[5]	GER4-040	0.63	3	63	0.92	NA	2791	8	39	39	NA	NA	NA	None	None	0.00	NA	9.10	Cone
[5]	GER4-041	0.63	3	63	0.92	NA	2791	8	39	39	NA	NA	NA	None	None	0.00	NA	9.44	Cone
[5]	GER4-042	0.63	3	63	0.92	NA	2791	8	39	39	NA	NA	NA	None	None	0.00	NA	9.78	Cone
[5]	GER4-043	0.63	3	63	0.92	NA	2791	8	39	39	NA	NA	NA	None	None	0.00	NA	9.89	Cone
[5]	GER4-044	0.63	3	63	0.92	NA	2791	8	39	39	NA	NA	NA	None	None	0.00	NA	11.13	Cone
[5]	GER4-045	0.63	3	63	0.92	NA	1401	12	39	39	NA	NA	NA	None	None	0.00	NA	6.52	Cone
[5]	GER4-046	0.63	3	63	0.92	NA	1401	12	39	39	NA	NA	NA	None	None	0.00	NA	7.19	Cone
[5]	GER4-047	0.63	3	63	0.92	NA	1401	12	39	39	NA	NA	NA	None	None	0.00	NA	8.32	Cone
[5]	GER4-048	0.63	3	63	0.92	NA	2791	12	39	39	NA	NA	NA	None	None	0.00	NA	8.43	Cone
[5]	GER4-049	0.63	3	63	0.92	NA	2791	12	39	39	NA	NA	NA	None	None	0.00	NA	8.77	Cone
[5]	GER4-050	0.63	3	63	0.92	NA	2791	12	39	39	NA	NA	NA	None	None	0.00	NA	8.99	Cone
[5]	GER4-051	0.63	3	63	0.92	NA	2791	12	39	39	NA	NA	NA	None	None	0.00	NA	8.99	Cone
[5]	GER4-052	0.63	3	63	0.92	NA	2791	12	39	39	NA	NA	NA	None	None	0.00	NA	9.44	Cone
[5]	GER4-053	0.63	3	63	0.92	NA	2791	12	39	39	NA	NA	NA	None	None	0.00	NA	10.12	Cone
[5]	GER4-054	0.63	3	63	0.92	NA	5703	12	39	39	NA	NA	NA	None	None	0.00	NA	12.14	Cone
[5]	GER4-055	0.63	3	63	0.92	NA	5703	12	39	39	NA	NA	NA	None	None	0.00	NA	12.59	Cone
[5]	GER4-056	0.63	3	63	0.92	NA	5703	12	39	39	NA	NA	NA	None	None	0.00	NA	12.81	Cone
[5]	GER4-057	0.63	3	63	0.92	NA	4585	12	39	39	NA	NA	NA	None	None	0.00	NA	12.93	Cone
[5]	GER4-058	0.63	3	63	0.92	NA	4585	12	39	39	NA	NA	NA	None	None	0.00	NA	13.04	Cone
[5]	GER4-059	0.63	3	63	0.92	NA	4585	12	39	39	NA	NA	NA	None	None	0.00	NA	13.26	Cone
[5]	GER4-060	0.63	3	63	0.92	NA	5703	12	39	39	NA	NA	NA	None	None	0.00	NA	13.26	Cone
[5]	GER4-061	0.63	3	63	0.92	NA	5703	12	39	39	NA	NA	NA	None	None	0.00	NA	13.49	Cone
[5]	GER4-062	0.63	3	63	0.92	NA	5703	12	39	39	NA	NA	NA	None	None	0.00	NA	13.71	Cone
[5]	GER4-063	0.87	4	63	0.88	NA	1695	6	39	39	NA	NA	NA	None	None	0.00	NA	10.39	Cone
[5]	GER4-064	0.87	4	63	0.88	NA	1695	6	39	39	NA	NA	NA	None	None	0.00	NA	10.43	Cone
[5]	GER4-065	0.87	4	63	0.88	NA	1695	6	39	39	NA	NA	NA	None	None	0.00	NA	10.75	Cone
[5]	GER4-066	0.87	4	63	0.88	NA	3491	6	39	39	NA	NA	NA	None	None	0.00	NA	15.02	Cone
[5]	GER4-067	0.87	4	63	0.88	NA	3491	6	39	39	NA	NA	NA	None	None	0.00	NA	15.83	Cone
[5]	GER4-068	0.87	4	63	0.88	NA	3491	6	39	39	NA	NA	NA	None	None	0.00	NA	16.01	Cone

[5]	GER4-069	0.87	4	63	0.88	NA	3749	8	39	39	NA	NA	NA	None	None	0.00	NA	15.56	Cone
[5]	GER4-070	0.87	4	63	0.88	NA	3749	8	39	39	NA	NA	NA	None	None	0.00	NA	16.01	Cone
[5]	GER4-071	0.87	4	63	0.88	NA	3749	8	39	39	NA	NA	NA	None	None	0.00	NA	17.09	Cone
[5]	GER4-072	0.87	4	63	0.88	NA	5703	8	39	39	NA	NA	NA	None	None	0.00	NA	17.65	Cone
[5]	GER4-073	0.87	4	63	0.88	NA	5703	8	39	39	NA	NA	NA	None	None	0.00	NA	17.98	Cone
[5]	GER4-074	0.87	4	63	0.88	NA	5703	8	39	39	NA	NA	NA	None	None	0.00	NA	18.32	Cone
[5]	GER4-075	0.87	4	63	0.88	NA	5703	8	39	39	NA	NA	NA	None	None	0.00	NA	18.43	Cone
[5]	GER4-076	0.87	4	63	0.88	NA	5703	8	39	39	NA	NA	NA	None	None	0.00	NA	18.77	Cone
[5]	GER4-077	0.87	4	63	0.88	NA	5703	8	39	39	NA	NA	NA	None	None	0.00	NA	20.68	Cone
[5]	GER4-078	0.87	4	63	0.88	NA	3429	12	39	39	NA	NA	NA	None	None	0.00	NA	13.94	Cone
[5]	GER4-079	0.87	4	63	0.88	NA	3429	12	39	39	NA	NA	NA	None	None	0.00	NA	14.39	Cone
[5]	GER4-080	0.87	4	63	0.88	NA	3429	12	39	39	NA	NA	NA	None	None	0.00	NA	14.57	Cone
[5]	GER4-081	0.87	4	63	0.88	NA	3429	12	39	39	NA	NA	NA	None	None	0.00	NA	14.75	Cone
[5]	GER4-082	0.87	4	63	0.88	NA	3085	12	39	39	NA	NA	NA	None	None	0.00	NA	15.20	Cone
[5]	GER4-083	0.87	4	63	0.88	NA	3429	12	39	39	NA	NA	NA	None	None	0.00	NA	15.38	Cone
[5]	GER4-084	0.87	4	63	0.88	NA	3429	12	39	39	NA	NA	NA	None	None	0.00	NA	15.38	Cone
[5]	GER4-085	0.87	4	63	0.88	NA	3491	12	39	39	NA	NA	NA	None	None	0.00	NA	15.51	Cone
[5]	GER4-086	0.87	4	63	0.88	NA	4326	12	39	39	NA	NA	NA	None	None	0.00	NA	16.41	Cone
[5]	GER4-087	0.87	4	63	0.88	NA	3085	12	39	39	NA	NA	NA	None	None	0.00	NA	16.46	Cone
[5]	GER4-088	0.87	4	63	0.88	NA	3491	12	39	39	NA	NA	NA	None	None	0.00	NA	16.64	Cone
[5]	GER4-089	0.87	4	63	0.88	NA	4326	12	39	39	NA	NA	NA	None	None	0.00	NA	16.64	Cone
[5]	GER4-090	0.87	4	63	0.88	NA	4326	12	39	39	NA	NA	NA	None	None	0.00	NA	16.64	Cone
[5]	GER4-091	0.87	4	63	0.88	NA	3085	12	39	39	NA	NA	NA	None	None	0.00	NA	17.00	Cone
[5]	GER4-092	0.87	4	63	0.88	NA	4486	12	39	39	NA	NA	NA	None	None	0.00	NA	17.09	Cone
[5]	GER4-093	0.87	4	63	0.88	NA	3491	12	39	39	NA	NA	NA	None	None	0.00	NA	17.09	Cone
[5]	GER4-094	0.87	4	63	0.88	NA	3085	12	39	39	NA	NA	NA	None	None	0.00	NA	17.09	Cone
[5]	GER4-095	0.87	4	63	0.88	NA	3749	12	39	39	NA	NA	NA	None	None	0.00	NA	17.27	Cone
[5]	GER4-096	0.87	4	63	0.88	NA	3749	12	39	39	NA	NA	NA	None	None	0.00	NA	17.45	Cone
[5]	GER4-097	0.87	4	63	0.88	NA	4326	12	39	39	NA	NA	NA	None	None	0.00	NA	17.54	Cone
[5]	GER4-098	0.87	4	63	0.88	NA	3085	12	39	39	NA	NA	NA	None	None	0.00	NA	17.71	Cone
[5]	GER4-099	0.87	4	63	0.88	NA	3085	12	39	39	NA	NA	NA	None	None	0.00	NA	17.80	Cone
[5]	GER4-100	0.87	4	63	0.88	NA	4326	12	39	39	NA	NA	NA	None	None	0.00	NA	17.98	Cone
[5]	GER4-101	0.87	4	63	0.88	NA	3749	12	39	39	NA	NA	NA	None	None	0.00	NA	17.98	Cone
[5]	GER4-102	0.87	4	63	0.88	NA	4486	12	39	39	NA	NA	NA	None	None	0.00	NA	18.43	Cone
[5]	GER4-103	0.87	4	63	0.88	NA	4486	12	39	39	NA	NA	NA	None	None	0.00	NA	18.55	Cone
[5]	GER4-104	0.87	4	63	0.88	NA	4326	12	39	39	NA	NA	NA	None	None	0.00	NA	19.11	Cone
[5]	GER4-105	0.63	4	63	0.92	NA	1906	8	39	39	NA	NA	NA	None	None	0.00	NA	9.71	Cone
[5]	GER4-106	0.63	4	63	0.92	NA	1906	8	39	39	NA	NA	NA	None	None	0.00	NA	10.70	Cone
[5]	GER4-107	0.63	4	63	0.92	NA	1906	8	39	39	NA	NA	NA	None	None	0.00	NA	11.24	Cone
[5]	GER4-108	0.63	4	63	0.92	NA	1401	12	39	39	NA	NA	NA	None	None	0.00	NA	9.44	Cone
[5]	GER4-109	0.63	4	63	0.92	NA	1401	12	39	39	NA	NA	NA	None	None	0.00	NA	10.34	Cone

[5]	GER4-110	0.63	4	63	0.92	NA	1401	12	39	39	NA	NA	NA	None	None	0.00	NA	11.47	Cone
[5]	GER4-111	0.63	4	63	0.92	NA	4585	12	39	39	NA	NA	NA	None	None	0.00	NA	19.78	Cone
[5]	GER4-112	0.63	4	63	0.92	NA	4585	12	39	39	NA	NA	NA	None	None	0.00	NA	20.46	Cone
[5]	GER4-113	0.63	4	63	0.92	NA	4585	12	39	39	NA	NA	NA	None	None	0.00	NA	22.03	Cone
[5]	GER4-114	0.75	5	63	0.79	NA	2495	12	39	39	NA	NA	NA	None	None	0.00	NA	16.19	Cone
[5]	GER4-115	0.75	5	63	0.79	NA	2495	12	39	39	NA	NA	NA	None	None	0.00	NA	16.19	Cone
[5]	GER4-116	0.75	5	63	0.79	NA	2495	12	39	39	NA	NA	NA	None	None	0.00	NA	19.60	Cone
[5]	GER4-117	0.87	5	63	0.88	NA	3749	12	39	39	NA	NA	NA	None	None	0.00	NA	21.22	Cone
[5]	GER4-118	0.87	5	63	0.88	NA	3749	12	39	39	NA	NA	NA	None	None	0.00	NA	21.94	Cone
[5]	GER4-119	0.87	5	63	0.88	NA	3749	12	39	39	NA	NA	NA	None	None	0.00	NA	22.66	Cone
[5]	GER4-121	0.87	6	63	0.88	NA	2310	12	39	39	NA	NA	NA	None	None	0.00	NA	19.24	Cone
[5]	GER5-01	0.37	2	63	0.33	NA	1697	2	39	39	NA	NA	NA	None	None	0.00	NA	2.16	Cone
[5]	GER5-02	0.37	2	63	0.33	NA	1697	2	39	39	NA	NA	NA	None	None	0.00	NA	2.38	Cone
[5]	GER5-03	0.37	2	63	0.33	NA	1697	2	39	39	NA	NA	NA	None	None	0.00	NA	2.54	Cone
[5]	GER5-04	0.37	2	63	0.33	NA	3495	2	39	39	NA	NA	NA	None	None	0.00	NA	4.00	Cone
[5]	GER5-05	0.37	2	63	0.33	NA	3495	2	39	39	NA	NA	NA	None	None	0.00	NA	4.50	Cone
[5]	GER5-06	0.37	2	63	0.33	NA	3495	2	39	39	NA	NA	NA	None	None	0.00	NA	4.59	Cone
[5]	GER5-07	0.63	3	63	0.92	NA	2799	2	39	39	NA	NA	NA	None	None	0.00	NA	5.04	Cone
[5]	GER5-08	0.63	3	63	0.92	NA	2799	2	39	39	NA	NA	NA	None	None	0.00	NA	5.58	Cone
[5]	GER5-09	0.63	3	63	0.92	NA	4308	2	39	39	NA	NA	NA	None	None	0.00	NA	6.02	Cone
[5]	GER5-10	0.63	3	63	0.92	NA	2799	2	39	39	NA	NA	NA	None	None	0.00	NA	6.16	Cone
[5]	GER5-11	0.63	3	63	0.92	NA	4308	2	39	39	NA	NA	NA	None	None	0.00	NA	6.47	Cone
[5]	GER5-12	0.63	3	63	0.92	NA	4308	2	39	39	NA	NA	NA	None	None	0.00	NA	6.65	Cone
[5]	GER5-22	0.63	3	63	0.92	NA	2799	3	39	39	NA	NA	NA	None	None	0.00	NA	7.42	Cone
[5]	GER5-23	0.63	3	63	0.92	NA	2799	3	39	39	NA	NA	NA	None	None	0.00	NA	7.51	Cone
[5]	GER5-24	0.63	3	63	0.92	NA	4308	3	39	39	NA	NA	NA	None	None	0.00	NA	7.55	Cone
[5]	GER5-25	0.63	3	63	0.92	NA	2799	3	39	39	NA	NA	NA	None	None	0.00	NA	7.82	Cone
[5]	GER5-26	0.63	3	63	0.92	NA	4308	3	39	39	NA	NA	NA	None	None	0.00	NA	7.87	Cone
[5]	GER5-27	0.63	3	63	0.92	NA	4308	3	39	39	NA	NA	NA	None	None	0.00	NA	8.63	Cone
[5]	GER5-13	0.63	3	63	0.92	NA	2466	2	39	39	NA	NA	NA	None	None	0.00	NA	3.78	Cone
[5]	GER5-14	0.63	3	63	0.92	NA	2466	2	39	39	NA	NA	NA	None	None	0.00	NA	3.96	Cone
[5]	GER5-15	0.63	3	63	0.92	NA	2466	2	39	39	NA	NA	NA	None	None	0.00	NA	4.41	Cone
[5]	GER5-16	0.63	3	63	0.92	NA	5845	2	39	39	NA	NA	NA	None	None	0.00	NA	5.93	Cone
[5]	GER5-17	0.63	3	63	0.92	NA	5845	2	39	39	NA	NA	NA	None	None	0.00	NA	5.93	Cone
[5]	GER5-18	0.63	3	63	0.92	NA	5845	2	39	39	NA	NA	NA	None	None	0.00	NA	6.56	Cone
[5]	GER5-28	0.63	3	63	0.92	NA	2263	3	39	39	NA	NA	NA	None	None	0.00	NA	4.09	Cone
[5]	GER5-29	0.63	3	63	0.92	NA	2263	3	39	39	NA	NA	NA	None	None	0.00	NA	4.18	Cone
[5]	GER5-30	0.63	3	63	0.92	NA	2263	3	39	39	NA	NA	NA	None	None	0.00	NA	5.71	Cone
[5]	GER5-31	0.63	3	63	0.92	NA	4786	3	39	39	NA	NA	NA	None	None	0.00	NA	6.92	Cone
[5]	GER5-32	0.63	3	63	0.92	NA	4786	3	39	39	NA	NA	NA	None	None	0.00	NA	8.09	Cone
[5]	GER5-33	0.63	3	63	0.92	NA	4786	3	39	39	NA	NA	NA	None	None	0.00	NA	9.17	Cone

[5]	GER5-19	0.87	4	63	0.88	NA	5773	2	39	39	NA	NA	NA	None	None	0.00	NA	8.63	Cone
[5]	GER5-20	0.87	4	63	0.88	NA	5773	2	39	39	NA	NA	NA	None	None	0.00	NA	9.17	Cone
[5]	GER5-21	0.87	4	63	0.88	NA	5773	2	39	39	NA	NA	NA	None	None	0.00	NA	10.07	Cone
[5]	GER5-34	0.87	4	63	0.88	NA	2799	3	39	39	NA	NA	NA	None	None	0.00	NA	11.02	Cone
[5]	GER5-35	0.87	4	63	0.88	NA	2799	3	39	39	NA	NA	NA	None	None	0.00	NA	11.96	Cone
[5]	GER5-36	0.87	4	63	0.88	NA	5773	3	39	39	NA	NA	NA	None	None	0.00	NA	12.41	Cone
[5]	GER5-37	0.87	4	63	0.88	NA	2799	3	39	39	NA	NA	NA	None	None	0.00	NA	13.13	Cone
[5]	GER5-38	0.87	4	63	0.88	NA	5773	3	39	39	NA	NA	NA	None	None	0.00	NA	13.31	Cone
[5]	GER5-39	0.87	4	63	0.88	NA	5773	3	39	39	NA	NA	NA	None	None	0.00	NA	13.67	Cone
[5]	GER5-40	0.87	4	63	0.88	NA	2799	5	39	39	NA	NA	NA	None	None	0.00	NA	14.12	Cone
[5]	GER5-41	0.87	4	63	0.88	NA	2799	5	39	39	NA	NA	NA	None	None	0.00	NA	14.75	Cone
[5]	GER5-42	0.87	4	63	0.88	NA	2799	5	39	39	NA	NA	NA	None	None	0.00	NA	15.02	Cone
[5]	GER5-43	0.87	4	63	0.88	NA	4308	5	39	39	NA	NA	NA	None	None	0.00	NA	15.56	Cone
[5]	GER5-44	0.87	4	63	0.88	NA	4308	5	39	39	NA	NA	NA	None	None	0.00	NA	18.25	Cone
[5]	GER5-45	0.87	4	63	0.88	NA	4308	5	39	39	NA	NA	NA	None	None	0.00	NA	18.93	Cone
[6]	GER4-160	1.18	10	131	1.82	NA	2727	21	NA	NA	NA	NA	NA	None	None	0.00	NA	66.16	Cone
[6]	GER4-161	1.18	10	131	1.82	NA	2727	22	NA	NA	NA	NA	NA	None	None	0.00	NA	67.91	Cone
[6]	GER4-162	1.18	10	131	1.82	NA	2727	22	NA	NA	NA	NA	NA	None	None	0.00	NA	58.97	Cone
[6]	GER4-163	1.18	10	131	1.82	NA	2727	22	NA	NA	NA	NA	NA	None	None	0.00	NA	59.93	Cone
[6]	GER4-164	1.18	10	131	1.82	NA	2727	22	NA	NA	NA	NA	NA	None	None	0.00	NA	60.86	Cone
[6]	GER4-165	1.18	10	131	1.82	NA	2727	22	NA	NA	NA	NA	NA	None	None	0.00	NA	61.51	Cone
[6]	GER4-166	1.18	10	131	1.82	NA	2727	22	NA	NA	NA	NA	NA	None	None	0.00	NA	62.50	Cone
[6]	GER4-167	1.18	10	131	1.82	NA	2727	22	NA	NA	NA	NA	NA	None	None	0.00	NA	64.27	Cone
[6]	GER4-168	1.18	10	131	1.82	NA	3408	28	NA	NA	NA	NA	NA	None	None	0.00	NA	65.19	Cone
[6]	GER4-169	1.57	14	131	2.62	NA	2727	29	NA	NA	NA	NA	NA	None	None	0.00	NA	101.30	Cone
[6]	GER4-170	1.57	14	131	2.62	NA	2727	29	NA	NA	NA	NA	NA	None	None	0.00	NA	101.61	Cone
[6]	GER4-171	1.57	14	131	2.62	NA	2727	29	NA	NA	NA	NA	NA	None	None	0.00	NA	104.69	Cone
[6]	GER4-172	1.57	14	131	2.62	NA	2727	29	NA	NA	NA	NA	NA	None	None	0.00	NA	105.21	Cone
[6]	GER4-173	1.57	14	131	2.62	NA	2727	29	NA	NA	NA	NA	NA	None	None	0.00	NA	107.84	Cone
[6]	GER4-174	1.57	14	131	2.62	NA	2727	29	NA	NA	NA	NA	NA	None	None	0.00	NA	105.77	Cone
[6]	GER4-175	1.57	14	131	2.62	NA	2727	29	NA	NA	NA	NA	NA	None	None	0.00	NA	106.92	Cone
[6]	GER4-176	1.57	14	131	2.62	NA	2727	29	NA	NA	NA	NA	NA	None	None	0.00	NA	94.78	Cone
[6]	GER4-177	1.57	14	131	2.62	NA	2727	NA	NA	NA	NA	NA	NA	None	None	0.00	NA	88.80	Cone
[6]	GER4-178	1.57	14	131	2.62	NA	2727	NA	NA	NA	NA	NA	NA	None	None	0.00	NA	98.76	Cone
[6]	GER4-180	1.97	21	131	5.32	NA	2350	NA	NA	NA	NA	NA	NA	None	None	0.00	NA	164.40	Cone
[6]	GER4-181	1.97	21	131	5.32	NA	2350	NA	NA	NA	NA	NA	NA	None	None	0.00	NA	173.13	Cone
[6]	GER4-182	1.97	21	131	5.32	NA	2350	NA	NA	NA	NA	NA	NA	None	None	0.00	NA	189.27	Cone
[6]	GER4-183	1.97	21	131	5.32	NA	2915	NA	NA	NA	NA	NA	NA	None	None	0.00	NA	189.65	Cone
[6]	GER4-184	1.97	21	131	5.32	NA	2915	NA	NA	NA	NA	NA	NA	None	None	0.00	NA	193.40	Cone
[6]	GER4-185	1.97	21	131	5.32	NA	2350	NA	NA	NA	NA	NA	NA	None	None	0.00	NA	193.72	Cone
[6]	GER4-186	1.97	21	131	5.32	NA	2915	NA	NA	NA	NA	NA	NA	None	None	0.00	NA	198.73	Cone

[6]	GER4-187	1.97	21	131	5.32	NA	2915	NA	NA	NA	NA	NA	NA	None	None	0.00	NA	206.28	Cone
[6]	GER4-188	1.97	21	131	5.32	NA	3408	NA	NA	NA	NA	NA	NA	None	None	0.00	NA	199.00	Cone
[6]	GER4-189	1.97	21	131	5.32	NA	2350	NA	NA	NA	NA	NA	NA	None	None	0.00	NA	188.52	Cone
[6]	GER4-190	1.97	21	131	5.32	NA	2915	NA	NA	NA	NA	NA	NA	None	None	0.00	NA	191.63	Cone
[6]	GER4-191	1.97	21	131	5.32	NA	2915	NA	NA	NA	NA	NA	NA	None	None	0.00	NA	206.67	Cone
[6]	GER4-192	1.97	21	131	5.32	NA	2350	NA	NA	NA	NA	NA	NA	None	None	0.00	NA	172.47	Cone
[6]	GER4-173	1.57	14	131	2.62	NA	2727	29	NA	NA	NA	NA	NA	None	None	0.00	NA	107.84	Cone
[6]	GER4-174	1.57	14	131	2.62	NA	2727	29	NA	NA	NA	NA	NA	None	None	0.00	NA	105.77	Cone
[6]	GER4-175	1.57	14	131	2.62	NA	2727	29	NA	NA	NA	NA	NA	None	None	0.00	NA	106.92	Cone
[6]	GER4-176	1.57	14	131	2.62	NA	2727	29	NA	NA	NA	NA	NA	None	None	0.00	NA	94.78	Cone
[6]	GER4-177	1.57	14	131	2.62	NA	2727	NA	NA	NA	NA	NA	NA	None	None	0.00	NA	88.80	Cone
[6]	GER4-178	1.57	14	131	2.62	NA	2727	NA	NA	NA	NA	NA	NA	None	None	0.00	NA	98.76	Cone
[6]	GER4-180	1.97	21	131	5.32	NA	2350	NA	NA	NA	NA	NA	NA	None	None	0.00	NA	164.40	Cone
[6]	GER4-181	1.97	21	131	5.32	NA	2350	NA	NA	NA	NA	NA	NA	None	None	0.00	NA	173.13	Cone
[6]	GER4-182	1.97	21	131	5.32	NA	2350	NA	NA	NA	NA	NA	NA	None	None	0.00	NA	189.27	Cone
[6]	GER4-183	1.97	21	131	5.32	NA	2915	NA	NA	NA	NA	NA	NA	None	None	0.00	NA	189.65	Cone
[6]	GER4-184	1.97	21	131	5.32	NA	2915	NA	NA	NA	NA	NA	NA	None	None	0.00	NA	193.40	Cone
[6]	GER4-185	1.97	21	131	5.32	NA	2350	NA	NA	NA	NA	NA	NA	None	None	0.00	NA	193.72	Cone
[6]	GER4-186	1.97	21	131	5.32	NA	2915	NA	NA	NA	NA	NA	NA	None	None	0.00	NA	198.73	Cone
[6]	GER4-187	1.97	21	131	5.32	NA	2915	NA	NA	NA	NA	NA	NA	None	None	0.00	NA	206.28	Cone
[6]	GER4-188	1.97	21	131	5.32	NA	3408	NA	NA	NA	NA	NA	NA	None	None	0.00	NA	199.00	Cone
[6]	GER4-189	1.97	21	131	5.32	NA	2350	NA	NA	NA	NA	NA	NA	None	None	0.00	NA	188.52	Cone
[6]	GER4-190	1.97	21	131	5.32	NA	2915	NA	NA	NA	NA	NA	NA	None	None	0.00	NA	191.63	Cone
[6]	GER4-191	1.97	21	131	5.32	NA	2915	NA	NA	NA	NA	NA	NA	None	None	0.00	NA	206.67	Cone
[6]	GER4-192	1.97	21	131	5.32	NA	2350	NA	NA	NA	NA	NA	NA	None	None	0.00	NA	172.47	Cone
[6]	GER5-46	1.18	10	131	1.82	NA	2915	9	NA	NA	NA	NA	NA	None	None	0.00	NA	44.87	Cone
[6]	GER5-47	1.18	10	131	1.82	NA	2915	9	NA	NA	NA	NA	NA	None	None	0.00	NA	46.87	Cone
[6]	GER5-48	1.18	10	131	1.82	NA	2915	9	NA	NA	NA	NA	NA	None	None	0.00	NA	46.92	Cone
[6]	GER5-49	1.18	10	131	1.82	NA	2915	9	NA	NA	NA	NA	NA	None	None	0.00	NA	50.72	Cone
[6]	GER5-56	1.18	10	131	1.82	NA	2350	11	NA	NA	NA	NA	NA	None	None	0.00	NA	47.66	Cone
[6]	GER5-57	1.18	10	131	1.82	NA	2350	11	NA	NA	NA	NA	NA	None	None	0.00	NA	49.01	Cone
[6]	GER5-50	1.57	14	131	2.62	NA	2915	9	NA	NA	NA	NA	NA	None	None	0.00	NA	73.56	Cone
[6]	GER5-51	1.57	14	131	2.62	NA	2915	9	NA	NA	NA	NA	NA	None	None	0.00	NA	83.29	Cone
[6]	GER5-58	1.57	14	131	2.62	NA	2350	14	NA	NA	NA	NA	NA	None	None	0.00	NA	61.64	Cone
[6]	GER5-59	1.57	14	131	2.62	NA	2350	15	NA	NA	NA	NA	NA	None	None	0.00	NA	74.34	Cone
[6]	GER5-60	1.57	14	131	2.62	NA	2350	15	NA	NA	NA	NA	NA	None	None	0.00	NA	93.59	Cone
[6]	GER5-61	1.57	14	131	2.62	NA	2350	15	NA	NA	NA	NA	NA	None	None	0.00	NA	78.89	Cone
[7]	GER4-122	0.87	7	63	0.89	NA	3049	16	NA	NA	NA	NA	NA	None	None	0.00	NA	39.00	Cone
[7]	GER4-126	0.87	7	63	0.89	NA	3332	18	NA	NA	NA	NA	NA	None	None	0.00	NA	42.04	Cone
[7]	GER4-127	0.87	7	63	0.89	NA	3332	18	NA	NA	NA	NA	NA	None	None	0.00	NA	44.96	Cone
[7]	GER4-128	0.87	7	63	0.89	NA	3466	18	NA	NA	NA	NA	NA	None	None	0.00	NA	46.54	Cone

[7]	GER4-129	0.87	7	63	0.89	NA	3651	18	NA	NA	NA	NA	NA	None	None	0.00	NA	50.13	Cone
[7]	GER4-130	0.87	7	63	0.89	NA	3638	18	NA	NA	NA	NA	NA	None	None	0.00	NA	50.13	Cone
[7]	GER4-131	0.87	7	63	0.89	NA	4068	18	NA	NA	NA	NA	NA	None	None	0.00	NA	50.13	Cone
[7]	GER4-132	0.87	7	63	0.89	NA	3332	18	NA	NA	NA	NA	NA	None	None	0.00	NA	50.81	Cone
[7]	GER4-133	0.87	7	63	0.89	NA	3638	18	NA	NA	NA	NA	NA	None	None	0.00	NA	51.26	Cone
[7]	GER4-134	0.87	7	63	0.89	NA	3417	18	NA	NA	NA	NA	NA	None	None	0.00	NA	51.71	Cone
[7]	GER4-135	0.87	7	63	0.89	NA	3332	18	NA	NA	NA	NA	NA	None	None	0.00	NA	53.05	Cone
[7]	GER4-136	0.87	7	63	0.89	NA	3651	18	NA	NA	NA	NA	NA	None	None	0.00	NA	53.73	Cone
[7]	GER4-137	0.87	7	63	0.89	NA	3687	18	NA	NA	NA	NA	NA	None	None	0.00	NA	54.18	Cone
[7]	GER4-138	0.87	7	63	0.89	NA	3638	18	NA	NA	NA	NA	NA	None	None	0.00	NA	58.23	Cone
[7]	GER4-140	0.87	7	63	0.89	NA	1917	26	NA	NA	NA	NA	NA	None	None	0.00	NA	28.78	Cone
[7]	GER4-141	0.87	7	63	0.89	NA	2016	26	NA	NA	NA	NA	NA	None	None	0.00	NA	28.87	Cone
[7]	GER4-142	0.87	7	63	0.89	NA	2016	26	NA	NA	NA	NA	NA	None	None	0.00	NA	30.35	Cone
[7]	GER4-143	0.87	7	63	0.89	NA	1917	NA	NA	NA	NA	NA	NA	None	None	0.00	NA	31.16	Cone
[7]	GER4-144	0.87	7	63	0.89	NA	2483	NA	NA	NA	NA	NA	NA	None	None	0.00	NA	40.80	Cone
[7]	GER4-145	0.87	7	63	0.89	NA	2483	NA	NA	NA	NA	NA	NA	None	None	0.00	NA	40.98	Cone
[7]	GER4-146	0.87	7	63	0.89	NA	2445	NA	NA	NA	NA	NA	NA	None	None	0.00	NA	41.07	Cone
[7]	GER4-147	0.87	7	63	0.89	NA	2445	NA	NA	NA	NA	NA	NA	None	None	0.00	NA	45.19	Cone
[7]	GER5-52	0.87	7	163	0.89	NA	2727	NA	NA	NA	NA	NA	NA	None	None	0.00	NA	24.57	Cone
[7]	GER5-53	0.87	7	163	0.89	NA	2727	NA	NA	NA	NA	NA	NA	None	None	0.00	NA	28.44	Cone
[7]	GER5-54	0.87	7	163	0.89	NA	2727	NA	NA	NA	NA	NA	NA	None	None	0.00	NA	25.72	Cone
[7]	GER5-55	0.87	7	163	0.89	NA	2727	NA	NA	NA	NA	NA	NA	None	None	0.00	NA	28.24	Cone
[8]	GER4-149	1.18	10	138	1.82	NA	5410	NA	NA	NA	NA	NA	NA	None	None	0.00	NA	92.58	Cone
[8]	GER4-150	1.18	10	138	1.82	NA	4177	NA	NA	NA	NA	NA	NA	None	None	0.00	NA	92.64	Cone
[8]	GER4-151	1.18	10	138	1.82	NA	5410	NA	NA	NA	NA	NA	NA	None	None	0.00	NA	93.32	Cone
[8]	GER4-152	1.18	10	138	1.82	NA	5410	NA	NA	NA	NA	NA	NA	None	None	0.00	NA	97.93	Cone
[8]	GER4-153	1.18	10	138	1.82	NA	4177	NA	NA	NA	NA	NA	NA	None	None	0.00	NA	98.11	Cone
[8]	GER4-154	1.18	10	138	1.82	NA	8717	NA	NA	NA	NA	NA	NA	None	None	0.00	NA	112.18	Cone
[8]	GER4-155	1.18	10	138	1.82	NA	8659	NA	NA	NA	NA	NA	NA	None	None	0.00	NA	120.27	Cone
[8]	GER4-156	1.18	10	138	1.82	NA	8717	NA	NA	NA	NA	NA	NA	None	None	0.00	NA	125.69	Cone
[8]	GER4-157	1.18	10	138	1.82	NA	8833	NA	NA	NA	NA	NA	NA	None	None	0.00	NA	138.82	Cone
[8]	GER4-158	1.18	10	138	1.82	NA	8833	NA	NA	NA	NA	NA	NA	None	None	0.00	NA	139.49	Cone
[8]	GER4-159	1.18	10	138	1.82	NA	8833	NA	NA	NA	NA	NA	NA	None	None	0.00	NA	140.33	Cone
[9]	1T	1.00	3	134	2.35	0.61	3340	9	9	9	18	18	9	None	None	0.00	NA	14.00	Cone
[9]	2T	1.00	3	134	11.78	0.61	3340	9	9	9	18	18	9	None	None	0.00	NA	16.20	Conc
[9]	3T	1.00	3	134	27.48	0.61	3060	9	9	9	18	18	9	None	None	0.00	NA	16.80	Conc
[9]	4T	1.00	5	134	2.35	0.61	3050	9	9	9	18	18	9	None	None	0.00	NA	23.90	Conc
[9]	5T	1.00	5	134	11.78	0.61	3050	9	9	9	18	18	9	None	None	0.00	NA	29.40	Conc
[9]	6T	1.00	5	134	27.48	0.61	3060	9	9	9	18	18	9	None	None	0.00	NA	32.20	Conc
[9]	7T	1.00	7	134	2.35	0.61	2720	9	9	9	18	18	9	None	None	0.00	NA	25.40	Conc
[9]	8T	1.00	5	134	2.35	0.61	3180	9	9	9	18	18	9	None	None	0.00	NA	24.20	Conc

[9]	9T	0.75	5	134	11.78	0.61	3180	9	9	9	18	18	9	None	None	0.00	NA	30.40	Conc
[9]	10T	0.75	5	134	2.35	0.61	3120	23	23	23	46	46	7	None	None	0.00	NA	22.50	Cone
[9]	11T	0.75	5	134	11.78	0.61	3100	23	23	23	46	46	7	None	None	0.00	NA	26.40	Cone
[9]	12T	0.75	5	134	27.48	0.61	2940	23	23	23	46	46	7	None	None	0.00	NA	27.40	Conc
[10]	1a	0.63	5	60	0.92	0.31	3600	NA	NA	NA	18	72	30	None	None	0.00	NA	21.00	Steel
[10]	1b	0.63	5	60	0.92	0.31	3600	NA	NA	NA	18	72	30	None	None	0.00	NA	15.50	Steel
[10]	1c	0.63	5	60	0.92	0.31	3600	NA	NA	NA	18	72	30	None	None	0.00	NA	19.50	Steel
[10]	2a	0.63	7	120	0.92	0.31	3600	NA	NA	NA	18	72	30	None	None	0.00	NA	37.50	Steel
[10]	2b	0.63	7	120	0.92	0.31	3600	NA	NA	NA	18	72	30	None	None	0.00	NA	37.40	Steel
[10]	2c	0.63	7	120	0.92	0.31	3600	NA	NA	NA	18	72	30	None	None	0.00	NA	37.40	Steel
[10]	3a	0.63	7	60	0.92	0.31	3600	NA	NA	NA	18	72	30	None	None	0.00	NA	16.60	Steel
[10]	3b	0.63	7	60	0.92	0.31	3600	NA	NA	NA	18	72	30	None	None	0.00	NA	16.70	Steel
[11]	C8-A1	0.63	2	NA	0.63	0.23	1279	6	6	6	12	12	6	None	None	0.00	NA	4.32	Cone
[11]	C8-A2	0.63	2	NA	0.63	0.23	1279	6	6	6	12	12	6	None	None	1.00	NA	4.59	Cone
[11]	C8-A3	0.63	2	NA	0.63	0.23	1279	6	6	6	12	12	6	None	None	2.00	NA	5.17	Cone
[11]	C8-B4	0.63	1	NA	0.63	0.23	1217	2	6	6	12	12	6	None	None	3.00	NA	2.16	Cone
[11]	C8-B5	0.63	3	NA	0.63	0.23	1217	2	6	6	12	12	6	None	None	4.00	NA	3.64	Cone
[11]	C8-B6	0.63	2	NA	0.63	0.23	1217	2	6	6	12	12	6	None	None	5.00	NA	3.53	Cone
[11]	C8-C7	0.63	2	NA	0.63	0.23	1307	2	6	6	12	12	6	None	None	6.00	NA	1.89	Cone
[11]	C8-C8	0.63	2	NA	0.63	0.23	1307	2	6	6	12	12	6	None	None	7.00	NA	1.57	Cone
[11]	C8-C9	0.63	2	NA	0.63	0.23	1307	2	6	6	12	12	6	None	None	8.00	NA	1.75	Cone
[11]	C8-G19	0.63	3	NA	0.72	0.23	1353	6	6	6	12	12	6	None	None	9.00	NA	6.41	Cone
[11]	C8-G20	0.63	3	NA	0.72	0.23	1353	6	6	6	12	12	6	None	None	10.00	NA	6.65	Cone
[11]	C8-G21	0.63	3	NA	0.72	0.23	1353	6	6	6	12	12	6	None	None	11.00	NA	6.43	Cone
[11]	C8-A22	0.63	4	NA	0.63	0.23	1505	6	6	6	12	12	6	None	None	12.00	NA	8.39	Cone
[11]	C8-A23	0.63	4	NA	0.63	0.23	1505	6	6	6	12	12	6	None	None	13.00	NA	5.87	Cone
[11]	C8-A24	0.63	3	NA	0.63	0.23	1505	6	6	6	12	12	6	None	None	14.00	NA	6.34	Cone
[11]	C8-H25	0.32	2	NA	0.63	0.23	1353	6	6	6	12	12	6	None	None	15.00	NA	2.36	Cone
[11]	C8-H26	0.32	2	NA	0.63	0.23	1353	6	6	6	12	12	6	None	None	16.00	NA	2.38	Cone
[11]	C8-H27	0.32	2	NA	0.63	0.23	1353	6	6	6	12	12	6	None	None	17.00	NA	3.19	Cone
[11]	C16-A1	0.63	2	NA	0.63	0.23	2495	6	6	6	12	12	6	None	None	0.00	NA	5.93	Cone
[11]	C16-A2	0.63	1	NA	0.63	0.23	2495	6	6	6	12	12	6	None	None	1.00	NA	7.64	Cone
[11]	C16-A3	0.63	2	NA	0.63	0.23	2495	6	6	6	12	12	6	None	None	2.00	NA	4.50	Cone
[11]	C16-B4	0.63	2	NA	0.63	0.23	2965	2	6	6	12	12	6	None	None	3.00	NA	4.61	Cone
[11]	C16-B5	0.63	2	NA	0.63	0.23	2965	2	6	6	12	12	6	None	None	4.00	NA	5.78	Cone
[11]	C16-B6	0.63	2	NA	0.63	0.23	2965	2	6	6	12	12	6	None	None	5.00	NA	5.44	Cone
[11]	C16-C7	0.63	2	NA	0.63	0.23	2714	2	6	6	12	12	6	None	None	6.00	NA	4.18	Cone
[11]	C16-C8	0.63	2	NA	0.63	0.23	2714	2	6	6	12	12	6	None	None	7.00	NA	4.05	Cone
[11]	C16-C9	0.63	2	NA	0.63	0.23	2714	2	6	6	12	12	6	None	None	8.00	NA	4.70	Cone
[11]	C16-G19	0.63	3	NA	0.72	0.23	2310	6	6	6	12	12	6	None	None	9.00	NA	8.03	Cone
[11]	C16-G20	0.63	3	NA	0.72	0.23	2310	6	6	6	12	12	6	None	None	10.00	NA	7.58	Cone

[11]	C16-G21	0.63	3	NA	0.72	0.23	2310	6	6	6	12	12	6	None	None	11.00	NA	8.41	Cone
[11]	C16-A22	0.63	4	NA	0.63	0.23	2603	6	6	6	12	12	6	None	None	12.00	NA	9.89	Cone
[11]	C16-A23	0.63	4	NA	0.63	0.23	2603	6	6	6	12	12	6	None	None	13.00	NA	10.57	Cone
[11]	C16-A24	0.63	4	NA	0.63	0.23	2603	6	6	6	12	12	6	None	None	14.00	NA	8.79	Cone
[11]	C16-H25	0.32	2	NA	0.63	0.23	2286	6	6	6	12	12	6	None	None	15.00	NA	3.73	Cone
[11]	C16-H26	0.32	2	NA	0.63	0.23	2286	6	6	6	12	12	6	None	None	16.00	NA	4.95	Cone
[11]	C16-H27	0.32	2	NA	0.63	0.23	2286	6	6	6	12	12	6	None	None	17.00	NA	3.60	Cone
[12]	#1	1.35	7	100	2.20	1.43	2900	24	24	24	48	48	38	None	None	0.00	NA	70.00	Cone
[12]	#2	1.35	11	100	2.20	1.43	2820	24	24	24	48	48	38	None	None	0.00	NA	109.40	Cone
[12]	#3	1.35	15	100	2.20	1.43	3080	24	24	24	48	48	38	None	None	0.00	NA	128.50	Steel
[12]	#4	1.00	7	90	1.50	0.79	3280	24	24	24	48	48	38	None	None	0.00	NA	73.00	Cone
[12]	#5	1.00	11	90	1.50	0.79	3320	24	24	24	48	48	38	None	None	0.00	NA	102.60	Steel
[12]	#6	1.00	15	90	1.50	0.79	2740	24	24	24	48	48	38	None	None	0.00	NA	100.80	Steel
[12]	#12	1.25	7	125	1.82	1.23	2850	24	24	24	48	48	38	None	None	0.00	NA	53.80	Cone
[12]	#13	1.25	11	125	1.82	1.23	2940	24	24	24	48	48	38	None	None	0.00	NA	110.00	Cone
[13]	12DC5701	0.75	4	120	0.79	0.33	4382	39	NA	NA	NA	NA	NA	None	None	0.00	NA	30.80	Cone
[13]	12DC5702	0.75	4	120	0.79	0.33	4382	39	NA	NA	NA	NA	NA	None	None	0.00	NA	27.52	Cone
[13]	12DC5703	0.75	4	120	0.79	0.33	4382	39	NA	NA	NA	NA	NA	None	None	0.00	NA	28.29	Cone
[13]	12DC5704	0.75	4	120	0.79	0.33	4382	39	NA	NA	NA	NA	NA	None	None	0.00	NA	27.52	Cone
[13]	12DC5705	0.75	4	120	0.79	0.33	4382	39	NA	NA	NA	NA	NA	None	None	0.00	NA	28.67	Cone
[13]	12DC5707	0.75	4	120	0.79	0.33	4244	39	NA	NA	NA	NA	NA	Parallel	None	0.00	NA	30.12	Cone
[13]	12DC5708	0.75	4	120	0.79	0.33	4244	39	NA	NA	NA	NA	NA	Parallel	None	0.00	NA	29.55	Cone
[13]	12DC5709	0.75	4	120	0.79	0.33	4244	39	NA	NA	NA	NA	NA	Parallel	None	0.00	NA	30.12	Cone
[13]	12DC5710	0.75	4	120	0.79	0.33	4244	39	NA	NA	NA	NA	NA	Parallel	None	0.00	NA	30.03	Cone
[13]	12DC5712	0.75	4	120	0.79	0.33	4244	39	NA	NA	NA	NA	NA	Parallel	None	0.00	NA	27.75	Cone
[13]	11SC5701	0.75	4	120	0.79	0.33	4382	39	NA	NA	NA	NA	NA	None	None	0.00	NA	23.46	Cone
[13]	11SC5702	0.75	4	120	0.79	0.33	4382	39	NA	NA	NA	NA	NA	None	None	0.00	NA	21.43	Cone
[13]	11SC5703	0.75	4	120	0.79	0.33	4382	39	NA	NA	NA	NA	NA	None	None	0.00	NA	22.98	Cone
[13]	11SC5704	0.75	4	120	0.79	0.33	4382	39	NA	NA	NA	NA	NA	None	None	0.00	NA	21.14	Cone
[13]	11SC5705	0.75	4	120	0.79	0.33	4382	39	NA	NA	NA	NA	NA	None	None	0.00	NA	21.24	Cone
[13]	11SC5706	0.75	4	120	0.79	0.33	4381	39	NA	NA	NA	NA	NA	Parallel	None	0.00	NA	18.05	Cone
[13]	11SC5707	0.75	4	120	0.79	0.33	4381	39	NA	NA	NA	NA	NA	Parallel	None	0.00	NA	20.28	Cone
[13]	11SC5708	0.75	4	120	0.79	0.33	4381	39	NA	NA	NA	NA	NA	Parallel	None	0.00	NA	19.02	Cone
[13]	11SC5709	0.75	4	120	0.79	0.33	4381	39	NA	NA	NA	NA	NA	Parallel	None	0.00	NA	19.89	Cone
[13]	11SC5710	0.75	4	120	0.79	0.33	4381	39	NA	NA	NA	NA	NA	Parallel	None	0.00	NA	18.63	Cone
[14]	SS-10-90	0.47	5	68	0.47	0.15	4153	8	5	5	9	16	28	None	Stirrup	0.40	51.92	10.56	Steel
[14]	SS-15-90	0.47	7	68	0.47	0.15	4153	8	5	5	9	16	28	None	Stirrup	0.40	51.92	10.45	Steel
[14]	SS-20-90	0.47	9	68	0.47	0.15	4153	8	5	5	9	16	28	None	Stirrup	0.40	51.92	10.43	Steel
[14]	SS'-20-90	0.47	9	68	0.47	0.15	4153	8	5	5	9	16	28	None	Stirrup	0.40	51.92	10.36	Steel
[14]	TS-10-90	0.47	5	68	0.47	0.15	4153	8	5	5	9	16	28	None	Stirrup	0.40	51.92	10.19	Steel
[14]	TS-15-90	0.47	7	68	0.47	0.15	4153	8	5	5	9	16	28	None	Stirrup	0.40	51.92	9.90	Steel

[14]	TS-20-90	0.47	9	68	0.47	0.15	4153	8	5	5	9	16	28	None	Stirrup	0.40	51.92	10.10	Steel
[14]	TT-10-90	0.47	5	68	0.47	0.15	4153	8	5	5	9	16	28	None	Stirrup	0.40	51.92	9.90	Steel
[14]	TT-15-90	0.47	7	68	0.47	0.15	4153	8	5	5	9	16	28	None	Stirrup	0.40	51.92	9.90	Steel
[14]	TT-20-90	0.47	9	68	0.47	0.15	4153	8	5	5	9	16	28	None	Stirrup	0.40	51.92	9.96	Steel
[15]	A-6	1.25	8	150	1.91	1.23	7375	16	16	16	65	65	24	None	None	0.00	NA	76.32	Cone
[15]	A-7	1.25	8	150	1.91	1.23	7375	16	16	16	65	65	24	None	None	0.00	NA	72.63	Cone
[15]	A-8	1.25	8	150	1.91	1.23	7375	16	16	16	65	65	24	None	None	0.00	NA	73.82	Cone
[15]	A-9	1.25	8	150	1.91	1.23	7375	16	16	16	65	65	24	None	None	0.00	NA	81.20	Cone
[15]	A-10	1.25	8	150	1.91	1.23	7375	16	16	16	65	65	24	None	None	0.00	NA	80.23	Cone
[15]	A11	1.00	8	150	1.62	0.79	7375	16	16	16	65	65	24	None	None	0.00	NA	68.04	Cone
[15]	A12	1.00	8	150	1.62	0.79	7375	16	16	16	65	65	24	None	None	0.00	NA	72.13	Cone
[15]	A13	1.00	8	150	1.62	0.79	7375	16	16	16	65	65	24	None	None	0.00	NA	72.86	Cone
[15]	A14	1.00	8	150	1.62	0.79	7375	16	16	16	65	65	24	None	None	0.00	NA	71.13	Cone
[15]	A15	1.00	8	150	1.62	0.79	7375	16	16	16	65	65	24	None	None	0.00	NA	69.08	Cone
[15]	B-6	1.25	8	150	1.91	1.23	11722	16	16	16	65	65	24	None	None	0.00	NA	85.90	Cone
[15]	B-7	1.25	8	150	1.91	1.23	11722	16	16	16	65	65	24	None	None	0.00	NA	81.90	Cone
[15]	B-8	1.25	8	150	1.91	1.23	11722	16	16	16	65	65	24	None	None	0.00	NA	78.06	Cone
[15]	B-9	1.25	8	150	1.91	1.23	11722	16	16	16	65	65	24	None	None	0.00	NA	84.76	Cone
[15]	B-10	1.25	8	150	1.91	1.23	11722	16	16	16	65	65	24	None	None	0.00	NA	71.81	Cone
[15]	C-6	1.25	8	150	1.91	1.23	11234	16	16	16	65	65	24	None	None	0.00	NA	91.74	Cone
[15]	C-7	1.25	8	150	1.91	1.23	11234	16	16	16	65	65	24	None	None	0.00	NA	86.74	Cone
[15]	C-8	1.25	8	150	1.91	1.23	11234	16	16	16	65	65	24	None	None	0.00	NA	93.38	Cone
[15]	C-9	1.25	8	150	1.91	1.23	11234	16	16	16	65	65	24	None	None	0.00	NA	89.04	Cone
[15]	C-10	1.25	8	150	1.91	1.23	11234	16	16	16	65	65	24	None	None	0.00	NA	87.81	Cone
[15]	B-11	1.00	8	150	1.62	0.79	11722	16	16	16	65	65	24	None	None	0.00	NA	78.07	Cone
[15]	B-12	1.00	8	150	1.62	0.79	11722	16	16	16	65	65	24	None	None	0.00	NA	82.11	Cone
[15]	B-13	1.00	8	150	1.62	0.79	11722	16	16	16	65	65	24	None	None	0.00	NA	81.86	Cone
[15]	B-14	1.00	8	150	1.62	0.79	11722	16	16	16	65	65	24	None	None	0.00	NA	78.76	Cone
[15]	B-15	1.00	8	150	1.62	0.79	11722	16	16	16	65	65	24	None	None	0.00	NA	77.22	Cone
[15]	C-11	1.00	8	150	1.62	0.79	11234	16	16	16	65	65	24	None	None	0.00	NA	87.77	Cone
[15]	C-12	1.00	8	150	1.62	0.79	11234	16	16	16	65	65	24	None	None	0.00	NA	84.24	Cone
[15]	C-13	1.00	8	150	1.62	0.79	11234	16	16	16	65	65	24	None	None	0.00	NA	85.62	Cone
[15]	C-14	1.00	8	150	1.62	0.79	11234	16	16	16	65	65	24	None	None	0.00	NA	81.58	Cone
[15]	C-15	1.00	8	150	1.62	0.79	11234	16	16	16	65	65	24	None	None	0.00	NA	86.44	Cone
[15]	D-1	0.75	4	150	0.79	0.44	11951	16	16	16	65	65	24	None	None	0.00	NA	26.02	Cone
[15]	D-2	0.75	4	150	0.79	0.44	11951	16	16	16	65	65	24	None	None	0.00	NA	26.55	Cone
[15]	D-3	0.75	4	150	0.79	0.44	11951	16	16	16	65	65	24	None	None	0.00	NA	25.13	Cone
[15]	D-4	0.75	4	120	0.79	0.44	11951	16	16	16	65	65	24	None	None	0.00	NA	18.36	Cone
[15]	D-5	0.75	4	150	0.79	0.44	11951	16	16	16	65	65	24	None	None	0.00	NA	26.15	Cone
[15]	D-6	0.75	4	150	0.79	0.44	11951	16	16	16	65	65	24	None	None	0.00	NA	24.78	Cone
[15]	F-1	0.75	4	150	0.79	0.44	12042	16	16	16	65	65	24	None	None	0.00	NA	24.46	Cone

[15]	F-2	0.75	4	150	0.79	0.44	12042	16	16	16	65	65	24	None	None	0.00	NA	25.24	Cone
[15]	F-3	0.75	4	150	0.79	0.44	12042	16	16	16	65	65	24	None	None	0.00	NA	23.05	Cone
[15]	F-4	0.75	4	120	0.79	0.44	12042	16	16	16	65	65	24	None	None	0.00	NA	20.98	Cone
[15]	F-5	0.75	4	150	0.79	0.44	12042	16	16	16	65	65	24	None	None	0.00	NA	25.45	Cone
[15]	F-6	0.75	4	150	0.79	0.44	12042	16	16	16	65	65	24	None	None	0.00	NA	26.18	Cone
[15]	H-1	0.75	4	150	0.79	0.44	7451	16	16	16	65	65	24	None	None	0.00	NA	25.34	Cone
[15]	H-2	0.75	4	150	0.79	0.44	7451	16	16	16	65	65	24	None	None	0.00	NA	27.70	Cone
[15]	H-3	0.75	4	150	0.79	0.44	7451	16	16	16	65	65	24	None	None	0.00	NA	28.48	Cone
[15]	H-5	0.75	4	150	0.79	0.44	7451	16	16	16	65	65	24	None	None	0.00	NA	26.78	Cone
[15]	H-6	0.75	4	150	0.79	0.44	7451	16	16	16	65	65	24	None	None	0.00	NA	27.19	Cone
[15]	E-1	1.00	6	150	1.29	0.79	11951	16	16	16	65	65	24	None	None	0.00	NA	49.32	Cone
[15]	E-2	1.00	6	150	1.29	0.79	11951	16	16	16	65	65	24	None	None	0.00	NA	49.93	Cone
[15]	E-3	1.00	6	150	1.29	0.79	11951	16	16	16	65	65	24	None	None	0.00	NA	51.65	Cone
[15]	E-4	1.00	6	150	1.29	0.79	11951	16	16	16	65	65	24	None	None	0.00	NA	49.12	Cone
[15]	E-5	1.00	6	150	1.29	0.79	11951	16	16	16	65	65	24	None	None	0.00	NA	52.37	Cone
[15]	G-1	1.00	6	150	1.29	0.79	12042	16	16	16	65	65	24	None	None	0.00	NA	52.43	Cone
[15]	G-2	1.00	6	150	1.29	0.79	12042	16	16	16	65	65	24	None	None	0.00	NA	53.90	Cone
[15]	G-3	1.00	6	150	1.29	0.79	12042	16	16	16	65	65	24	None	None	0.00	NA	51.35	Cone
[15]	G-4	1.00	6	150	1.29	0.79	12042	16	16	16	65	65	24	None	None	0.00	NA	52.68	Cone
[15]	G-5	1.00	6	150	1.29	0.79	12042	16	16	16	65	65	24	None	None	0.00	NA	53.51	Cone
[15]	I-1	1.00	6	150	1.29	0.79	7451	16	16	16	65	65	24	None	None	0.00	NA	46.89	Cone
[15]	I-2	1.00	6	150	1.29	0.79	7451	16	16	16	65	65	24	None	None	0.00	NA	47.64	Cone
[15]	I-3	1.00	6	150	1.29	0.79	7451	16	16	16	65	65	24	None	None	0.00	NA	51.57	Cone
[15]	I-4	1.00	6	150	1.29	0.79	7451	16	16	16	65	65	24	None	None	0.00	NA	49.80	Cone
[15]	I-5	1.00	6	150	1.29	0.79	7451	16	16	16	65	65	24	None	None	0.00	NA	45.33	Cone
[16]	M-S2-90	0.63	14	73	5.40	0.23	5700	8	5	5	9	16	28	None	Long. bars	8.10	53.37	18.79	Steel
[16]	M-T4-90	0.63	14	73	5.40	0.23	5700	8	5	5	9	16	28	None	Long. bars	8.10	53.37	17.92	Steel
[17]	CIP-uncrack	0.75	4	120	0.91	0.33	4700	4	NA	NA	88	30	NA	None	None	0.00	NA	22.82	Cone
[17]	CIP-cracked	0.75	4	120	0.91	0.33	4700	4	NA	NA	88	30	NA	None	None	0.00	NA	19.85	Cone
[18]	NC-1	0.88	4	NA	0.88	0.60	4068	14	14	14	28	28	8	None	None	0.00	NA	16.83	Cone
[18]	NC-2	0.88	4	NA	0.88	0.60	4068	14	14	14	28	28	8	None	None	0.00	NA	17.14	Cone
[18]	NC-3	0.88	4	NA	0.88	0.60	4068	14	14	14	28	28	8	None	None	0.00	NA	16.81	Cone
[19]	M12-5	0.42	8	79	0.96	0.14	2959	2	8	8	16	16	18	None	None	0.00	NA	11.18	Steel
[19]	M12-10	0.42	8	79	0.96	0.14	2959	2	8	8	16	16	18	None	None	0.00	NA	10.76	Steel
[19]	M12-15	0.42	8	79	0.96	0.14	2959	2	8	8	16	16	18	None	None	0.00	NA	11.42	Steel
[19]	M12-16	0.42	8	79	0.96	0.14	2959	4	8	8	16	16	18	None	None	0.00	NA	11.49	Steel
[19]	M12-17	0.42	8	79	0.96	0.14	2959	5	8	8	16	16	18	None	None	0.00	NA	11.24	Steel
[19]	M12-22	0.42	8	79	0.96	0.14	2959	8	8	8	16	16	18	None	None	0.00	NA	10.80	Steel
[19]	M16-38	0.61	12	66	1.65	0.23	4308	2	8	8	16	16	18	None	None	0.00	NA	16.51	Steel
[19]	M16-51	0.61	12	66	1.65	0.23	4308	8	8	8	16	16	18	None	None	0.00	NA	16.51	Steel
[20]	MT-H-200	0.63	13	66	5.40	0.31	4438	8	5	5	9	16	18	None	Long. bars	8.10	49.89	20.04	Steel

[20]	MT-H-200NB	0.63	13	66	5.40	0.31	4438	8	5	5	9	16	18	None	Long. bars	8.10	49.89	19.73	Steel
[21]	Headed stud 1	0.75	4	49	0.55	0.44	3727	NA	NA	NA	NA	NA	NA	None	None	0.00	NA	9.44	Cone
[21]	Headed stud 2	0.75	4	49	0.55	0.44	3727	NA	NA	NA	NA	NA	NA	None	None	0.00	NA	9.89	Cone
[21]	Headed stud 3	0.75	4	49	0.55	0.44	3727	NA	NA	NA	NA	NA	NA	None	None	0.00	NA	11.47	Cone
[21]	Headed stud 4	0.75	4	49	0.55	0.44	3727	NA	NA	NA	NA	NA	NA	None	None	0.00	NA	11.50	Cone
[21]	Headed stud 5	0.75	4	49	0.55	0.44	3727	NA	NA	NA	NA	NA	NA	None	None	0.00	NA	11.69	Cone
[22]	HS-1	0.47	3	75	0.29	0.17	4641	13	13	13	25	25	11	None	None	0.00	NA	10.30	Cone
[22]	HS-2	0.47	3	75	0.29	0.17	4641	13	13	13	25	25	11	None	None	0.00	NA	9.85	Cone
[22]	HS-3	0.63	4	75	0.45	0.31	4641	13	13	13	25	25	11	None	None	0.00	NA	16.30	Cone
[22]	HS-4	0.63	4	75	0.45	0.31	4641	13	13	13	25	25	11	None	None	0.00	NA	18.34	Cone
[22]	HS-5	0.63	4	75	0.45	0.31	4641	13	13	13	25	25	11	None	None	0.00	NA	18.01	Cone
[23]	T1-1	1.00	4	125	12.25	0.61	3983	20	20	20	40	40	16	None	None	0.00	NA	23.32	Cone
[23]	T2-1	1.00	4	125	12.25	0.61	3983	20	20	20	40	40	16	Partial	None	0.00	NA	22.80	Cone
[23]	T3-1	1.00	4	125	12.25	0.61	3983	20	20	20	40	40	16	Partial	None	0.00	NA	24.93	Cone
[23]	T4-1	1.00	4	125	12.25	0.61	3983	20	20	20	40	40	16	Partial	None	0.00	NA	22.79	Cone
[23]	T5-1	1.00	4	125	12.25	0.61	3983	20	20	20	40	40	16	Partial	None	0.00	NA	21.24	Cone
[23]	T6-1	1.00	4	125	12.25	0.61	3983	20	20	20	40	40	16	Partial	None	0.00	NA	24.98	Cone
[23]	T7-1	1.00	4	125	12.25	0.61	3983	20	20	20	40	40	16	Partial	None	0.00	NA	16.51	Cone
[23]	T8-1	1.00	4	125	12.25	0.61	3983	20	20	20	40	40	16	Partial	None	0.00	NA	24.75	Cone
[23]	T9-1	1.00	4	125	12.25	0.61	3983	20	20	20	40	40	16	Partial	None	0.00	NA	14.95	Cone
[23]	T10-1	1.00	4	125	12.25	0.61	3983	20	20	20	40	40	16	Partial	None	0.00	NA	24.37	Cone
[23]	T11-1	1.00	4	125	12.25	0.61	3983	20	20	20	40	40	16	Partial	None	0.00	NA	23.62	Cone
[23]	T12-1	1.00	4	125	12.25	0.61	3983	20	20	20	40	40	16	Partial	None	0.00	NA	22.00	Cone
[23]	T13-1	1.00	4	125	12.25	0.61	3983	20	20	20	40	40	16	Partial	None	0.00	NA	21.11	Cone
[23]	T14-1	1.00	4	125	12.25	0.61	3983	20	20	20	40	40	16	Partial	None	0.00	NA	24.34	Cone
[23]	T15-1	1.00	4	125	12.25	0.61	3983	20	20	20	40	40	16	Partial	None	0.00	NA	14.77	Cone
[23]	T16-1	1.00	4	125	12.25	0.61	3983	20	20	20	40	40	16	Partial	None	0.00	NA	21.53	Cone
[23]	T17-1	1.00	4	125	12.25	0.61	3983	20	20	20	40	40	16	Partial	None	0.00	NA	23.81	Cone
[23]	T18-1	1.00	4	125	12.25	0.61	3983	20	20	20	40	40	16	Partial	None	0.00	NA	23.21	Cone
[23]	T19-1	1.00	4	125	12.25	0.61	3983	20	20	20	40	40	16	Partial	None	0.00	NA	21.95	Cone
[23]	T20-1	1.00	4	125	12.25	0.61	3983	20	20	20	40	40	16	Partial	None	0.00	NA	24.23	Cone
[23]	T21-1	1.00	4	125	12.25	0.61	3983	20	20	20	40	40	16	Partial	None	0.00	NA	14.51	Cone
[24]	T1-A	2.75	25	155	22.33	5.94	5771	74	63	63	148	125	73	None	None	0.00	NA	596.14	Cone
[24]	T1-B	2.75	25	155	22.33	5.94	5630	74	63	63	148	125	73	None	None	0.00	NA	613.51	Cone
[24]	T1-C	2.75	25	155	22.33	5.94	5508	74	63	63	148	125	73	None	None	0.00	NA	559.49	Cone
[24]	T1-D	2.75	25	155	22.33	5.94	5464	74	63	63	148	125	73	None	None	0.00	NA	528.62	Cone
[24]	T2-A	3.75	35	155	45.70	11.04	5177	95	82	82	189	165	70	None	None	0.00	NA	727.66	Cone
[24]	T2-B	3.75	35	155	45.70	11.04	5248	95	82	82	189	165	70	None	None	0.00	NA	730.22	Cone
[24]	T2-C	3.75	35	155	45.70	11.04	5291	95	82	82	189	165	70	None	None	0.00	NA	741.43	Cone
[24]	T2-D	3.75	35	155	45.70	11.04	5320	95	82	82	189	165	70	None	None	0.00	NA	699.77	Cone
[24]	T3-A	4.25	45	155	64.35	14.18	5448	113	81	81	225	162	90	None	None	0.00	NA	1129.82	Cone

[24]	T3-B	4.25	45	155	64.35	14.18	5348	113	81	81	225	162	90	None	None	0.00	NA	1283.96	Cone
[24]	T3-C	4.25	45	155	64.35	14.18	5305	113	81	81	225	162	90	None	None	0.00	NA	1254.92	Cone
[24]	T3-D	4.25	45	155	64.35	14.18	5220	113	81	81	225	162	90	None	None	0.00	NA	1210.38	Cone
[24]	T4-A	2.75	25	155	22.33	5.94	5945	74	63	63	148	125	73	None	Stirrups	6.32	60.00	754.33	Unfinish
[24]	T4-B	2.75	25	155	22.33	5.94	5917	74	63	63	148	125	73	None	Stirrups	6.32	60.00	782.25	Unfinish
[24]	T4-C	2.75	25	155	22.33	5.94	5903	74	63	63	148	125	73	None	Stirrups	6.32	60.00	751.28	Unfinish
[24]	T4-D	2.75	25	155	22.33	5.94	5817	74	63	63	148	125	73	None	Stirrups	6.32	60.00	754.61	Unfinish
[24]	T5-A	2.75	25	155	22.33	5.94	6144	74	63	63	148	125	73	None	Stirrups	12.64	60.00	805.52	Unfinish
[24]	T5-B	2.75	25	155	22.33	5.94	6130	74	63	63	148	125	73	None	Stirrups	12.64	60.00	761.38	Unfinish
[24]	T5-C	2.75	25	155	22.33	5.94	6130	74	63	63	148	125	73	None	Stirrups	12.64	60.00	750.35	Unfinish
[24]	T5-D	2.75	25	155	22.33	5.94	6116	74	63	63	148	125	73	None	Stirrups	12.64	60.00	746.67	Unfinish
[25]	B-3	0.79	6	65	0.91	0.33	4192	17	3	3	35	6	12	None	Stirrups	0.13	42.79	11.96	Cone
[25]	B-4	0.79	8	65	0.91	0.33	4192	17	3	3	35	6	12	None	Stirrups	0.13	42.79	10.61	Cone
[25]	B-5	0.79	10	65	0.91	0.33	4192	17	3	3	35	6	12	None	Stirrups	0.13	42.79	14.12	Cone
[26]	2052010	0.75	4	76	0.91	0.65	5650	4	12	24	56	42	17	None	None	0.00	NA	19.66	Cone
[26]	2122010	0.75	4	76	0.91	0.65	5650	4	12	24	56	42	17	None	None	1.00	NA	21.22	Cone
[26]	3252010	0.75	4	76	0.91	0.65	5650	4	12	24	56	42	17	None	None	2.00	NA	18.44	Cone
[26]	3252010_2	0.75	4	76	0.91	0.65	5650	4	12	24	56	42	17	None	None	3.00	NA	17.96	Cone
[26]	3252010	0.75	6	76	0.91	0.65	5650	4	16	24	56	42	17	None	None	4.00	NA	28.30	Cone
[26]	3302010	0.75	6	76	0.91	0.65	5650	4	16	24	56	42	17	None	None	5.00	NA	25.20	Cone
[26]	3312010	0.75	6	76	0.91	0.65	5650	4	16	24	56	42	17	None	None	6.00	NA	28.14	Steel
[26]	4062010	0.75	6	76	0.91	0.65	5650	4	16	24	56	42	17	None	None	7.00	NA	27.80	Steel
[26]	1292010	0.75	6	76	0.91	0.65	5650	6	16	24	56	42	17	None	None	8.00	NA	28.37	Steel

The references are list as follows.

Ref. #	Name
[1]	Nordlin, E.F.; Ames, W.H.; and Post, E.R., (1968) Evaluation of Concrete Anchor Bolts, Caltrans Report 19601- 762500- 36390, 60 pp.
[2]	McMackin, P. .I.; Slutter, R. G.; and Fisher, J. W., "Headed Steel Anchors Under Combined Loading," AISC Engineering Journal, 2nd Quarter, Apr. 1973, pp. 43-52.
[3]	Hasselwander, G. B.; Jirsa, J. O.; Breen, J. E.; and Lo., K.,"Strength and Behavior of Anchor Bolts Embedded Near Edges of Concrete Piers," Research Report 29-2F, Center for Transportation Research, the University of Texas at Austin, Austin, TX, May 1974,
[4]	Cannon, R. W.; Burdette, E. G.; and Funk, R. R., "Anchorage to Concrete," Tennessee Valley Authority, Knoxville, Dec. 1975.
[5]	Bode, H. and Hanenkamp, W. (1985). Zur tragfähigkeit von kopfbolzen bei zugbeanspruchung. Bauingenieur,. 361–367. In Shirvani thesis
[6]	Versuche mit Kopfbolzen, durchgeführt am IBS, München und der FMPA Stuttgart, 1985, unpublished In Shirvani thesis
[7]	Versuche mit Kopfbolzen, durchgeführt von Hochtief und der VA der Universität Karlsruhe, 1983, unpublished In Shirvani thesis
[8]	Versuche mit Kopfbolzen, durchgeführt an der Universität Bochum, 1985, unpublished In Shirvani thesis
[5]~[8]	Shirvani, Mansour, "Behavior of Tensile Anchors in Concrete: Statistical Analysis and Design Recommendations," MS Thesis, The University of Texas at Austin, 1998
[9]	Hawkins, N. M. (1987). "Strength in shear and tension of cast-in-place anchor bolts." Special Publication, ACI SP-103, 233-255.
[10]	Cook, R. A., Collins D. M., Klingner, R. E., and Polyzois. D. (1992). "Load-Deflection Behavior of Cast-in-Place and Retrofit Concrete Anchors." ACI Structural Journal, V. 89, No. 6, pp. 639-649.
[11]	T. Balough, G. Kovacshazy and A. Frigey (1992) "Pull-out Tests on Steel Embedments in Concrete" ACI Special Publication 130. pp. 221-234
[12]	Carraio, P. J., Krauss, K. W. and Kim, J. B., Tension Tests of Heavy-Duty Anchors with Embedments of 8 to 19 Inches , ACI Structural Journal, May-June 1996, pp. 1-9.
[13]	Hallowell, J., Tensile and Shear Behavior of Anchors in Uncracked and Cracked Concrete Under Static and Dynamic Loading," M.S. Thesis, The University of Texas at Austin, December, 1996.
[14]	Ohashi, Y. and Nakashima, YS. (1997) "Experimental study on mechanical characteristics of exposed portions of anchor bolts," Summaries of technical papers of Annual Meeting Architectural Institute of Japan. C-1, Structures III, Timber structures steel str
[15]	Primavera, E.J., J.P. Pinelli and E.H. Kalajian. 1997. Tensile Behavior of Cast-in-Place and Undercut Anchors in High Strength Concrete. ACI Structures Journal 94:5
[16]	Nakashima, S. "Behaviour of exposed portions of anchor bolts subjected to reversed cyclic combined tension and shear forces," Annual Meeting Architectural Institute of Japan. C-1 Structure III, pp. 229-232 (in Japanese)
[17]	Rodriguez, M., Lotze, D., Gross, J. H., Zhang, Y., Klingner, R. E. and Graves, III, H. L., "Dynamic Behavior of Tensile Anchors to Concrete," Structures Journal, American Concrete Institute, Farmington Hills, Michigan, vol. 98, no. 4, July-August 2001, pp
[18]	Yong, Y., Kim, H., and Kim, S. (2001) Assessment of Fracture Behaviors for CIP Anchors Fastened to Cracked and Uncracked Concretes KCI Concrete Joumal. Vol l3 No. 2 pp. 33-41
[19]	KAWANO Hisao, KUTANI Kazuhide, and MASUDA Kanshi "EXPERIMENTAL STUDIES ON THE SHEAR RESISTANCE OF ANCHOR BOLTS IN EXPORSED TYPE OF STEEL COLUMN BASES [in Japanese]" Journal of structural and construction engineering. Transactions of AIJ (567), 141-148, 2
[20]	Yoshimori, K. and Nakashima, S. (2004) "Experimental study on mechanical characteristics of exposed portions of anchor bolts subjected to tension or shear." Research reports of Architectural Institute of Japan, Vol. 44, pp. 333-336.
[21]	Hoehler, M. S., "Behavior and Testing of Fastenings to Concrete for Use in Seismic Applications, PhD dissertation, Universität Stuttgart, Stuttgart, Germany, 2006, 261 pp.
[22]	Solomos G, Berra M "Testing of Anchorages in Concrete Under Dynamic Tensile Loading" MATERIALS AND STRUCTURES 39; 2006. p. 695-706.
[23]	J.B. Jang, Y.P. Suh The experimental investigation of a crack's influence on the concrete breakout strength of a cast-in-place anchor Nuclear Engineering and Design 236 (2006) 948–953.
[24]	Nam Ho Lee, Kang Sik Kim, Chang Joon Bang, and Kwang Ryeon Park, "Tensile-Headed Anchors with Large Diameter and Deep Embedment in Concrete" ACI Structural Journal, V. 104, No. 4, 2007.
[25]	ANDO Yutaro , SAKAI Satoru , NAKANO Katsuhiko (2007) "Study on Structural Performance of Anchor bolt Embedded in RC Footing Beams ," Architectural Institute of Japan, (50), 117-120,
[26]	Petersen, D. (2011) Seismic bahavior and design of cast-in-place anchors, MS Thesis, UW-Milwaukee

Appendix B Collected Data on Cast-in Anchors in Shear

No.	No. of	d_a (in)	h_{ef} (in)	F_{ut} (ksi)	A_{brg}	$A_{se,V}$ (in^2)	f'_c (psi)	c_{a1} (in)	c_{a2}	c_{a3} (in)	c_{a4} (in)	x (in)	y (in)	h (in)	Crack	Reinf.	A_s (in^2)	V (kips)	e_v(in)	Mode
Ref.	Reported	Anchor	Embed	Steel	Head	Effective	Conc.	Front	Side	Side	Back	Block	Block	Block	in	Anchor	Reinf.	Measured	Shear	Reported
Pape	Test	Dia.	Depth	Strength	Area	Area	Strength	Edge	Edge	Edge 2	Edge	Length	Width	Height	Concrete	Pattern	Area	Shear	Offset	Failure
[1]	4A2	0.50	3.5	71	0.2	0.20	3840	20	10	14	10	24	30	7	None	None	0.00	14.40	0.00	Steel
[1]	4B2	0.50	3.5	71	0.2	0.20	4390	20	10	14	10	24	30	7	None	None	0.00	13.90	0.00	Steel
[1]	5A2	0.63	3.4	68	0.2	0.31	3790	20	10	14	10	24	30	7	None	None	0.00	23.80	0.00	Steel
[1]	5B2	0.63	3.4	68	0.2	0.31	4250	20	10	14	10	24	30	7	None	None	0.00	22.50	0.00	Steel
[1]	6A2	0.75	3.4	70	0.3	0.44	3870	20	10	14	10	24	30	7	None	None	0.00	32.00	0.00	Steel
[1]	6B2	0.75	3.4	70	0.3	0.44	4240	20	10	14	10	24	30	7	None	None	0.00	32.50	0.00	Steel
[2]	1-A	0.75	2.6	71	0.8	0.44	5080	14	10	10	14	20	28	6	None	None	0.00	29.30	0.00	Steel
[2]	2-A	0.75	2.6	71	0.8	0.44	5080	14	10	10	14	20	28	6	None	None	0.00	32.50	0.00	Steel
[2]	3-A	0.75	2.6	71	0.8	0.44	5080	14	10	10	14	20	28	6	None	None	0.00	30.60	0.00	Steel
[2]	1-SA	0.63	2.7	70	0.7	0.31	4010	14	10	10	14	20	28	6	None	None	0.00	19.50	0.00	Steel
[2]	2-SA	0.63	2.7	70	0.7	0.31	4010	14	10	10	14	20	28	6	None	None	0.00	20.80	0.00	Steel
[2]	3-SA	0.63	2.7	70	0.7	0.31	4010	14	10	10	14	20	28	6	None	None	0.00	19.90	0.00	Steel
[2]	1-B	0.75	2.6	71	0.8	0.44	4780	14	10	10	14	20	28	6	None	None	0.00	27.40	0.00	Steel
[2]	2-B	0.75	2.6	71	0.8	0.44	4780	14	10	10	14	20	28	6	None	None	0.00	25.40	0.00	Steel
[2]	3-B	0.75	2.6	71	0.8	0.44	4780	14	10	10	14	20	28	6	None	None	0.00	25.40	0.00	Steel
[2]	1-SB	0.63	2.7	70	0.7	0.31	4030	14	10	10	14	20	28	6	None	None	0.00	18.20	0.00	Steel
[2]	2-SB	0.63	2.7	70	0.7	0.31	4030	14	10	10	14	20	28	6	None	None	0.00	16.90	0.00	Steel
[2]	3-SB	0.63	2.7	70	0.7	0.31	4030	14	10	10	14	20	28	6	None	None	0.00	18.80	0.00	Steel
[2]	1-2B	0.75	2.6	71	0.8	0.44	4780	14	10	10	14	20	28	6	None	None	0.00	26.10	0.00	Steel
[2]	2-2B	0.75	2.6	71	0.8	0.44	4780	14	10	10	14	20	28	6	None	None	0.00	25.50	0.00	Steel
[2]	3-2B	0.75	2.6	71	0.8	0.44	4780	14	10	10	14	20	28	6	None	None	0.00	25.00	0.00	Steel
[2]	1-C	0.75	2.6	71	0.8	0.44	4280	14	10	10	14	20	28	6	None	None	0.00	21.60	0.00	Steel
[2]	2-C	0.75	2.6	71	0.8	0.44	4280	14	10	10	14	20	28	6	None	None	0.00	21.50	0.00	Steel
[2]	3-C	0.75	2.6	71	0.8	0.44	4280	14	10	10	14	20	28	6	None	None	0.00	22.60	0.00	Steel
[2]	1-D	0.75	2.6	71	0.8	0.44	4920	14	10	10	14	20	28	6	None	None	0.00	21.60	0.00	Steel
[2]	2-D	0.75	2.6	71	0.8	0.44	4920	14	10	10	14	20	28	6	None	None	0.00	23.30	0.00	Steel
[2]	3-D	0.75	2.6	71	0.8	0.44	4920	14	10	10	14	20	28	6	None	None	0.00	24.40	0.00	Steel
[2]	1-E	0.75	2.6	71	0.8	0.44	4300	14	10	10	14	20	28	6	None	None	0.00	23.10	0.00	Steel
[2]	2-E	0.75	2.6	71	0.8	0.44	4300	14	10	10	14	20	28	6	None	None	0.00	22.50	0.00	Steel
[2]	3-E	0.75	2.6	71	0.8	0.44	4300	14	10	10	14	20	28	6	None	None	0.00	21.60	0.00	Steel
[2]	1-SE	0.63	2.7	70	0.7	0.31	4000	14	10	10	14	20	28	6	None	None	0.00	15.70	0.00	Steel
[2]	2-SE	0.63	2.7	70	0.7	0.31	4000	14	10	10	14	20	28	6	None	None	0.00	15.70	0.00	Steel
[2]	3-SE	0.63	2.7	70	0.7	0.31	4000	14	10	10	14	20	28	6	None	None	0.00	17.00	0.00	Steel
[2]	1-2E	0.75	2.6	71	0.8	0.44	4400	14	10	10	14	20	28	6	None	None	0.00	21.20	0.00	Steel
[2]	2-2E	0.75	2.6	71	0.8	0.44	4400	14	10	10	14	20	28	6	None	None	0.00	23.10	0.00	Steel
[2]	3-2E	0.75	2.6	71	0.8	0.44	4400	14	10	10	14	20	28	6	None	None	0.00	22.70	0.00	Steel

[3]	A2-6	0.75	3.6	64	0.8	0.44	5270	2	12	12	12	84	24	24	None	None	0.00	4.35	0.00	Cone
[3]	A3-6	0.75	3.6	64	0.8	0.44	5270	2	12	12	12	84	24	24	None	None	0.00	4.70	0.00	Cone
[3]	B1-7	0.75	3.6	64	0.8	0.44	4060	2	12	12	12	84	24	24	None	None	0.00	2.90	0.00	Cone
[3]	C3-6	0.75	3.6	64	0.8	0.44	4910	2	12	12	12	84	24	24	None	None	0.00	3.30	0.00	Cone
[3]	A1-7	0.75	3.6	64	0.8	0.44	5270	4	12	12	12	84	24	24	None	None	0.00	9.90	0.00	Cone
[3]	A1-8	0.75	3.6	64	0.8	0.44	5270	4	12	12	12	84	24	24	None	None	0.00	10.20	0.00	Cone
[3]	A2-7	0.75	3.6	64	0.8	0.44	5270	6	12	12	12	84	24	24	None	None	0.00	20.00	0.00	Cone
[3]	A2-8	0.75	3.6	64	0.8	0.44	5270	6	12	12	12	84	24	24	None	None	0.00	19.00	0.00	Cone
[3]	A3-7	0.75	3.6	64	0.8	0.44	5270	8	12	12	12	84	24	24	None	None	0.00	30.00	0.00	Steel
[3]	A3-8	0.75	3.6	64	0.8	0.44	5270	8	12	12	12	84	24	24	None	None	0.00	32.00	0.00	Steel
[3]	B3-7	0.75	3.6	64	0.8	0.44	4900	10	12	12	12	84	24	24	None	None	0.00	28.60	0.00	Cone
[3]	B3-8	0.75	3.6	64	0.8	0.44	4900	10	12	12	12	84	24	24	None	None	0.00	28.50	0.00	Cone
[4]	76-42	0.75	6.0	60	0.8	0.44	4815	4	20	20	36	40	40	12	None	None	0.00	19.12	0.00	Cone
[4]	76-43	0.75	6.0	60	0.8	0.44	4815	5	20	20	36	40	40	12	None	None	0.00	15.81	0.00	Cone
[4]	76-48	0.75	6.0	60	0.8	0.44	4850	6	20	20	36	40	40	12	None	None	0.00	22.62	0.00	Cone
[4]	76-51	0.75	6.0	61	0.8	0.44	4900	6	20	20	36	40	40	12	None	None	0.00	30.36	0.00	Cone
[5]	S1	0.50	6.0	74	0.6	0.20	7704	18	4	4	6	8	24	15	None	None	0.00	5.67	0.50	Unfinished
[5]	S2	0.63	6.0	74	0.9	0.31	6775	18	4	4	6	8	24	15	None	None	0.00	8.67	0.50	Unfinished
[5]	S3	0.75	6.0	74	0.8	0.44	6910	18	4	4	6	8	24	15	None	None	0.00	14.14	0.50	Unfinished
[5]	S4	0.63	6.0	74	0.9	0.31	5800	18	4	4	6	8	24	15	None	None	0.00	13.33	0.00	Steel
[5]	S5	0.63	6.0	74	0.9	0.31	5211	18	4	4	6	8	24	15	None	None	0.00	13.34	0.00	Steel
[5]	S6	0.63	6.0	74	0.9	0.31	4674	18	4	4	6	8	24	15	None	None	0.00	12.89	0.00	Steel
[6]	#1-1A4CH	1.00	9.1	68	1.2	0.79	4200	4	13	13	22	26	26	24	None	Hairpin	0.40	16.60	0.00	Bond
[6]	#2-1B4CH	1.00	9.1	68	1.2	0.79	4200	4	13	13	22	26	26	24	None	Hairpin	0.40	14.60	0.00	Bond
[6]	#3-1C4CH	1.00	9.1	68	1.2	0.79	4200	4	13	13	22	26	26	24	None	Hairpin	0.40	26.30	0.00	Cone
[6]	#4-1D4CH	1.00	9.1	68	1.2	0.79	4200	4	13	13	22	26	26	24	None	Hairpin	0.40	24.90	0.00	Cone
[6]	#5-1E4CH	1.00	9.1	62	1.2	0.79	4200	4	13	13	22	26	26	24	None	Hairpin	0.40	25.20	0.00	Cone
[6]	#6-1F4CH	1.00	9.1	62	1.2	0.79	4200	4	13	13	22	26	26	24	None	Hairpin	0.40	25.20	0.00	Cone
[6]	#7-1A4CN	1.00	9.1	66	1.2	0.79	4200	4	13	13	22	26	26	24	None	None	0.00	16.50	0.00	Cone
[6]	#8-1B4CN	1.00	9.1	66	1.2	0.79	4200	4	13	13	22	26	26	24	None	None	0.00	12.60	0.00	Cone
[6]	#9-1C4CN	1.00	9.1	62	1.2	0.79	4200	4	13	13	22	26	26	24	None	None	0.00	11.70	0.00	Cone
[6]	#10-1A4CU	1.00	9.1	62	1.2	0.79	4200	4	13	13	13	26	17	24	None	Surface	0.40	21.10	0.00	Cone
[6]	#11-1B4CU	1.00	9.1	62	1.2	0.79	4200	4	13	13	13	26	17	24	None	Surface	0.40	16.80	0.00	Cone
[6]	#19-1A6CH	1.00	9.1	62	1.2	0.79	4200	6	26	26	34	52	40	24	None	Hairpin	0.40	30.90	0.00	Steel
[6]	#20-1B6CH	1.00	9.1	62	1.2	0.79	4200	6	26	26	34	52	40	24	None	Hairpin	0.40	36.30	0.00	Steel
[6]	#21-1A6CN-22	1.00	9.1	68	1.2	0.79	4200	6	26	26	34	52	40	24	None	None	0.00	21.00	0.00	Cone
[6]	#22-1B6CN-22	1.00	9.1	68	1.2	0.79	4200	6	26	26	34	52	40	24	None	None	0.00	21.00	0.00	Cone
[6]	#23-1A6CN-33	1.00	9.1	68	1.2	0.79	4200	6	26	26	34	52	40	24	None	None	0.00	17.30	0.00	Cone
[6]	#24-1B6CN-33	1.00	9.1	68	1.2	0.79	4200	6	26	26	34	52	40	24	None	None	0.00	19.90	0.00	Cone
[6]	#25-1A6CN-44	1.00	9.1	68	1.2	0.79	4200	6	26	26	34	52	40	24	None	None	0.00	20.10	0.00	Cone
[6]	#26-1B6CN-44	1.00	9.1	68	1.2	0.79	4200	6	26	26	34	52	40	24	None	None	0.00	18.60	0.00	Cone

[6]	#27-1A8CH	1.00	9.1	62	1.2	0.79	4200	8	26	26	34	52	40	24	None	Hairpin	0.40	39.00	0.00	Steel
[6]	#28-1B8CH	1.00	9.1	62	1.2	0.79	4200	8	26	26	32	52	40	24	None	Hairpin	0.40	35.50	0.00	Steel
[6]	#29-1A8CN	1.00	9.1	66	1.2	0.79	4200	8	26	26	32	52	40	24	None	None	0.00	32.40	0.00	Steel
[6]	#30-1B8CN	1.00	9.1	66	1.2	0.79	4200	8	26	26	32	52	40	24	None	None	0.00	32.40	0.00	Steel
[6]	#35-1A12CN	1.00	9.1	66	1.2	0.79	4200	12	26	26	28	52	40	24	None	None	0.00	35.00	0.00	Cone
[6]	#36-1B12CN	1.00	9.1	66	1.2	0.79	4200	12	26	26	28	52	40	24	None	None	0.00	35.00	0.00	Cone
[6]	#37-2A6CH	2.00	18.4	67	4.7	3.14	4200	6	26	26	34	52	40	24	None	Hairpin	0.40	46.80	0.00	Cone
[6]	#38-2B6CH	2.00	18.4	67	4.7	3.14	4200	6	26	26	34	52	40	24	None	Hairpin	0.40	46.20	0.00	Cone
[6]	#39-2C6CH	2.00	18.4	72	4.7	3.14	4200	6	26	26	34	52	40	24	None	Hairpin	0.62	73.30	0.00	Cone
[6]	#40-2D6CH	2.00	18.4	72	4.7	3.14	4200	6	26	26	34	52	40	24	None	Hairpin	0.62	77.30	0.00	Cone
[6]	#41-2A6CN	2.00	18.4	67	4.7	3.14	4200	6	26	26	34	52	40	24	None	None	0.00	26.30	0.00	Cone
[6]	#42-2B6CN	2.00	18.4	67	4.7	3.14	4200	6	26	26	34	52	40	24	None	None	0.00	25.40	0.00	Cone
[6]	#49-2A12CH	2.00	18.4	67	4.7	3.14	4200	12	26	26	28	52	40	24	None	Hairpin	0.62	77.90	0.00	Cone
[6]	#50-2B12CH	2.00	18.4	67	4.7	3.14	4200	12	26	26	28	52	40	24	None	Hairpin	0.62	80.00	0.00	Cone
[6]	#51-2A12CN	2.00	18.4	67	4.7	3.14	4200	12	26	26	28	52	40	24	None	None	0.00	55.10	0.00	Cone
[6]	#52-2B12CN	2.00	18.4	67	4.7	3.14	4200	12	26	26	28	52	40	24	None	None	0.00	60.00	0.00	Cone
[6]	#73-1A6CH-COMB	1.00	9.1	62	1.2	0.79	4200	6	26	26	34	52	40	24	None	Hairpin	0.40	38.00	2.00	Steel
[6]	#74-1B6CH-COMB	1.00	9.1	62	1.2	0.79	4200	6	26	26	34	52	40	24	None	Hairpin	0.40	38.00	2.00	Steel
[6]	#75-1A8CN-COMB	1.00	9.1	62	1.2	0.61	4200	8	26	26	34	52	40	24	None	0.00	0.00	20.50	2.00	Steel
[6]	#76-1B8CN-COMB	1.00	9.1	62	1.2	0.61	4200	8	26	26	34	52	40	24	None	0.00	0.00	19.70	2.00	Steel
[6]	#81-1A6CH-hs-	1.00	9.1	124	1.2	0.79	4200	6	26	26	34	52	40	24	None	Hairpin	0.40	38.00	2.00	Cone
[6]	#82-1B6CH-hs-	1.00	9.1	124	1.2	0.79	4200	6	26	26	34	52	40	24	None	Hairpin	0.40	38.90	2.00	Cone
[6]	#85-2A6CH-COMB	2.00	18.4	67	4.7	3.14	4200	6	26	26	34	52	40	24	None	Hairpin	0.62	59.30	2.00	Cone
[6]	#86-2B6CH-COMB	2.00	18.4	67	4.7	3.14	4200	6	26	26	34	52	40	24	None	Hairpin	0.62	64.00	2.00	Cone
[6]	#89-2A6CH-hs-	2.00	18.4	105	4.7	3.14	4200	6	26	26	34	52	40	24	None	Hairpin	0.62	58.90	2.00	Cone
[6]	#90-2B6CH-hs-	2.00	18.4	105	4.7	3.14	4200	6	26	26	34	52	40	24	None	Hairpin	0.62	64.70	2.00	Cone
[7]	B1-1	0.75	8.0	61	0.8	0.44	4262	12	24	24	24	96	36	24	None	None	0.00	23.80	0.00	Steel
[7]	B1-2	0.75	8.0	61	0.8	0.44	4262	12	24	24	24	96	36	24	None	None	0.00	24.50	0.00	Steel
[7]	B1-3	0.75	8.0	61	0.8	0.44	4262	12	24	24	24	96	36	24	None	None	0.00	22.80	0.00	Steel
[7]	B1-4	0.75	8.0	61	0.8	0.44	4262	12	24	24	24	96	36	24	None	None	0.00	25.50	0.00	Steel
[7]	B1-5	0.75	8.0	61	0.8	0.44	4262	12	24	24	24	96	36	24	None	None	0.00	25.00	0.00	Steel
[7]	B1-6	0.75	8.0	61	0.8	0.44	4262	12	24	24	24	96	36	24	None	None	0.00	25.50	0.00	Steel
[7]	B1-7	0.75	8.0	61	0.8	0.44	4262	12	24	24	24	96	36	24	None	None	0.00	23.00	0.00	Steel
[7]	B1-8	0.75	8.0	61	0.8	0.44	4262	12	24	24	24	96	36	24	None	None	0.00	23.00	0.00	Steel
[7]	B2-1	0.75	8.0	61	0.8	0.44	4200	2	24	24	34	96	36	24	None	None	0.00	3.85	0.00	Cone
[7]	B2-2	0.75	8.0	61	0.8	0.44	4200	2	24	24	34	96	36	24	None	None	0.00	1.50	0.00	Cone
[7]	B2-3	0.75	8.0	61	0.8	0.44	4200	2	24	24	34	96	36	24	None	None	0.00	4.00	0.00	Cone
[7]	B2-4	0.75	8.0	61	0.8	0.44	4200	4	24	24	32	96	36	24	None	None	0.00	6.75	0.00	Cone
[7]	B2-5	0.75	8.0	61	0.8	0.44	4200	4	24	24	32	96	36	24	None	None	0.00	6.00	0.00	Cone
[7]	B2-6	0.75	8.0	61	0.8	0.44	4200	4	24	24	32	96	36	24	None	None	0.00	6.00	0.00	Cone
[7]	B2-7	0.75	8.0	61	0.8	0.44	4200	6	24	24	30	96	36	24	None	None	0.00	10.00	0.00	Cone

[7]	B2-8	0.75	8.0	61	0.8	0.44	4200	4	24	24	32	96	36	24	None	None	0.00	7.50	0.00	Cone
[7]	B2-9	0.75	8.0	61	0.8	0.44	4200	6	24	24	30	96	36	24	None	None	0.00	9.30	0.00	Cone
[7]	B2-10	0.75	8.0	61	0.8	0.44	4200	8	24	24	28	96	36	24	None	None	0.00	19.00	0.00	Cone
[7]	B2-11	0.75	8.0	61	0.8	0.44	4200	2	24	24	34	96	36	24	None	None	0.00	4.10	0.00	Cone
[7]	B2-12	0.75	8.0	61	0.8	0.44	4200	8	24	24	28	96	36	24	None	None	0.00	16.70	0.00	Cone
[7]	B2-13	0.75	8.0	61	0.8	0.44	4200	8	24	24	28	96	36	24	None	None	0.00	19.50	0.00	Cone
[7]	B2-14	0.75	8.0	61	0.8	0.44	4200	6	24	24	30	96	36	24	None	None	0.00	14.50	0.00	Cone
[7]	B3-1	0.75	8.0	61	0.8	0.44	6200	4	24	24	32	96	36	24	None	Hairpin	0.62	23.00	0.00	Cone
[7]	B3-2	0.75	8.0	61	0.8	0.44	6200	4	24	24	32	96	36	24	None	Hairpin	0.62	23.00	0.00	Cone
[7]	B3-3	0.75	8.0	61	0.8	0.44	6200	4	24	24	32	96	36	24	None	Hairpin	0.62	22.50	0.00	Cone
[7]	B3-4	0.75	8.0	61	0.8	0.44	6200	2	24	24	34	96	36	24	None	Hairpin	0.62	22.80	0.00	Cone
[7]	B3-6	0.75	8.0	61	0.8	0.44	6200	2	24	24	34	96	36	24	None	Hairpin	0.62	22.00	0.00	Cone
[7]	B3-7	0.75	8.0	61	0.8	0.44	6200	4	24	24	32	96	36	24	None	Hairpin	0.62	23.00	0.00	Cone
[7]	B3-8	0.75	8.0	61	0.8	0.44	6200	4	24	24	32	96	36	24	None	Hairpin	0.62	23.00	0.00	Cone
[7]	B3-9	0.75	8.0	61	0.8	0.44	6200	4	24	24	32	96	36	24	None	Hairpin	0.62	22.00	0.00	Cone
[7]	B3-11	0.75	8.0	61	0.8	0.44	6200	2	24	24	34	96	36	24	None	Hairpin	0.62	18.50	0.00	Cone
[7]	B3-13	0.75	8.0	61	0.8	0.44	6200	2	24	24	34	96	36	24	None	Hairpin	0.62	15.50	0.00	Cone
[7]	B3-15	0.75	8.0	61	0.8	0.44	6200	2	24	24	34	96	36	24	None	Hairpin	0.62	22.00	0.00	Cone
[8]	Bottom-1	0.50	6.0	70	0.6	0.20	5750	6	8	8	6	16	12	16	None	None	0.00	12.78	0.00	Steel
[8]	Bottom-2	0.50	6.0	70	0.6	0.20	5750	6	8	8	6	16	12	16	None	None	0.00	12.69	0.00	Steel
[8]	Bottom-3	0.50	6.0	70	0.6	0.20	5750	6	8	8	6	16	12	16	None	None	0.00	12.53	0.00	Steel
[8]	Side-1	0.50	6.0	70	0.6	0.20	5750	6	8	8	6	16	12	16	None	None	0.00	12.46	0.00	Steel
[8]	Side-2	0.50	6.0	70	0.6	0.20	5750	6	8	8	6	16	12	16	None	None	0.00	12.21	0.00	Steel
[8]	Side-3	0.50	6.0	70	0.6	0.20	5750	6	8	8	6	16	12	16	None	None	0.00	12.07	0.00	Steel
[8]	Toploose-1	0.50	6.0	70	0.6	0.20	4950	6	8	8	6	16	12	16	None	None	0.00	9.91	0.00	Steel
[8]	Toploose-2	0.50	6.0	70	0.6	0.20	4950	6	8	8	6	16	12	16	None	None	0.00	8.17	0.00	Steel
[8]	Toploose-3	0.50	6.0	70	0.6	0.20	4950	6	8	8	6	16	12	16	None	None	0.00	9.16	0.00	Steel
[8]	Topfixed-1	0.50	6.0	70	0.6	0.20	4950	6	8	8	6	16	12	16	None	None	0.00	8.71	0.00	Steel
[8]	Topfixed-2	0.50	6.0	70	0.6	0.20	4950	6	8	8	6	16	12	16	None	None	0.00	10.25	0.00	Steel
[8]	Topfixed-3	0.50	6.0	70	0.6	0.20	4950	6	8	8	6	16	12	16	None	None	0.00	8.50	0.00	Steel
[9]	1S	1.00	3.0	134	11.8	0.79	3080	9	9	9	9	18	18	9	None	Surface	1.76	23.72	0.00	Pryout
[9]	2S	1.00	5.0	134	11.8	0.79	3010	9	9	9	9	18	18	9	None	Surface	2.76	25.16	0.00	Unfinished
[9]	3S	1.00	3.0	134	11.8	0.79	2900	9	9	9	9	18	18	9	None	Surface	3.76	22.07	0.00	Pryout
[9]	4S	1.00	7.0	134	11.8	0.79	3020	9	9	9	9	18	18	9	None	Surface	4.76	27.73	0.00	Unfinished
[9]	5S	1.00	5.0	134	2.4	0.79	2900	9	9	9	9	18	18	9	None	Surface	5.76	22.58	0.00	Unfinished
[9]	6S	1.00	3.0	134	2.4	0.79	3100	9	9	9	9	18	18	9	None	Surface	6.76	19.50	0.00	Pryout
[9]	7S	1.00	3.0	134	11.8	0.79	4930	9	9	9	9	18	18	9	None	Surface	7.76	27.22	0.00	Pryout
[9]	8S	1.00	5.0	134	11.8	0.79	4930	9	9	9	9	18	18	9	None	Surface	8.76	29.28	0.00	Unfinished
[9]	9S	0.75	5.0	134	11.8	0.44	3080	9	9	9	9	18	18	9	None	Surface	9.76	21.66	0.00	Unfinished
[9]	10S	0.75	7.0	134	11.8	0.44	3080	9	9	9	9	18	18	9	None	Surface	10.76	23.72	0.00	Unfinished
[9]	11S	0.75	3.0	134	11.8	0.44	3040	9	9	9	9	18	18	9	None	Surface	11.76	23.10	0.00	Pryout

[9]	12S	0.75	5.0	134	2.4	0.44	3040	9	9	9	9	18	18	9	None	Surface	12.76	21.04	0.00	Unfinished
[9]	13S	0.75	3.0	134	2.4	0.44	3080	9	9	9	9	18	18	9	None	Surface	13.76	20.22	0.00	Pryout
[9]	14S	0.75	3.0	134	11.8	0.44	5040	9	9	9	9	18	18	9	None	Surface	14.76	28.25	0.00	Pryout
[9]	15S	0.75	5.0	134	2.4	0.44	5040	9	9	9	9	18	18	9	None	Surface	15.76	26.00	0.00	Unfinished
[10]	OSU-A1	0.50	1.6	65	0.3	0.20	5960	3	24	96	34	0	0	12	None	None	0.00	5.70	0.00	Cone
[10]	OSU-A2	0.50	1.6	65	0.3	0.20	5960	5	48	72	31	0	0	12	None	None	0.00	13.30	0.00	Cone
[10]	OSU-A10	0.50	1.6	65	0.3	0.20	5960	3	24	96	34	0	0	12	None	None	0.00	6.60	0.00	Cone
[10]	OSU-A11	0.50	1.6	65	0.3	0.20	5960	5	48	72	31	0	0	12	None	None	0.00	13.50	0.00	Steel
[10]	OSA-A19	0.50	5.6	65	0.3	0.20	5960	3	3	118	34	0	0	12	None	None	0.00	3.40	0.00	Cone
[11]	A-13-1	0.51	12.8	70	0.3	0.21	2998	2	8	8	14	16	16	10	None	None	0.00	2.43	0.00	Cone
[11]	A-13-2	0.51	12.8	70	0.3	0.21	2998	3	8	8	13	16	16	10	None	None	0.00	5.56	0.00	Cone
[11]	A-13-3	0.51	12.8	70	0.3	0.21	2998	4	8	8	12	16	16	10	None	None	0.00	7.36	0.00	Cone
[11]	A-13-4	0.51	12.8	70	0.3	0.21	2998	5	8	8	11	16	16	10	None	None	0.00	9.92	0.00	Steel
[11]	A-19-1	0.75	18.7	70	0.7	0.44	2998	3	9	9	15	18	18	12	None	None	0.00	5.62	0.00	Cone
[11]	A-19-2	0.75	18.7	70	0.7	0.44	2998	4	9	9	14	18	18	12	None	None	0.00	8.27	0.00	Cone
[11]	A-19-3	0.75	18.7	70	0.7	0.44	2998	5	9	9	13	18	18	12	None	None	0.00	10.25	0.00	Cone
[11]	A-19-4	0.75	18.7	70	0.7	0.44	2998	6	9	9	12	18	18	12	None	None	0.00	16.20	0.00	Steel
[11]	A-19-5	0.75	18.7	70	0.7	0.44	2998	7	9	9	11	18	18	12	None	None	0.00	16.20	0.00	Steel
[11]	A-19-6	0.75	18.7	70	0.7	0.44	2998	8	9	9	10	18	18	12	None	None	0.00	20.39	0.00	Steel
[11]	A-16-1	0.61	15.2	71	0.5	0.29	3195	3	10	10	15	20	18	12	None	None	0.00	6.53	0.00	Cone
[11]	A-16-2	0.61	15.2	71	0.5	0.29	3195	4	10	10	14	20	18	12	None	None	0.00	7.74	0.00	Cone
[11]	A-16-3	0.61	15.2	71	0.5	0.29	3195	5	10	10	13	20	18	12	None	None	0.00	10.10	0.00	Cone
[11]	A-16-4	0.61	15.2	71	0.5	0.29	3195	6	10	10	12	20	18	12	None	None	0.00	14.07	0.00	Cone
[11]	B-16-1	0.61	15.2	71	0.5	0.29	3195	5	2	18	13	20	18	12	None	None	0.00	5.69	0.00	Cone
[11]	B-16-2	0.61	15.2	71	0.5	0.29	3195	5	3	17	13	20	18	12	None	None	0.00	7.56	0.00	Cone
[11]	B-16-3	0.61	15.2	71	0.5	0.29	3195	5	4	16	13	20	18	12	None	None	0.00	8.55	0.00	Cone
[11]	B-16-4	0.61	15.2	71	0.5	0.29	3195	5	5	15	13	20	18	12	None	None	0.00	10.08	0.00	Cone
[11]	A-25-1	0.96	25.0	65	1.5	0.73	3230	5	11	11	17	22	22	14	None	None	0.00	13.56	0.00	Cone
[11]	A-25-2	0.96	25.0	65	1.5	0.73	3230	7	11	11	15	22	22	14	None	None	0.00	17.86	0.00	Cone
[11]	A-25-3	0.96	25.0	65	1.5	0.73	3230	9	11	11	13	22	22	14	None	None	0.00	26.68	0.00	Steel
[11]	A-36-1	1.41	28.8	61	2.7	1.56	3230	6	11	11	16	22	22	14	None	None	0.00	15.98	0.00	Cone
[11]	A-36-2	1.41	28.8	61	2.7	1.56	3230	8	11	11	14	22	22	14	None	None	0.00	26.46	0.00	Cone
[11]	A-36-3	1.41	28.8	61	2.7	1.56	3230	10	11	11	12	22	22	14	None	None	0.00	31.31	0.00	Cone
[11]	A-56-1	2.16	43.2	69	5.3	3.67	3230	9	11	11	13	22	22	14	None	None	0.00	28.11	0.00	Cone
[11]	A-56-2	2.16	43.2	69	5.3	3.67	3230	10	11	11	12	22	22	14	None	None	0.00	36.38	0.00	Cone
[11]	A-56-3	2.16	43.2	69	5.3	3.67	3230	11	11	11	11	22	22	14	None	None	0.00	39.68	0.00	Cone
[11]	C-13-1	0.51	12.8	71	0.3	0.21	2988	3	8	8	13	16	16	12	None	None	0.00	4.67	0.00	Cone
[11]	D-13-1	0.51	12.8	71	0.3	0.21	3672	3	8	8	13	16	16	12	None	None	0.00	4.12	0.00	Cone
[11]	E-13-1	0.51	12.8	71	0.3	0.21	4487	3	8	8	13	16	16	12	None	None	0.00	5.20	0.00	Cone
[11]	C-16-1	0.61	15.2	72	0.5	0.29	2988	3	8	8	13	16	16	12	None	None	0.00	5.78	0.00	Cone
[11]	D-16-1	0.61	15.2	72	0.5	0.29	3672	3	8	8	13	16	16	12	None	None	0.00	5.69	0.00	Cone

[11]	E-16-1	0.61	15.2	72	0.5	0.29	4487	3	8	8	13	16	16	12	None	None	0.00	6.72	0.00	Cone
[11]	C-19-1	0.75	18.7	68	0.7	0.44	2988	4	8	8	12	16	16	12	None	None	0.00	8.46	0.00	Cone
[11]	D-19-1	0.75	18.7	68	0.7	0.44	3672	4	8	8	12	16	16	12	None	None	0.00	7.71	0.00	Cone
[11]	E-19-1	0.75	18.7	68	0.7	0.44	4487	4	8	8	12	16	16	12	None	None	0.00	8.38	0.00	Cone
[11]	C-25-1	0.96	24.0	67	1.5	0.73	2988	5	8	8	11	16	16	12	None	None	0.00	11.24	0.00	Cone
[11]	D-25-1	0.96	24.0	67	1.5	0.73	3672	5	8	8	11	16	16	12	None	None	0.00	11.55	0.00	Cone
[11]	E-25-1	0.96	24.0	67	1.5	0.73	4487	5	8	8	11	16	16	12	None	None	0.00	14.11	0.00	Cone
[11]	F-13-2	0.51	13.0	8	0.3	0.20	3001	3	2	3	11	4	14	8	None	None	0.00	2.20	0.00	Cone
[11]	F-16-2	0.61	16.0	10	0.5	0.29	3001	4	2	4	10	5	14	10	None	None	0.00	3.04	0.00	Cone
[11]	F-19-2	0.75	19.0	10	0.7	0.44	3001	5	2	5	11	7	16	10	None	None	0.00	5.25	0.00	Cone
[11]	F-25-2	0.96	25.0	12	1.5	0.72	3001	7	3	7	11	10	18	12	None	None	0.00	10.80	0.00	Cone
[11]	H-19-2	0.75	19.0	65	0.5	0.44	3414	5	4	5	7	9	12	10	None	None	0.00	9.41	0.00	Cone
[11]	H-19-3	0.75	19.0	65	0.5	0.44	3414	5	4	5	7	9	12	10	None	None	0.00	7.50	0.00	Cone
[11]	H-19-4	0.75	19.0	65	0.5	0.44	3414	5	3	5	7	8	12	10	None	None	0.00	7.28	0.00	Cone
[11]	H-19-5	0.75	19.0	65	0.5	0.44	3414	5	3	5	7	8	12	10	None	None	0.00	7.19	0.00	Cone
[11]	H-19-6	0.75	19.0	65	0.5	0.44	3414	5	2	5	7	7	12	10	None	None	0.00	5.47	0.00	Cone
[11]	H-19-7	0.75	19.0	65	0.5	0.44	3414	5	2	5	7	7	12	10	None	None	0.00	5.16	0.00	Cone
[11]	H-19-9	0.75	19.0	65	0.5	0.44	3414	4	3	4	4	7	8	8	None	None	0.00	5.73	0.00	Cone
[11]	H-19-10	0.75	19.0	65	0.5	0.44	3414	4	3	4	4	6	8	8	None	None	0.00	5.84	0.00	Cone
[11]	H-19-11	0.75	19.0	65	0.5	0.44	3414	4	3	4	4	6	8	8	None	None	0.00	5.89	0.00	Cone
[11]	H-19-12	0.75	19.0	65	0.5	0.44	3414	4	2	4	4	6	8	8	None	None	0.00	4.56	0.00	Cone
[11]	H-19-13	0.75	19.0	65	0.5	0.44	3414	4	2	4	4	5	8	8	None	None	0.00	4.52	0.00	Cone
[11]	H-19-14	0.75	19.0	65	0.5	0.44	3414	4	1	4	4	5	8	8	None	None	0.00	3.35	0.00	Cone
[11]	H-19-16	0.75	19.0	65	0.5	0.44	3414	2	2	2	6	5	8	8	None	None	0.00	2.51	0.00	Cone
[11]	H-19-17	0.75	19.0	65	0.5	0.44	3414	2	2	2	6	4	8	8	None	None	0.00	2.09	0.00	Cone
[11]	H-19-18	0.75	19.0	65	0.5	0.44	3414	2	2	2	6	4	8	8	None	None	0.00	1.83	0.00	Cone
[11]	H-19-19	0.75	19.0	65	0.5	0.44	3414	2	1	2	6	4	8	8	None	None	0.00	1.81	0.00	Cone
[11]	H-19-20	0.75	19.0	65	0.5	0.44	3414	2	1	2	6	4	8	8	None	None	0.00	1.72	0.00	Cone
[11]	P-22-1	0.86	17.6	65	0.9	0.59	2290	3	9	9	15	18	18	14	None	Hoop	0.40	5.62	0.00	Cone
[11]	P-22-2	0.86	17.6	65	0.9	0.59	2290	4	9	9	14	18	18	14	None	Hoop	0.40	6.55	0.00	Cone
[11]	P-22-3	0.86	17.6	65	0.9	0.59	2290	4	9	9	14	18	18	14	None	Hoop	0.40	7.01	0.00	Cone
[11]	P-22-4	0.86	17.6	65	0.9	0.59	2290	4	9	9	14	18	18	14	None	Hoop	0.40	7.76	0.00	Cone
[11]	P-22-5	0.86	17.6	65	0.9	0.59	2290	5	9	9	13	18	18	14	None	Hoop	0.40	9.77	0.00	Cone
[11]	Q-22-1	0.86	17.6	65	0.9	0.59	2290	3	9	9	15	18	18	14	None	Hoop	0.40	5.97	0.00	Cone
[11]	Q-22-2	0.86	17.6	65	0.9	0.59	2290	3	9	9	15	18	18	14	None	Hoop	0.40	5.58	0.00	Cone
[11]	Q-22-3	0.86	17.6	65	0.9	0.59	2290	3	9	9	15	18	18	14	None	Hoop	0.40	5.95	0.00	Cone
[11]	Q-22-4	0.86	17.6	65	0.9	0.59	2290	3	9	9	15	18	18	14	None	Hoop	0.40	4.83	0.00	Cone
[11]	Q-22-5	0.86	17.6	65	0.9	0.59	2290	3	9	9	15	18	18	14	None	Hoop	0.40	5.38	0.00	Cone
[11]	Q-22-6	0.86	17.6	65	0.9	0.59	2290	5	9	9	13	18	18	14	None	Hoop	0.40	8.86	0.00	Cone
[11]	Q-22-7	0.86	17.6	65	0.9	0.59	2290	5	9	9	13	18	18	14	None	Hoop	0.40	9.46	0.00	Cone
[11]	Q-22-8	0.86	17.6	65	0.9	0.59	2290	5	9	9	13	18	18	14	None	Hoop	0.40	9.96	0.00	Cone

[11]	Q-22-9	0.86	17.6	65	0.9	0.59	2290	5	9	9	13	18	18	14	None	Hoop	0.40	9.30	0.00	Cone
[11]	Q-22-10	0.86	17.6	65	0.9	0.59	2290	5	9	9	13	18	18	14	None	Hoop	0.40	9.26	0.00	Cone
[12]	S1	0.63	8.0	86	0.8	0.31	2663	2	16	16	10	16	16	18	None	None	0.00	2.41	0.00	Cone
[12]	S2	0.63	8.0	86	0.8	0.31	2663	4	16	16	8	16	16	18	None	None	0.00	8.14	0.00	Cone
[12]	S3	0.63	8.0	86	0.8	0.31	2663	6	16	16	6	16	16	18	None	None	0.00	19.29	0.00	Steel
[12]	S4	0.63	8.0	86	0.8	0.31	2663	8	16	16	4	16	16	18	None	None	0.00	17.63	0.00	Steel
[12]	S5	0.63	8.0	86	0.8	0.31	2663	2	16	16	10	16	16	18	None	None	0.00	1.51	0.00	Cone
[12]	S6	0.63	8.0	86	0.8	0.31	2663	4	16	16	8	16	16	18	None	None	0.00	8.92	0.00	Cone
[12]	S7	0.63	8.0	86	0.8	0.31	2663	6	16	16	6	16	16	18	None	None	0.00	12.77	0.00	Cone
[12]	S8	0.63	8.0	86	0.8	0.31	2663	8	16	16	4	16	16	18	None	None	0.00	16.41	0.00	Steel
[12]	S9	0.63	8.0	86	0.8	0.31	3726	6	16	16	6	16	16	40	None	None	0.00	13.44	0.00	Cone
[12]	S10	0.63	8.0	86	0.8	0.31	3726	6	16	16	6	16	16	40	None	None	0.00	9.91	0.00	Cone
[12]	S11	0.63	8.0	86	0.8	0.31	3044	2	16	16	10	16	16	40	None	None	0.00	2.36	0.00	Cone
[12]	S12	0.63	8.0	86	0.8	0.31	3044	2	16	16	10	16	16	40	None	None	0.00	2.09	0.00	Cone
[12]	S13	0.63	8.0	86	0.8	0.31	3044	4	16	16	8	16	16	40	None	None	0.00	8.59	0.00	Cone
[12]	S14	0.63	8.0	86	0.8	0.31	3044	8	16	16	4	16	16	40	None	None	0.00	20.70	0.00	Steel
[12]	S15	0.63	8.0	86	0.8	0.31	3142	2	16	16	10	16	16	40	None	None	0.00	2.43	0.00	Cone
[12]	S16	0.63	8.0	86	0.8	0.31	3142	4	16	16	8	16	16	40	None	None	0.00	7.71	0.00	Cone
[12]	S17	0.63	8.0	86	0.8	0.31	3142	8	16	16	4	16	16	40	None	None	0.00	16.30	0.00	Cone
[12]	S18	0.63	8.0	86	0.8	0.31	3142	2	16	16	10	16	16	40	None	None	0.00	3.08	0.00	Cone
[12]	S19	0.63	8.0	86	0.8	0.31	3142	4	16	16	8	16	16	40	None	None	0.00	8.59	0.00	Cone
[12]	S20	0.63	8.0	86	0.8	0.31	3142	6	16	16	6	16	16	40	None	None	0.00	15.42	0.00	Steel
[13]	1SCR5701	0.75	4.0	120	0.7	0.44	4210	4	13	24	50	74	54	14	None	None	0.00	8.61	0.00	Cone
[13]	1SCR5702	0.75	4.0	120	0.7	0.44	4210	4	13	24	50	74	54	14	None	None	0.00	7.95	0.00	Cone
[13]	1SCR5703	0.75	4.0	120	0.7	0.44	4210	4	13	24	50	74	54	14	None	None	0.00	7.10	0.00	Cone
[13]	1SCR5704	0.75	4.0	120	0.7	0.44	4210	4	13	24	50	74	54	14	None	None	0.00	9.18	0.00	Cone
[13]	1SCR5705	0.75	4.0	120	0.7	0.44	4210	4	13	24	50	74	54	14	None	None	0.00	8.61	0.00	Cone
[13]	2SCR5701	0.75	4.0	120	0.7	0.44	4225	4	13	24	50	74	54	14	None	None	0.00	12.32	0.00	Cone
[13]	2SCR5702	0.75	4.0	120	0.7	0.44	4225	4	13	24	50	74	54	14	None	None	0.00	10.33	0.00	Cone
[13]	2SCR5703	0.75	4.0	120	0.7	0.44	4225	4	13	24	50	74	54	14	None	None	0.00	7.96	0.00	Cone
[13]	2SCR5704	0.75	4.0	120	0.7	0.44	4225	4	13	24	50	74	54	14	None	None	0.00	11.09	0.00	Cone
[13]	2SCR5705	0.75	4.0	120	0.7	0.44	4225	4	13	24	50	74	54	14	None	None	0.00	11.47	0.00	Cone
[13]	3SCR5701	0.75	4.0	120	0.7	0.44	4635	4	13	24	50	74	54	14	Parallel	None	0.00	7.45	0.00	Cone
[13]	3SCR5702	0.75	4.0	120	0.7	0.44	4635	4	13	24	50	74	54	14	Parallel	None	0.00	6.06	0.00	Cone
[13]	3SCR5703	0.75	4.0	120	0.7	0.44	4635	4	13	24	50	74	54	14	Parallel	None	0.00	7.15	0.00	Cone
[13]	3SCR5704	0.75	4.0	120	0.7	0.44	4635	4	13	24	50	74	54	14	Parallel	None	0.00	8.24	0.00	Cone
[13]	3SCR5705	0.75	4.0	120	0.7	0.44	4635	4	13	24	50	74	54	14	Parallel	None	0.00	6.95	0.00	Cone
[13]	4DCR5701	0.75	4.0	120	0.7	0.44	4225	4	13	24	50	74	54	14	None	None	0.00	9.29	0.00	Cone
[13]	4DCR5702	0.75	4.0	120	0.7	0.44	4225	4	13	24	50	74	54	14	None	None	0.00	10.43	0.00	Cone
[13]	4DCR5703	0.75	4.0	120	0.7	0.44	4225	4	13	24	50	74	54	14	None	None	0.00	6.92	0.00	Cone
[13]	4DCR5704	0.75	4.0	120	0.7	0.44	4225	4	13	24	50	74	54	14	None	None	0.00	10.14	0.00	Cone

[13]	4DCR5705	0.75	4.0	120	0.7	0.44	4225	4	13	24	50	74	54	14	None	None	0.00	12.32	0.00	Cone
[14]	M-1	0.75	4.6	70	0.7	0.44	4714	8	7	7	8	74	54	6	None	None	0.00	24.30	0.00	Steel
[14]	M-2	0.75	4.6	70	0.7	0.44	4714	8	7	7	8	74	54	6	None	None	0.00	24.46	0.00	Steel
[15]	A-P	0.51	3.6	81	0.6	0.20	6309	7	7	7	7	14	14	6	None	None	0.00	13.44	0.00	Steel
[15]	B-P	0.51	3.6	81	0.6	0.20	5816	7	7	7	7	14	14	6	None	None	0.00	12.72	0.00	Steel
[16]	Tes-2	0.49	2.0	60	0.6	0.19	4000	9	9	9	9	20	18	4	None	None	0.00	10.66	0.00	Steel
[16]	Tes-7	0.49	2.0	60	0.6	0.19	4000	9	9	9	9	20	18	4	None	None	0.00	11.42	0.00	Steel
[16]	Tes-8	0.49	2.0	60	0.6	0.19	4000	9	9	9	9	20	18	4	None	None	0.00	10.34	0.00	Steel
[16]	Tes-10	0.49	2.0	60	0.6	0.19	4000	9	9	9	9	20	18	4	None	None	0.00	11.78	0.00	Steel
[17]	SS-10-0	0.47	4.7	68	0.5	0.18	4153	8	5	5	8	9	16	28	None	Stirrup	0.40	8.60	0.00	Steel
[17]	SS-15-0	0.47	7.1	68	0.5	0.18	4153	8	5	5	8	9	16	28	None	Stirrup	0.40	9.13	0.00	Steel
[17]	SS-20-0	0.47	9.4	68	0.5	0.18	4153	8	5	5	8	9	16	28	None	Stirrup	0.40	8.58	0.00	Steel
[17]	SS'-20-0	0.47	9.4	68	0.5	0.18	4153	8	5	5	8	9	16	28	None	Stirrup	0.40	9.11	0.00	Steel
[17]	TS-10-0	0.47	4.7	68	0.5	0.13	4153	8	5	5	8	9	16	28	None	Stirrup	0.40	6.22	0.00	Steel
[17]	TS-15-0	0.47	7.1	68	0.5	0.13	4153	8	5	5	8	9	16	28	None	Stirrup	0.40	6.72	0.00	Steel
[17]	TS-20-0	0.47	9.4	68	0.5	0.13	4153	8	5	5	8	9	16	28	None	Stirrup	0.40	6.22	0.00	Steel
[17]	TT-10-0	0.47	4.7	68	0.5	0.13	4153	8	5	5	8	9	16	28	None	Stirrup	0.40	6.19	0.00	Steel
[17]	TT-15-0	0.47	7.1	68	0.5	0.13	4153	8	5	5	8	9	16	28	None	Stirrup	0.40	6.02	0.00	Steel
[17]	TT-20-0	0.47	9.4	68	0.5	0.13	4153	8	5	5	8	9	16	28	None	Stirrup	0.40	5.56	0.00	Steel
[18]	B-0-0-S-M	0.47	9.4	70	0.5	0.18	4551	8	5	5	8	9	16	28	None	Stirrup	0.24	8.51	0.00	Steel
[18]	B-10-0-S-M	0.47	9.4	70	0.5	0.18	4551	8	5	5	8	9	16	28	None	Stirrup	0.24	7.94	0.39	Steel
[18]	B-20-0-S-M	0.47	9.4	70	0.5	0.18	4551	8	5	5	8	9	16	28	None	Stirrup	0.24	7.72	0.79	Steel
[18]	B-40-0-S-M	0.47	9.4	70	0.5	0.18	4551	8	5	5	8	9	16	28	None	Stirrup	0.24	7.50	1.57	Steel
[18]	C-0-4-S-M	0.47	9.4	70	0.5	0.18	4551	2	5	5	14	9	16	28	None	None	0.00	1.76	0.00	Cone
[18]	R-0-4-S-M	0.47	9.4	70	0.5	0.18	4551	2	5	5	14	9	16	28	None	None	0.00	1.59	0.00	Cone
[18]	C-0-6-S-M	0.47	9.4	70	0.5	0.18	4551	3	5	5	13	9	16	28	None	None	0.00	4.08	0.00	Cone
[18]	R-0-6-S-M	0.47	9.4	70	0.5	0.18	4551	3	5	5	13	9	16	28	None	None	0.00	3.51	0.00	Cone
[18]	C-0-8-S-M	0.47	9.4	70	0.5	0.18	4551	4	5	5	12	9	16	28	None	None	0.24	4.19	0.00	Cone
[18]	R-0-8-S-M	0.47	9.4	70	0.5	0.18	4551	4	5	5	12	9	16	28	None	Stirrup	0.24	5.93	0.00	Cone
[18]	C-0-0-S-M	0.47	9.4	70	0.5	0.18	4551	8	5	5	8	9	16	28	None	Stirrup	0.24	8.42	0.00	Steel
[18]	M-S2-00	0.63	13.4	73	0.7	0.31	5700	8	5	5	8	9	16	28	None	Stirrup	0.24	15.08	0.00	Steel
[18]	M-S2-00F	0.63	13.4	73	0.7	0.31	5700	8	5	5	8	9	16	28	None	Stirrup	0.24	15.24	0.00	Steel
[18]	M-S2-00G	0.63	13.4	73	0.7	0.31	5700	8	5	5	8	9	16	28	None	Stirrup	0.24	13.11	1.50	Steel
[18]	M-T4-00	0.63	13.4	73	0.7	0.24	5700	8	5	5	8	9	16	28	None	Stirrup	0.24	11.24	0.00	Steel
[18]	M-T4-00F	0.63	13.4	73	0.7	0.24	5700	8	5	5	8	9	16	28	None	Stirrup	0.24	11.62	0.00	Steel
[18]	M-T4-00G	0.63	13.4	73	0.7	0.24	5700	8	5	5	8	9	16	28	None	Stirrup	0.24	10.45	1.50	Steel
[19]	PM-01	0.63	3.6	84	0.9	0.31	5961	8	10	10	10	50	50	5	None	None	0.00	16.03	0.00	Steel
[19]	PM-02	0.63	3.6	84	0.9	0.31	5961	8	10	10	10	50	50	5	None	None	0.00	15.89	0.00	Steel
[19]	NPM-01	0.63	3.6	77	0.9	0.31	4728	8	10	10	10	50	50	5	None	None	0.00	15.58	0.00	Steel
[19]	NPM-02	0.63	3.6	77	0.9	0.31	4728	8	10	10	10	50	50	5	None	None	0.00	15.43	0.00	Steel
[20]	V1301A	0.49	2.6	82	0.3	0.19	6700	2	20	10	55	60	60	16	None	None	0.00	5.20	0.00	Cone

[20]	V1301B	0.49	2.6	82	0.3	0.19	6680	3	20	20	55	60	60	16	None	None	0.00	4.50	0.00	Cone
[20]	V1302A	0.49	2.6	82	0.3	0.19	6680	4	20	20	55	60	60	16	None	None	0.00	11.60	0.00	Cone
[20]	V1302B	0.49	2.6	82	0.3	0.19	6680	4	20	20	55	60	60	16	None	None	0.00	11.50	0.00	Cone
[20]	V1303A	0.49	2.6	82	0.3	0.19	5690	6	20	20	55	60	60	16	None	None	0.00	17.00	0.00	Steel
[20]	V1303B	0.49	2.6	82	0.3	0.19	5690	6	20	20	55	60	60	16	None	None	0.00	17.50	0.00	Steel
[20]	V1321A	0.50	4.9	79	0.3	0.19	6700	2	20	20	55	60	60	16	None	None	0.00	3.90	0.00	Cone
[20]	V1321B	0.50	4.9	79	0.3	0.19	6680	2	20	20	55	60	60	16	None	None	0.00	5.00	0.00	Cone
[20]	V1322A	0.50	4.9	79	0.3	0.19	6680	4	20	20	55	60	60	16	None	None	0.00	11.90	0.00	Cone
[20]	V1322B	0.50	4.9	79	0.3	0.19	6580	4	20	20	55	60	60	16	None	None	0.00	10.60	0.00	Cone
[20]	V1323B	0.50	4.9	79	0.3	0.19	5700	5	20	20	55	60	60	16	None	None	0.00	16.30	0.00	Steel
[20]	V1323C	0.50	4.9	79	0.3	0.19	5290	6	20	20	55	60	60	16	None	None	0.00	16.70	0.00	Steel
[20]	V1311A	0.62	3.7	78	0.5	0.31	6430	3	20	20	55	60	60	16	None	None	0.00	7.70	0.00	Cone
[20]	V1311B	0.62	3.7	78	0.5	0.31	5160	3	20	20	55	60	60	16	None	None	0.00	6.20	0.00	Cone
[20]	V1312B	0.62	3.7	78	0.5	0.31	6450	5	20	20	55	60	60	16	None	None	0.00	16.20	0.00	Cone
[20]	V1313A	0.62	3.7	78	0.5	0.31	5690	8	20	20	55	60	60	16	None	None	0.00	25.30	0.00	Steel
[20]	V1313B	0.62	3.7	78	0.5	0.31	5690	8	20	20	55	60	60	16	None	None	0.00	26.80	0.00	Cone
[20]	V1314A	0.62	3.7	78	0.5	0.31	5770	8	20	20	55	60	60	16	None	None	0.00	24.90	0.00	Steel
[20]	V1314B	0.62	3.7	78	0.5	0.31	5770	8	20	20	55	60	60	16	None	None	0.00	25.10	0.00	Cone
[20]	V1C01A	0.62	3.7	78	0.5	0.31	6580	3	3	20	55	60	60	16	None	None	0.00	4.40	0.00	Cone
[20]	V1C01B	0.62	3.7	78	0.5	0.31	6720	3	3	20	55	60	60	16	None	None	0.00	4.80	0.00	Cone
[20]	V1C02A	0.62	3.7	78	0.5	0.31	6700	2	4	20	55	60	60	16	None	None	0.00	4.40	0.00	Cone
[20]	V1C02B	0.62	3.7	78	0.5	0.31	6720	3	4	20	55	60	60	16	None	None	0.00	4.80	0.00	Cone
[20]	V1C03A	0.62	3.7	78	0.5	0.31	6470	3	5	20	55	60	60	16	None	None	0.00	5.50	0.00	Cone
[20]	V1C03B	0.62	3.7	78	0.5	0.31	6490	3	6	20	55	60	60	16	None	None	0.00	6.40	0.00	Cone
[20]	V1C11A	0.62	3.7	78	0.5	0.31	6550	4	4	20	55	60	60	16	None	None	0.00	9.00	0.00	Cone
[20]	V1C11B	0.62	3.7	78	0.5	0.31	6550	4	4	20	55	60	60	16	None	None	0.00	9.30	0.00	Cone
[20]	V1C21A	0.62	3.7	78	0.5	0.31	5690	5	3	20	55	60	60	16	None	None	0.00	8.90	0.00	Cone
[20]	V1C21B	0.62	3.7	78	0.5	0.31	5690	5	3	20	55	60	60	16	None	None	0.00	8.90	0.00	Cone
[20]	V1C22A	0.62	3.7	78	0.5	0.31	5700	5	4	20	55	60	60	16	None	None	0.00	7.20	0.00	Cone
[20]	V1C22B	0.62	3.7	78	0.5	0.31	5700	5	4	20	55	60	60	16	None	None	0.00	6.50	0.00	Cone
[20]	V1C23A	0.62	3.7	78	0.5	0.31	5770	5	5	20	55	60	60	16	None	None	0.00	12.20	0.00	Cone
[20]	V1C23B	0.62	3.7	78	0.5	0.31	5770	5	5	20	55	60	60	16	None	None	0.00	11.50	0.00	Cone
[20]	V1C31A	0.62	3.7	78	0.5	0.31	5830	6	3	20	55	60	60	16	None	None	0.00	12.30	0.00	Cone
[20]	V1C31B	0.62	3.7	78	0.5	0.31	5830	6	3	20	55	60	60	16	None	None	0.00	9.40	0.00	Cone
[20]	V1C31C	0.62	3.7	78	0.5	0.31	5290	6	3	20	55	60	60	16	None	None	0.00	10.40	0.00	Cone
[20]	V1C32A	0.62	3.7	78	0.5	0.31	5160	6	6	20	55	60	60	16	None	None	0.00	11.40	0.00	Cone
[20]	V1C32B	0.62	3.7	78	0.5	0.31	5160	7	7	20	55	60	60	16	None	None	0.00	13.50	0.00	Cone
[20]	V1C41A	0.62	3.7	78	0.5	0.31	5160	9	2	20	55	60	60	16	None	None	0.00	10.30	0.00	Cone
[20]	V1C42A	0.62	3.7	78	0.5	0.31	5160	7	5	20	55	60	60	16	None	None	0.00	15.00	0.00	Cone
[20]	V1C42B	0.62	3.7	78	0.5	0.31	5160	8	5	20	55	60	60	16	None	None	0.00	14.30	0.00	Cone
[20]	V1C43A	0.62	3.7	78	0.5	0.31	5160	8	8	20	55	60	60	16	None	None	0.00	16.60	0.00	Cone

[20]	V1C43B	0.62	3.7	78	0.5	0.31	5160	8	8	20	55	60	60	16	None	None	0.00	17.80	0.00	Cone
[20]	V1312A	0.62	3.7	78	0.5	0.31	6490	5	8	20	55	60	60	16	None	None	0.00	13.10	0.00	Cone
[21]	3-1a	0.75	4.0	120	0.7	0.44	4700	4	20	24	26	88	30	14	None	None	0.00	8.80	0.00	Cone
[21]	3-1b	0.75	4.0	120	0.7	0.44	4700	4	20	24	26	88	30	14	None	Hairpin	0.88	22.90	0.00	Cone
[21]	3-1c	0.75	4.0	120	0.7	0.44	4700	4	20	24	26	88	30	14	None	Hairpin	0.88	17.30	0.00	Cone
[21]	3-3a	0.75	4.0	120	0.7	0.44	4700	4	20	24	26	88	30	14	None	None	0.00	7.20	0.00	Cone
[21]	3-3b	0.75	4.0	120	0.7	0.44	4700	4	20	24	26	88	30	14	None	Hairpin	0.88	22.10	0.00	Cone
[21]	3-3c	0.75	4.0	120	0.7	0.44	4700	4	20	24	26	88	30	14	None	Hairpin	0.88	16.10	0.00	Cone
[22]	M12-1	0.42	8.4	79	1.0	0.14	2959	2	8	8	14	16	16	18	None	None	0.00	1.85	0.00	Cone
[22]	M12-6	0.42	8.4	79	1.0	0.14	2959	2	8	8	14	16	16	18	None	None	0.00	2.29	0.00	Cone
[22]	M12-11	0.42	8.4	79	1.0	0.14	2959	2	8	8	13	16	16	18	None	None	0.00	2.78	0.00	Cone
[22]	M12-18	0.42	8.4	79	1.0	0.14	2959	8	8	8	8	16	16	18	None	None	0.00	8.31	0.00	Steel
[22]	W1/2-23	0.51	10.2	69	1.3	0.21	4047	3	8	8	13	16	16	18	None	None	0.00	5.93	0.00	Cone
[22]	W1/2-24	0.51	10.2	69	1.3	0.21	4047	4	8	8	12	16	16	18	None	None	0.00	6.04	0.00	Cone
[22]	W1/2-25	0.51	10.2	69	1.3	0.21	4047	4	8	8	12	16	16	18	None	None	0.00	7.25	0.00	Cone
[22]	W1/2-26	0.51	10.2	69	1.3	0.21	4047	4	8	8	11	16	16	18	None	None	0.00	9.68	0.00	Steel
[22]	W1/2-27	0.51	10.2	69	1.3	0.21	4047	5	8	8	11	16	16	18	None	None	0.00	9.46	0.00	Steel
[22]	M16-34	0.61	12.3	66	1.7	0.30	4308	2	8	8	14	16	16	18	None	None	0.00	2.91	0.00	Cone
[22]	M16-39	0.61	12.3	66	1.7	0.30	4308	2	8	8	13	16	16	18	None	None	0.00	3.59	0.00	Cone
[22]	M16-43	0.61	12.3	66	1.7	0.30	4308	3	8	8	13	16	16	18	None	None	0.00	4.34	0.00	Cone
[22]	M16-47	0.61	12.3	66	1.7	0.30	4308	8	8	8	8	16	16	18	None	None	0.00	16.29	0.00	Steel
[22]	M20-52	0.78	15.5	66	2.6	0.47	3829	3	8	8	13	16	16	18	None	None	0.00	4.43	0.00	Cone
[22]	M20-56	0.78	15.5	66	2.6	0.47	3829	3	8	8	13	16	16	18	None	None	0.00	5.36	0.00	Cone
[22]	M20-60	0.78	15.5	66	2.6	0.47	3829	4	8	8	12	16	16	18	None	None	0.00	6.00	0.00	Cone
[23]	S1M	0.51	3.7	60	0.6	0.20	3570	10	10	10	10	20	20		None	None	0.00	9.63	0.00	Steel
[23]	S3M	0.51	3.7	60	0.6	0.20	5000	10	10	10	10	20	20		None	None	0.00	13.38	0.00	Steel
[23]	S9M	0.51	3.7	60	0.6	0.20	2675	10	10	10	10	20	20		None	None	0.00	14.50	0.00	Steel
[24]	No.1-1	0.75	4.6	60	0.8	0.44	4660	7	5	5	21	10	28	24	None	None	0.00	22.48	0.00	Steel
[24]	No.2-5	0.75	4.6	60	0.8	0.44	4660	7	5	5	21	10	28	24	None	None	0.00	28.25	0.00	Steel
[25]	V1401A	0.49	2.6	82	0.3	0.19	6700	46	12	108	2	120	48	16	None	None	0.00	15.80	0.00	Steel
[25]	V1401B	0.49	2.6	82	0.3	0.19	6580	46	20	100	2	120	48	16	None	None	0.00	16.20	0.00	Steel
[25]	V1402A	0.49	2.6	82	0.3	0.19	6680	45	29	91	3	120	48	16	None	None	0.00	16.50	0.00	Steel
[25]	V1402B	0.49	2.6	82	0.3	0.19	6680	45	41	79	3	120	48	16	None	None	0.00	15.80	0.00	Steel
[25]	V1403A	0.49	2.6	82	0.3	0.19	6680	44	55	65	4	120	48	16	None	None	0.00	17.60	0.00	Steel
[25]	V1403B	0.49	2.6	82	0.3	0.19	6680	44	49	71	4	120	48	16	None	None	0.00	14.50	0.00	Steel
[25]	V1404A	0.49	2.6	82	0.3	0.19	5690	43	19	101	5	120	48	16	None	None	0.00	17.10	0.00	Steel
[25]	V1404B	0.49	2.6	82	0.3	0.19	5690	43	34	86	5	120	48	16	None	None	0.00	17.50	0.00	Steel
[25]	V1405A	0.49	2.6	82	0.3	0.19	5700	42	50	70	6	120	48	16	None	None	0.00	17.40	0.00	Steel
[25]	V1405B	0.49	2.6	82	0.3	0.19	5700	42	55	65	6	120	48	16	None	None	0.00	18.10	0.00	Steel
[25]	V1411A	0.62	3.7	78	0.5	0.31	6580	46	20	100	3	120	48	16	None	None	0.00	22.80	0.00	Steel
[25]	V1411B	0.62	3.7	78	0.5	0.31	6700	46	12	108	3	120	48	16	None	None	0.00	21.80	0.00	Steel

[25]	V1411C	0.62	3.7	78	0.5	0.31	6430	46	24	24	3	120	48	16	None	None	0.00	24.20	0.00	Steel
[25]	V1412A	0.62	3.7	78	0.5	0.31	6470	43	32	36	5	120	48	16	None	None	0.00	26.80	0.00	Steel
[25]	V1412B	0.62	3.7	78	0.5	0.31	6470	43	17	36	5	120	48	16	None	None	0.00	25.50	0.00	Steel
[25]	V1413A	0.62	3.7	78	0.5	0.31	5700	41	40	80	8	120	48	16	None	None	0.00	23.90	0.00	Steel
[25]	V1413B	0.62	3.7	78	0.5	0.31	5700	41	25	92	8	120	48	16	None	None	0.00	24.10	0.00	Steel
[26]	C-1-nf 291	0.56	7.0	60	0.5	0.25	2710	2	10	10	10	20	12	24	None	None	0.00	8.33	2.00	Conc
[26]	C-1-nf 292	0.56	7.0	60	0.5	0.25	2710	2	10	10	10	20	12	24	None	None	0.00	7.84	2.00	Conc
[26]	D-1-nf 300	0.56	7.0	60	0.5	0.25	2710	2	10	10	10	20	12	24	None	None	0.00	8.42	2.00	Conc
[26]	D-1-nf 301	0.56	7.0	60	0.5	0.25	2710	2	10	10	10	20	12	24	None	None	0.00	8.01	2.00	Conc
[27]	S1-A	2.50	25.0	155	23.4	4.44	5959	20	41	41	60	84	75	45	None	None	0.00	#####	0.00	Cone
[27]	S1-B	2.50	25.0	155	23.4	4.44	6018	20	41	41	60	84	75	45	None	None	0.00	99.92	0.00	Cone
[27]	S1-C	2.50	25.0	155	23.4	4.44	6141	20	41	41	60	84	75	45	None	None	0.00	#####	0.00	Cone
[27]	S1-D	2.50	25.0	155	23.4	4.44	6154	20	41	41	60	84	75	45	None	None	0.00	#####	0.00	Cone
[27]	S1-E	2.50	25.0	155	23.4	4.44	6192	20	41	41	60	84	75	45	None	None	0.00	#####	0.00	Cone
[27]	S2-A	3.00	25.0	155	31.4	6.51	6230	20	41	41	60	84	75	45	None	None	0.00	#####	0.00	Cone
[27]	S2-B	3.00	25.0	155	31.4	6.51	6272	20	41	41	60	84	75	45	None	None	0.00	#####	0.00	Cone
[27]	S2-C	3.00	25.0	155	31.4	6.51	6287	20	41	41	60	84	75	45	None	None	0.00	#####	0.00	Cone
[27]	S2-D	3.00	25.0	155	31.4	6.51	6358	20	41	41	60	84	75	45	None	None	0.00	#####	0.00	Cone
[27]	S2-E	3.00	25.0	155	31.4	6.51	6358	20	41	41	60	84	75	45	None	None	0.00	#####	0.00	Cone
[27]	S3-A	3.50	25.0	155	54.0	8.96	6272	20	41	41	60	84	75	45	None	None	0.00	#####	0.00	Cone
[27]	S3-B	3.50	25.0	155	54.0	8.96	6258	20	41	41	60	84	75	45	None	None	0.00	#####	0.00	Cone
[27]	S3-C	3.50	25.0	155	54.0	8.96	6230	20	41	41	60	84	75	45	None	None	0.00	#####	0.00	Cone
[27]	S3-D	3.50	25.0	155	54.0	8.96	6216	20	41	41	60	84	75	45	None	None	0.00	#####	0.00	Cone
[27]	S3-E	3.50	25.0	155	54.0	8.96	6201	20	41	41	60	84	75	45	None	None	0.00	#####	0.00	Cone
[27]	S4-A	3.00	30.0	155	31.4	6.51	6130	20	41	41	60	84	75	45	None	None	0.00	#####	0.00	Cone
[27]	S4-B	3.00	30.0	155	31.4	6.51	6130	20	41	41	60	84	75	45	None	None	0.00	#####	0.00	Cone
[27]	S4-C	3.00	30.0	155	31.4	6.51	6173	20	41	41	60	84	75	45	None	None	0.00	#####	0.00	Cone
[27]	S4-D	3.00	30.0	155	31.4	6.51	6187	20	41	41	60	84	75	45	None	None	0.00	#####	0.00	Cone
[27]	S4-E	3.00	30.0	155	31.4	6.51	6201	20	41	41	60	84	75	45	None	None	0.00	#####	0.00	Cone
[27]	S6-A	2.50	25.0	155	23.4	4.44	5625	15	32	32	60	84	75	45	None	None	0.00	58.06	0.00	Cone
[27]	S6-B	2.50	25.0	155	23.4	4.44	5645	15	32	32	60	84	75	45	None	None	0.00	62.80	0.00	Cone
[27]	S6-C	2.50	25.0	155	23.4	4.44	5645	15	32	32	60	84	75	45	None	None	0.00	58.06	0.00	Cone
[27]	S6-D	2.50	25.0	155	23.4	4.44	5665	15	32	32	60	84	75	45	None	None	0.00	63.23	0.00	Cone
[27]	S7-A	2.50	25.0	155	23.4	4.44	5120	30	76	76	60	84	75	45	None	None	0.00	#####	0.00	Cone
[27]	S7-B	2.50	25.0	155	23.4	4.44	5234	30	76	76	60	84	75	45	None	None	0.00	#####	0.00	Cone
[27]	S7-C	2.50	25.0	155	23.4	4.44	5248	30	76	76	60	84	75	45	None	None	0.00	#####	0.00	Cone
[27]	S8-A	2.50	25.0	155	23.4	4.44	5652	15	32	32	60	84	75	45	None	Surface	4.74	#####	0.00	Not
[27]	S8-B	2.50	25.0	155	23.4	4.44	5652	15	32	32	60	84	75	45	None	Surface	4.74	#####	0.00	Not
[27]	S8-C	2.50	25.0	155	23.4	4.44	5652	15	32	32	60	84	75	45	None	Surface	4.74	#####	0.00	Not
[27]	S8-D	2.50	25.0	155	23.4	4.44	5652	15	32	32	60	84	75	45	None	Surface	4.74	#####	0.00	Not
[27]	S9-1	2.50	25.0	155	23.4	4.44	5652	15	32	32	60	84	75	45	None	Hairpin	4.04	#####	0.00	Not

[27]	S9-2	2.50	25.0	155	23.4	4.44	5652	15	32	32	60	84	75	45	None	Hairpin	4.74	#####	0.00	Not
[27]	S9-A	2.50	25.0	155	23.4	4.44	5652	15	32	32	60	84	75	45	None	Hairpin	4.74	#####	0.00	Not
[27]	S9-B	2.50	25.0	155	23.4	4.44	5652	15	32	32	60	84	75	45	None	Hairpin	4.74	#####	0.00	Not
[27]	S9-C	2.50	25.0	155	23.4	4.44	5652	15	32	32	60	84	75	45	None	Hairpin	4.74	#####	0.00	Not
[27]	S9-D	2.50	25.0	155	23.4	4.44	5652	15	32	32	60	84	75	45	None	Hairpin	4.74	83.74	0.00	Not
[27]	S10-A	2.50	25.0	155	23.4	4.44	5652	15	32	32	60	84	75	45	None	Hairpin	3.53	105.1	0.00	Not
[27]	S10-B	2.50	25.0	155	23.4	4.44	5652	15	32	32	60	84	75	45	None	Hairpin	3.53	131.7	0.00	Not
[27]	S10-C	2.50	25.0	155	23.4	4.44	5652	15	32	32	60	84	75	45	None	Hairpin	3.53	87.71	0.00	Not
[27]	S10-D	2.50	25.0	155	23.4	4.44	5652	15	32	32	60	84	75	45	None	Hairpin	3.53	100.3	0.00	Not
[28]	Q2	0.87	5.1	NA	NA	0.59	3442	3	NA	NA	NA	NA	NA	NA	None	Surface	0.35	7.64	0.00	Cone
[28]	Q9	0.87	5.1	NA	NA	0.59	3442	3	NA	NA	NA	NA	NA	NA	None	Surface	0.35	6.99	0.00	Cone
[28]	Q3	0.87	5.1	NA	NA	0.59	3442	6	NA	NA	NA	NA	NA	NA	None	Surface	0.35	21.54	0.00	Cone
[28]	Q6	0.87	5.1	NA	NA	0.59	3442	10	NA	NA	NA	NA	NA	NA	None	Surface	0.70	37.27	0.00	Cone
[28]	8.1/10	0.87	7.3	NA	NA	0.59	3687	3	NA	NA	NA	NA	NA	NA	None	Surface	0.35	6.81	0.00	Cone
[28]	8.1/11	0.87	7.3	NA	NA	0.59	3687	3	NA	NA	NA	NA	NA	NA	None	Surface	0.35	6.29	0.00	Cone
[28]	8.1/12	0.87	7.3	NA	NA	0.59	3687	3	NA	NA	NA	NA	NA	NA	None	Surface	0.35	8.12	0.00	Cone
[28]	8.1/13	0.87	7.3	NA	NA	0.59	3687	3	NA	NA	NA	NA	NA	NA	None	Surface	0.35	7.04	0.00	Cone
[28]	8.2/6	0.87	7.3	NA	NA	0.59	3687	3	NA	NA	NA	NA	NA	NA	None	Surface	0.35	6.86	0.00	Cone
[28]	8.3/5	0.87	7.3	NA	NA	0.59	2827	3	NA	NA	NA	NA	NA	NA	None	Surface	0.35	5.10	0.00	Cone
[28]	8.3/10	0.87	7.3	NA	NA	0.59	2827	3	NA	NA	NA	NA	NA	NA	None	Surface	0.35	7.33	0.00	Cone
[28]	8.4/4	0.87	7.3	NA	NA	0.59	2827	3	NA	NA	NA	NA	NA	NA	None	Surface	0.35	6.14	0.00	Cone
[28]	8.4/12	0.87	7.3	NA	NA	0.59	2827	3	NA	NA	NA	NA	NA	NA	None	Surface	0.35	4.92	0.00	Cone
[28]	8.4/3	0.87	7.3	NA	NA	0.59	2827	3	NA	NA	NA	NA	NA	NA	None	Surface	0.35	7.42	0.00	Cone
[28]	8.1/6	0.87	7.3	NA	NA	0.59	3687	6	NA	NA	NA	NA	NA	NA	None	Surface	0.35	19.99	0.00	Cone
[28]	8.1/5	0.87	7.3	NA	NA	0.59	3687	10	NA	NA	NA	NA	NA	NA	None	Surface	0.70	33.43	0.00	Cone
[28]	8.4/6	0.87	7.3	NA	NA	0.59	3687	10	NA	NA	NA	NA	NA	NA	None	Surface	0.70	33.07	0.00	Cone
[28]	1_1_a	0.79	7.9	NA	NA	0.49	3196	2	NA	NA	NA	NA	NA	NA	None	Surface	0.35	15.85	0.00	Spalling
[28]	1_1_b	0.79	7.9	NA	NA	0.49	3196	2	NA	NA	NA	NA	NA	NA	None	Surface	0.35	16.21	0.00	Spalling
[28]	1_2_a	0.79	7.9	NA	NA	0.49	3196	4	NA	NA	NA	NA	NA	NA	None	Surface	0.35	24.98	0.00	Spalling
[28]	1_2_b	0.79	7.9	NA	NA	0.49	3196	4	NA	NA	NA	NA	NA	NA	None	Surface	0.35	22.97	0.00	Spalling
[28]	1_3_a	0.79	7.9	NA	NA	0.49	3196	8	NA	NA	NA	NA	NA	NA	None	Surface	0.35	35.12	0.00	Steel
[28]	1_3_b	0.79	7.9	NA	NA	0.49	3196	8	NA	NA	NA	NA	NA	NA	None	Surface	0.35	32.77	0.00	Steel
[28]	2_1_a	0.79	7.9	NA	NA	0.49	3196	4	NA	NA	NA	NA	NA	NA	None	Surface	0.35	19.94	0.00	Spalling
[28]	2_1_b	0.79	7.9	NA	NA	0.49	3196	4	NA	NA	NA	NA	NA	NA	None	Surface	0.35	18.27	0.00	Spalling
[28]	2_2_a	0.79	7.9	NA	NA	0.49	3196	8	NA	NA	NA	NA	NA	NA	None	Surface	0.35	33.99	0.00	Steel
[28]	2_2_b	0.79	7.9	NA	NA	0.49	3196	8	NA	NA	NA	NA	NA	NA	None	Surface	0.35	32.99	0.00	Steel
[28]	2_3_a	0.79	7.9	NA	NA	0.49	3196	8	NA	NA	NA	NA	NA	NA	None	Surface	0.35	30.38	0.00	Steel
[28]	2_3_b	0.79	7.9	NA	NA	0.49	3196	8	NA	NA	NA	NA	NA	NA	None	Surface	0.35	30.09	0.00	Steel
[28]	3_1_a	0.79	7.9	NA	NA	0.49	3196	4	NA	NA	NA	NA	NA	NA	None	Surface	0.70	22.71	0.00	Steel
[28]	3_1_b	0.79	7.9	NA	NA	0.49	3196	4	NA	NA	NA	NA	NA	NA	None	Surface	0.70	21.38	0.00	Steel
[28]	3_4_a	0.79	7.9	NA	NA	0.49	3196	8	NA	NA	NA	NA	NA	NA	None	Surface	0.70	33.50	0.00	Steel

[28]	3_4_b	0.79	7.9	NA	NA	0.49	3196	8	NA	NA	NA	NA	NA	NA	None	Surface	0.70	31.62	0.00	Steel
[28]	3_5_a	1.18	7.9	NA	NA	1.10	3196	8	NA	NA	NA	NA	NA	NA	None	Surface	0.70	38.86	0.00	Steel
[28]	3_5_b	1.18	7.9	NA	NA	1.10	3196	8	NA	NA	NA	NA	NA	NA	None	Surface	0.70	33.33	0.00	Steel
[28]	10_1_a	0.79	7.9	NA	NA	0.49	3196	2	NA	NA	NA	NA	NA	NA	None	Surface	0.35	16.19	0.00	Rundstahl
[28]	10_1_b	0.79	7.9	NA	NA	0.49	3196	2	NA	NA	NA	NA	NA	NA	None	Surface	0.35	15.80	0.00	Rundstahl
[28]	10_2_a	0.94	7.9	NA	NA	0.70	3196	8	NA	NA	NA	NA	NA	NA	None	Surface	0.35	31.61	0.00	Rundstahl
[28]	10_2_b	0.94	7.9	NA	NA	0.70	3196	8	NA	NA	NA	NA	NA	NA	None	Surface	0.35	31.22	0.00	Rundstahl
[28]	11_1_a	0.94	7.9	NA	NA	0.70	3196	8	NA	NA	NA	NA	NA	NA	None	Surface	0.35	26.72	0.00	ohne
[28]	11_1_b	0.94	7.9	NA	NA	0.70	3196	8	NA	NA	NA	NA	NA	NA	None	Surface	0.35	23.35	0.00	ohne
[28]	12_1_a	0.79	7.9	NA	NA	0.49	3196	2	NA	NA	NA	NA	NA	NA	None	Surface	0.00	6.96	0.00	ohne
[28]	12_1_b	0.79	7.9	NA	NA	0.49	3196	2	NA	NA	NA	NA	NA	NA	None	Surface	0.00	8.47	0.00	ohne
[28]	12_2_a	0.94	7.9	NA	NA	0.70	3196	8	NA	NA	NA	NA	NA	NA	None	Surface	0.00	24.19	0.00	ohne
[28]	12_2_b	0.94	7.9	NA	NA	0.70	3196	8	NA	NA	NA	NA	NA	NA	None	Surface	0.00	23.67	0.00	ohne
[29]	#2-5	0.50	7.0	69	NA	0.20	3300	3	12	12	14	72	16	12	None	None	0.00	9.18	2.00	Wood
[29]	#2-6	0.50	7.0	69	NA	0.20	3300	3	12	12	14	72	16	12	None	None	0.00	9.18	2.00	Wood
[29]	#2-7	0.50	7.0	69	NA	0.20	3300	2	12	12	14	72	16	12	None	None	0.00	7.08	2.00	Cone
[29]	#2-8	0.50	7.0	69	NA	0.20	3300	2	12	12	14	72	16	12	None	None	0.00	7.08	2.00	Cone
[29]	#2-9	0.50	7.0	69	NA	0.20	3300	2	12	12	14	72	16	12	None	None	0.00	7.08	2.00	Cone
[29]	#2-10	0.50	7.0	69	NA	0.20	3300	2	12	12	14	72	16	12	None	None	0.00	7.08	2.00	Cone
[29]	#2-11	0.50	7.0	69	NA	0.20	3300	2	12	12	14	72	16	12	None	None	0.00	7.08	2.00	Cone
[29]	#2-12	0.50	7.0	69	NA	0.20	3300	2	12	12	14	72	16	12	None	None	0.00	7.08	2.00	Cone
[29]	#2-13	0.50	7.0	69	NA	0.20	3300	2	12	12	14	72	16	12	Yes	None	0.00	6.52	2.00	Cone
[29]	#2-14	0.50	7.0	69	NA	0.20	3300	2	12	12	14	72	16	12	Yes	None	0.00	6.52	2.00	Cone
[29]	#2-15	0.50	7.0	69	NA	0.20	3300	2	12	12	14	72	16	12	Yes	None	0.00	6.52	2.00	Cone
[29]	#2-16	0.50	7.0	69	NA	0.20	3300	2	12	12	14	72	16	12	Yes	None	0.00	6.52	2.00	Cone
[29]	#2-17	0.50	7.0	69	NA	0.20	3300	2	12	12	14	72	16	12	Yes	None	0.00	6.52	2.00	Cone
[29]	#2-18	0.50	7.0	69	NA	0.20	3300	2	12	12	14	72	16	12	Yes	None	0.00	6.52	2.00	Cone
[30]	#2232010	0.75	4.0	76	0.9	0.33	5650	4	12	16	15	40	38	17	None	None	0.00	14.46	0.00	Cone
[30]	#2222010	0.75	4.0	76	0.9	0.33	5650	4	12	16	15	40	38	17	None	None	0.00	14.18	0.00	Cone
[30]	#1132010	0.75	6.0	76	0.9	0.33	5650	4	16	24	15	56	38	17	None	None	0.00	13.41	0.00	Cone
[30]	#3012010	0.75	6.0	76	0.9	0.33	5650	4	16	24	15	56	38	17	None	None	0.00	15.82	0.00	Cone
[30]	#3092010	0.75	6.0	76	0.9	0.33	5650	6	16	16	15	48	38	17	None	None	0.00	16.11	0.00	Steel
[30]	#3102010	0.75	6.0	76	0.9	0.33	5650	6	16	16	15	48	38	17	None	None	0.00	17.74	0.00	Steel
[30]	#3222010	0.75	6.0	76	0.9	0.33	5650	6	16	16	15	48	38	17	None	None	0.00	16.84	0.00	Steel
[30]	#3232010	0.75	6.0	76	0.9	0.33	5650	6	16	16	15	48	38	17	None	None	0.00	16.17	0.00	Steel
[30]	#9132010	0.75	6.0	76	0.9	0.33	3525	4	16	16	15	48	38	17	None	Surf.	0.40	22.19	0.00	Steel
[30]	#9132010_2	0.75	6.0	76	0.9	0.33	3525	4	16	16	15	48	38	17	None	Surf.	0.40	22.47	0.00	Steel
[30]	#9282010	1.00	6.0	131	1.5	0.61	3800	6	16	16	15	48	38	17	None	Surf.	0.80	39.18	0.00	Steel
[30]	#9292010	1.00	6.0	131	1.5	0.61	3800	6	16	16	15	48	38	17	None	Surf.	0.80	44.11	0.00	Steel
[30]	#10062010	1.00	6.0	131	1.5	0.61	3800	6	9	9	15	48	38	17	None	Surf.	0.80	38.40	0.00	Steel
[30]	#10062010_2	1.00	6.0	131	1.5	0.61	3800	6	9	9	15	48	38	17	None	Surf.	0.80	34.71	0.00	Steel

[30]	#10072010	1.00	6.0	131	1.5	0.61	3800	6	9	9	15	48	38	17	None	Surf.	0.80	33.40	0.00	Steel
[30]	#10292010 SG	1.00	6.0	131	1.5	0.61	3800	6	16	16	15	48	38	17	None	Surf.	0.80	36.13	0.00	Steel
[30]	#11192010 SG	1.00	6.0	131	1.5	0.61	3800	6	16	16	15	48	38	17	None	Surf.	0.80	39.33	0.00	Steel
[31]	GER-1	0.79	4.7	60	NA	0.49	3597	2	4	NA	NA	NA	NA	NA	None	None	0.00	1.57	0.00	Cone
[31]	GER-2	0.79	4.7	60	NA	0.49	3597	2	4	NA	NA	NA	NA	NA	None	None	0.00	1.82	0.00	Cone
[31]	GER-3	0.98	5.9	60	NA	0.76	3597	2	4	NA	NA	NA	NA	NA	None	None	0.00	2.43	0.00	Cone
[31]	GER-4	0.98	5.9	60	NA	0.76	3597	2	4	NA	NA	NA	NA	NA	None	None	0.00	2.43	0.00	Cone
[31]	GER-5	0.55	3.3	60	NA	0.24	3597	2	4	NA	NA	NA	NA	NA	None	None	0.00	1.28	0.00	Cone
[31]	GER-6	0.55	3.3	60	NA	0.24	3597	2	4	NA	NA	NA	NA	NA	None	None	0.00	1.57	0.00	Cone
[31]	GER-7	0.55	3.3	60	NA	0.24	3597	2	4	NA	NA	NA	NA	NA	None	None	0.00	1.87	0.00	Cone
[31]	GER-8	0.55	3.3	60	NA	0.24	3597	2	4	NA	NA	NA	NA	NA	None	None	0.00	1.87	0.00	Cone
[31]	GER-9	1.04	8.3	60	NA	0.85	5384	3	5	NA	NA	NA	NA	NA	None	None	0.00	4.18	0.00	Cone
[31]	GER-10	1.04	8.3	60	NA	0.85	5384	3	6	NA	NA	NA	NA	NA	None	None	0.00	4.59	0.00	Cone
[31]	GER-11	1.04	8.3	60	NA	0.85	5627	3	6	NA	NA	NA	NA	NA	None	None	0.00	6.29	0.00	Cone
[31]	GER-12	0.98	5.9	60	NA	0.76	3597	3	6	NA	NA	NA	NA	NA	None	None	0.00	3.28	0.00	Cone
[31]	GER-13	0.98	5.9	60	NA	0.76	3597	3	6	NA	NA	NA	NA	NA	None	None	0.00	3.87	0.00	Cone
[31]	GER-14	0.55	3.3	60	NA	0.24	3597	3	5	NA	NA	NA	NA	NA	None	None	0.00	2.99	0.00	Cone
[31]	GER-15	0.55	3.3	60	NA	0.24	3597	3	5	NA	NA	NA	NA	NA	None	None	0.00	2.99	0.00	Cone
[31]	GER-16	0.79	4.7	60	NA	0.49	3597	3	6	NA	NA	NA	NA	NA	None	None	0.00	3.28	0.00	Cone
[31]	GER-17	0.79	4.7	60	NA	0.49	3597	3	6	NA	NA	NA	NA	NA	None	None	0.00	3.57	0.00	Cone
[31]	GER-18	0.79	4.7	60	NA	0.49	3597	3	6	NA	NA	NA	NA	NA	None	None	0.00	3.57	0.00	Cone
[31]	GER-19	0.79	4.7	60	NA	0.49	3597	3	6	NA	NA	NA	NA	NA	None	None	0.00	3.87	0.00	Cone
[31]	GER-20	1.04	8.3	60	NA	0.85	5384	3	6	NA	NA	NA	NA	NA	None	None	0.00	6.11	0.00	Cone
[31]	GER-21	1.04	8.3	60	NA	0.85	5384	3	8	NA	NA	NA	NA	NA	None	None	0.00	5.89	0.00	Cone
[31]	GER-22	1.04	8.3	60	NA	0.85	5384	3	11	NA	NA	NA	NA	NA	None	None	0.00	6.63	0.00	Cone
[31]	GER-23	1.04	8.3	60	NA	0.85	5384	3	6	NA	NA	NA	NA	NA	None	None	0.00	6.65	0.00	Cone
[31]	GER-24	1.04	8.3	60	NA	0.85	5384	5	8	NA	NA	NA	NA	NA	None	None	0.00	9.13	0.00	Cone
[31]	GER-25	0.98	5.9	60	NA	0.76	3713	5	8	NA	NA	NA	NA	NA	None	None	0.00	8.14	0.00	Cone
[31]	GER-26	0.98	5.9	60	NA	0.76	3713	5	8	NA	NA	NA	NA	NA	None	None	0.00	8.99	0.00	Cone
[31]	GER-27	0.98	5.9	60	NA	0.76	3713	5	8	NA	NA	NA	NA	NA	None	None	0.00	8.99	0.00	Cone
[31]	GER-28	0.98	5.9	60	NA	0.76	3713	5	8	NA	NA	NA	NA	NA	None	None	0.00	8.99	0.00	Cone
[31]	GER-29	0.79	4.7	60	NA	0.49	3713	5	8	NA	NA	NA	NA	NA	None	None	0.00	7.71	0.00	Cone
[31]	GER-30	0.79	4.7	60	NA	0.49	3713	5	8	NA	NA	NA	NA	NA	None	None	0.00	7.71	0.00	Cone
[31]	GER-31	0.79	6.3	60	NA	0.49	4363	5	12	NA	NA	NA	NA	NA	None	None	0.00	12.45	0.00	Cone
[31]	GER-32	0.79	6.3	60	NA	0.49	4734	5	12	NA	NA	NA	NA	NA	None	None	0.00	13.38	0.00	Cone
[31]	GER-33	1.04	8.3	60	NA	0.85	4734	5	12	NA	NA	NA	NA	NA	None	None	0.00	12.61	0.00	Cone
[31]	GER-34	1.10	8.8	60	NA	0.95	4734	5	12	NA	NA	NA	NA	NA	None	None	0.00	12.39	0.00	Cone
[31]	GER-35	1.10	8.8	60	NA	0.95	4734	5	12	NA	NA	NA	NA	NA	None	None	0.00	15.42	0.00	Cone
[31]	GER-36	1.04	8.3	60	NA	0.85	5384	6	11	NA	NA	NA	NA	NA	None	None	0.00	13.49	0.00	Cone
[31]	GER-37	0.79	6.1	60	NA	0.49	4363	5	12	NA	NA	NA	NA	NA	None	None	0.00	12.45	0.00	Cone
[31]	GER-38	0.79	6.1	60	NA	0.49	4734	5	12	NA	NA	NA	NA	NA	None	None	0.00	13.38	0.00	Cone

[31]	GER-39	1.10	7.4	60	NA	0.95	4734	5	12	NA	NA	NA	NA	NA	None	None	0.00	12.12	0.00	Cone
[31]	GER-40	1.10	7.4	60	NA	0.95	4734	5	12	NA	NA	NA	NA	NA	None	None	0.00	12.68	0.00	Cone
[31]	GER-41	1.10	7.4	60	NA	0.95	4734	5	12	NA	NA	NA	NA	NA	None	None	0.00	15.89	0.00	Cone
[31]	GER-42	1.10	7.4	60	NA	0.95	4734	5	12	NA	NA	NA	NA	NA	None	None	0.00	14.95	0.00	Cone
[31]	GER-43	1.04	7.1	60	NA	0.85	4734	5	12	NA	NA	NA	NA	NA	None	None	0.00	13.58	0.00	Cone
[31]	GER-44	1.04	7.1	60	NA	0.85	4734	5	12	NA	NA	NA	NA	NA	None	None	0.00	11.67	0.00	Cone
[31]	GER-45	1.10	7.1	60	NA	0.95	4514	9	12	NA	NA	NA	NA	NA	None	None	0.00	21.04	0.00	Cone
[31]	GER-46	1.42	8.6	60	NA	1.58	4084	9	12	NA	NA	NA	NA	NA	None	None	0.00	29.76	0.00	Cone
[31]	GER-47	1.57	9.3	60	NA	1.95	4084	9	12	NA	NA	NA	NA	NA	None	None	0.00	42.31	0.00	Cone
[31]	GER-48	1.04	7.1	60	NA	0.85	4084	9	12	NA	NA	NA	NA	NA	None	None	0.00	28.62	0.00	Cone
[31]	GER-49	1.42	8.6	60	NA	1.58	4084	9	12	NA	NA	NA	NA	NA	None	None	0.00	30.93	0.00	Cone
[31]	GER-50	1.04	7.1	60	NA	0.85	3342	9	6	NA	NA	NA	NA	NA	None	None	0.00	17.29	0.00	Cone
[31]	GER-51	1.10	7.4	60	NA	0.95	4873	5	6	NA	NA	NA	NA	NA	None	None	0.00	10.97	0.00	Cone
[31]	GER-52	1.04	7.1	60	NA	0.85	4873	5	6	NA	NA	NA	NA	NA	None	None	0.00	10.16	0.00	Cone
[31]	GER-53	1.42	8.6	60	NA	1.58	4873	6	6	NA	NA	NA	NA	NA	None	None	0.00	12.72	0.00	Cone
[31]	GER-54	1.10	7.4	60	NA	0.95	4873	5	4	NA	NA	NA	NA	NA	None	None	0.00	8.72	0.00	Cone
[31]	GER-55	1.04	12.0	60	NA	0.85	5384	3	3	NA	NA	NA	NA	NA	None	None	0.00	2.83	0.00	Cone
[31]	GER-56	1.04	12.0	60	NA	0.85	5384	8	3	NA	NA	NA	NA	NA	None	None	0.00	7.53	0.00	Cone
[31]	GER-57	1.04	12.0	60	NA	0.85	5384	3	3	NA	NA	NA	NA	NA	None	None	0.00	3.42	0.00	Cone
[31]	GER-58	1.04	12.0	60	NA	0.85	5384	5	3	NA	NA	NA	NA	NA	None	None	0.00	5.10	0.00	Cone
[31]	GER-59	1.04	12.0	60	NA	0.85	5384	6	3	NA	NA	NA	NA	NA	None	None	0.00	6.65	0.00	Cone
[31]	GER-60	1.04	12.0	60	NA	0.85	5384	8	3	NA	NA	NA	NA	NA	None	None	0.00	10.75	0.00	Cone
[31]	GER-61	1.04	12.0	60	NA	0.85	5384	3	5	NA	NA	NA	NA	NA	None	None	0.00	4.18	0.00	Cone
[31]	GER-62	1.04	12.0	60	NA	0.85	5384	3	5	NA	NA	NA	NA	NA	None	None	0.00	4.72	0.00	Cone
[31]	GER-63	1.04	12.0	60	NA	0.85	5384	5	5	NA	NA	NA	NA	NA	None	None	0.00	7.17	0.00	Cone
[31]	GER-64	1.04	12.0	60	NA	0.85	5384	6	5	NA	NA	NA	NA	NA	None	None	0.00	9.67	0.00	Cone
[31]	GER-65	1.04	12.0	60	NA	0.85	5384	3	6	NA	NA	NA	NA	NA	None	None	0.00	4.59	0.00	Cone
[31]	GER-66	1.04	12.0	60	NA	0.85	5384	3	6	NA	NA	NA	NA	NA	None	None	0.00	6.11	0.00	Cone
[31]	GER-67	1.04	12.0	60	NA	0.85	5384	5	6	NA	NA	NA	NA	NA	None	None	0.00	8.88	0.00	Cone
[31]	GER-68	1.04	12.0	60	NA	0.85	5384	6	6	NA	NA	NA	NA	NA	None	None	0.00	12.99	0.00	Cone
[31]	GER-69	1.04	12.0	60	NA	0.85	5384	3	8	NA	NA	NA	NA	NA	None	None	0.00	5.89	0.00	Cone
[31]	GER-70	1.04	12.0	60	NA	0.85	5384	5	8	NA	NA	NA	NA	NA	None	None	0.00	9.13	0.00	Cone
[31]	GER-71	1.04	12.0	60	NA	0.85	5384	6	8	NA	NA	NA	NA	NA	None	None	0.00	14.88	0.00	Cone
[31]	GER-72	1.04	12.0	60	NA	0.85	5384	8	8	NA	NA	NA	NA	NA	None	None	0.00	21.13	0.00	Cone
[31]	GER-73	1.04	12.0	60	NA	0.85	5384	3	11	NA	NA	NA	NA	NA	None	None	0.00	6.63	0.00	Cone
[31]	GER-74	1.04	12.0	60	NA	0.85	5384	6	11	NA	NA	NA	NA	NA	None	None	0.00	13.49	0.00	Cone

Reference list

Ref. #	Name
Shear-1	Viest, I. M. Investigation of Stud Shear Connectors for Composite Concrete and Steel T-Beams Journal of the American Concrete Institute, Vol. 27, April, 1956.
Shear-2	Ollgaard, J. G.; Slutter, R. G.; and Fisher, J. W., "Shear Strength of Stud Connectors in Lightweight and Normal Weight Concrete," AISC Engineering Journal, V. 8, No. 2, Apr. 1971, pp.55-64.
Shear-3	McMackin, P. .I.; Slutter, R. G.; and Fisher, J. W., "Headed Steel Anchors Under Combined Loading," AISC Engineering Journal, 2nd Quarter, Apr. 1973, pp. 43-52.
Shear-4	Bailey, John W., and Burdette, Edwin G., "Edge Effects on Anchorage to Concrete," Civil Engineering Research Series No. 31, The University of Tennessee, Knoxville, Aug. 1977, 120 pp.
Shear-4	Muratli, Hakki, Klingner, R. E. and Graves, III, H. L., "Behavior of Shear Anchors in Concrete: Statistical Analysis and Design Recommendations," ACI Structural Journal, vol. 101, no. 6, November-December 2004, pp. 821-829.
Shear-5	Neille, D. (1977) Behavior of headed stud connections for precast pannels under monotonic and cyclic shear loading, MS thesis, Univeristy of British Comlumbia, 242pp.
Shear-6	Swirsky P h., el al., "Lateral Resistance of Anchor Bolts installed in Concrete," Report No. FHWA-CA-ST-4167-77-12, pp.lOO, California Department of Transportation, Sacramento, May 1978.
Shear-7	Klingner, R.E., Mendonca, J.A. and Malik J.B. (1982). Effect of reinforcing details on the shear resistance of anchor bolts under reversed cyclic loading. ACI Journal, 79: 1, pp. 471-479.
Shear-7	Klingner R. C. and Mendonca, J. A,, "Shear Capacity of Short Anchor Bolls and Welded Studs: A Lilerature Review," Journal of the American Concrete Institute, Proceedings Vol. 79, No. 5, September-October 1982, pp. 339-350
Shear-8	Kuhn, J.M. and Buckner, C.D. (1986), "Effect of Concrete Placement on Shear Strength of Headed Studs," Journal of Structural Engineering, ASCE, Vol. 112, No. 8, August, pp. 1965-1971.
Shear-9	Hawkins, N. M. (1987). "Strength in shear and tension of cast-in-place anchor bolts." Special Publication, ACI SP-103, 233-255.
Shear-10	"Stud Groups Loaded in Shear near a Free Edge," by Wong, Donahey, and Lloyd from 1998.
Shear-11	kawano Hisao , Kutani Kazuhide , Masuda Kanshi (1989) "An Experimental Study on the Shear Strength of Anchor Bolts Embedded in Concrete [in Japanese]" Annual Meeting Architectural Institute of Japan. C-1, Structures III
Shear-12	Ueda, T, Kitipornchai, S., and Ling, K., "Experimental investigation of anchor bolts under shear," Journal of Structural Engineering, A.S.C.E., Vol.116, No.4, 1990, pp.910-924.
Shear-13	Hallowell, J., Tensile and Shear Behavior of Anchors in Uncracked and Cracked Concrete Under Static and Dynamic Loading," M.S. Thesis, The University of Texas at Austin, December, 1996.
Shear-14	Gattesco, N. and Giuriani, E. "Experimental study on stud shear connectors subjected to cyclic loading." J. Constr. Steel Res., 38(1), 1–21
Shear-15	Nakajima, A., Saiki, I., Kokai, M., Doi, K., Takabayashi, Y. and Ooe, H., Cyclic shear force-slip behavior of studs under alternating and pulsating load condition, Engineering Structures, Vol.25, pp.537-545, 2003.
Shear-16	Taplin, G. and Grundy, P. (1997) Incremental slip of stud shear connectors under repeated loading IABSE reports Vol.999.
Shear-17	Ohashi, Y. and Nakashima, YS. (1997) "Experimental study on mechanical characteristics of exposed portions of anchor bolts," Summaries of technical papers of Annual Meeting Architectural Institute of Japan. C-1, Structures III, Timber structures steel str
Shear-18	Nakashima, S. (1998) Mechanical characteristics of exposed portions of anchor bolts subjected to shearing forces Summaries of technical papers of Annual Report, Architectural Institute of Japan, Vol. 38, pp. 349-352
Shear-19	Bursi, O. S., Gramola, G.: Behaviour of headed stud shear connectors under low cycle high amplitude displacements. Materials and Structures, May 1999, Vol. 32,pp. 290-297.
Shear-20	Anderson, N. S. and Meinheit, D. F. [2000], "Design Criteria for Headed Stud Groups in Shear: Part 1 – Steel Capacity and Back Edge Effects," PCI Journal, V. 45, No. 5, September/October, pp. 46-75.
Shear-21	Gross, J. H., Klingner, R. E. and Graves, III, H. L., "Dynamic Behavior of Single and Double Near-Edge Anchors Loaded in Shear," Structures Journal, American Concrete Institute, Farmington Hills, Michigan, vol. 98, no. 5, September-October 2001, pp. 665-
Shear-22	kawano Hisao, Kutani Kazuhide, And Masuda Kanshi "EXPERIMENTAL STUDIES ON THE SHEAR RESISTANCE OF ANCHOR BOLTS IN EXPORSED TYPE OF STEEL COLUMN BASES [in Japanese]" Journal of structural and construction engineering. Transactions of AIJ (567), 141-148, 2

Shear-23	Civjan SA, Singh P. Behavior of shear studs subjected to fully reversed cyclic loading. Journal of Structural Engineering, ASCE 2003;129(11):1466–74.
Shear-24	Saari, W., Hajjar, J. F., Schultz, A. E., and Shield, C. K. (2004). "Behavior of Shear Studs in Steel Frames with Reinforced Concrete Infill Walls," Journal of Constructional Steel Research, Vol. 60, No. 10, October, pp. 1453-1480.
Shear-25	Anderson, N. S. and Meinheit, D. F. [2000], "Design Criteria for Headed Stud Groups in Shear" WJE research report Chapter 14
Shear-26	Fennel, A., Voss, T., Moore, K., and Mochizuki, G. (2009) Report on laboratory testing of anchor bolts connecting wood sill plates to concrete with minimum edge distances, Structural Engineers Association of Northern California, 50 pp.
Shear-27	Nam Ho Lee, Kwang Ryeon Park, Yong Pyo Suh (2010) "Shear behavior of headed anchors with large diameters and deep embedment in concrete," Nuclear Engineering and Design
Shear-28	Schmid, K. (2010) Structural behavior and design of anchor near the edge with hanger steel under shear PhD Thesis, University of Stuttgart
Shear-29	DeRenzis, A., Kochkin, V., and Ehrlich, G. (2010) Evaluation of Wood Sole Plate Anchorage to Concrete Under Monotonic and Cyclic Loading, 2010 Structures Congress, pp. 808-819.
Shear-30	Petersen, D. (2010) Seismic behavior and design of cast-in-place anchors, MS Thesis, UW-Milwaukee
Shear-31	German tests stored in ACI 355 database assembled by Prof. Klingner at the University of Texas.